THE PHOTOPHYSICAL PROPERTIES AND APPLICATIONS OF RUTHENIUM(II) POLYPYRIDYL COMPLEXES AS LUMINESCENT PROBES OF PROTEINS.

BY

MIRIAM WALSH, BSc. (HONS.)
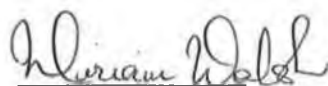
A THESIS PRESENTED TO DUBLIN CITY UNIVERSITY FOR THE DEGREE OF DOCTOR OF PHILOSOPHY.

SUPERVISOR PROF. JOHANNES G. VOS.
SCHOOL OF CHEMICAL SCIENCES,
DUBLIN CITY UNIVERSITY.

JUNE 1997.

i

This thesis is dedicated to my parents.

This thesis has not previously been submitted as an exercise for a degree at this, or at any other university. Except where otherwise indicated, this work has been carried out by the author alone.

Miriam Walsh

Acknowledgements.

I could almost write a book mentioning all the people who have helped me in various ways during the course of my PhD, but I will somehow restrict it to 2 pages. Firstly, I must sincerely thank my supervisor Prof. Han Vos (Han the man), whose encouragement and support helped me greatly! His ideas, opinions and patience were greatly appreciated and I thank him for the extended use of his office. His fashion tips were also useful but never followed and yes Han, I will get my hair done! Thanks to the academic and technical staff of D.C.U. chemistry dept, to Conor Long and his research group, especially Siobhan for any laser aid! and also Dermot Diamond and Suzanne Walsh for their help during the double exponential timewarp! Thanks to Paddy Kane for his timely help in the molecular modelling.

I would like to thank Prof. Richard O Kennedy and his research group for their useful advice and for the supply of biological compounds. Special thanks to Eli Ryan(Burke) for her valuable assistance during the early stages of my postgrad. Further thanks are due to Ann for her ideas and help during my enzyme work, and to Ciaran Fagan and Ann-Marie for advice and use of their laboratory. Special thanks to staff at Coldchon Ltd., for their use of photocopying facilities and for their understanding and tolerance during the final stages.

Most sincere thanks to all my fellow research group, both past and present, Andy, Helen, Tia (back for more questions!), Dave, Margaret, Frances, Noel, Joe, Rachel (I don't like Mondays) and the more recent bunch Christine, Luke, Una and Bronagh (an honorary member) who made life almost enjoyable in AG12! Special thanks to Frances for her help in the final stages of this thesis. Last but definitely not least, special thanks to Karen, my partner in crime, whose quirky ways and great sense of humour provided plenty of laughs along the way and who made ruthenium research all the more interesting! Her friendship and help will always be appreciated and long may it last (at least until she buys that hat!).

Further thanks to all of the other postgrads in the chemistry department, Ciara, James, Ciaran, Orla, Pat (the philosopher), Fiona, Aisling, Declan, Mary Mac, Mick x 3, Teresa, Joe, Ben, Mrs. Karen J., to name but a few. Shane, Ollie, James and Cormac, ta for the good craic and nice clean talk at coffee breaks.

To my sporting buddies from DCU, Dunnie, Maureen (Mo), Ann, Liz, Aoibhinn, Eilish, Angela, Vinnie, Derek, Alan, the list is neverending... I never thought soccer, camogie and badminton could be so much fun even when losing! Thanks for all the laughs, tears (not always gracious losers) and good sport we had over the years, they'll always be remembered fondly!

A special thanks to Mags (I dont know, I'm from Carla), (& Conor), Brid (& Aidan), Ann (& Donie) and Sue-Ann (& Mark) for the fun get-togethers and great friendship throughout college years and beyond !

To all occupants of 32 Botanic Ave. past and present, thanks for the great craic there, in particular Karen, Ann, Frances, Maureen x 2, Susana, Maria, Pamela, Ruijjie, Sven and Astrid. Best of luck in the future! To the gang of Barr Aille, Sinead, Susan, Liz and Yvónne, although ye meant well (NOT) your constant "thesis, thesis" chants were not appreciated at the time but they did the trick!

Outside DCU, back in T-town, a special thanks to Quack, a good and close pal. Her friendship, support and willingness to party kept me going through good and bad. I'm still waiting for that big day to wear my dress! A special mention to Span the man to thank him for his continuing support, patience and understanding, particularly through the rough patches.

Finally, I would like to thank all the Walsh clan (& Corrways) forever multiplying, and particularly my parents, Catherine and Michael, for their support, guidance and love. This thesis is dedicated to them and I thank them for everything. I'm particularly indebted to my mother, the best in the world, for her faith and pride in me as well as her eternal patience and good humour. You have made all this worthwhile, Mam.

Abstract.

This thesis involves the characterisation of Ru(II) polypyridyl complexes when covalently linked to proteins and a study of their propensity to monitor conformational variances which these proteins undergo in solution.

In the first section of this thesis, the Ru(II) complexes are covalently bound to various synthetic and natural proteins via selected binding sites on the biomolecules, and these protein-bound labels are extensively characterised via the spectroscopic and luminescent properties of the labels. Thereafter, these protein-bound labels are employed as spectroscopic probes of the conformational changes which the bound proteins undergo in solution via variations in the photophysical properties of these labels found to accompany structural changes of the proteins. Although the emission spectra of the labels are somewhat sensitive to the conformational properties of the bound protein, the decay lifetimes were found to be the most sensitive reporter, due to their sensitivity to their local environment. The α-helix to random coil transition of poly-amino acids were thereby probed by changes in the decay lifetimes of the labels. This section also investigates the potential of the decay lifetime of the labels as a probe of the unfolding process of natural proteins. Investigations into the effects of a number of parameters (i.e. label type and position on protein, temperature, chemical denaturants) on the probing potential of the labels were carried out.

The final section involves the labelling of an enzyme with the same Ru(II) complexes. Firstly, the effect of the labelling on the activity of the enzyme was studied to determine the effect of such modification on the natural conformational properties of the enzyme. Correlation between the acid-induced loss of activity (i.e denaturation) of the enzyme and changes in the decay lifetimes of the labels were found suggesting the potential application of such fluorescent complexes as probes in real biological matrices without adverse effects on the natural characteristics of the system.

Table of Contents.

Chapter 1.
Introduction

1.1   General introduction.

The overall aim of this thesis is the application of ruthenium polypyridyl complexes as fluorescent probes in biological systems, concentrating on the monitoring of conformational changes which the bound biomolecules naturally undergo in solution.

Firstly, in order to emphasise the usefulness of ruthenium polypyridyls in this field, it is natural to commence with a review of the properties of these complexes, in particular, those relevant to this thesis. This chapter will survey the literature in relation to the use of ruthenium complexes as fluorescent labels in various biological systems, notably DNA and proteins such as enzymes and antibodies. Other applications discovered involving specific interactions between ruthenium complexes and compounds of biological significance will be discussed, ranging from the use of such complexes as anti-cancer agents, to their use in the study of biological electron-transfer processes to the chemiluminescent detection of compounds of biological significance. The aim of such a review is to illustrate the broad applicability of ruthenium complexes in the fields of biology, biochemistry and medicine and hence to clarify why such complexes were chosen in the study of the conformational properties of biomolecules in this thesis.

1.2   The structural and physical properties of ruthenium polypyridyl complexes.

Ru^{2+} is a d_6 system and the polypyridyl ligands are usually colourless molecules possessing σ-donor orbitals localised on the nitrogen atoms and π-donor and π^*-acceptor orbitals more or less delocalised on aromatic rings. The compound $[Ru(bpy)_3]^{2+}$ where bpy = 2,2'-bipyridine and other $[Ru(L-L)_3]^{2+}$ compounds where L-L=bidentate polypyridyl ligand, exhibit D_3 symmetry and the π and π^* orbitals of the

ligands may be symmetrical (χ) or anti-symmetrical (Ψ) with respect to rotation around the C_2 axis, retained by each Ru(bpy) unit [1]. The x-ray crystal structure for $[Ru(bpy)_3]^{2+}$ shows that the metal to ligand (Ru-N) bond lengths are short, indicating significant back-bonding between Ru(II) and the π^* orbitals of bpy [1]. The structure of the parent compound $[Ru(bpy)_3]^{2+}$ is depicted in Figure 1.1 below.
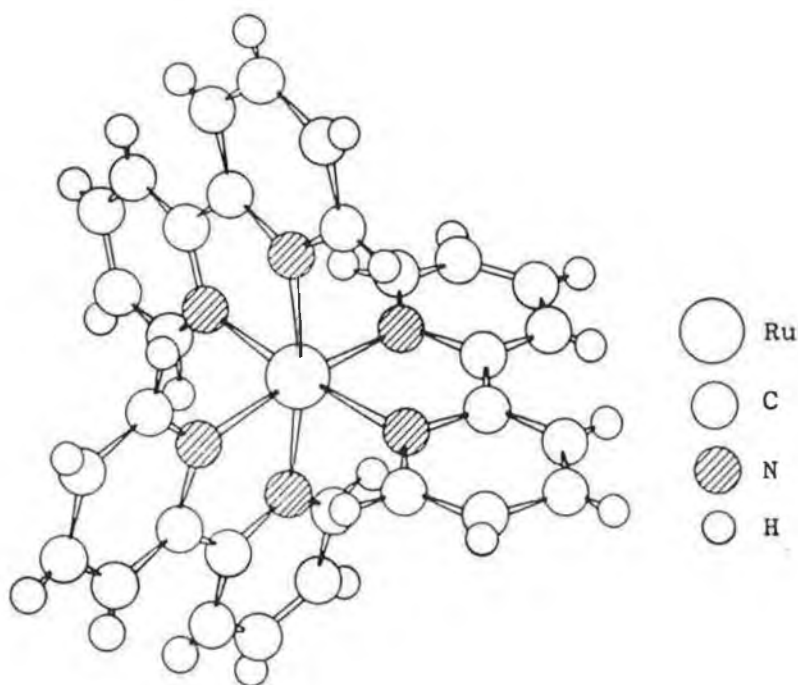
Figure 1.1 Structure of [Ru(bpy)₃]²⁺ [4].

1.3. The photophysical properties of $[Ru(bpy)_3]^{2+}$ in solution.

The lowest excited state for most Ru(II) polypyridyl complexes is a ^{3}MLCT (metal to ligand charge transfer) transition, [5, 6, 7] which undergoes slow radiationless decay, thus exhibiting long lived emission. [2] Due to the presence of an oxidising site on the metal and a reductive site on the ligands, the MLCT excited states possess two distinct redox sites. [1] Hence, the energy position of the MLCT state depends on the redox properties of the metal and ligands, in particular on the σ-donor or π-acceptor properties of the ligands [8]. The difference in energy between the filled d orbitals and the lowest unoccupied ligand-based orbital is related to the absorption and emission energy of the complexes. By a careful choice of ligands in a series of complexes of the same metal ion, the orbital nature of the lowest excited state and hence, its energy, emission lifetime, redox properties, emission quantum yield, chemical stability and oxidation and reduction potentials can be controlled [1].

Due to their unique combination of photochemistry, electrochemistry and chemical stability, Ru(II) polypyridyl complexes find applications as (a) photoluminescent compounds; (b) excited state reactants in electron and energy transfer processes and (c) as excited state products in electron transfer chemiluminescence [9].

$[Ru(bpy)_3]^{2+}$ has been recognised as a potential catalyst for the decomposition of water into its elements by irradiation with solar light [10], and recently, very high solar energy conversion efficiencies at dye sensitised photoelectrochemical cells have been realised [11-13].

1.3.1 Absorption spectroscopy.

The absorption spectrum of $[Ru(bpy)_3]^{2+}$ is illustrated in Figure 1.2. The intense transitions observed in the visible region are due to the metal to ligand charge transfer (MLCT) transition between the metal centred t_{2g} ground state and ligand π^*

states. [3, 8, 9, 10] The intense bands in the ultraviolet region are due to intraligand π-π* transitions, while the weaker absorption to the blue of the visible band has been assigned to a metal centred d-d* transition. The tail at longer wavelengths has been assigned to a weak spin-forbidden MLCT transition [2, 5].

It is believed that the excited electron is delocalised among the ligands in the ^{1}MLCT excited state but that as interaction between the ligands is weak, it localises on only one ligand when intersystem crossing to the ^{3}MLCT excited state takes place. [1] The photophysical pathway of $[Ru(bpy)_3]^{2+}$ is illustrated in Figure 1.3.
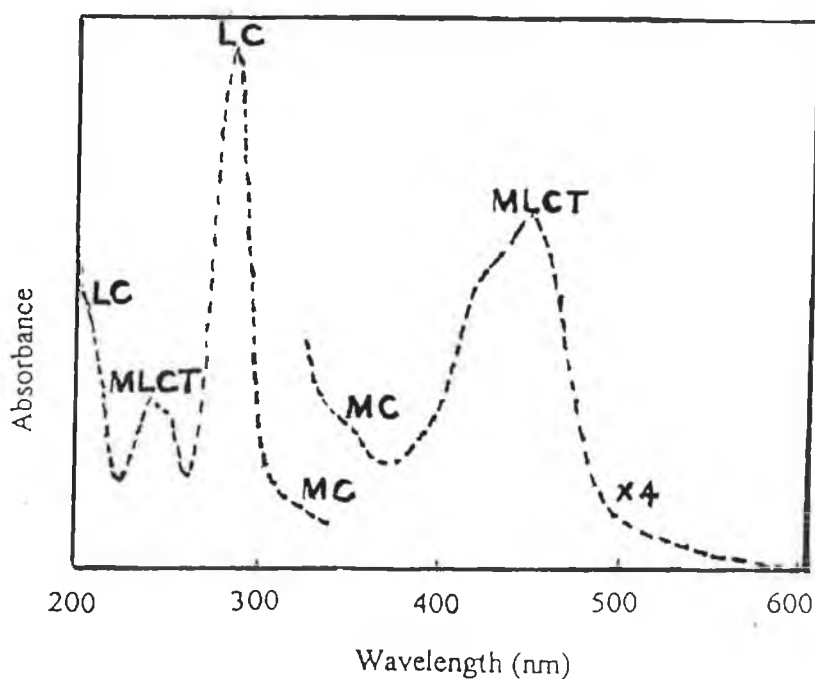
Figure 1.2 Absorption spectrum of $[Ru(bpy)_3]^{2+}$ in aqueous solution.

5
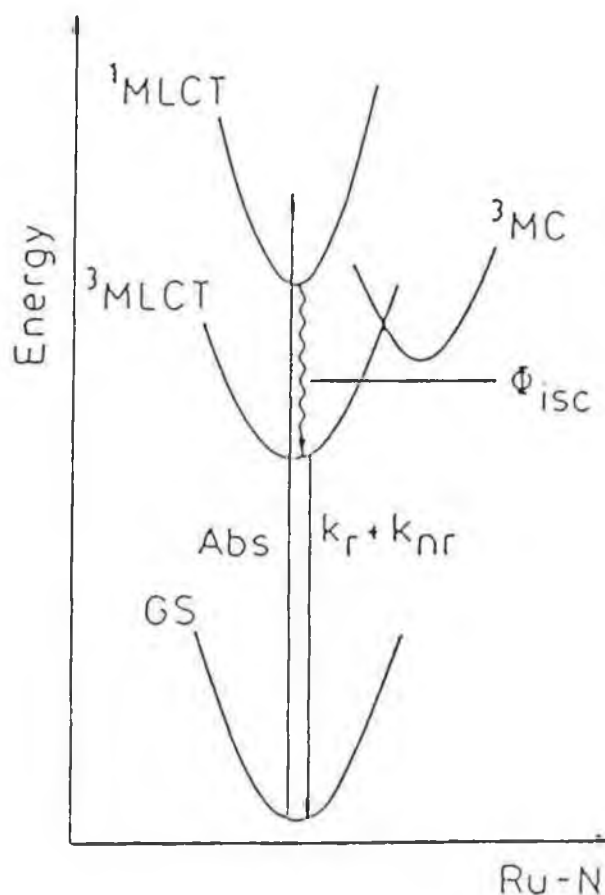
Figure 1.3 Schematic representation of the decay photophysical processes of
[Ru(bpy)$_3$]$^{2+}$.

1.3.2   Emission spectroscopy.

There has been extensive investigation into the nature and multiplicity of levels involved in the emission of ruthenium polypyridyl complexes and whether charge transfer in the electron is localised on one ligand or delocalised over all ligand orbitals. Recent results suggest that the best description is that of levels of MLCT nature which assume substantial triplet character and a single ligand localised excitation (Kober and Meyer model) [1, 14].

Figure 1.3 depicts the decay photophysical processes of $[Ru(bpy)_3]^{2+}$. It reveals how the electron is excited to a ligand centred ^{1}MLCT manifold, singlet in character. Fast intersystem crossing occurs with unit efficiency from the singlet state to the triplet manifold of three closely spaced ^{3}MLCT states, with a fourth state occurring several hundred cm^{-1} to higher energy. The three lowest lying levels are quite close together ($\Delta E \sim 100$cm^{-1}) and have predominantly triplet character, whereas the presence of the fourth MLCT state is usually masked by the deactivating ^{3}MC state [7, 14].

At higher temperatures all of these states are populated, thus contributing to the excited state decay. Hence, a broad emission band results (excited state manifold considered an average). In contrast, at low temperatures the upper states contribute very little, and so a fine spectrum is observed due to a perturbed skeletal vibration of the aromatic ring due to the removal of the π^* electron. The maximum wavelength of emission is found at higher wavelength (ie. lower energy) at room temperature compared to low temperatures. This phenomenon known as the" rigidochromic effect" is due to the relaxation of the rigid matrix perturbation [1].

Emission from the triplet state to the ground state (k_r) or radiationless decay (k_{nr}) to the ground state can take place. The ^{3}MC state is responsible for a further deactivating pathway giving rise to either radiationless deactivation or photodecomposition of the complex.

Emission intensities are stronger at lower temperatures which is explained by the energy difference (ΔE) between the emitting ^{3}MLCT state and the deactivating ^{3}MC state [7, 16-19]. At room temperature, thermal population of this ^{3}MC state is possible [8, 20] resulting in a decrease in emission intensity (ie k_r will decrease). At low temperatures, thermal population of the ^{3}MC state is not possible and so emission is more intense due to an increase in k_r. The ^{3}MC dd state lies about 4000cm^{-1} above the ^{3}CT manifold and has a high rate of radiationless decay. As well as being responsible for thermal deactivation the ^{3}MC state is accountable for photochemical reactions eg. racemisation and photosubstitution [21-23]. Non-

radiactive decay occurs less efficiently from the ^{3}CT manifold, is important at low temperatures and is dependent on the vibrational activity and on the solvent [24]. For most complexes there is a radiationless deactivation path which is somewhat "frozen" at low temperatures when the solvent matrix is rigid, but which only becomes important when the solvent matrix becomes "fluid" at room temperature [25].

1.3.3   Temperature dependence of emission lifetime.

Temperature dependence studies of luminescence behaviour can yield information concerning energy, electronic nature and deactivation rates of the luminescent and reactive states.

The main features concerning the temperature dependence of the luminescence decay of $[Ru(bpy)_3]^{2+}$ are as follows [26];

(a) an Arrhenius type behaviour in the rigid glass region (84-100K);

(b) a discontinuity in the glass fluid transition region (~100-150 K) ;

(c) an Arrhenius type behaviour in the 150-250 K temperature range having basically the same parameters as in the rigid glass and ;

(d) another steeper Arrhenius type region for temperatures over 250 K.

Equation 1.1 given below describes this complex behaviour, where $K_{0'}$ is a temperature-independent term;

$$\frac{1}{\tau} = K_{0'} + \frac{Bi}{1 + \exp[C(1/T - 1/T_b)]} + A_1 e^{-\Delta E1/RT} + A_2 e^{-\Delta E2/RT} \qquad (1.1)$$

8

Consequently, the lifetimes of many polypyridyl complexes of Ru(II) in fluid solution are highly temperature dependent, with the lifetimes expressible as the sum of a temperature independent and several temperature dependent terms, as outlined in equation 1.1.

The second term in equation 1.1 describes the behaviour in the glass-fluid transition while the two exponential terms account for the Arrhenius behaviour at low and high temperatures. Emission of $[Ru(bpy)_3]^{2+}$ and related complexes originates from a group of closely spaced MLCT levels with similar decay properties. On melting of the matrix, large amplitude vibrational modes play a part, enhancing the rate of radiationless deactivation processes, thereby resulting in a decrease in intensity and lifetime. On complete melting of the glass, the slightly activated Arrhenius behaviour continues because the emission always originates from the same group of MLCT excited states. As earlier mentioned, a ^3MC excited state, which lies about $4000cm^{-1}$ above the emitting levels becomes accessible at higher temperatures. As it is strongly distorted relative to the ground state, it undergoes fast radiationless decay including ligand substitution and racemisation reactions. The fourth MLCT excited state at several hundred cm^{-1} higher than the other three levels, with mainly singlet character, is not involved in the temperature dependence behaviour as it is " masked " by the surface crossing to the ^3MC level [1, 26]. Figure 1.4 represents the temperature dependence of $[Ru(bpy)_3]^{2+}$ in nitrile solution.

1.3.4   *Chemistry and quenching reactions of the $[Ru(bpy)_3]^{2+}$ excited state.*

On absorption of a photon by a molecule in any photochemical or photophysical process the excited state formed is a high energy unstable species which must undergo some type of deactivation process. Excited state deactivation can occur in a number of ways, as illustrated in Figure 1.5.
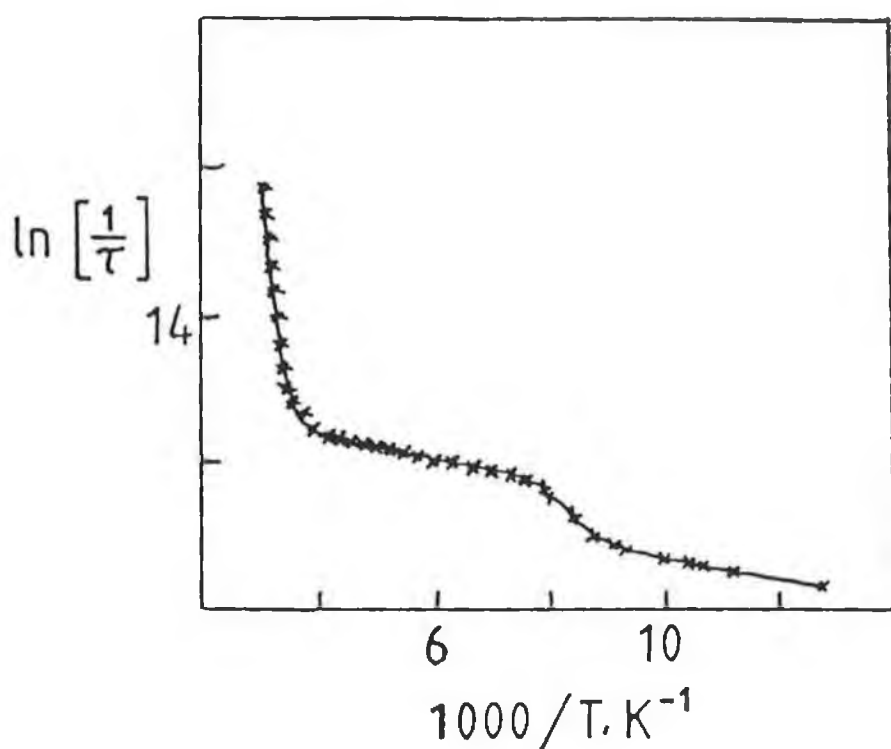
Figure 1.4 Temperature dependence behaviour of [Ru(bpy)₃]²⁺ in nitrile solution.

Deactivation may occur via several processes including the following;

 (i) the disappearance of the original molecule after undergoing some photochemical reaction ;

 (ii) the emission of light as luminescence;

 (iii) the degradation of the excess energy into heat (radiationless deactivation);

 (iv) Some type of interaction with other species present in solution (quenching).
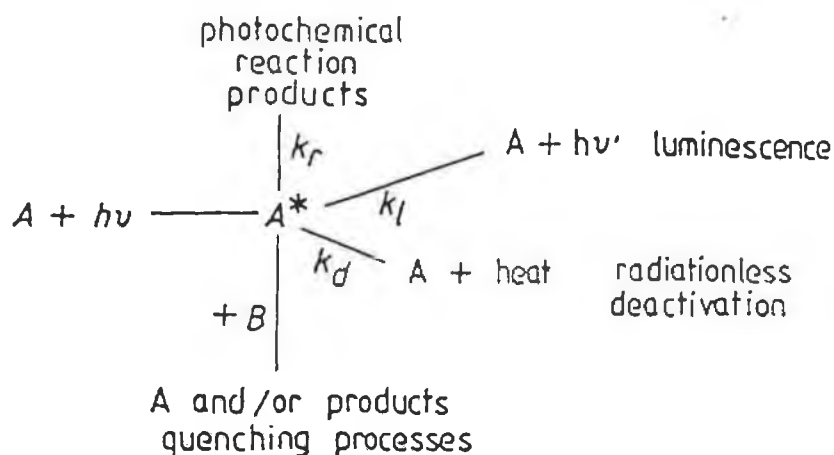
Figure 1.5 Schematic representation of the excited state deactivation processes.

Processes involving radiationless deactivation, quenching or photochemical reactions compete with the luminescence decay process of the excited state. A sufficiently long lived excited state may become involved in energy and electron transfer processes in fluid solution (ie. an encounter with a molecule of another solute and interacting bimolecularly, leading to quenching of the excited state.) This is true of the lowest excited state of $[Ru(bpy)_3]^{2+}$ (^{3}MLCT) which lives long enough for such encounters to take place. It also possesses suitable properties to play the role of energy donor, electron donor or electron acceptor.

11

(i) $*[Ru(bpy)_3]^{2+} + Q$ ------> $[Ru(bpy)_3]^{2+} + Q*$ (1.2)

(ii) $*[Ru(bpy)_3]^{2+} + Q$ ------> $[Ru(bpy)_3]^{3+} + Q^-$ (1.3)

(iii) $*[Ru(bpy)_3]^{2+} + Q$ ------> $[Ru(bpy)_3]^+ + Q^+$ (1.4)

The higher energy content of the excited state leads to its status as both a stronger reductant and stronger oxidant than the corresponding ground state [1]. The excited state acts as (i) an energy donor as in equation (1.2); (ii) a reductant as in equation (1.3); and (iii) an oxidant as in equation (1.4) [1, 14].

Energy transfer in equation (1.2) above is a physical process where, through contact, an excited state molecule transfers its energy to another molecule. Equations (1.3) and (1.4) above involve electron transfer from or to the excited molecule and the simultaneous oxidation/reduction of another species in solution. The ability to undergo energy transfer is related to the zero-zero spectroscopic energy E^{0-0} of the donor-acceptor pair (spectral overlap) and that of electron transfer to the redox potential. Kinetic factors are associated with the activation energy (E_a) needed to re-organise the inner/outer shells, before electron transfer can occur [2].

The designation of quenching processes to energy transfer requires direct observation of the acceptor phosphorescence or photoreactions from the excitation into the acceptor-excited states [15]. Bimolecular quenching of the excited state of $[Ru(bpy)_3]^{2+}$ has been extensively investigated using metal ions, such as Eu^{3+}, Cr^{2+} and quinones. One such example of energy transfer for $[Ru(bpy)_3]^{2+}$ is by $[Cr(CN)_6]^{3-}$ confirmed by the phosphorescence from the chromium complex. As $[Cr(CN)_6]^{3-}$ is not easily oxidised or reduced both reductive and oxidative $*[Ru(bpy)_3]^{2+}$ electron transfer quenching by $[Cr(CN)_6]^{3-}$ is thermodynamically forbidden [1, 2, 27]. $[Cr(bpy)_3]^{3+}$ can however be easily reduced, hence oxidative electron transfer prevails over the energy transfer (hence, the application of $[Cr(bpy)_3]^{2+}$ absorption spectroscopy in flash photolysis experiments) [1, 2, 28].

Below, an example of reductive electron transfer quenching, by Eu^{2+} is displayed [29, 30].

$$[Ru(bpy)_3]^{2+} + Eu^{2+}(aqueous) \text{-----}> \ [Ru(bpy)_3]^{1+} + Eu^{3+}(aqueous) \qquad (1.5)$$

The increased absorption due to the formation of $[Ru(bpy)_3]^+$ occurs at the same rate as the luminescence emission depletion of $*[Ru(bpy)_3]^{2+}$ indicating kinetically that reductive quenching is involved [15].

The mean lifetime of an excited state is given by the following equation;

$$1/\tau = k_{obs} \qquad (1.6)$$

where k_{obs} is the decay rate constant and τ is the average lifetime of the excited state, decaying by all possible decay mechanisms, each with its own decay constant so that;

$$1/\tau = k_r + k_{nr} + k_q[Q] \qquad (1.7)$$

where k_r is the rate constant for emission, k_{nr} is the rate constant for non-radiative decay, k_q is the rate constant for bimolecular quenching with Q, a quencher (eg. $^3O_2$) and [Q] is the concentration of the quenching agent [31]. Therefore, by substitution, the Stern-Volmer equation is derived below;

$$1/\tau = 1/\tau_0 + k_q[Q] \qquad (1.8)$$

which describes the effect of a quenching agent Q in solution on the emission lifetime [31-33]. Thus, a plot (Stern-Volmer) of $1/\tau$ versus [Q] yields k_q, the bimolecular quenching rate constant (slope). Quenching of the excited state of $[Ru(bpy)_3]^{2+}$ has been widely investigated and is known to be quenched by a variety of inorganic species [1, 2].

13

Compounds containing unpaired electrons can act as efficient quenching agents, notably molecular oxygen and other paramagnetic species. These are particularly effective in removing energy from the triplet state molecules and therefore causes particular problems in phosphorescence and with molecules possessing relatively long fluorescence lifetimes. Oxygen is one of the few molecules which effectively quenches *$[Ru(bpy)_3]^{2+}$(k_q =3.3 x $10^9 M^{-1}s^{-1}$). Singlet oxygen formation by energy transfer and electron transfer mechanisms has been proposed. The lifetime of *$[Ru(bpy)_3]^{2+}$ is reduced by about a third in aerated aqueous solutions, however, bubbling with nitrogen or argon reduces oxygen quenching to less than 1% [4].

It is difficult to deduce from a single study which of the three mechanisms (eqn1.2-1.4) is responsible for quenching. One can clarify which process is responsible for Stern-Volmer behaviour by examining the dependence of the quenching constants (k_q) for a given quencher on the excited state reduction potential of a series of closely related Ru(II) polypyridyl complexes. A dependence indicates quenching by electron transfer while the absence of any dependence suggests quenching by energy transfer mechanisms [15].

1.4. Interactions of ruthenium polypyridyl complexes with biomolecules.

1.4.1 Metal-DNA Interactions.

The design of molecules targetted specifically for DNA sites is important as DNA molecules contain all the genetic information necessary for cellular function [34]. The control or regulation of what genetic information is expressed on a chemical level must depend upon the binding of proteins or small molecules to specific sites along the DNA strand. There is much interest in understanding how this recognition process takes place, how the DNA structure varies along the strand to direct specific binding at some sites and not others and what factors determine this specificity in

binding. Hence, in recent years extensive research has been carried out in this field in attempts to produce analogues to these DNA binding proteins in order to better understand such highly specific recognition processes.

DNA binding molecules can interact in both a noncovalent and covalent manner. They tend to interact noncovalently in the following ways;

(a) by full intercalation where the molecule is inserted between the hydrophobic base pairs of DNA and is subsequently stabilised through π-stacking ;

(b) Hydrophobic/electrostatic/hydrogen bond interactions leading to binding to the minor or major groove and ;

(c) external binding on the surface of the helix.

The various binding modes of DNA binding molecules to DNA are illustrated in Figure 1.6. In order for intercalation to take place the base pairs of the helix must separate and the helix must unwind in order to accomodate the planar intercalator, one necessity for intercalation being that the intercalative moiety is flat [35]. Intercalation is the most common mode of binding of small spectroscopic probes such as ethidium and small drugs like antimycin to DNA. Significantly, intercalating compounds can be useful as probes of DNA structure as the aromatic chromophore of the intercalating cation can provide a sensitive handle to monitor conformation and flexibility of the helix [35].

Many intercalators show antibacterial or anticancer activity and because the inserted residue often resembles a base pair in shape and thickness, intercalators are commonly frame shift mutagens [36]. Several natural antitumour antibiotics, for example, daunomycins contain planar aromatic moieties and their pharmacological activity originates in particular from their ability to intercalate into DNA [37, 38]. Significantly, metal complexes are uniquely suited for specific interaction with DNA, binding in both covalent and noncovalent manners. Their shapes, charges and propensity for binding to nucleic acid sites have rendered their co-ordination com

15

plexes suitable as probes to examine DNA structure and potentially useful reagents in site-specific drug design [37].
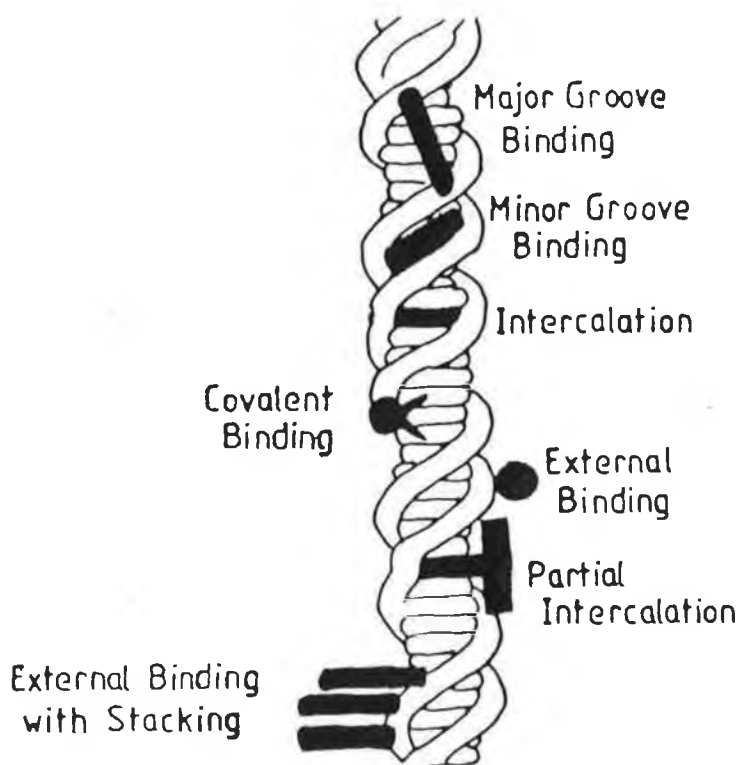
Figure 1.6. Schematic representation of the available binding sites of DNA.

Co-ordination complexes offer unique well-defined geometries useful in designing reagents to match specific local DNA conformations. The high redox activity of many metal complexes can also be exploited in directing chemistry at specific sites along the DNA strand. Furthermore, the inorganic photochemistry of certain cationic transition metal complexes may be harnessed to render them useful for footprinting and mapping experiments in-vitro and in-vivo [37]. The co-ordination about the metal centre with easily varied ligands and stereochemically well-defined geometries further allows one to match structure of the anchored inter

calator to the local shape of the DNA helix, and hence the intercalative binding mode is particularly important in their use as DNA probes [38].

The formation of metal complex-DNA adducts can have a significant effect on the biological function of DNA, as verified by the antitumour drug cis-platin of the structural form $Pt(NH)_3Cl_2$ [38]. DNA binding drugs commonly exert their activity by altering DNA structure either by covalent modification, forming adducts which inhibit DNA processing enzymes, or by the introduction of lesions that irreparably damage DNA [38]. Electron transfer reactions of metal complexes offer pathways for the oxidative cleavage of DNA structure and will be subsequently discussed in this literature review.

Lippard and co-workers were among the first to discover that metal complexes could intercalate into DNA and RNA. [39] Initial studies were carried out on the square planar platinum(II) complexes containing aromatic terpyridyl or phenanthroline ligands. Generally, charged tetra co-ordinated planar platinum complexes were found to intercalate into DNA whereas the neutral dichloroplatinum complexes could bind covalently to DNA through co-ordination to its nitrogen bases [39].

Methidium-Fe(II)-EDTA reagents have been reported as both well characterised planar intercalators and DNA cleaving agents [40], while recently the cleavage of DNA by electrochemical activation of Mn^{III} and Fe^{II} complexes of meso-tetrakis(N-methyl-4-pyridiniumyl)porphine was reported [41]. Non-planar metal complexes such as tetrahedral zinc complexes $[Zn(phen)Cl_2]^{2+}$ and $[Cu(phen)_2]^{1+}$ were also found to bind to and cause efficient strand cleavage to DNA [40, 42, 43].

Covalent binding may also take place as in addition to the harder phosphate anion sites along the backbone which the cationic metals interact electrostatically with, the endocyclic nitrogen lone pairs on the purines and pyrimidines provide favourable sites for coordination to transition metal ions and particularly so for the softer heavier metal. In fact, DNA is an extremely good ligand for metals, hence the clinical success of the simple coordination complex cis-dichloro-diammine platinum(II) ie. cis-DDP. This complex acts as an antitumour drug whose mode of ac-

17

tion involves direct co-ordination of cis-DDP to neighbouring guanines through their N-7 nitrogen atoms, hence forming intrastrand crosslinks [38, 44].

Octahedral transition metal (Ru, Zn, Co, Rh) polypyridyl complexes can also interact with DNA/RNA via both covalent and noncovalent modes [40, 42, 43] and extensive studies involving probes and cleaving agents for DNA in recent years has involved such complexes, in particular those of Ru.

Covalent attachment to biomolecules is particularly relevant in this thesis as all the binding methods used lead to covalent bond formation between the protein/polypeptide molecules and the ruthenium(II) polypyridyl complexes. Nevertheless, much of the literature in this thesis reviews the non-covalent interactions between ruthenium polypyridyl complexes and biomolecules, in particular the electrostatic and intercalative binding modes to DNA.

As the aim is to review DNA-ruthenium polypyridyl interactions, firstly the specific advantages and unique properties these complexes possess, in addition to those listed in general for transition metal complexes must be discussed. Then, their applications as probes and cleaving agents of DNA will be discussed, firstly in regard to their chirality and their use as probes for DNA handedness and then in relation to their use as sensitisers for the photocleavage of DNA. It is also necessary to discuss the effects of binding on the physical properties of DNA as well as on the spectroscopic properties of the complexes, in order to appreciate how exactly these complexes work as such sensitive probes. Finally, the use of certain ruthenium complexes as anticancer agents, in terms of their effect on DNA is discussed.

1.4.1.1 Ruthenium polypyridyl-DNA interactions.

$[Ru(bpy)_3]^{2+}$ is a prototype example of a polypyridyl complex and interactions of such complexes with biomolecules have been widely studied over recent years, in

18

particular their interactions with DNA and polynucleotides, which have been the subject of active investigation and much controversy of late.

Ruthenium polypyridyl complexes are rigid, planar, chiral and contain a co-ordinately saturated metal ion at their core. These features are critical to their application as DNA binders and photocleavage reagents but are also applicable to most transition metal polypyridyl complexes [40, 42]. However, ruthenium polypyridyl complexes display intense MLCT absorption in the visible region which significantly is distinct from where biomolecules absorb (UV region) and hence the spectroscopic properties of the biopolymer do not interfere with those of the label, and in the case of DNA binding, it provides a spectroscopic tool to monitor the binding process [1, 45]. Also, other critical properties include the intense emission they display, the large Stokes shift they possess, and the long lived luminescence emission they exhibit, with room temperature lifetimes in aqueous solution of 100-600ns [1]. Furthermore, these complexes possess a redox active site essential for the ability to act as DNA photocleaving molecules [40, 43].

Ru(II) complexes, as for other octahedral transition metals, can bind covalently and noncovalently to DNA [43]. The common feature is the incorporation of planar aromatic ligands which can interact noncovalently, intercalatively and electrostatically with biomolecules. Covalent linkage to DNA has also been reported using ruthenium phenanthroline compounds [46]. Extensive investigations have been carried out studying the effects of various ligands on the mode of binding and the extent of changes in the bound ruthenium complexes photophysical properties, among other factors affecting DNA binding [47-55].

Intercalative binding leads to perturbation of the photophysical properties of ruthenium complexes such as emission lifetime, intensity and steady-state polarisation due to the close approach of the metal complex to the helix on sandwiching one of the ligands between the adjacent base pairs. Several methods of recognising the intercalative mode of binding exist based on the following basic features of this binding mode [51, 52];

19

(a) the helix becomes stretched and unwound at each binding site which can
be followed using electrophoretic mobility assays;

(b) the helix is stabilised upon intercalation which becomes evident by
increases in melting temperature of DNA;

(c) the probe becomes oriented due to being held rigidly coplanar with the
DNA base, and for these effects fluorescence depolarisation and anisotropic
effects are used to indicate the retention of polarisation of emitted light only
if intercalation occurs;

(d) the spectroscopic properties of the probe are affected by intercalation.

In brief, the techniques used to study such binding modes are either based
on the physical changes the DNA undergoes or the spectroscopic changes one sees
in the probe [56]. Using several of these monitoring techniques, initial studies led to
the distinction between intercalators, a prime example being $[Ru(phen)_3]^{2+}$ and
external binders such as $[Ru(bpy)_3]^{2+}$, the differences being attributed to the insuf-
ficient π electron overlap provided by the bipyridine ligand for effective intercala-
tion into the DNA base pairs. Certain mixed complexes which exhibit intermediate
behaviour include $[Ru(bpy)_2(phen)]^{2+}$ and $[Ru(bpy)_2(DIP)]^{2+}$ [48, 53]. However,
in recent years the exact mode of binding of $[Ru(phen)_3]^{2+}$ has become a very
controversial subject and is discussed in greater detail in the following section.

Studies of various $Ru(L-L)_3$ complexes and their mixed complexes have
concluded that maximum intercalating ability is acquired with a ligand of greater
capacity to stack and overlap with base pairs and that binding affinity increases
with increasing hydrophobicity of the ancillary ligands. Also for complexes which
bind appreciably, enantiomeric selectivity is observed (Section 1.3.1.2.) [51]. For
most complexes, binding to DNA leads to enhancement of luminescence, probably
due to an increase in the average lifetime of the complex upon binding to DNA and
also to the protection of the complexes excited state from oxygen [48]. Multi-

20

exponential decay behaviour is observed for these bound complexes, with two decay components, one much longer and the other shorter than the unbound species. While the longer lifetime is probably the composite of similar decays from the complexes when bound to different base sequences, externally and intercalatively, the nature of the shorter lifetime is more uncertain. In contrast, the luminescence quenching of $[Ru(TAP)_3]^{2+}$ when bound to DNA is explained by photoredox interaction with guanines (See section 1.3.1.3.) [47, 48].

2,2'-bipyridyl

(bpy)

4,7-diphenyl-1,10-phenanthroline

(DIP)

1,4,5,8,9,12-hexaazatriphenylene (HAT)

3,4,7,8-tetramethyl-1,10-phenanthroline (TMP)
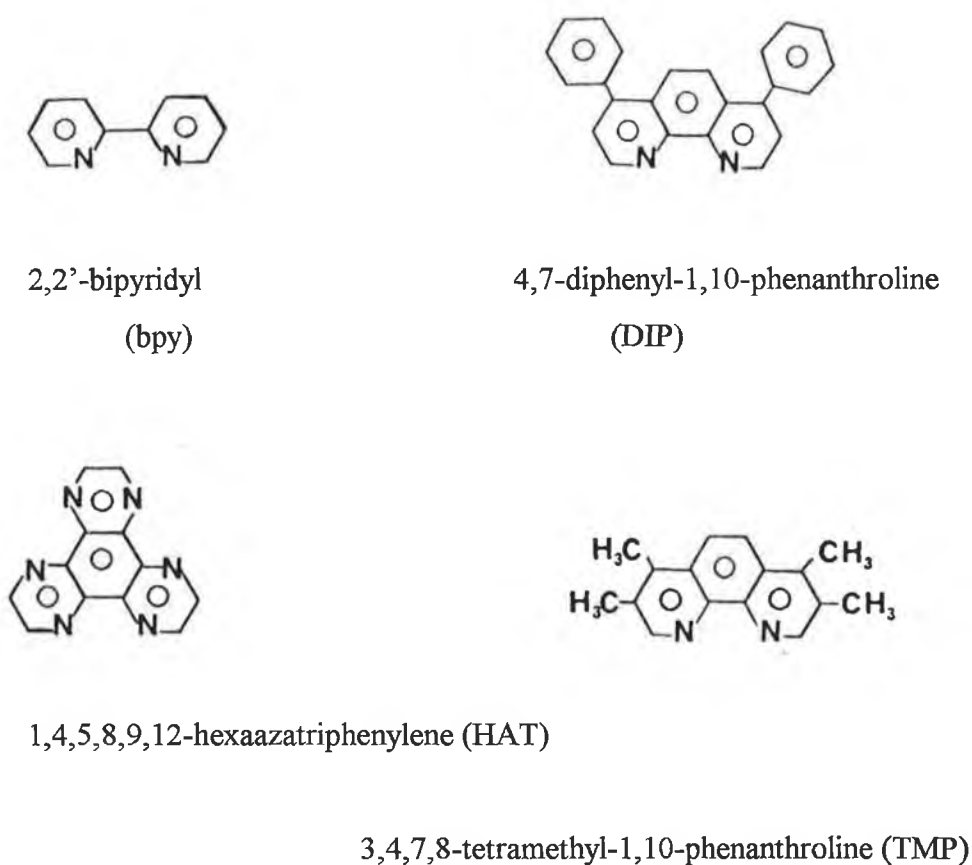
Figure 1.8. Structures and abbreviations of ligands cited in the text.

The nature of interactions of homoleptic and heteroleptic Ru polypyridyls containing such ligands as bpy, phen, DIP, trimethylphenanthroline (TMP), tetra-azaphenanthrene (TAP) and 1,4,5,8,9,12-hexaazatriphenylene (HAT) has yielded much information on factors affecting binding to DNA and on the properties required for DNA cleavage [48, 51]. Interestingly, $[Ru(TMP)_3]^{2+}$ is the only complex, on addition of DNA not to exhibit double exponential decay behaviour and is explained in terms of its size, being too large to bind against the well defined groove of B-DNA, hence the single lifetime is that of the unbound species [47].

Of particular interest is the discovery of a ruthenium polypyridyl complex $[Ru(bpy)_2(dppz)]^{2+}$, where dppz = dipyrido phenazine, which has implications as a highly sensitive reporter molecule for double stranded DNA [56], and whose structure is depicted in Figure 1.9. This compound does not exhibit any luminescence in aqueous solution at ambient temperatures but in the presence of DNA to which it binds avidly, it exhibits intense luminescence, subsequently revealed to be due to the protection of the phenazine ring from quenching by interaction with water [56, 57]. Hence, its description as a molecular "light switch" for DNA. Work carried out by Barton and co-workers on related complexes has led to the discovery that substitutions could be made in the ancillary ligands while still maintaining the remarkable "light switch" effect. Substitution on the dppz ligand however leads to complexes which all luminesce to some degree in aqueous solution in the absence of DNA and are therefore less efficient "light switches" [57]. More recent reports describe the tethering of an oligonucleotide to a Ru(II) dipyridophenazine complex to yield a sequence specific molecular light switch since the oligonucleotide functionalised with a Ru(II)dppz complex can be used to target single-stranded DNA in a sequence specific fashion (See Figure 1.10) [58]. Hence, their potential in the development of novel hybridisation probes for heterogenous and homogenous assays.

Further studies of the interactions of enantiomeric forms of $[Ru(phen)_2dppz]^{2+}$ with DNA have been carried out [59], illustrating the increasing

attention these novel Ru(II) dppz derivatives are receiving due to their unique spectroscopic probing qualities.

In relation to covalent linkage, [Ru(phen)$_2$Cl$_2$] shares with cis-dichlorodiammine platinum(II) (cis-DDP) characteristics of both structure and reactivity [46]. Like cis-DDP the neutral [Ru(phen)$_2$Cl$_2$] contains two cis-oriented chlorine ions which are good leaving groups, allowing the chlorines to be exchanged and the metal to form covalent bonds with the base atoms of DNA. Hence, [Ru(phen)$_2$Cl$_2$] represents an octahedral analogue for cis-DDP, but one that is chiral [46].
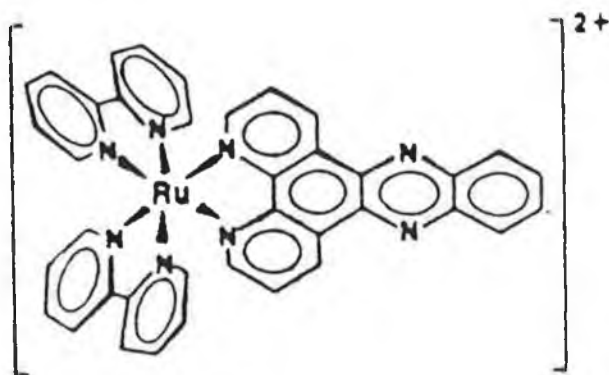
Figure 1.9. Structure of the complex [Ru(bpy)$_2$(dppz)]$^{2+}$ [56].

DNA oligomers and duplexes containing a covalently attached derivative of [Ru(bpy)$_3$]$^{2+}$ have been described [60]. These display potential as photochemically activated DNA cleavage agents, fundamental to their use in the construction of macromolecules with specifically located redox active subunits [60]. Bathophenan-

throline ruthenium complexes have also been covalently attached to DNA, and used as nonradioactive label molecules for oligonucleotides [61-63]. [Ru(TAP)$_3$]$^{2+}$ and related complexes have been receiving increasing attention of late, [55, 64] whereby evidence has been subsequently found of adduct formation between such complexes with DNA, being sufficiently oxidising to abstract an electron from guanine in DNA [64]. A recent publication describes evidence for a new kind of photochemical adduct between a metal complex and nucleotide where the binding of [Ru(TAP)$_3$]$^{2+}$ proceeds through covalent binding of the guanine to one of the TAP ligands. Initial electron transfer from the guanine to the metal complex excited state has been proposed to lead to such a compound [65].
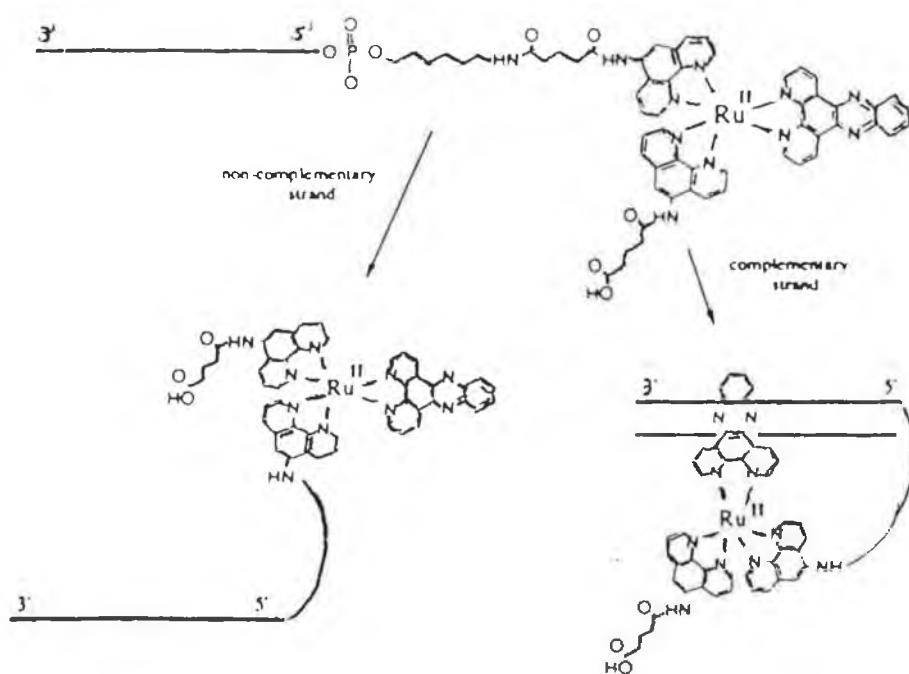
Figure 1.10. Schematic representation of the tethering of a dppz complex of ruthenium(II) to an oligonucleotide [58].

24

like three-bladed propellers and have two enantiomeric forms corresponding to right
(Δ) and left (Λ) handed screws. (See Figure 1.11) [69-72].
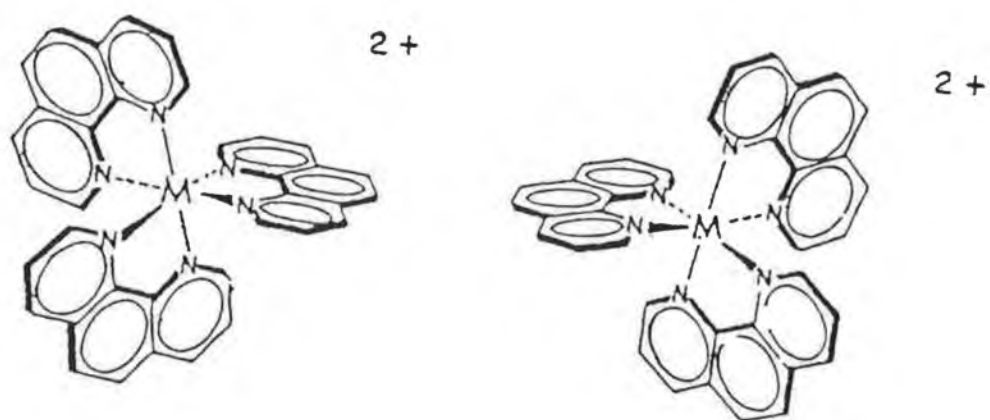
Figure 1.11. Enantiomeric forms of [Ru(phen)$_3$]$^{2+}$ [42].

In order to understand the applications of ruthenium complexes as probes for DNA structure, the distinguishing factors between the various forms of DNA A, B and Z are stressed herein. The A and B forms are right-handed helical structured DNA whereas the Z form is the left-handed DNA. The general structure of a helix is two anti-parallel polymer strands with the bases paired through Watson and Crick hydrogen bonds. B-DNA is the most predominant form and is a regular right-handed helix with the base pairs oriented basically perpendicular to the axis of the helix and contains distinctive minor and major grooves of well defined width and depth. In contrast, A-DNA has a very shallow but wide major groove and is found in double stranded RNA segments. Z-DNA zig-zags and is basically a long slender helix with a wide and shallow major groove and a minor groove pinched down into the narrow crevice. As well as these regular forms however, various structural variations can be found along the DNA strands, such as bends, kinks, left-handed sites, hairpin loops and cruciforms [73].

Originally, ruthenium polypyridyl complexes were believed to bind electrostatically to single or double stranded (ds)DNA at low ionic strength as well as intercalatively to dsDNA [73]. However due to much controversy surrounding the exact mode of binding which these complexes used as probes for DNA handedness undergo, a summary of different theories put forward will be given below.

Barton and co-workers had proposed that binding of ruthenium tris(phenanthroline) complexes occurs through two mechanisms: (1) intercalation, based on the observation that binding causes the DNA duplex to unwind, and (2) "surface" interactions [45, 52, 54, 74]. Preliminary studies involving such complexes report that on binding of the chiral complexes by intercalation enantiomeric selectivity is observed with B-DNA with the Δ-enantiomer, a right-handed propeller like structure displaying a greater affinity than Λ-[Ru(phen)$_3$]$^{2+}$ for the right handed helix [45, 52, 74]. The basis for this selectivity is illustrated in Figure 1.12. With one phenanthroline ligand intercalated, the two non-intercalated ligands of the isomer fit closely along the right-handed helical groove, while the non-intercalated ligands of

the Λ isomer are repelled sterically by the phosphate backbone of the duplex. This is because the disposition of the left-handed isomer is opposed to the right-handed helical groove of B-DNA [45].
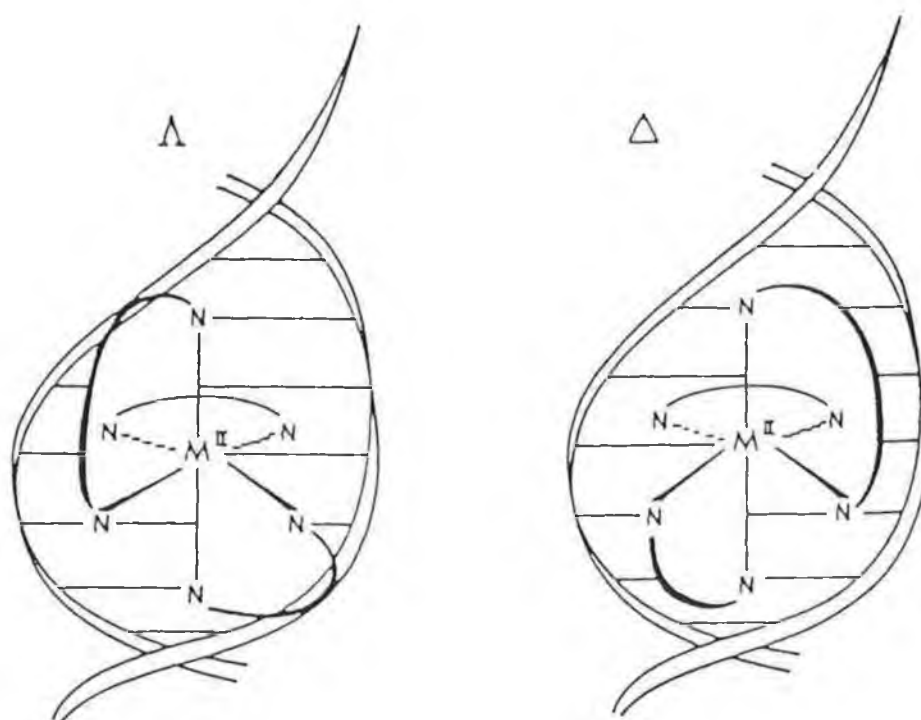
Figure 1.12. Lamda (Λ) and delta (Δ) tris(phenanthroline) metal complexes, a schematic illustration of such complexes intercalated into right-handed DNA [42].

Further studies show the isomers of $[Ru(DIP)_3]^{2+}$ to exhibit enhanced enantiomeric selectivity, with only Δ-$[Ru(DIP)_3]^{2+}$ binding to B-DNA. This is explained in terms of the increased bulkiness on the non-intercalated phenanthroline ligands which completely block the intercalation of the isomer into a right handed helix. Hence, its enantioselectivity is due to the steric effects of the phenyl " wings " of the chelate [54, 75].

The complex $[Ru(phen)_2Cl_2]$ already mentioned for its covalent binding to B-DNA has been shown to exhibit striking enantiomeric selectivity distinct from that seen on intercalation [46]. Unlike intercalation, it appears that the left-handed isomer is favoured, as is found for the groove bound mode. Similar alignment for covalent and intercalative binding is not possible as one of the non-stacked phenanthroline ligand is considerably crowded by the right-handed helical column. Further studies of such stereoselective covalent binding was recently reported by Thorp and co-workers, who investigated an extensive series of aquaruthenium(II) complexes of the type $[L_5Ru(OH_2)]^{2+}$ and $[L_4Ru(OH_2)_2]^{2+}$ [76]. These mono- and diaqua complexes are shown to bind covalently to calf thymus DNA and the results correlate well with those of Barton and Lolis on $[Ru(phen)_2Cl_2]$ [46]. The reactions proceed with a surprisingly high stereoselectivity that favours covalent binding of the Λ isomer with $[Ru(phen)_2(py)OH_2]^{2+}$ showing an enantiomeric excess of 80% [76].

One interesting application found for these "DNA handedness probes" is reported by Barton and co-workers where the potential of these complexes as probes for DNA structure in a protein-bound complex was examined [77]. The binding of the enzyme Restriction Endonuclease EcoRI to DNA is reported to alter the enantiomeric preference of the conformation-specific intercalators $[Ru(phen)_3]^{2+}$ and $[Ru(DIP)_3]^{2+}$ for DNA, providing evidence under solution conditions that binding by the restriction enzyme causes a conformational change in the DNA helix [77].

Another application is the combination of such chiral probes with DNA photocleavage properties. An example of such a complex is $[Ru(TMP)_3]^{2+}$ which shows preferential binding to A-DNA, displays enantiomeric discrimination in its binding and upon irradiation with visible light cleaves A-form helices preferentially [78] (See section 1.4.1.3).

The possibility that these compounds could only partially insert one phenanthroline ring was first raised by Barton et al. [45, 54,] and later by Kelly at al. [53], Gorner et al. [49] and Haworth et al. [79] who argued that complete insertion, as occurs with the classical intercalators ethidium and acridinium, is blocked by the two external phenanthroline rings which clash with the DNA backbone. Energy minimisation calculations revealed that each isomer has two binding modes, partial insertion (as opposed to classical intercalation) and external or electrostatic binding, with binding proposed to occur in the major groove of DNA [79]. However, Norden et al. concluded from their studies that each isomer bound to DNA by a single binding mode and that neither isomer is bound by intercalation [80] which was further supported by Eriksson et al. [81, 82] who showed that both isomers bind primarily in the minor groove. Binding is not by classical intercalation but rather involves the insertion of two phenanthroline rings into the minor groove, leading to slight distortions of DNA structure. Rehmann and Barton concluded from NMR studies that Δ Ru prefers intercalation while Λ Ru prefers surface binding [83]. Hard et al. also studied the enantioselectivity of both isomers for both right and left handed DNA, reporting their findings that Δ Ru binds more tightly to both the B and Z forms than the Λ isomer [84].

Further studies undertaken by Satyanarayana and co-workers [85, 86] provide evidence that each isomer does indeed bind to DNA via a single mode, and that neither isomer bind by classical intercalation, seen as neither enantiomer lengthens short, rod-like DNA. In fact, the binding of the isomers to DNA was shown to be entropically driven, hence the interactions are largely electrostatic in nature and therefore unlike other DNA intercalating agents. Both isomers show a

30

modest site specificity with the Δ Ru preferring GC base pairs while the Λ isomer prefers AT base pairs. Notably, however, neither isomer was found to discriminate in any significant way between B and Z DNA.

Recent studies were carried out on Ru-dppz complexes, novel structural analogues based on $[Ru(phen)_3]^{2+}$ (See section 1.4.1.) to determine their mode of binding to DNA. Such studies provide reasonable evidence for an intercalative mode of binding for both isomers although the thermodynamics of their DNA binding is unlike those observed for the proven intercalators ethidium and dauno-mycin. The Δ isomer binds to DNA approximately twice as strongly as the Λ iso-mer, which represents at best only a modest enantiomeric selectivity [59].

Based on these significant findings, the potential of ruthenium enantiomers as specific probes of DNA conformation would appear rather limited, as they bind weakly to DNA, have only a modest base specificity and cannot distinguish be-tween very different DNA conformations. Although the question of the ability of such tris-chelate metal complexes to discriminate between B and Z forms of DNA has remained debatable and details of DNA complex interactions are far from well understood, it would appear that the exciting potential that these complexes were believed to exhibit has been greatly exaggerated and their applicability is much more limited than originally anticipated.

1.4.1.3 Ruthenium polypyridyl complexes as sensitisers for DNA photocleavage.

As earlier mentioned, one means by which DNA binding drugs exert their activity is the introduction of lesions that damage DNA irreversibly. In addition to the rigid asymmetric framework provided by ruthenium coordination geometries and the spectroscopic sensitivity to assay binding through the metals electronic transitions,

31

ruthenium polypyridyl complexes can also provide a rich source of reactivity through redox chemistry. Hence, the means exist to couple modes of recognition to site-specific reactions of ruthenium polypyridyl complexes along the helix, rendering them useful in the design of specific DNA cleaving agents and drugs.

The DNA cleaving abilities of $[Cu(phen)_2]^{2+}$ and other polypyridyl complexes of Co, Ru, Rh, Pt, Fe, Cr and Mn have been realised. The investigation of ruthenium polypyridyl complexes containing bpy, bpz, phen, DIP, TMP, HAT and TAP ligands (See Figure 1.8) led to the discovery of unique complexes that bind to and photoinduce redox processes with DNA. Such novel complexes include complexes with two or more HAT/TAP ligands. This behaviour is due to their ability to oxidise guanine when bound to DNA [47, 48, 51]. Significantly, the photochemistry of $[Ru(TAP)_3]^{2+}$ (See Figure 1.13) with mononucleotides appears to follow photosubstitutions that would take place on natural DNA or synthetic polynucleotides. In such cases, the photoreactions lead to a photoanchoring of the $[Ru(TAP)_2]^{2+}$ moiety on DNA [87]. The complex Λ-$Ru(TAP)_3]^{2+}$ and $[Ru(bpy)_n(TAP)_{3-n}]^{2+}$ have been studied and have also been found to be very efficient DNA photocleavage agents [47, 48, 88].

As earlier reported, adduct formation occurs between these complexes and DNA. The radical cation of guanine (G) produced on abstraction of an electron from G in DNA appears responsible for the more efficient induction of single stranded breaks in DNA [65]. In contrast, $[Ru(phen)_3]^{2+}$, $[Ru(bpy)_3]^{2+}$ and related complexes proceed by different mechanisms ie. the mediation of the formation of singlet oxygen which results in the photocleavage of DNA [88, 89].

$[Ru(TMP)_3]^{2+}$, already discussed as a probe for DNA handedness due to its preferential binding to A-DNA, also cleaves these helical forms with enantiomeric selectivity ie. the Λ-isomer cleaves the A-form with twice the efficiency of the right-handed isomer [79].
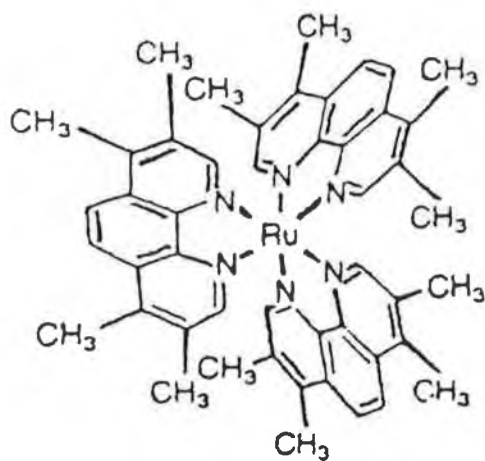
(a) $[Ru(TMP)_3]^{2+}$
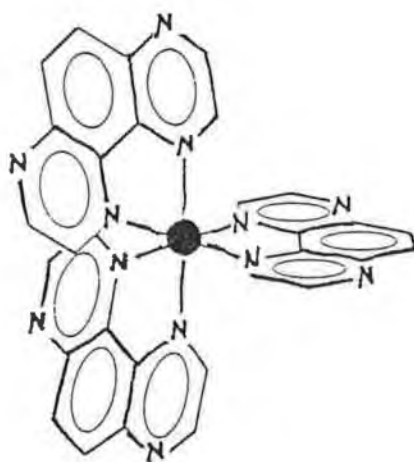
(b) $[Ru(TAP)_3]^{2+}$

Figure 1.13 Structures of the DNA photocleavage reagents (a) $[Ru(TMP)_3]^{2+}$ and (b) $[Ru(TAP)_3]^{2+}$.

The effects of $[Ru(TMP)_3]^{2+}$ and $[Ru(phen)_3]^{2+}$ on the photocleavage of tRNA have been compared, revealing that they both indeed preferentially photocleave at the guanine residues, however showing contrasting efficiencies of cleavage due to the protection of some of the guanine residues as a result of the molecular shape of $[Ru(TMP)_3]^{2+}$ [90]. Hence, these complexes may be used as probes of new tRNAs as well as being useful in the elucidation of major secondary and even tertiary structural features of other RNA molecules.

An alternative method to photosensitised DNA damage found using ruthenium complexes has been realised. This involves the damage of DNA via photosensitised radical production. $[Ru(bpy)_3]^{2+}$ bound to nucleic acids in the presence of $K_2S_2O_8$ sensitises the production of the reactive species SO_4^- and $[Ru(bpy)_3]^{3+}$ close to the strand which lead to single strand break formation [91].

A complex leading to double stranded cleavage through a metal-activated mechanism has also been reported. $[Ru(DIP)_2Macro]^{2+}$ is an analogue of $[Ru(DIP)_3]^{2+}$ with one of the three DIP ligands modified with two polyamine armlike segments that can themselves complex metal ions (See Figure 1.14). The complex binds to DNA while the two modified arms deliver complexed metal ions to each strand of the DNA helix for double stranded cleavage [92]. It effectively cleaves double stranded DNA in the presence of the redox active Cu(II) and less efficiently for the redox inactive Zn(II) [92, 93]. The metal activated cleavage by this complex may occur via nucleophilic attack at the phosphodiester backbone leading to hydrolysis of the anionic diester. Hence, the potential of such complexes as artificial restriction enzymes is indicated.

Finally, new families of DNA cleavage agents (electrocatalytic or thermal), based on oxoruthenium(IV) have been studied. Ru(II) is produced quantitatively which also binds to DNA covalently in a slow follow-up reaction [94, 95]. These active cleavage agents can be generated electrochemically or chemically via oxidation of the corresponding $[Ru(tpy)(L)OH_2]^{2+}$ complexes, where tpy = 2,2',2"-

terpyridine with only the complex where L = dipyridophenazine (dppz) intercalating classically. The excited state of $[Ru(tpy)(dppz)OH_2]^{2+}$ is not emissive in aqueous solution but does emit in the presence of double stranded DNA, thereby exhibiting the "light switch" effect earlier noted for $[Ru(bpy)_2(dppz)]^{2+}$. The cleavage reaction leads to the release of nucleic acid bases, implicating sugar oxidation as the reaction pathway. [95, 96] The majority of the binding of these complexes to DNA is non-covalent, however, over long time periods, a very small fraction becomes covalently bound to DNA via replacement of an aqua ligand by a nucleophile in DNA, presumably N7 of the guanine.

Complex binds to DNA; polyamine groups bind metal ions for cleavage of phosphodiester backbone
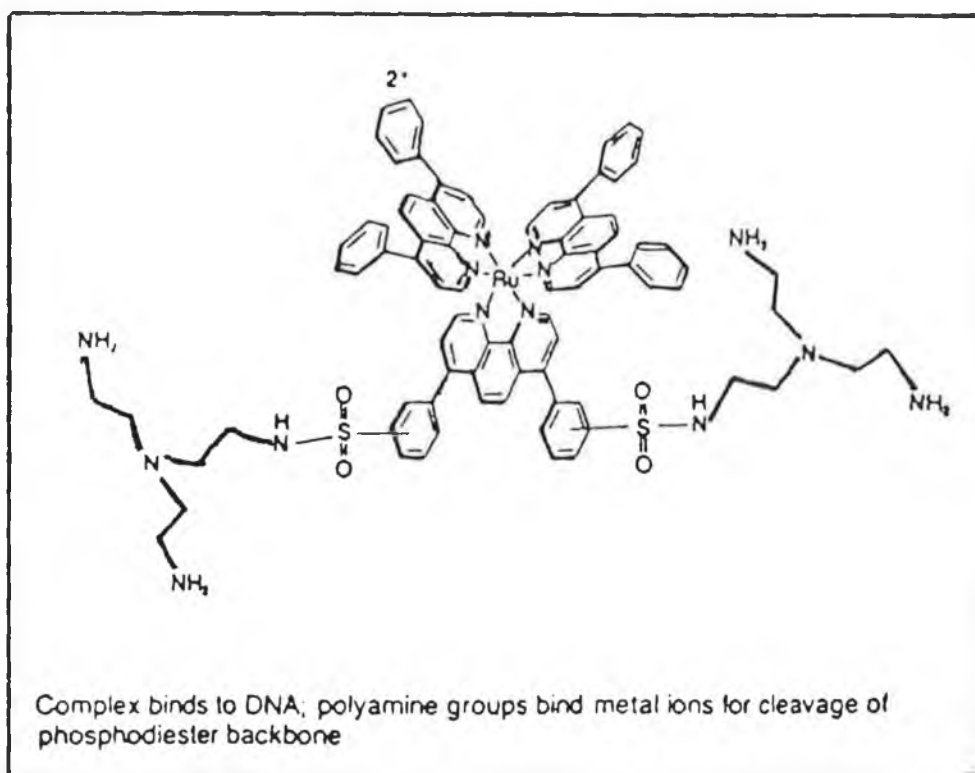
Figure 1.14. Structure of the complex $[Ru(DIP)_2Macro]^{n+}$ [92].

Since the discovery of cis-dichloro-diammine platinum(II) ie. cis-DDP as the first organometallic complex to be used in chemotherapeutic treatment of human malignant neoplasm, much research has been carried out on other transition metal complexes such as ruthenium in an attempt to find equivalent compounds, in particular with lower host toxicity levels.

Ru(II) compounds reveal similarities to the antiviral, antibacterial and antineoplastic activities of cis-DDP [97]. Since this discovery, many Ru(II) complexes have been synthesised, showing promising antineoplastic activity for application in cancer treatment. Being directly below Fe in the periodic table and existing in both the di- and tripositive oxidation states in aqueous solution, there is evidence that absorption of $[RuCl_3.3H_2O]$ into the body parallels that of iron. It is concentrated by the villi of the small intestine and then widely distributed. A portion remains in the blood for a relatively long period and may be taken up by the plasma protein transferrin because like Fe(III), Ru(III) has a high affinity for phenolate ligands which are involved in the transferrin-Fe binding site. Rapidly growing cells such as those in neoplasms have a high iron requirement and hence have a large number of receptors for transferrin. Release of Ru(III) from transferrin may be facilitated by cellular reduction to Ru(II) which then separates and binds to cellular structures, while the transferrin is free to migrate back out of the cell. Thus, the chemistry of specific ruthenium complexes leading to their accumulation in tumours is an important factor in their use as anticancer agents [98a].

The target molecule for ruthenium containing anticancer agents appears to be DNA. Besides intercalation, as already discussed, smaller complexes or those with shapes unsuitable for intercalation are more likely to attach to the surface of DNA either through electrostatic or Van Der Waals forces. Unlike the square planar geometry of the active form of platinum anticancer drugs, these Ru ions are usually six coordinate with octahedral structures. The two additional coordination sites allow

new modes of binding to nucleic acids and with some ligands provide for the chirality in the complexes and so in their interactions with the DNA helix.

In addition to binding to DNA, many complexes can interfere with nucleic acid metabolism in some way or other. In vitro studies have demonstrated that Ru(II) and Ru(III) compounds are active in inhibiting DNA synthesis and possess mutagenic activity [98a]. Several mechanisms which have been suggested, following the preferential binding to G7 sites include the following ;

(1) the failure of replicating enzymes to recognise the metallated G;

(2) additional metal binding following or inducing helix disruption;

(3) Subsequent protein intra- or inter-strand crosslinking by the metal;

(4) chemical reactions of the guanine residue induced by the presence of the metal ion;

(5) Fenton's chemistry occurring at the metal ion to generate radicals capable of strand cleavage;

Ruthenium compounds with nitrogen ligands localise in tumour tissue as well as exhibiting good antitumour activity. These ligands undergo solvent mediated ligand substitution in aqueous solution and the nitrogen ligands possess sufficient strength to remain intact following electron transfer. Such complexes with applications as " prodrugs ", introduced into the organism as Ru(III) or Ru(IV) with nitrogen and acido ligands remain fairly stable to substitution as long as these oxidation states are maintained. Upon reduction to a lower oxidation state, the metal immediately loses the acido ligand and engages in rapid exchange of water molecules at the open site. Consequently, tissue binding is favoured in areas low in oxygen and high in reductants, such as the reducing hypoxic environment of many tumours where reduction but not reoxidation of Ru should produce a higher Ru(II)/Ru(III) ratio than in the surrounding more aerated tissue [98a].

The complex fac-$[Ru(NH_3)_2Cl_2]$ was among the first discovered to display excellent antitumour activity, however its poor solubility precludes it from adequate

formulation as a drug [98b]. Because of this, complexes with one or two fewer nitrogen ligands and one or two more halides were developed to arrive at species which are more soluble due to their anionic charge. Although the mechanisms of action involved are not clear, complexes of the form cis-$[X_2L_4Ru]X$, $[X_3L_3Ru]$ and $M[X_4L_2Ru]$ give promising results, where X = Cl or Br, L = NH_3 or a nitrogen heterocycle and M = any monopositive cation.

Of the more recent water soluble complexes coordinated with heterocyclic ligands in the trans position $HB[(RuB_2Cl_4)]$ and the corresponding pentachloro derivatives $(HB)_2[(RuBCl_5)]$ have been identified as the most active antitumour agents. Their general structural forms are presented in Figure 1.15. Representatives of this class are $[RuIm_2Cl_4]$ and $[RuImCl_5]$ where I = imidazole ring, shown in Figure 1.16. The antitumour activity of $ImH(RuIm_2Cl_4)$ [99, 100b] and $ImH_2(RuImCl_5)$ [100a] has been investigated and reveal promising properties for clinical use including a non-toxic treatment of colorectal tumours.
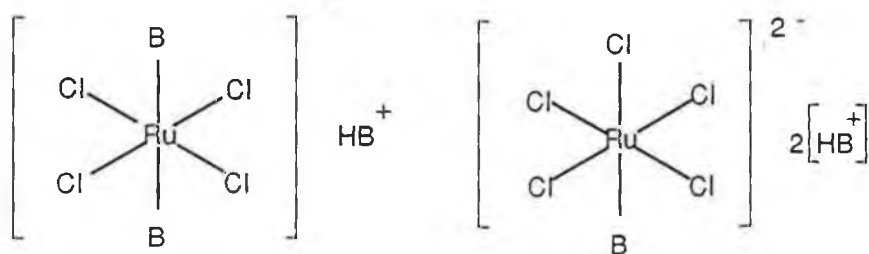
Figure 1.15. Structures of complexes HB[RuB₂Cl₄] and 2HB[RuBCl₅] where B= nitrogen heterocycle.

38

Another branch of tumour inhibiting complexes is cis-dichlorotetrakis (dimethylsulfoxide) ruthenium(II) and related compounds [101]. Despite its octahedral geometry and absence of amino ligands, this complex presents some interesting resemblances to cis-[Pt(NH$_3$)$_2$Cl$_2$] such as neutrality, two cis-chloride ligands, high stability of 2+ oxidation state and a high affinity for nitrogen donor ligands [102]. Furthermore, DMSO is known to cross the cell membrane easily while the complex is quite soluble in water.

ImH(RuIm$_2$Cl$_4$) (ImH)$_2$(RuImCl$_5$)
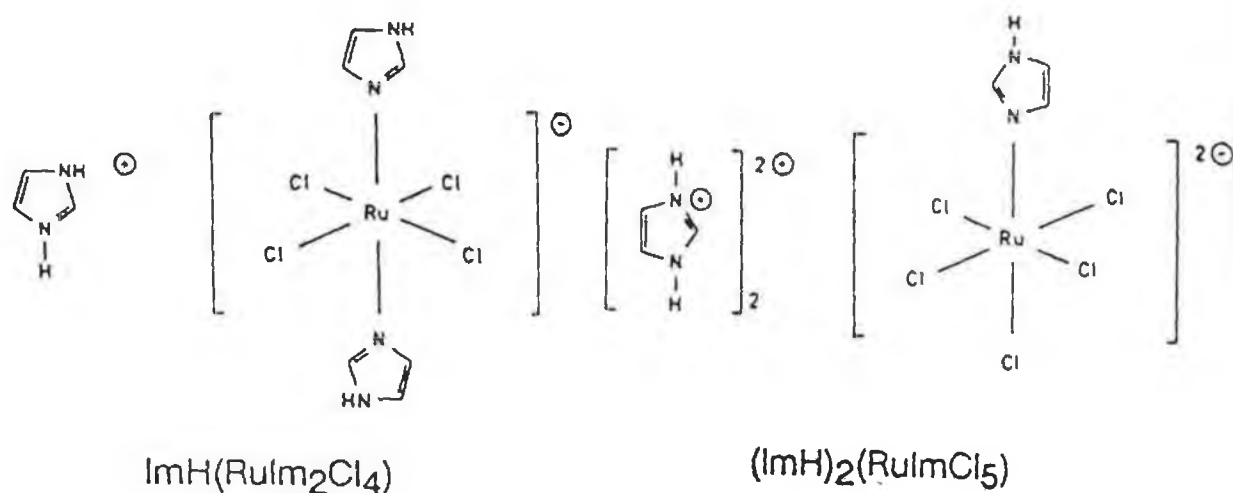
Figure 1.16. Structures of the complexes RuIm$_2$Cl$_4^-$ and RuImCl$_5^{2-}$ where Im=Imidazole ring.

In vitro studies of cis- and trans-[RuCl$_2$(DMSO)$_4$] have suggested that N7 of the guanine is the major target of the cis-complex when binding to DNA. The trans isomer also covalently binds to DNA but with a markedly higher reaction rate and leads to marked modification of calf thymus DNA structure. The progressive destruction of the ordered DNA structure could be related to the formation of bi-functional adducts along the chain. The trans isomer appears to have a remarkably higher reactivity than the cis isomer, due to differences in their structures. [98c] In vivo studies reveal both isomers to possess mutagenic activity against bacterial strains, with the trans form less so, while exhibiting a higher cytotoxicity and mutagenic activity when tested against a eucaryotic system [98c].

Experimental results indeed show that Ru(II) DMSO complexes possess a significant antitumour and antimetastatic activity, also exhibiting interesting therapeutic potential when combined with surgical amputation of the primary tumour [101-103]. NMR structural characterisation of the reaction product between trans [RuCl$_2$(DMSO)$_4$] and d(GpG) has been carried out revealing the formation of a stable compound characterised by a covalent bifunctional coordination of the bases to the metal centre [104]. The compound displays structural features similar to those exhibited by the corresponding cisplatin complex, indicating that such a way of interaction with DNA is not exclusive to Pt or to metals with square planar coordination geometries. The anti-metastatic effect of the trans isomer is of the same order as that obtained with an equitoxic dosage of cis-DDP.

The promising antimetastatic activity displayed by a related complex Na[trans-RuCl$_4$(DMSO)Im] reported recently [105], as well as another novel complex trans HInd[RuCl$_4$(Ind)$_2$] [106] indicates the possibility that related complexes may represent a new generation of antitumour compounds capable of selectively interacting with metastasis formation of solid tumours. The structures of some interesting Ru-DMSO complexes are illustrated below in Figure 1.17.

The increasing attention ruthenium complexes are receiving as anticancer agents stresses the exciting potential they hold in this area and is yet another significant application of the interaction of ruthenium complexes with DNA.
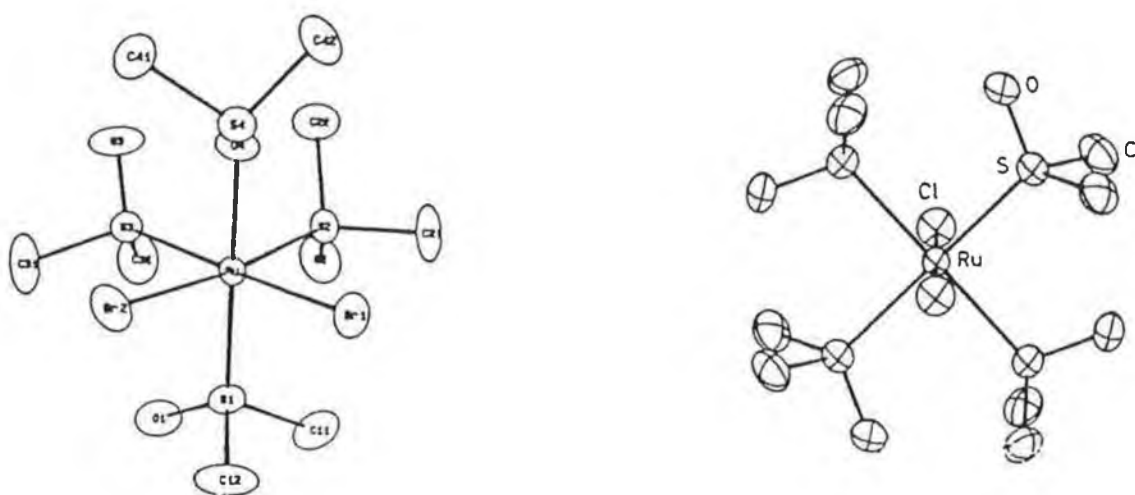
Figure 1.17. Ortep drawing of (a) cis-Ru(DMSO)₄Cl₂ and (b) trans-Ru(DMSO)₄Cl₂ with the atom labelling scheme.

1.4.2. Study of Biological Electron Transfer Reactions.

The study of rates and mechanisms of electron transfer reactions is fundamental to understanding many vital processes as several important biological processes involve series of electron transfer reactions that are very efficiently controlled. An under-

standing of how electrons are transferred over large distances is therefore essential to the characterisation of fundamental redox processes in biology, such as oxidative phosphorylation and photosynthesis. Consequently, the study of intramolecular electron transfer across rigid and flexible polypeptides, proteins and DNA in solution has received much attention in recent years.

The active sites of the electron transfer centres only make up a small percentage by weight of the total electron transfer protein, indicating that the surrounding protein may play a major role in modulating the properties of these electron transfer centres, such as structural changes where the polypeptide chain allows specific protein-protein interactions by direct electron transfer.

In order to obtain new information on the kinetics and mechanisms by which electron transfer proteins operate, the electron transfer redox reactions of cytochrome c, iron-sulfur proteins and copper blue proteins have been studied using various small molecule reagents including $[Cr(OH_2)_6]^{2+}$, $[Fe(phen)_3]^{2+}$, a series of substituted $[Co(phen-X)_3]^{n+}$, and notably $[Ru(NH_3)_6]^{2+}$ and related complexes [107-111].

The efficiency of electron transfer has been suggested to be attenuated by proteins, membranes and other biological structures [107, 108]. Studies of electron transfer involving the interior of structurally characterised metalloproteins modified with pentammine ruthenium complexes have shown that electron transfer can occur over large distances through protein interiors [109, 110]. Such factors as donor-acceptor distance, thermodynamic driving force and the nature of the intervening medium were deemed critical in determining rates of electron transfer.

Ruthenium complexes have been attached to surface histidines of structurally characterised proteins, including cytochrome c, myoglobin derivatives and hemoglobins, so as not to modify the structure of the native protein. From these studies, it is apparent that the effects of the structure of the intervening medium (specific conformation between donor and acceptor groups) and the orientation of the donor-

acceptor unit on electron transfer are far less understood than other factors such as solvent environment and distance [109-115].

Beratan, Onuchic and coworkers have examined the effects of protein structure on distant electronic couplings via the pathway analysis of various protein electron-transfer reactions [116]. Although such theoretical methods contain the minimal description needed to adequately model the basic mechanisms of protein-mediated electron tunnelling, it makes reasonable predictions about primary, secondary, tertiary and quaternary structural effects on electron transfer rates. Measurements of electron transfer rates in ruthenium-modified proteins have been carried out to test the methods reliability [116].

Electron-tunnelling in ruthenium-modified cytochrome c has been reported whereby the rates and the couplings correlate well with the lengths of sigma-tunnelling pathways comprised of covalent bonds, hydrogen bonds and through space jumps from the histidines to the heme group [117]. Site directed mutants of human myoglobin [Mb], an oxygen-storage protein have been prepared in order to investigate the electron transfer in ruthenium zinc porphyrin derivatives of recombinant human myoglobins, so as to compare this to the data obtained for Ru-modified cytochrome c [118, 119].

The characterisation of a Ru-modified derivative of the [2Fe-2S] ferredoxin FdI component of *A. variabilis* by attachment of $[Ru(NH_3)_5]^{3+}$ to a surface histidine has been carried out [120]. Ferredoxins isolated from higher plants and algae are involved in redox processes including those related to photosynthesis and are characterised by a one electron redox change. Such results further correlate with the theory that the electron transfer is indeed highly sensitive to the intervening protein medium, but the exact role that the protein matrix plays in mediating the electron transfer process is not well understood [119, 120].

Electron transfer across polypeptides has also been studied, by studying electron transfer in osmium-ruthenium binuclear complexes bridged with oligoproline peptides [121, 122]. Significantly, these are suitable as rigid chemical spacers in studies of long-range intramolecular electron transfer as a function of

distance between donor and acceptor. The results reveal that rapid rates of electron transfer across polypeptides can be observed for a metal-to-metal separation of > 20 Å [121].

A report by Mecklenburg discusses the photoinduced electron transfer in amino acid assemblies [123], where various combinations of donor, acceptor and chromophores to yield multifunctional amino acids and peptides are constructed in order to explore excited-state electron transfer in such amide-based complexes [123].

In addition to various proteins, DNA is used as a biological medium through which long range electron transfer is investigated. Barton and co-workers have studied several donor-acceptor systems, including Ru(II) and Co(II) polypyridyls, which undergo photoinduced electron transfer. From these systems, the role of the DNA double helix in mediating electron transfer has been investigated and various aspects of the DNA environment, such as local electrostatic fields, hydrophobic patches, lipophilic interactions and the dimensionality of space surrounding the double helix have been monitored [124-126]. A reduced dimensionality in diffusion of DNA-binding proteins appears to be a major factor contributing to their ability to rapidly locate sequences along the DNA. Firstly, stereoselective electron transfer in the presence of DNA is reported [124]. Due to the long range of movement and decreased dimensionality, the electron transfer rates are greatly enhanced in the presence of DNA, with the DNA essentially acting as a catalyst of electron transfer [124].

Further reports by Barton suggest that the apparent rate enhancement in the presence of DNA could be due to a combination of factors including (1) the increase in local concentration of bound donor-acceptor pairs; (2) facilitated diffusion of the bound pair along the DNA helix in a reduced dimensional space and; (3) long range electron transfer between donor and acceptor pairs with DNA as the intervening medium [125]. The more mobile surface-bound ruthenium complex promotes long range transfer with greater efficiency than the intercalated species, despite the closeness of the intercalated form to the extensive framework of the

stacked bases. Hence, the efficiency of electron transfer apparently depends upon the binding mode, ie. the orientation of donor and acceptor on the biopolymer, as well as upon the electronic states of donor and acceptor, and how well these electronic states couple with the intervening DNA [125].

Rapid photoinduced electron transfer over a distance of greater than 40 Å between metallointercalators, a donor $[Ru(phen)_2dppz]^{2+}$ and acceptor $[Rh(phi)_2phen]^{3+}$ that are tethered to a DNA duplex have been reported [126]. Significantly, complete quenching is observed only when the acceptor is covalently bound to the same duplex as the donor, indicating that the intervening DNA helix facilitates the donor-acceptor interaction despite the large distance separating the metallointercalors on the helix [126].

Meade and coworkers have recently reported a novel approach of preparing ruthenium-modified duplex DNA derivatives, where the donor and acceptor are separated by any number of base pairs [127]. (See Figure 1.18.) The stacked aromatic heterocycles of the DNA duplex apparently serve as an efficient medium for coupling electron donors and acceptors over very long distances, indeed comparable to distances found in biological systems [126, 128]. Furthermore, the electronic coupling between donor and acceptor for modified DNA derivatives appears to display a remarkable dependence on nucleic acid sequence [128].

In brief, the many publications concerning the use of ruthenium complexes in the study of electron transfer across biological materials are indicative of the heightened interest in this field in recent years, and the exciting potential ruthenium complexes hold in the study of such natural biological processes.
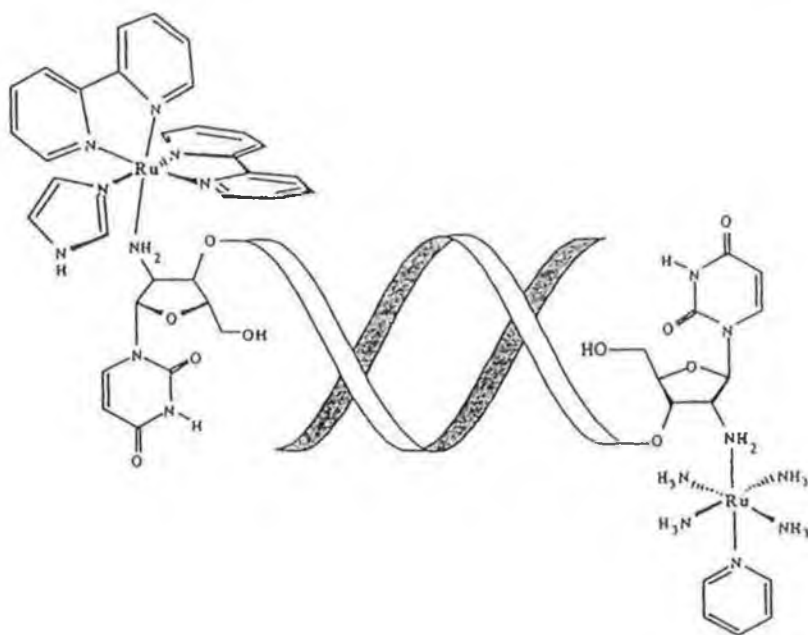
Figure 1.18. Schematic representation of duplex DNA labelled with ruthenium based donors and acceptors [127].

1.4.3. Chemiluminescent reactions with biological compounds.

During the early studies of ruthenium complexes of the form $[Ru(L-L)_3]^{3+}$, where L = bpy or phen, the most striking behaviour observed was their ability to undergo chemiluminescent reduction. Addition of acidic solutions of $[Ru(L-L)_3]^{3+}$ to aque-

ous NaOH solution results in orange chemiluminescence, clearly visible in a dimly lit room. Further studies of Ru(II) and Ru(III) compounds revealed that Ru(II) complexes also exhibit intense luminescence emission and that the chemiluminescent spectrum obtained from the Ru(III) complexes is fundamentally identical to the luminescence spectra for its Ru(II) equivalent compounds.

$[Ru(bpy)_3]^{3+}$ can react with a variety of compounds, including oxalate and other organic acids to yield chemiluminescence, thereby allowing the detection of such compounds. [129, 130] The detection of oxalate has biological significance, particularly in medical analysis, as high concentrations of oxalate in the blood accompany a number of maladies including renal failure, vitamin deficiencies and intestinal diseases.

Chemiluminescence (CL) is observed when part of the energy of an exothermic chemical reaction is released as light. This occurs between oxalate and $[Ru(bpy)_3]^{3+}$ with a rather specific electron transfer. The mechanism of the reaction is as described below.

$$[Ru(bpy)_3]^{2+} \quad\quad ----> \quad [Ru(bpy)_3]^{3+} + e- \quad\quad (1.9)$$

$$[Ru(bpy)_3]^{3+} + C_2O_4^{2-} \quad ----> \quad [Ru(bpy)_3]^{2+} + C_2O_4^{-} \quad\quad (1.10)$$

$$C_2O_4^{-} \quad\quad\quad ----> \quad CO_2 + CO_2^{-} \quad\quad (1.11)$$

$$CO_2^{-} + [Ru(bpy)_3]^{3+} \quad ----> \quad CO_2 + [Ru(bpy)_3]^{2+*} \quad\quad (1.12)$$
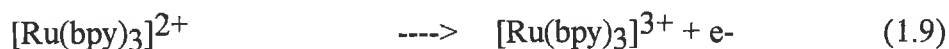
Alternatively, $[Ru(bpy)_3]^{2+*}$ may be produced as follows;

$$CO_2^{-} + [Ru(bpy)_3]^{2+} \quad ----> \quad CO_2 + [Ru(bpy)_3]^{+} \quad\quad (1.13)$$

$$[Ru(bpy)_3]^{+} + [Ru(bpy)_3]^{3+} ----> \quad [Ru(bpy)_3]^{2+} + [Ru(bpy)_3]^{2+*} \quad (1.14)$$

47

Above is an example of electrogenerated chemiluminescence where the reaction between electrogenerated $[Ru(bpy)_3]^{3+}$ and oxalate yields luminescence in aqueous solution. The key factors in the production of the excited state are the large free energy change associated with the rapid electron transfer reactions (1.11) and (1.14) and the production of a strong reductant, CO_2^- by oxidation of oxalate $(C_2O_4^-)$. These unique factors contribute to the specificity of the reaction. Intense orange emission results when the excited state decays to the ground state. The emission intensity is shown to be directly proportional to the concentration of oxalate, thereby rendering $[Ru(bpy)_3]^{3+}$ a useful probe for oxalate in biological matrices [130].

A more recent application for $[Ru(bpy)_3]^{3+}$ involves the chemiluminescence detection of amino acids, peptides and proteins [131]. The sensitive detection of over 20 amino acids, some peptides and a few proteins has been studied with the flow injection analytical technique. Amino acids generally are not well suited for detection without prior derivatisation due to the absence of a strong chromophore, whereas the $[Ru(bpy)_3]^{3+}$ reagent has the potential to be generated in line prior to the detection cell, which can make the system more rugged and easy to use. Hence, the advantages of using chemiluminescence reagents such as $[Ru(bpy)_3]^{3+}$ includes fast reaction kinetics, a high reaction efficiency to enhance selectivity and the capability of reacting directly with amino acids thereby increasing sensitivity.

The observed CL for the reaction of $[Ru(bpy)_3]^{3+}$ with amines is related to the first ionisation potential of the non-bonding orbital of the nitrogen atom. The observed CL results from the formation of an amine radical by reaction of the amine with $[Ru(bpy)_3]^{3+}$. The radical then reacts with a second $[Ru(bpy)_3]^{3+}$ ion, producing an excited $[Ru(bpy)_3]^{2+*}$, which subsequently decays to the ground state with the emission of a photon [131]. A similar mechanism has been proposed for the reaction with amino acids and is revealed below [132].

48

$$H_3N^+CHRCOO^- \quad + \quad OH^- \quad ----> \quad H_2NCHRCOO^- \qquad (1.15)$$

$$H_2NCHRCOO^- \quad + \quad [Ru(bpy)_3]^{3+} \quad ---->$$
$$H_2N^+CHRCOO^- \quad + \quad [Ru(bpy)_3]^{2+} \qquad (1.16)$$

$$H_2N^+CHRCOO^- \quad + \quad [Ru(bpy)_3]^{3+} \quad ---->$$
$$NH{=}CRCOO^- \quad + \quad [Ru(bpy)_3]^{2+*} \quad + \quad 2H^+ \qquad (1.17)$$

$$[Ru(bpy)_3]^{2+*} \quad ----> \quad [Ru(bpy)_3]^{2+} \quad + \quad h\nu_{600} \qquad (1.18)$$

$$NH{=}CRCOO^- \quad + \quad H_2O \quad ----> \quad RCOCOO^- \quad + \quad NH_3 \qquad (1.19)$$
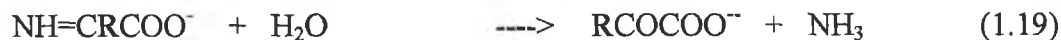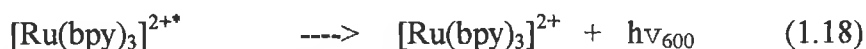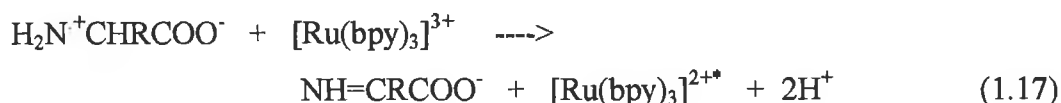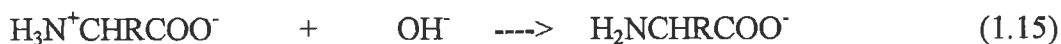
Brune and co-workers have investigated the effect of pH on the reaction of $[Ru(bpy)_3]^{3+}$ with amino-acids and found this to be the key experimental parameter in the application of this reaction as a detection technique [132].

Early studies of the oxidation of amino acids suggest that the reactive species is the anion of the amino acid. If so, the reaction should be faster at pH values $> pK_a$ of the N-terminal amine of the amino acid. In accordance with this, the maximum chemiluminescence signal for amino acids occurs at pH values above pH 7. In fact, optimum chemiluminescence emission is observed between pH 10 and 11 (where a significant percentage of the amino acid exists in anionic form). A background reaction between the hydroxide ion and $[Ru(bpy)_3]^{3+}$ is observed to be less pH-dependent and does not occur with the same efficiency as the amino-acid reaction and hence does not limit this technique. An example of results found are for glutamic acid whose $pK_a = 9.2$ (See Figure 1.19). At pHs more than pH 8, the reaction occurs with greater facility than with the hydroxide ion and therefore, chemi-

49

luminescence increases dramatically over the pH range 9-11. This system is very sensitive with a detection limit of about 30 pmole found for valine.

It was further concluded from these initial studies that the presence of peptide bonds may not be essential for peptide or protein detection rendering such a technique feasible for some peptides and proteins including insulin, myoglobin and ribonuclease, as studied by Danielson and co-workers [131].
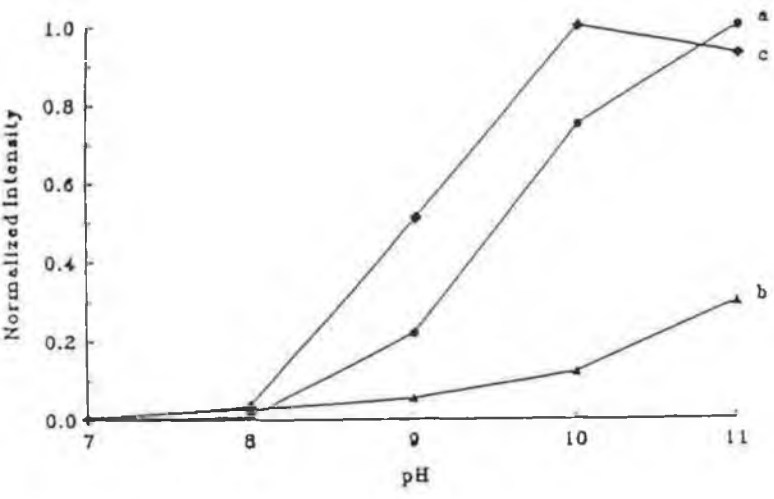
Figure 1.19. pH Dependence of Chemiluminescence of Glutamic Acid [132]. (a) Background-corrected glutamic acid signal; (b) background signal from OH⁻ reaction; (c) signal to noise ratio (SNR) obtained from (a) and the noise measured on (b).

More recent studies were carried out, again by Brune and co-workers on the role of electron-donating/withdrawing character, pH and stoichiometry on the chemiluminescent reaction of $[Ru(bpy)_3]^{3+}$ with amino acids [133]. According to Brune, electron-withdrawing R groups tend to decrease chemiluminescence (ie. alcohols, serine and threonine) while electron-donating R groups have the opposite effect (ie. alkyl side chains, leucine and valine) A postcolumn chemiluminescent technique for the detection of underivatised amino acids indicates the potential of such a system following a protein digest. As smaller amounts of protein are being isolated for sequencing, new and improved methods for separating and detecting the amino acids are constantly in demand and hence its implications in protein sequencing.

In such systems, the chemiluminescence derived from such a technique should be directly proportional to the quantity of amino acid present, the method should have a wide dynamic working range and it should be sensitive to the detection of all amino acids. The characteristics of the $[Ru(bpy)_3]^{3+}$/amino acid reaction, consequently render it suitable. The reaction of aliphatic tertiary amines using the chemiluminescence reagent $[Ru(bpy)_3]^{3+}$ has also been applied to the detection of antibiotics such as clindamycin and erythromycin [131].

Downey and Niemen have studied the chemiluminescence detection of NADH using $[Ru(bpy)_3]^{3+}$ immobilised on a Nafion film, this being the first research carried out concerning NADH detection using $[Ru(bpy)_3]^{3+}$ electrochemiluminescence [134]. NAD^+ is required to catalyse enzyme reactions of dehydrogenases, while NADH is produced by the enzyme reaction, the amount being related to the substrate concentration (hence substrate concentration can be determined by measuring NADH concentration). Recent reports have been made on the construction of a flow injection analysis system for a reduced form of nicotamide adenine dinucleotide (NADH) by electrogenerated chemiluminescence using $[Ru(bpy)_3]^{3+}$ [135]. Such a system has significant advantages, in particular its

simplicity as only $[Ru(bpy)_3]^{2+}$ is needed as a reagent since its chemiluminescence requires no enzymes for NADH determination.

Finally, the electrogenerated chemiluminescence (ECL) yielded from the oxidation of $[Ru(phen)_3]^{2+}$ at a gold electrode in the presence of oxalate has been used to characterise the nature of the interaction of the Ru(II) chelate with calf thymus DNA [136]. The decrease in ECL emission from the excited state, $[Ru(phen)_3]^{2+*}$, in the presence of DNA has been attributed to the binding of the chelate to the DNA strand. Detection of luminescence is possible with high precision, and compared to voltammetric and spectrophotometric measurements, very low concentrations of complex can be used ie. micromolar to nanomolar [136].

1.4.4 Covalent linkage of ruthenium polypyridyl complexes to proteins.

In our last section aimed at discussing the usefulness of ruthenium polypyridyl com plexes, the covalent linkage of ruthenium based labels with proteins will be the main concern. In order to fully understand the reactions carried out, and to visualise where on the proteins the labels are bound to, a brief discussion of the reactive groups of proteins and how these labels couple to form stable covalent bonds is essential.

1.4.4.1 Reactive groups of proteins [137-139].

Proteins/peptides are amino acid polymers containing a number of reactive side chains which can be used to attach reporter molecules. Under appropriate conditions, each reagent normally reacts only with the indicated target side chain(s). Depending on the protein, the reagent and the particular conditions, however, complete modification of all such side chains is not always obtained.

As well as, or as an alternative to these intrinsic reactive groups, specific reactive moieties can be introduced into the polymer chain by chemical modification, whereby these groups serve as " handles " for attaching a wide variety of molecules. Conjugation usually involves binding to the amino side-chains, in particular the ε-amino group of lysines, the phenolic moiety of tyrosines, the carboxyl groups of glutamate and aspartate and the sulphydryl groups of cysteines. As a general rule, modifications that have the least effect on side-chain character should have the least effect on protein structure and properties. Modifications of lysine residues that retain their usual cationic charge, for example, generally have relatively little effect on the biological activities and other properties of many proteins. However, a lack of specificity of the reactions is a common feature.

One of the most reactive groups of a protein is the aliphatic ε-amine of the amino acid lysine. Lysines are usually present and are often quite abundant while, among the 20 or so amino acid side chains normally present in proteins, ε-amino groups of lysine residues are usually among the most common and most accessible of the potentially reactive groups. Lysine amines are good nucleophiles above pH 8 (pKa = 9.18) and therefore, react cleanly and easily with a variety of reagents to form stable bonds. The α-amino groups of the N- terminal amino acid are also reactive, are less basic and so are reactive at approximately pH 7.0. Sometimes they can be modified selectively, in the presence of lysines. There is usually at least one α-amino acid in a protein, and in the case of proteins that have multiple peptide chains or several subunits, there can be more. Therefore, the most commonly used method of protein modification is through these aliphatic amine groups.

$$\text{Protein-NH}_2 \quad + \quad RX \quad \longrightarrow \quad \text{Protein-NHR} \quad + \quad HX. \qquad (1.20)$$

Proteins contain carboxylic acids at the COO^- terminal position and within the side chains of the amino acids aspartine and glutamine. Due to their low reactivity in water, thay are usually converted into reactive esters by use of a water soluble carbodiimide, when used in the selective modification of proteins, and then

reacted with a nucleophilic reagent such as an amine or hydrazide (See equation 1.21.).

$$\underset{\text{Prot}}{\text{Prot}}\ \overset{\text{O}}{\underset{\|}{\text{C}}}-\text{OH} \longrightarrow \text{Prot}\ \overset{\text{O}}{\underset{\|}{\text{C}}}-\text{OX} \quad + \quad \text{RNHNH}_2 \longrightarrow \text{Prot}\overset{\text{O}}{\underset{\|}{\text{C}}}\text{NHNHR}$$

$$(1.21)$$
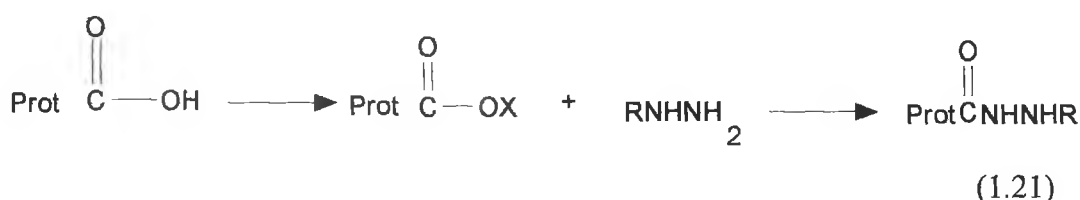
The amine reagent should be weakly basic so as to react specifically with the activated carboxylic acid in the presence of the other amines on the protein, as protein cross-linking can occur when the pH is raised to above pH 8.0, i.e. when the protein amines are partially unprotonated and reactive. Hence the suitability of hydrazides, which are weakly basic, in coupling reactions with carboxylic acids.

Another common reactive group in proteins is the thiol residue from the sulphur containing amino acid cystine and its reduction product cysteine, which are counted together as one of the 20 amino acids. Cysteine contains a free thiol group, which is more nucleophilic than amines and is generally the most reactive functional group in a protein. It reacts with some of the same modification reagents as for amines and can also react with reagents that are not very reactive towards amines. Thiols, unlike most amines, are reactive at neutral pH, hence they can be coupled to other molecules selectively in the presence of amines, as described in equation 1.22.

$$\text{NH}_2\text{-Protein-SH} + \text{RH} \quad \text{-------}> \text{NH}_2\text{-Protein-SR} + \text{HX} \quad (1.22)$$
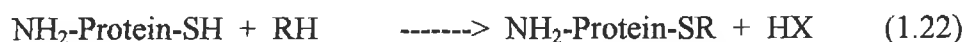
This selectivity makes the thiol group suitable as a linker for coupling two proteins together, as other methods only coupling amines may result in the formation of unwanted products, such as homodimers and oligomers. In the absence

54

of cysteine, some proteins also have the amino acid methionine. Since selective modification of methionine is difficult to achieve, it is seldom used to attach small molecules to proteins.

Chemical modification of other amino acid side chains has not been extensively used. The high pK_a of the guanidine functional group of arginine (pK_a = 12-13) requires more drastic reaction conditions than most proteins can survive. Also, tryptophan modification requires harsh conditions and is rarely used except as a method of analysis in structural or activity studies.

1.4.4.2. Protein modification reagents [139].

Reactive groups may also be introduced by chemical modification. The basic principles for understanding how to use such reagents are (1) the recognition of the reactive groups on the protein that can be modified; (2) knowledge of the type of chemical reactions these reactive groups will take part in; and (3) the nature of the chemical bonds that will result from these reactions.

Amine reactive reagents react primarily with lysines and the α-amino groups of proteins and peptides under both aqueous and nonaqueous conditions. The choice of amine modification reagent chosen for a reaction depends upon the reactivity and specificity required for that specific protein. Fluorochromes which modify these groups include the isothiocyanates, succinimidyl esters, isocyanates and sulphonyl halides (chlorides).

Reactive esters, for example N- hydroxysuccinimide (NHS) esters are very common reagents used for the modification of amines, with high selectivity towards aliphatic amines. The aliphatic amide products formed are very stable (optimum pH 8-9) and the reaction scheme is described in equation 1.23. The NHS esters formed are slowly hydrolysed by water but are stable to storage if kept well dessicated. Almost all molecules that contains a carboxylic acid or that can be chemically modified to contain a carboxylic acid can be converted into NHS esters, as shown

55

in equation 1.24, thereby rendering these reagents among the most powerful protein-modification reagents available.

$$\text{Protein-NH}_2 \quad + \quad \text{RC-O-N} \overset{O}{\underset{O}{\text{(ring)}}} \quad \longrightarrow \quad \text{Protein-NHCR} \quad + \quad \text{HO-N} \overset{O}{\underset{O}{\text{(ring)}}}$$

(1.23)

$$\text{RCOH} \quad + \quad \text{HO-N} \overset{O}{\underset{O}{\text{(ring)}}} \quad \overset{DCC}{\longrightarrow} \quad \text{RCON} \overset{O}{\underset{O}{\text{(ring)}}}$$

(1.24)
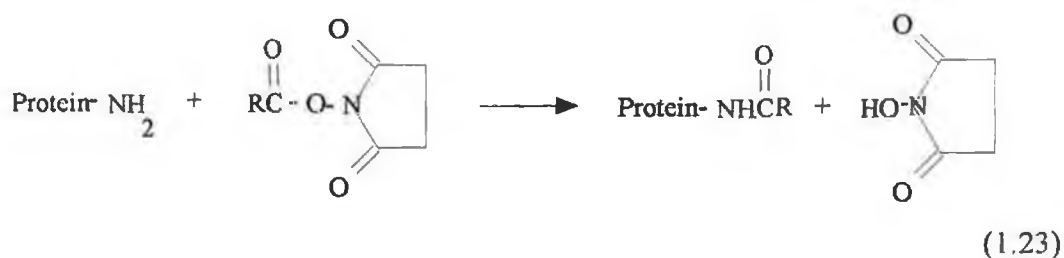
Isothiocyanates are other amine modification reagents of intermediate reactivity, forming thiourea bonds with proteins and such a reaction procedure is outlined in equation 1.25. They are more stable in water than the NHS esters and react with protein amines in aqueous solution at optimum pHs 9.0-9.5 . Due to this high pH, isothiocyanates may not be as suitable as NHS esters when modifying proteins that are sensitive to alkaline pH conditions.

56

$$\text{Prot}-\text{NH}_2 \quad + \quad \text{RN}=\text{C}=\text{S} \quad \longrightarrow \quad \text{Prot}-\overset{\overset{\text{S}}{\|}}{\text{NH}-\text{C}}-\text{NHR}$$

$$(1.25)$$
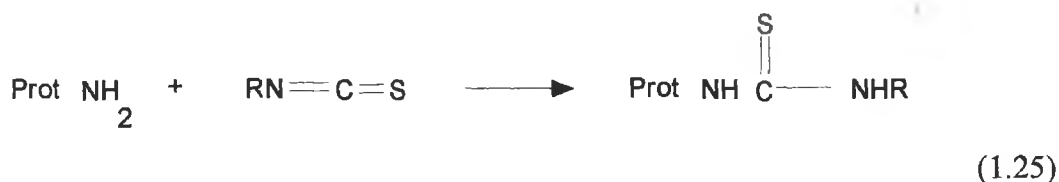
Aldehyde groups can also react with aliphatic and aromatic amines under mild aqueous conditions to form an intermediate known as a Schiff base, which can be selectively reduced by the mild reducing agent , such as sodium cyanoborohydride to give a stable alkylamine bond. This method, however, is not as frequently used as the activated ester method. Equation 1.26 below describes the reaction procedure involved.

$$\text{Prot}-\text{NH}_2 \quad + \quad \text{RCH}=\text{O} \quad \longrightarrow \quad \text{Prot}-\text{N}=\text{CHR} \quad \xrightarrow{\text{NaBH}_3\text{CN}} \quad \text{Prot}-\text{NHCH}_2\text{R}$$

$$(1.26)$$
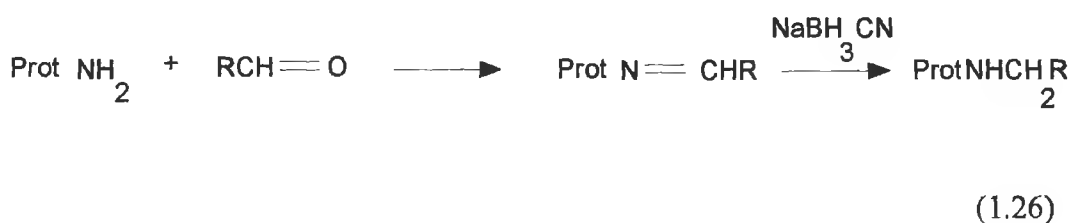
Sulphonyl halides are other highly reactive amine-modifying reagents. Although unstable in water, they form very stable sulfonamide bonds. As well as amines, sulfonyl halides also react with phenols (tyrosine), thiols (cysteine) and imidazoles (histidine) on proteins and are less selective than either the NHS esters or isothiocyanates.

Thiol reactive reagents which couple to thiol groups on proteins to give thioether-coupled products, react rapidly at neutral pH and can therefore be reacted with thiols selectively in the presence of amine groups. Examples include haloacetyl derivatives and maleimides, both which react with cysteine groups to form thioether bonds.

Other important modifications are carboxylic acids and aldehyde reactive reagents. One such example are amines and hydrazides which can be coupled to carboxylic acids of proteins via the activation of the carboxyl group by water soluble carbodiimide followed by reaction with an amine or hydrazide leading to stable amide bonds (See equation 1.27).

$$
\text{Protein -} \overset{\overset{\displaystyle O}{\|}}{\text{COH}} \quad + \quad RN = C = NR' \quad \longrightarrow \quad \text{Protein-}\overset{\overset{\displaystyle O}{\|}}{C}\,OC = NR
$$
$$
\text{HNR'}
$$

$$
\overset{\displaystyle R''NH_2}{\longrightarrow} \quad \text{Protein-}\overset{\overset{\displaystyle O}{\|}}{C}\,NHR'' \quad + \quad RNH\,\overset{\overset{\displaystyle O}{\|}}{C}\,NHR' \quad (1.27)
$$
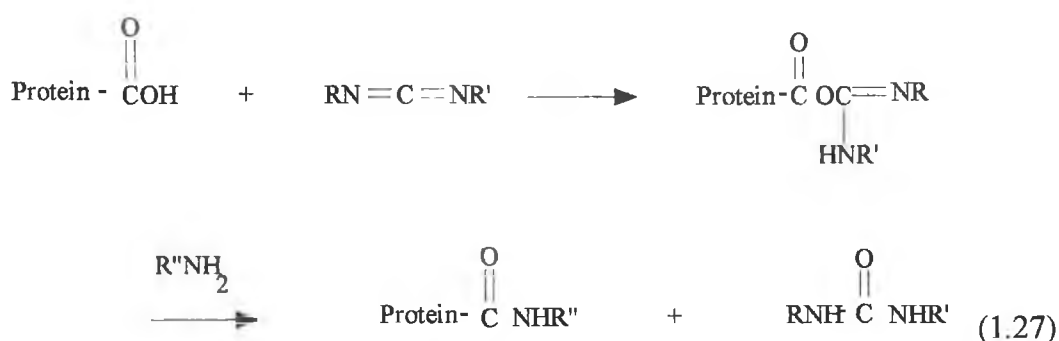
Amines and hydrazides can also react with aldehyde groups which can be generated on proteins by periodate oxidation of the carbohydrate moieties of the proteins. A Schiff base intermediate is formed which can be reduced to an alkylamine by reaction with $NaBH_4$, a mild and selective water soluble reducing agent. This reaction procedure is outlined below in equation 1.28.

$$
\text{Prot- gly} \quad + \quad NaIO_4 \quad \longrightarrow \quad \text{Prot CH} = O \quad \longrightarrow \quad \text{Prot CH}_2 NHR
$$
$$
(1.28)
$$
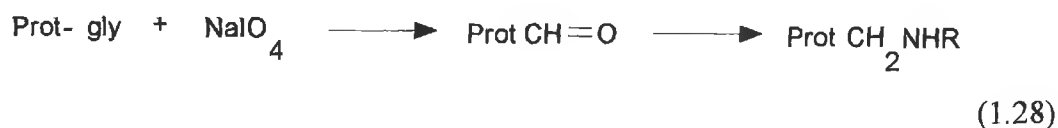
Much work has been carried out involving covalent linkage of ruthenium complexes to biomolecules and their use as probes of the systems in question. However, such applications will be discussed in greater detail in Chapter 4 where

our work involves similar probing studies and conjugation reactions. A summary of unusual applications found for ruthenium-modified biomolecules is given to demonstrate the broad applicability of such complexes in biological matrices.

1.4.5 *Diverse ruthenium-protein applications.*

Varied miscellanous applications have been found for ruthenium complexes, when bound to natural proteins, such as enzymes and antibodies, ranging from stabilising agents to their use as models of novel drugs.

One useful function of ruthenium complexes is the significant enhancement in conformational and thermal stabilisation of a protein obtained by cross-linking an engineered metal-binding site with a ruthenium complex inert to substitution [140]. Cross-linking two histidines on opposite strands of a β-sheet with $[Ru^{II}(bpy)_2]$ significantly increases the unfolding free energy of *Saccharomyces cerevisiae* iso-1-cytochrome c and increases its melting temperature with a minimal change in the cytochrome c FeIII/II reduction potential [140]. (See Figure 1.20)

A significant medical application for ruthenium complexes is based on their complexation to drugs, one example being the drug clotrimazole which acts against the tropical disease trypanasoma-cruzi, as they lead to enhancement of the drug's efficacy as well as exhibiting a low toxicity [141]. However, more detailed studies on the mechanisms of action of this complex, as well as further modifications of this and other related metal derivatives, are still in the early stages.

Regulation of protein and enzyme activities by external stimuli is necessary for the design of biocatalysts with a variety of potential biotechnological and medical applications. Chemical modification of enzymes with nonnatural functional groups such as photochromic or redox active molecules has been revealed as a promising approach. Hamachi and coworkers report light-driven acti

59

vation of a semi-synthetic myoglobin [Mb] that is directly modified at the heme co-factor active site [142]. The reconstituted protein with a photo-sensitisable $[Ru(bpy)_3]^{2+}$ at its heme is activated by visible light to function as a dioxygen storage protein. The active centre of Ru-Mb (protohemin) is reduced from the ferric to ferrous state by photoinduced electron transfer, followed by the reaction with dioxygen gas [142]. As opposed to earlier approaches, (a) a cofactor reconstitution method is applicable for the active site directed introduction of nonnatural functional groups and (b) a long range electron transfer rate can significantly influence the overall activity of the semisynthetic protein (See Figure 1.21).
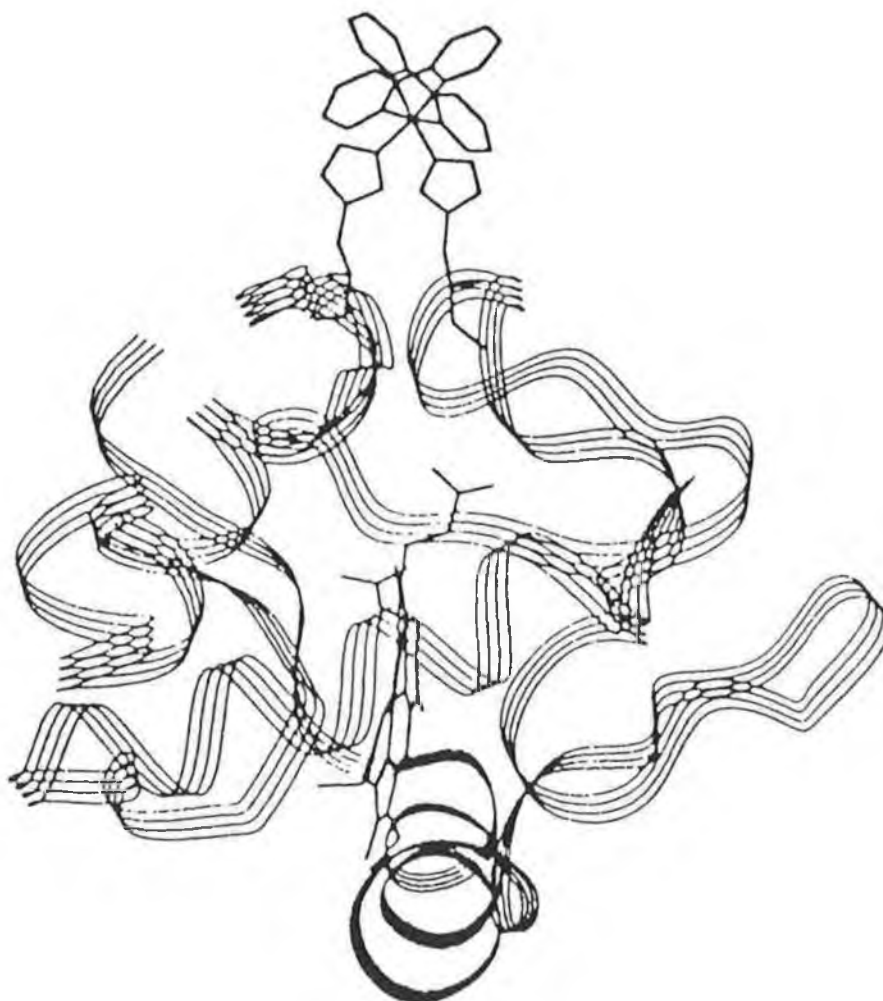
Figure 1.20 Energy-minimised model of Ru^{II}_2-H_{39} H_{38} cytochrome c [140].
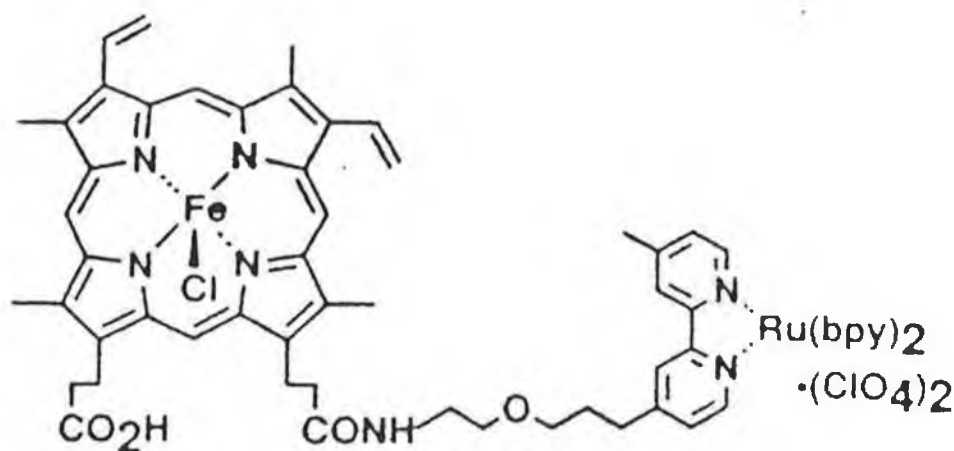
Figure 1.21 Structure of the protoheme derivative covalently bound to
[Ru(bpy)₃]²⁺ [142].

The binding of a complex cobalt ruthenium polyamine (see Figure 1.22), by DNA and a lipopolysaccharide has been investigated with implications as a model for a novel class of drug [143]. The aim was to study the value of heavy metal polycations compared to polyamines such as spermine, in their binding to macromolecules such as DNA and lipopolysaccharides, and consequently an attempt to design a prototype drug which would displace biological polycations from polyanion

partners. As simpler metal complex ammines such as $[Co(NH_3)]^{3+}$ bind quite strongly to such anions, this study involved testing to see if the affinity of polyamines could be matched by extended flexible complex metal cations such as the Ru-Co complex illustrated below (Figure 1.22). As expected, this complex binds strongly to DNA and lipopolysaccharides and it does not saturate the negative charge of the anions. Surprisingly however, the anions increase both the reagents photosensitivity and sensitivity to oxidation in air. As the Ru undergoes reversible one electron oxidation, implications include the attack by a drug based on the design of Ru-Co since DNA is susceptible to attack by free radicals [143].
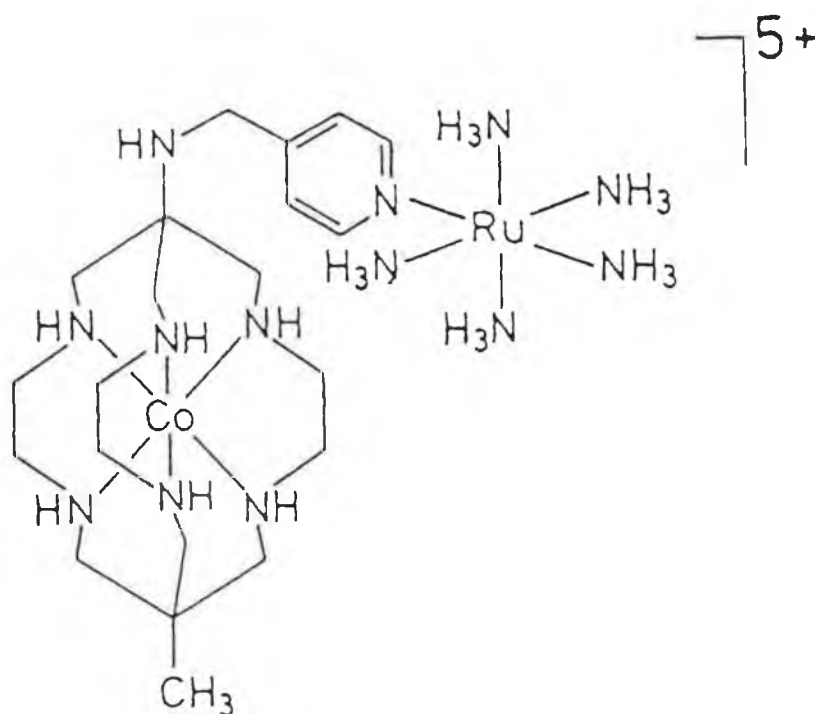
Figure 1.22 Structure of Ru-Co complex {Co[H₃CsarNHCH₂pyRu(NH₃)₅]} [143].

1.5. Scope of thesis.

This thesis is concerned with the study of ruthenium(II) polypyridyl complexes incorporated into biological systems in a covalent manner. There are two main goals of these studies. The first objective is the preparation and characterisation of ruthenium modified-proteins via specific sites along the biopolymer. The second and indeed converse goal is to use the existing extensive knowledge on the photophysics of these complexes to probe the conformational variances that the bound biomolecules undergo in solution.

In Chapter 3, the properties of the ruthenium labels bound to specific binding sites on the poly-amino acids and proteins are described. The main aim of this chapter is to verify the success of the conjugation procedures attempted and to study the effects of reaction conditions, label form and protein structure on the extent of these conjugation reactions.

The decay behaviour of ruthenium polypyridyl complexes is known to be very sensitive to its local environment. Therefore, in Chapter 4 and 5 the pH sensitivity of the emitting properties of the labels, in particular the emission intensities and lifetimes when bound to selected proteins is investigated. The aim here is to determine how the emission properties of such fluorescent labels can be used as a sensitive reporter, to follow acid-induced conformational changes of the bound biomolecules in solution due to variances in the nature of its surroundings. Chapter 4 investigates the probing potential of the absorption and emission spectra of the labels while Chapter 5 examines the potential of the decay lifetimes. The effect of chemical denaturants on the decay lifetimes of the protein-bound labels is also examined in an attempt to investigate the possibility of monitoring the unfolding of real proteins.

Finally, the photophysical properties, particularly the decay lifetimes of the labels are examined when bound to the enzyme lysozyme as enzyme activity studies should allow us to study the effects, if any, of such labelling on the function and conformational properties of the enzyme. In addition, this allows the establishment of

the extent of usefulness of such complexes in real biological processes as the denaturation of the protein is implied and hence can probably be monitored by the loss of activity of lysozyme towards its substrate.

Finally, Chapter 6 aims to bring the information in this thesis together and to give an overview of how exactly ruthenium polypyridyl complexes succeed in following certain conformational variances of the bound biomolecules, including secondary structure changes of polypeptides and the unfolding of proteins. Brief suggestions of further work which could be done in the future to extend the applicability and usefulness of such complexesin biological matrices are also given.

1.5.   References.

[1]   A. Juris, V. Balzani, F. Barigelletti, S. Campagna, P. Belser and A. Von Zelewsky, *Coord. Chem. Rev.*, **1988**, 84, 85.

[2]   K.Kalyanasundaram, *Coord. Chem. Rev.*, **1982**, 46, 159.

[3]   K.R. Seddon, *Coord. Chem. Rev.* , **1982**, 41, 79.

[4]   E.A. & K.R. Seddon, The Chemistry of Ruthenium, Elsevier, **1984**.

[5]   E.M. Kober and T.J. Meyer, *Inorg. Chem.*, **1982**, 21, 3967.

[6]   E.M. Kober and T.J. Meyer, *Inorg. Chem.*, **1983**, 22, 1614.

[7]   E.M. Kober and T.J. Meyer, *Inorg. Chem.*, **1984**, 23, 3877

[8]   J.V. Casper and T.J. Meyer, *Inorg. Chem.*, **1983**, 22, 2444.

[9]   R.J. Crutchley and A.B.P. Lever, *Inorg. Chem.*, **1982**, 21, 2276.

[10]   K. Kalyanasundaram, M. Gratzel and E. Pelizzetti, *Coord. Chem. Rev.*, **1986**, 69, 57.

[11]   B. O Reagan and M. Gratzel, *Nature*, **1991**, 353, 737.

[12]   A. Hay and M. Gratzel, *J. Phys. Chem.*, **1993**, 97, 6272.

[13]   K. Rao, D. Hall, M. Evans, M. Gratzel, M. Seibert and N. Vlachopoulous, *J. Photochem. Photobiol.*, **1990**, 5, 379.

[14]   R. Hage, R. Prins, J.G. Haasnoot, J. Reedijk and J.G. Vos, *J. Chem. Soc., Dalton Trans.*, **1987**, 1389.

[15]   R.J. Watts, *J. Chem. Ed.*, **1983**, 60, 834.

[16]   G.A. Heath, L.J. Yellowless and P.S. Braterman, *Chem. Phys. Lett.*, **1982**, 92, 646.

[17]   G.A. Heath, L.J. Yellowless and P.S. Braterman and A.Harriman, *J. Chem. Soc., Dalton Trans.*, **1983**, 1801.

[18]   W.M. Wacholtz, R.A. Auerbach, R.H. Schmehl, M. Ollino and W.R. Cherry, *Inorg. Chem.*, **1985**, 24, 1785.

[19]   W.J. Vining, J.V. Casper and T.J. Meyer, *J. Phys. Chem.*, **1985**, 89, 1095.

[20]   V. Balzani, F. Barigelletti, A. Juris, P.Belser and A. von Zelewsky, *Inorg. Chem.*, **1985**, 24, 202.

[21]   J. van Houten and R.J. Watts, *J. Am. Chem. Soc.*, **1976**, 98, 4853.

[22]   J. van Houten and R.J. Watts, *Inorg. Chem.*, **1978**, 17, 3381.

[23]   B. Durham, J.V. Casper, J.K. Nagle and T.J. Meyer, *J. Am. Chem. Soc.*, **1982**, 104, 4803.

[24]   J.V. Casper and T.J. Meyer, *J. Am. Chem. Soc.*, **1983**, 105, 5583.

[25]   V. Balzani, F. Barigelletti, A. Juris, P.Belser and A. von Zelewsky, *J. Phys. Chem.*, **1985**, 89, 3680.

[26]   V. Balzani, F. Barigelletti, A. Juris, P.Belser and A. von Zelewsky, *J. Phys. Chem.*, **1986**, 90, 5190.

[27]   A. Juris, M.F. Manfrin, M. Maestri and N. Serpone, *Inorg. Chem.*, **1978**, 17, 2258.

[28]   M. Maestri, V. Balzani, L. Moggi and F. Bolleta, *J. Chem. Soc. Commun.*, **1975**, 901.

[29]   C. Creutz and N. Sutin, *J. Am. Chem. Soc.*, **1976**, 98, 6384.

[30]   C. Creutz, *Inorg. Chem.*, **1978**, 17, 1046.

[31]   G.P. Porter, *J. Chem. Ed.*, **1983**, 60, 785.

[32]   C-T. Lin N. Sutin, W. Bottcher, M. Chou and C. Creutz, *J. Am. Chem. Soc.*, **1976**, 98, 6536.

[33]   C-T. Lin and N. Sutin, *J. Phys. Chem.*, **1976**, 80, 97.

[34]   A. Kornberg, DNA Replication (W.H. Freeman & Co.) San Francisco, **1979**.

[35]   S.J. Lippard, P.J. Bond, K.C. Wu, W.R. Bauer, *Science*, **1976**, 194, 726.

[36]   H.M. Berman, P.R. Young, *Ann. Rev. Biophys. Bioeng.*, **1981**, 10, 87.

[37]   E.F. Gale, E. Cundliffe, P.E. Reynolds, M.H. Richmond, M. Waring " Molecular Basis of Antibiotic Action " Wiley, London **1972**.

[38]   S. Neidle, *Prog. Med. Chem.*, **1979**, 16, 151.

[39]   (a) S.J. Lippard, *Acc. Chem. Res.*, **1978**, 11, 211
        (b) K.W. Jennete, S.J. Lippard, G.A. Vassikades and W. R. Bauer, *Proc. Natl. Acad. Sci. USA*, **1974**, 71, 3839.

[40]   C.V. Kumar, A.L.Raphael, J.K Barton, **1986**, Biomol. Stereodyn. III, Proc. of 4th Conversation in Discipl. Biomol. Stereodyns., R.H Sarma, M.H. Sarma Eds., Adenine Press. New York.

[41]   M. Rodriquez, T. Kodadek, M. Torres, A.J. Bard, *Bioconj. Chem*, **1990**, 1 ,123-131.

[42]   J.K Barton, *J. Biomol. Struct. Dyn.*, **1983**, 1, 621.

[43]   J.K Barton, *Comm. Inorg. Chem.*, **1985**, 3, 6, 321.

[44]   T.G. Spiroed, Nucl. Acid Metal Ion Interaction (John Wiley & Sons Inc., New York, *1980*).

[45]   J.K Barton, A.T. Danishefsky and J.M. Goldberg, *J. Am. Chem. Soc.*, **1984**, 106, 2172.

[46]   J.K Barton and E. Lolis, *J. Am. Chem. Soc.*, **1985**, 107, 708.

[47]   A. Kirsch-de Mesmaeker, G. Orellana, J.K Barton and N.J. Turro, *Photochem. Photobiol*, **1990**, 52, 3, 461.

[48]   A.B. Tossi and J.M. Kelly, *Photochem. Photobiol.*, **1989**, 49, 5, 545.

[49]   A.B. Tossi, H. Gorner, C. Stradowski and D. Schulte-Frohlinde, *J. Photochem. Photobiol. B*, **1988**, 2, 67.

[50]   L. Kittler, G. Lober, F.A. Gollmick and H. Bergman, *J. Electroanal. Chem.*, **1980**, 116, 503.

[51] A.M. Pyle, J.P. Rehmann, R. Meshoyrer, *J. Am. Chem. Soc.,* **1989**, 111, 3051.

[52] N.J. Turro, J.K. Barton and C.V. Kumar, *J. Am. Chem. Soc.,* **1985**, 107, 5518.

[53] D.J. McConnell, C. OhUigin, .B. Tossi and J.M. Kelly, *Nucl. Acid. Res.,* **1985**, 13, 7.

[54] J.M. Goldberg, C.V. Kumar, J.K Barton and N.J. Turro, *J. Am. Chem. Soc.,* **1986**, 108, 2081.

[55] J.P. Lecomte, G. Orellana and A. Kirsch-de Mesmaeker, *J. Phys. Chem.,* **1994**, 98, 5382.

[56] N.J. Turro, J.K. Barton, A.E. Friedman, J.C. Chambron and J-P. Sauvage, *J. Am. Chem. Soc.,* **1990**, 112, 4960.

[57] J.K. Barton, R.M. Hartshorn, *J. Am. Chem. Soc.,* **1992**, 114, 5919.

[58] J.K. Barton and Y. Jenkins, *J. Am. Chem. Soc.,* **1992**, 114, 22, 8736.

[59] I. Haq, P. Lincoln, D. Suh, B. Norden and J.B. Chaires, *J. Am. Chem. Soc.,***1995**, 117, 4788.

[60] J. Telser, K.A. Cruickshank, K.S Schanze and T.L. Nelzel, *J. Am. Chem. Soc.,* **1989**, 111, 7221.

[61] W. Bannwarth, *Anal. Biochem.,* **1989**, 181, 216.

[62] W. Bannwarth and D. Schmidt, *Tetr. Lett.,* **1989**, 30, 1513.

[63] R.L. Stallard, W. Bannwarth, C. Horming, R. Knorr, F.Muller and D. Schmidt, *Helv. Chim. Acta.,* **1988**, 71, 2085.

[64] J.M. Kelly, M.M. Feeney, A.B Tossi, J-P. Lecomte, *Anti-cancer Drug Des.,* **1990**, 5, 69.

[65] J.P. Lecomte, J.M. Kelly, M.M. Feeney, A.B. Tossi and A. Kirsch-de Mesmaeker, *J. Photochem. Photobiol., B: Biol.,* **1994**, 23, 69.

[66] B. Norden and F. Tjerneld, *FEBS Lett.,* **1976**, 67, 3, 368-370.

[67] J.K. Barton, J.J. Dannenberg and A.L. Raphael, *J. Am. Chem. Soc.,* **1982**, 104, 4967.

[68] A. Yamagashi, *J. Chem. Soc., Chem. Commun.,* **1983**, 572.

[69] J.K. Barton, *J. Biomol. Struct. Dyn.,* **1983**, 1 , 621.

[70]   J.K. Barton, J.M. Goldberg, A.T. Danishefsky, *J. Am. Chem. Soc.*, **1984**, 106, 2172.

[71]   C.V Kumar, N.J. Turro and J.K. Barton, *J. Am. Chem. Soc.*, **1985**, 107, 5518.

[72]   J.K. Barton, J.M. Goldberg and N.J. Turro, *J. Am. Chem. Soc.*, **1986**, 108, 2081.

[73]   J.K. Barton, *C & En.*, **1988**, 30.

[74]   J.K. Barton and C.J. Murphy, *Methods Enzymol.*, **1993**, 226, 576.

[75]   J.K. Barton, A.T. Danishefsky and L.A. Basile, *Proc. Natl. Acad. Sci. USA.*, **1984**, 81, 1961.

[76]   N. Grover, N. Gupta and H.H. Thorp, *J. Am. Chem. Soc.*, **1992**, 114, 3390.

[77]   J.K. Barton and S.R. Paranawithana, *Biochem*, **1986**, 25, 2205.

[78]   J.K. Barton and H-Y. Mei, *J. Am. Chem. Soc.*, **1986**, 108, 7414.

[79]   I.S Haworth, A.H. Elcock, A. Rodger and W.G. Richards, *J. Biomol. Struct. Dyn.*, **1991**, 9, 553.

[80]   C. Hiort, B. Norden and A. Rodgers , *J. Am. Chem. Soc.*, **1990**, 112, 1971.

[81]   M. Eriksson, M. Leijon, C. Hiort, B. Horden and A. Graslund, 1992, *J. Am. Chem. Soc.*, **1992**, 114, 4933.

[82]   M. Eriksson, M. Leijon, C. Hiort, B. Horden and A. Graslund, *Biochem*, **1994**, 33, 5031.

[83]   J.P Reymann and J.K Barton, *Biochem.*, **1990**, 29 (a) 1701, (b) 1710

[84]   T. Hard, P. Fan and D.R. Kearns, *Photochem. Photobiol.*, **1990**, 51, 77.

[85]   S. Satyanarayana, J.C. Dabrowiak and J.C. Chaires, *Biochem.*, **1992**, 31, 9319.

[86]   S. Satyanarayana, J.C. Dabrowiak and J.C. Chaires, *Biochem.*, **1993**, 32, 2573.

[87] J.-P. Lecomte and A. Kirsch-De Mesmaeker, *Bull. Soc. Chim. Belg.*, **1994**, 103, 5-6, 193.

[88]   J.M. Kelly, D.J. McConnell, C. OhUigin, A.B. Tossi, A. Kirsch-De Mesmaeker, A. Masschelein and J. Nasielski, *J. Chem. Soc., Chem. Commun.*, **1987**, 1821.

[89]   J.M. Kelly, D.J. McConnell, C. OhUigin, A.B. Tossi, C. Helene and T. Le Doan, *Free Rad., Metal Ions & Biopolymers*, **1989**, 144.

[90]   C.S Chow and J.K Barton, *J. Am. Chem. Soc.*, **1990**, 112, 2839.

[91]   A.B. Tossi, H. Gorner, A. Aboul-Enein and D. Schulte-Frohline, *Free Rad. Res. Comms.*, **1989**, 6, 2-3, 171.

[92]   L.A Basile and J.K Barton, *J. Am. Chem. Soc.*, **1987**, 109, 7548.

[93]   L.A Basile, A.L Raphael and J.K Barton, *J. Am. Chem. Soc.*, **1987**, 109, 7550.

[94]   H.H Thorp, *J. Inorg. Organometallic Polymers*, **1993**, 3, 1, 41.

[95]   Neyhart, N. Grover, S.R. Smith, W.A. Kalsbeck, T.A. Fairley, M. Cory and H.H Thorp, *J. Am. Chem. Soc.*, **1993,** 115, 11, 4423.

[96]   S.R. Smith, G.A. Neyhart, W.A. Kalsbeck and H.H. Thorp, *New J. Chem.*, **1994**, 18, 397.

[97]   M.J. Clarke, *Met. Ions Biol. Sys.*, **1980**, 11, 231.

[98]   *Prog. Clin. Med. Biochem.*, (a) **1989**, 10, 25. (b) **1989**, 10, 40. (c) **1989**, 10, 71.

[99]   B.K. Keppler, W. Rupp, *J. Cancer Res. Oncol.*, **1986**, 11, 166.

[100] (a) B. K. Keppler, W. Rupp, H. Endres, D. Wehe, *Inorg. Chem.*, **1987**, 26, 844.(b) B. K. Keppler, W. Rupp, H. Endres, U.M. Juhl, R. Niebl and W. Balzer, *Inorg. Chem.*, **1987**, 26, 4366.

[101] G. Sava, G. Mestroni, S. Zorzet and T. Giraldi, *J. Cancer Res. Oncol.*, **1984**, 20, 6 841.

[102] G. Mestroni, S. Zorzet, E. Alessio, G. Nardin, M. Calligaris and G. Sava, *Inorg. Chem.*, **1988**, 27, 4099.

[103] G. Mestroni, S. Zorzet, E. Alessio and G. Sava, *Pharm. Res.*, **1989**, 21, 5.

[104] E. Alessio, G. Esposito, S. Cauci, F. Fogolari, M. Scocchi, F. Quadrifoglio and P. Viglino, *Biochem.*, **1992**, 31, 31, 7094.

[105] G. Mestroni, S. Pacor, E. Alessio and G. Sava, *Clin. Eptl. Metastasis*, **1992**, 10, 4, 273.

[106] M. Hartmann and B.K. Keppler, *Comms. Inorg. Chem.*, **1995**, 16, 6, 339.

[107] A.G. Mauk, E. Bordignon and H.B. Gray, *J. Am. Chem. Soc.*, **1982**, 104, 7654.

[108] S.E. Peterson-Kennedy, J.L. McGourty, P.S. Ho, C.J.Sutoris, N. Liang, H. Zemel, N.N. Bough, E. Margohiosh and B.M. Hoffman, *Coord. Chem. Rev.*, **1985**, 64, 125.

[109] S.L. Mayo, W.R. Ellis, R.J. Crutchley and H.B. Gray, *Science*, **1986**, 233, 948.

[110] J.L. McGourty, W.V. Blough, B.M. Hoffman, *J. Am. Chem. Soc.*, **1983**, 105, 4472.

[111] J.R. Winkler, D.G. Nocera, K.M. Yocum, L. Bordignon and H.B. Gray, *J. Am. Chem. Soc.*, **1982**, 104, 5798.

[112] L.P. Pan., B. Durham, J. Wolinska and F. Millett, *Biochem.*, **1988**, 27, 7180.

[113] L.P. Pan., B. Durham, J.E. Long and F. Millett, *Biochem.*, **1989**, 28, 8659.

[114] N.M. Kostic, R. Margalit, C-M. Che and H.B Gray, *J. Am. Chem. Soc.*, **1983**, 105, 7765.

[115] J.L. McGourty, S.E. Peterson-Kennedy, W.Y. Ruo and B.M. Hoffman, *Biochem.*, **1987**, 26, 8302.

[116] J.N Onuchic, D.N. Beratan, J.R. Winkler and H.B. Gray, *Annu. Rev. Biomol. Struct.* **1992**, 21, 349.

[117] D.S. Wuttke, M.J. Bjerrum, I-J. Chang, J.R. Winkler and H.B Gray *Biochim. Biophys. Acta*, **1992**, 1101, 2, 168.

[118] D.R. Casimoro, L-L. Wong, J.L Colon, T.E. Zewert, J.H Richards, I-J. Chang, J.R. Winkler and H.B Gray, *J. Am. Chem. Soc.*, **1993**, 115, 4, 1485.

[119] L-H. Zang and A.H. Maki, *J. Am. Chem. Soc.*, **1990**, 112, 4346.

[120] E. Lloyd, N.P. Tomkinson, G.A. Salmon and A.G. Sykes, *Biochim. Biophys. Acta*, **1993**, 1202, 113.

[121] A. Vassilian, R.H. Magnuson, H. Schwarz and S.S. Isied, *J. Am. Chem. Soc.*,

1985, 107, 7432.

[122] A. Vassilian, J.F. Wishart, B. van Hemelryck, H. Schwarz and S.S. Isied, *J. Am. Chem. Soc.,* **1990,** 112, 7278.

[123] S.L. Mecklenburg, B.M. Peek, J.R. Schoonover, D.G McCafferty, C.G. Wall, B.W. Erickson and T.J. Meyer, *J. Am. Chem. Soc.,* **1993,** 115, 13, 5479.

[124] J.K. Barton, C.V. Kumar and N.J. Turro, *J. Am. Chem. Soc.,* **1986,** 108, 6391.

[125] M.D. Purugganan, C.V. Kumar, N.J. Turro and J.K. Barton, *Science,* **1988,** 241, 1645.

[126] C.J. Murphy, M.R. Arkin, Y. Jenkins, N.D. Ghatlia, S.H. Bossman, N.J. Turro and J.K. Barton, *Science,* **1993,** 262, 1025.

[127] T.J. Meade and J.F. Kayyem, *Angew. Chem. Int. Ed. Engl.,* **1995,** 34, 3, 352.

[128] S.M. Risser, D.N. Beratan and T.J Meade, *J. Am. Chem. Soc.,* **1993,** 115, 2508.

[129] I. Rubenstein and A.J. Bard, *J. Am. Chem. Soc.,* **1981,** 103, 512.

[130] C.R. Martin, I. Rubenstein and A.J. Bard, *Anal. Chem.,* **1983,** 55, 1580.

[131] J.B. Noffsinger and N.D. Danielson, *Anal. Chem.,* **1987,** 59, 865.

[132] S.N. Brune and D.R. Bobbitt, *Talanta,* **1991,** 38, 4, 419.

[133] S.N. Brune and D.R. Bobbitt, *Anal. Chem.,* **1992,** 64, 166.

[134] T.M. Downey and T.A. Nieman, *Anal. Chem.,* **1992,** 64, 261.

[135] K. Yokoyama, S. Sasaki, K. Ikebukuro, T.Takeuchi, I. Karube, Y. Tokitsu and Y. Masuda, *Talanta,* **1994,** 41, 6, 1035.

[136] M.T. Carter and A.J. Bard, *Bioconj. Chem.,* **1990,** 1. 257.

[137] R.P. Haughland, Handbook of Fluorescent Probes and Research Chemicals, Molecular Probes Inc., Oregon 97402, USA, 1989.

[138] M. Brinkley, *Bioconj. Chem.,* **1992,** 3, 1, 2.

[139] G.A. Means and R.E. Feeney, *Bioconj.Chem.,* **1990,** 1, 2.

[140] A. Muheim, R.J. Todd, D.R.Casimiro, H.B. Gray and F.H. Arnold, *J. Am. Chem. Soc.,* **1993**, 115, 2, 5312.

[141] R.A Sanchez-Delgado, K. Lazardi, L. Rincon and J.A. Urbina, *J. Med. Chem.,* **1993**, 36, 14, 2041.

[142] I. Hamachi, S. Tanaka and S. Shinkai, *J. Am. Chem. Soc.,* **1993**, 115, 22, 10458.

[143] A. Hammershoi, G. Nord, E. Rowatt, L.K. Skov and R.J.P. Williams, *J. Inorg. Biochem.,* **1993**, 49, 295

Chapter 2.

Experimental Procedures.

2.1   Introduction.

The synthetic procedures for the preparation of the ruthenium polypyridyl complexes and the methods of their conjugation reactions to various biomolecules are described in the following section. All synthetic reagents and solvents were of commercial grade and no further purification was employed. The instrumentation and chemical techniques used to characterise the prepared samples are also discussed herein.

The complexes and their respective bioconjugates are listed in numerical order for further reference and the table summarising the reference numbers of each complex/conjugate studied is listed in Table 3.1.

2.2. Synthesis of ruthenium polypyridyl complexes.

2.2.1   Preparation of the complexes $[Ru(L\text{-}L)_2(NH_2\,phen)]^{2+}$ [1].

where L-L=1,10-phenanthroline (phen) 2,2'-bipyridine (bpy) and 4,7'-diphenyl,1,10-phenanthroline (dpp).

The complexes were prepared according to literature methods [1].

2.2.2   Preparation of the complexes $[Ru(L\text{-}L)_2(NCSphen)]^{2+}$ [2].

These complexes were prepared as described in the literature [2], 0.20 mmol of the ruthenium amino complexes were placed in 10ml distilled water and stirred in the presence of an anion exchange resin (Amberlite exchange resin Cl⁻, activated by treatment with 2M NaOH, washed thoroughly and then treated with 2M HCl and washed thoroughly again.) in order to exchange the PF_6^- anion for Cl⁻ ions, thus rendering the compound soluble in aqueous solution. On removing the resin from the

74

filtrate, the dichloride compound was reacted with 0.01 M thiophosgene in acetone, by adding dropwise to the aqueous solution over 30 min. It was necessary to keep the reaction vessels in an ice-bath to prevent the evaporation of the thiophosgene.

All procedures were carried out with care due to the toxicity of thiophosgene, including the wearing of gloves and due to the volatility of thiophosgene, each reaction stage was carried out in the fumehood. The resulting solution was left overnight at room temperature in a covered vessel. The complexes $[Ru(dpp)_2(NCSphen)]^{2+}$ and $[Ru(phen)_2(NCSphen)]^{2+}$ precipitated and were isolated by filtration and dried under vacuum, on completion of the above reaction. In contrast, the complex $[Ru(bpy)_2(NCSphen)]^{2+}$ remained in solution at this stage, and was isolated by evaporation of the excess thiophosgene under reduced pressure, followed by precipitation using a saturated aqueous solution of NH_4PF_6. The compounds were then dried in vacuo. Recrystallisation of these isothiocyanate derivatives was not carried out due to their instability in aqueous solution.

2.2.3. *Synthesis of [Ru(bpy)$_2$(COOH$_2$bpy)](PF$_6$)$_2$.[3]*

The ligand 4,4'-carboxylic acid-2,2'bipyridine was prepared from 4,4'-dimethyl-2,2' bipyridine according to literature methods [3]. Synthesis of the ruthenium complex (a) and its conversion to the active ester (b) were carried out according to Bard [4].

2.3   Conjugation Procedures.

The various procedures involved in covalently binding ruthenium polypyridyl complexes to specific sites on selected biomolecules are described in this section.

2.3.1 Conjugation of $[Ru(L-L)_2(NH_2phen)]^{2+}$ to BSA and lysozyme. [1a, 1b]

(a) Conjugation of $[Ru(L-L)_2(NH_2phen)]^{2+}$ to albumins via carbohydrate moieties[1a] firstly involves the periodate oxidation of the albumin followed by conjugation to the amino complex. BSA (bovine serum albumin) 10-25 mg, was dissolved in 0.10M carbonate buffer (1-2 ml) and treated with 2.5 ml of 16 mmol $NaIO_4$ for two hours at 4 °C in the dark. [8] The ruthenium complex was dissolved in the minimum volume of dimethylformamide (DMF) and 0.10 M carbonate buffer, pH 9.2, keeping the total reaction volume to a minimum. The label solution was then added (50 molar excess unless otherwise stated) dropwise to the gently stirring protein solution using a micro-syringe. The conjugation reaction was allowed to proceed overnight at 4 °C, in the dark, with minimal agitation. Unbound ruthenium compound was removed by extensive dialysis against 0.10 M carbonate buffer, pH 9.2 (at least 4 changes of buffer). The oxidation of the protein leads to the formation of an unstable Schiffs base which was subsequently stabilised by adding 4/20 volumes of $NaBH_4$ (5 mg/ml) and reacted for one hour at 4°C, in the dark. Finally, the conjugate was further dialysed against two changes of carbonate buffer. [8]

(b) Conjugation of $[Ru(L-L)_2(NH_2phen)]^{2+}$ to albumins via glutamic acid residues [1b] involves the activation of the glutamic acid carboxylic acid side groups which are naturally quite inactive in aqueous solution. This was achieved by treating the albumin, already dissolved in 1-2 ml 0.05 M acetate buffer pH 4.8, with 0.05 ml of 1 x 10^{-3} M carbodiimide. [9] The ruthenium complex was then dissolved in the minimum volume of DMF/0.10 M carbonate buffer pH 9.2, added dropwise to the protein solution and the reaction allowed to proceed overnight at 4°C in the dark. Extensive dialysis was carried out against 0.10 M carbonate buffer pH 8-9.

2.3.2 Conjugation of [Ru(bpy)$_2$(NH$_2$phen)]$^{2+}$ to goat anti-mouse IgG. [1c]

Conjugation of the amino complex to IgG is as outlined in 2.3.1 except that 0.5 ml of IgG in PBS (phosphate buffered saline) ie 1-2 mg was used per conjugation. The buffer used was 0.05 M phosphate buffer pH 7.4 and the anti-IgG was oxidised using 1ml of 10 mmol NaIO$_4$ [10].

2.3.3 Conjugation of [Ru(L-L)$_2$(NH$_2$phen)]$^{2+}$ to Poly-L-Glutamate (PLGlu). [1d]

10 mg P-L-Glu was dissolved in 1-2 ml of 0.05 M acetate buffer pH 4.8 and then treated with 0.5 ml of 1 x 10^{-3} M solution of a water soluble carbodiimide for two hours at 4 ^{0}C in the dark, as undertaken in 2.3.1. The ruthenium complex was then dissolved in the minimum volume of DMF/0.10 M carbonate buffer pH 9.2, added dropwise to the protein solution and the reaction allowed to proceed overnight at 4^{0}C in the dark. Extensive dialysis was carried out against 0.10 M carbonate buffer pH 8.

2.3.4. Conjugation of [Ru(L-L)$_2$(NH$_2$phen)]$^{2+}$ to PLL. [1e]

This was carried out as described for PLGlu above (See 2.3.3.) as these amino complexes were bound to the terminal carboxylic acid groups of the polypeptide chain.

2.3.5. Conjugation of [Ru(L-L)$_2$(NCSphen)]$^{2+}$ to BSA, PLL and lysozyme [2a] [11] .

10mg BSA/PLL/lysozyme was dissolved in 1-2 ml 0.10 M carbonate buffer, pH 9.2. The isothiocyanate complexes were dissolved in 30:70 DMF/0.10M carbonate buffer pH 9.2 and were added dropwise in volumes equivalent to a 50 molar excess of the label to biomolecule (unless stated otherwise). The conjugation reaction was allowed to proceed overnight at 4 °C in the dark, with minimal agitation. The conjugate was extensively dialysed against 0.10 M carbonate buffer pH 9.2 [11].

2.3.6 Conjugation of [Ru(L-L)$_2$(NCSphen)]$^{2+}$ to PLGlu. [2b]

This was carried out as for PLL in section 2.3.5. However, 0.10M carbonate buffer pH 8-8.5 was employed throughout the procedure as opposed to the usual pH 9.2. This is due to the fact that the terminal amino groups have a lower pK_a of 8 compared to that of the lysine residues (pK_a=9.5).

2.3.7 Conjugation of the active ester of [Ru(bpy)$_2$(COOH$_2$bpy) to BSA and (PLL). [3a]

10 mg albumin/PLL was dissolved in 1-2 ml 0.10 M carbonate buffer, pH 8.2. The active ester solution was added dropwise in volumes equivalent to a 50 molar excess of the ester to biomolecule (unless stated otherwise). The conjugation reaction was allowed to proceed overnight at 4 °C in the dark, with minimal agitation. The conjugate was extensively dialysed against 0.10 M carbonate buffer pH 8.2 [11].

78

2.4. Chemical procedures.

2.4.1. Absorption and emission measurements.

UV/vis spectroscopy was carried out using a Shimadzu UV 3100 or UV3101PC instrument interfaced with an Elonex PC-433 personal computer. Emission spectra were obtained on a Perkin-Elmer LS50 or LS50B luminescence spectrometer interfaced with an Epson PCAX2E personal computer, employing Fluorescence Data Manager custom built software and equipped with a red sensitive Hamamatsu R 928 photomultiplier tube. An emission slit of 10nm was used at room temperature and the results were not corrected for photomultiplier response.

Quantum yields of emission, ϕ_{em} were carried out according to the method of optically dilute measurements described by Demas and Crosby [5]. The standard used was $[Ru(bpy)_3]^{2+}$, known to have a quantum yield of 0.028 in aqueous air equilibrated solution [6]. Normalisation of absorbance intensity was carried out prior to emission measurement and ϕ_{em} the emission quantum yield was determined by using the following equation (2.1);

$$\phi_{em}=0.028(A_s/A_{ref})(n_s/n_{ref})^2 \qquad (2.1)$$

where A_s and A_{ref} are the integrated areas of the emission band of the sample and reference complex respectively and n_s and n_{ref} are the solvent refractive indices of the sample and reference solutions respectively.

2.4.2 pK$_a$ measurements.

Measurements were carried out in Britton-Robinson buffer (0.04 M acetic acid, 0.04 M boric acid and 0.04M phosphoric acid) using the instrumentation described

above. The pH of the solutions was adjusted using 2 M H_2SO_4 or 2 M NaOH solution. Ground state pK_a values were determined by monitoring the intensity changes in absorption as a function of pH, using a Phillips PW9421 pH meter. The point of inflection of a plot of percentage change in absorbance versus pH was used to determine this value. To facilitate dissolution of samples in aqueous solutions a minimal volume of acetone was added. Measurements were carried out at room temperature.

2.4.3. *High performance liquid chromatography (HPLC).*

The purity of the ruthenium complexes was verified using an analytical cation exchange Waters HPLC system, consisting of a Waters pump, model 6000 or 501, fitted with a 20μ litre injecter loop, a Partisil SCX radial PAK cartridge and a 990 photodiode array detector connected to a NEC APCIII computer. The mobile phases used were (a) $CH_3CN:H_2O$ (80:20) containing 0.08M $LiClO_4$ (about pH 6-7); (b) mobile phase (a) adjusted to pH 2-3 with $HClO_4$. The flow rate was 2.5 ml/min.

2.4.4. *Size exclusion chromatography.*

As for the HPLC system described above, a Waters 990 Photodiode array system was employed, with a NEC APC111 computer for characterisation of the bioconjugates prepared. The column used was a BioSep-SEC-S2000 size exclusion column. The mobile phase used was 0.05M phosphate buffer pH 6.8, UV detection of 215nm was used and flow rates of 1.0 ml/min were applied, unless otherwise stated.

2.4.5. Column chromatography.

It was possible to use gel filtration chromatography to separate the free and protein-bound ruthenium complexes, as an alternative to dialysis, using Sephadex G-100 in a 1 by 10 column and phosphate buffered saline or 0.05M phosphate buffer pH6.8 as the eluents.

2.4.6. Infra-red spectroscopy.

Infra-red spectra were recorded on a Perkin-Elmer 983G Infrared Spectrometer using pressed KBr discs. This technique was used primarily to check for the presence of the isothiocyanate group in the complexes which were subequently used for conjugations to biomolecules, but also for the general characterisation of labels.

2.4.7 NMR spectroscopy.

^{1}H NMR spectra were recorded on a Bruker AC400 (400 Mhz) spectrometer. The measurements were carried out in $(CD_3)_2CO$ and DMSO. The peak positions are relative to TMS.

2.4.8 Lifetime measurements.

The lifetime measurements were carried out using a Q-switched Nd-YAG laser system as the excitation source, which operates at 1064 nm but can be frequency doubled, tripled or quadrupled to generate a second, third or fourth harmonic frequency at 532, 355 and 266 nm respectively. The third harmonic was exclusively used in

these experiments. The power of the laser pulse can be varied by applying different voltages across the amplifier flash tube. The pulse time is approximately 8 ns. The circular laser pulse is directed via two Pellin-Broca prisms upon the sample cuvette. When the pulse passes through the power meter, situated after the first prism but before the sample holder, the oscilloscope is triggered. The output of the sample cuvette and the emerging beam is focussed through two circular lens onto a F/3.4 monochromator. The detector, a Hamamatzu five stage photomultiplier is operated at 850 volts. The signal output is connected via a variable load resistor to the transient analyser, a Hewlett Packard 54510A oscilloscope. The oscilloscope is then linked to an Olivetti PCS 286 computer, whereby transient data can be stored and analysed.

The measurements were carried out in Britton Robinson buffer at 23^OC, as aerated solutions, unless otherwise stated.

2.4.9   Data analysis.

The fluorescence lifetime of a substance usually represents the average time duration the molecule remains in the excited state prior to its return to the ground state. The exponential decay of isolated fluorescent molecules can be described as follows;

$$\Phi(t) = \exp(-t/\tau) \qquad\qquad (2.2)$$

where τ is the emission lifetime.

However, the luminescence of molecules emitting from heterogenous systems such as proteins, frequently depart from first order kinetics [7]. Thus, a plot of the logarithm of emission intensity versus time is nonlinear. In kinetic studies of these systems the nonlinear semi-logarithmic plot is usually fitted to a multi-

exponential decay model. For the delta function excitation (ie. zero duration) with independently emitting noninteracting species the detector response is:

$$\Phi(t) = \sideset{}{^{i=1}}\sum_N K_i \exp(-t/\tau_i) \qquad (2.3)$$

$$\tau_I = 1/k_i \qquad (2.4)$$

where N is the number of emitting components. For the ith component, τ_i is the lifetime and K_i is the pre-exponential factor contributing to the signal at zero time. The K_i are functions of the spectral response of the detector, the concentration, emission and absorption characteristics of each component, the spectral transmission properties of the filters and the spectral distribution of the exciting light. [7]

For the studies reported in this thesis two different models were used to calculate the different lifetimes. The first is a simple monoexponential decay law [7], used to analyse the free labels lifetime;

$$\Phi(t) = A_1(1-\exp(-k_1 t)) \qquad (2.5)$$

where A_1 is the pre-exponential factor and k_1 is the decay rate constant.

A multi- exponential decay expression was used to analyse the data for the conjugate solutions, and is as follows;

$$\Phi(t) = [(A_1(1-\exp(-k_1 t))+(A_2(1-\exp(-k_2 t)))] \qquad (2.6)$$

where A_1 and A_2 are the emitting components respective pre-exponential factors and k_1 and k_2 are the decay rate constants. This model above assumes two populations of emitters, one which decays with rate constant k_1 and another which decays

83

with a rate constant k_2. It was possible to add on more terms for higher exponential fit .

In order to ascertain which decay behaviour is indeed observed, it was important to be able to judge the quality of the fit. From the best fit parameters, the expected curve was calculated. Even for the correct model, the theoretical and observed decays differed slightly due to noise. To visualise these discrepencies, a plot of the percentage errors versus time was made

$$\% \text{ error} = [(F(t_i)\text{-}D(t_i)/D(t_i)] \times 100 \qquad (2.7)$$

where $D(t_i)$ and $F(t_i)$ are the calculated best fit and observed decay data, respectively. For a good fit, the differences were small with a low % range ($< 5\%$) and randomly distributed plot, whereas a bad fit yielded a cosine wave distribution. As mentioned earlier, the absolute values of the pre-exponential factors depend on the experimental set-up. However, changes in the ratio of these factors A_1 and A_2 throughout an experiment may be deemed as significant so long as the experimental conditions remain constant throughout.

2.4.9.1 Calculations.

In order to understand more clearly the significance of the ratios of the various preexponential factors in a multi-exponential decay model and their dependence on the relative concentrations of their emitting species, as well as testing the precision of the lifetimes obtained, a set of appropriate experiments were carried out.

This involved the mixing of two fluorescent complexes of known single exponential decay behaviour. The relative concentrations of the two complexes were varied and the effect of this variable on the percentage of A_1 and A_2 examined and hence the reliability of the lifetime values deduced.

However, before studying a mixture, in order to ascertain the relationship between the concentration of an emitting species and its pre-exponential factor, a preliminary study on how A is influenced by the absolute concentration for one singly emitting fluorescent species in solution was undertaken. The experimental conditions (i.e. slit widths, path length etc.) were kept constant throughout, such that the concentration of the complex itself would be the only variable. Below in Table 2.1 the pre-exponential factors and lifetimes obtained for several concentrations of $[Ru(bpy)_3]^{2+}$ using the mono-exponential decay model (see equation 2.3) are listed. As can be seen from Table 2.1, the value of A is significantly dependent on the concentration of the complex. Although the higher concentrations yield the higher values of A, one is not directly proportional to the other. Hence, all this experiment verifies is the close association between the amount of an emitting species and its pre-exponential factor, with only one emitting component present. Significantly, however, it is to be noted that the variances between the lifetimes calculated for any two concentrations are within instrumental error (+- 10%) , all in the range 330-360ns. This indicates that the amount of an emitting species should not greatly affect it's decay lifetime.

Tables 2.2 and 2.3 below display results from a series of mixtures of two ruthenium complexes. Firstly, as presented in Table 2.2, $0.5 \times 10^{-4}M$ solutions of $[Ru(bpy)_3]^{2+}$ and $[Ru(dpp)_3]^{2+}$ in water were prepared and the mixtures made by taking various ratios of both solutions. Also, similar mixtures of $[Ru(bpy)_2(NH_2phen)]^{2+}$ (NH$_2$phen) and $[Ru(bpy)_2DHptr]^{2+}$ (dhptr) were prepared and analysed and their decay data are presented in Table 2.3. It was not possible to keep all experimental conditions constant throughout these experiments, however, as it was necessary to change the slit widths throughout it's course, to render analysis of the decay lifetimes possible.

Table 2.1. Decay profile data for various concentrations of $[Ru(bpy)_3]^{2+}$ using the single exponential decay model.

$[Ru(bpy)_3]^{2+}$ (mol/l)	A $^{\$}$	Lifetime (ns)
1×10^{-5}	6130	340
2×10^{-5}	7970	340
3×10^{-5}	14730	355
4×10^{-5}	17291	330
5×10^{-5}	21600	360

$^{\$}$ *Pre-exponential factor of the emitting species using the mono-exponential decay funciton $\Phi(t) = A_1(1-exp(-k_1 t))$.*

Table 2.2 reveals how, as the concentration of $[Ru(bpy)_3]^{2+}$ decreases, the contribution of its pre-exponential factor (i.e. $\%A_1$) also decreases, suggesting that there is indeed an inherent relationship between the concentration and the pre-exponential factor of an emitting component. However, the relationship would not be expected to be linear or even as closely related as found for a single emitting compound, due to certain variable contributing factors associated with such experiments, such as changes in slit width and applied voltages which complicate the analysis.

Table 2.2. Decay data for a series of solutions of varying ratios of $[Ru(bpy)_3]^{2+}$ (bpy) to $[Ru(dpp)_3]$ (dpp).

Bpy:dpp ratio	Lifetime bpy (ns)	% A_1 [$]	Lifetime dpp(ns)	% A_2 [$]
10:0	340	100	------	-----
9:1	355	92	750	8
7:3	388	85	760	15
5:5	378	74	800	26
3:7	410	63	770	37
1:9	410	51	800	49
0:10	------	----	740	100

[$] *Pre-exponential factors calculated using the multi-exponential decay function*

$\Phi(t) = [(A_1(1-\exp(-k_1t)) + (A_2(1-\exp(-k_2t))].$

Table 2.3. Decay data for a series of solutions containing varying ratios of $[Ru(bpy)_2(NH_2phen)]^{2+}$ (NH_2phen) and $[Ru(bpy)_2DHptr]^{2+}$ (dhptr).

NH_2phen:dhptr ratio	Lifetime NH_2phen (ns)	% A_1 [$]	Lifetime dhptr (ns)	% A_2 [$]
10:0	375	100	------	-----
9:1	375	93	90	7
7:3	360	82	100	18
5:5	410	52	110	48
3:7	390	38	90	62
1:9	350	34	90	66
0:10	-----	-----	100	100

[$] *Pre-exponential factors calculated using the multi-exponential decay function*

$\Phi(t) = [(A_1(1-\exp(-k_1t)) + (A_2(1-\exp(-k_2t))].$

Also, although both complexes absorb to a similar extent across the UV region, $[Ru(bpy)_3]^{2+}$ absorbs slightly more at the excitation wavelength, 355nm. This would explain why at a 1:1 ratio of bpy to dpp, rather than both pre-exponential factors contributing to the same extent , the pre-exponential factor of bpy contributes three times more than that of dpp. The lifetimes calculated for both complexes, when in the mixtures, were found to be quite reproducible, when compared to their corresponding lifetimes, when pure. From these results, it appears that the function used to analyse several lifetimes simultaneously is accurate and practical, even when one emitting species dominates greatly over another in concentration. Similar accurate results were obtained for the second mixture as presented in Table 2.3. The absorption of the $[Ru(bpy)_2(NH_2phen)]^{2+}$ solution was 0.433 at 355nm while that of $[Ru(bpy)_2DHptr]^{2+}$ was 0.326. In any samples in this thesis revealed to display multi-exponential decay behaviour, it would be expected that all emitting species would absorb similarly at 355 nm and hence this method of data analysis would seem appropriate for our work. The samples containing solely one complex were analysed using a single exponential model. Attempting to analyse a known single exponential decaying sample with the multi-exponential decay function (eqn 2.4) yielded two identical lifetimes and a wave function residual fit i.e. not a good fit.

Experiments were also carried out mixing two fluorescent complexes, one of which absorbs very much greater than the other at 355nm. As may be expected, a higher concentration of the greater absorbing component leads to problems in solving the lifetime of the minority species, due most probably to the masking of this species by the dominant component. For example, a 10:1 ratio of NH_2phen (400ns) to dpp (750ns), whose absorbances are at a ratio of 3:1 respectively at 355nm, the solving of the double exponential decay function with our model yielded two identical lifetimes close to that of NH_2phen i.e. approximately 400ns, indicating single exponential decay.

In conclusion, this model used shows certain limits and restrictions when one emitting species dominates greatly over the other, particularly in terms of absorbance, but this would not be expected to be a major factor in our solutions in this

thesis and hence permits us to assume our lifetime results reasonably accurate and reliable.

2.4.10. Molecular modelling.

Basic modelling of complexes and biomolecules was carried out using Hyperchem software. Molecular mechanics optimisation of complex structures was carried out using the Hyperchem Polak-Ribiere algorithm.

2.4.11 Stern-Volmer quenching studies.

The quenching rates of both the unbound labels and the bioconjugates by chemical denaturants were calculated by noting the height/area of the emission spectra of the quenched and unquenched after addition of increasing concentrations of quenching agents. In order to calculate the Stern-Volmer rate constant for every quenching agent, a plot of A_{NQ}/A_Q vs C_Q was obtained, where A_{NQ} = Area of emission spectrum of sample before addition of any quencher and A_Q = Area of emission spectrum after addition of X amount of quencher. This equation was also valid with the insertion of decay lifetimes rather than emission spectra areas/heights.

2.5. Biological procedures.

2.5.1 Buffers .

The buffers used were (a) 0.01M-0.10 M carbonate buffer, prepared from 0.01M-0.10 M sodium hydrogen carbonate/0.01M-0.10 M sodium carbonate in distilled water pHs 8.0-9.2 (b) 0.05-0.10 M phosphate buffer, pH 6.8 and 7.4, prepared from 0.05-0.10 M sodium dihydrogen phosphate/0.05-0.10 M di-sodium hydrogen phosphate in distilled water; (c) 0.05M-0.10 M acetate buffer pH 4.8, prepared from 0.05M-0.10 M glacial acetic acid/0.05M-0.10 M sodium acetate in distilled water and (d) Britton-Robinson buffer prepared from 0.04 M boric acid, 0.04 M phosphoric acid and 0.04 M glacial acetic acid in distilled water.

2.5.2. Estimation of the conjugation ratio.

The amount of ruthenium complex present was determined by its absorption at λ_{max} (450-480nm). The extinction coefficients of the unbound labels were previously measured in 0.10 M carbonate buffer pH 9.2 and no allowance was made for a change in the extinction coefficient upon binding to the biomolecules. The protein concentration was determined using methods subsequently described. The conjugation ratio was estimated according to Nairn [12], as described by equation 2.8 below:

$$\text{Moles Fluorochrome/Moles Protein} = x.\text{Abs.}/Cp \qquad (2.8)$$

where x = molecular weight of protein/extinction coefficient of label, Abs. = Absorbance of label at λ_{max}. and Cp = concentration of protein in mg/ml (as determined by protein assays described in 2.5.3.)

2.5.3 Determination of protein concentration.

Three methods were used to determine the amount of protein in the conjugate solutions.(a) The Folin-Lowry method [13] and (b) the Bradford method [14] were used in the determination of both PLL and bsa while (c) the glutamine/glutamate assay was employed specifically for the determination of PLGlu.

2.5.3.1 Folin-Lowry assay.

Standard protein solutions ranging from 0.0 to 0.20 mg/ml were prepared and suitable dilutions of the unknowns were made up. 5.0 ml of " alkaline solution " prepared from a 50:1 ratio of alkaline sodium carbonate solution (20g/l Na_2CO_3 in 0.10M NaOH) to copper sulphate-sodium potassium tartrate solution (5g/l $CuSO_4.5H_2O$ in 10g/l Na, K tartrate) was added, the solution was allowed to stand at room temperature for 10 minutes. 0.50 ml of 1:1 diluted Folin-Ciocalteu reagent was added with immediate mixing. After 30 mins the absorbance at 750nm was read. A standard curve was prepared and the protein concentration of the unknown sample was estimated.

2.5.3.2 The Bradford assay.

2.5 ml of the 1 in 5 diluted Bio-rad Bradford reagent was added to 0.10 ml of each sample/standard. The resulting solution was vortexed. The absorbance was read at 595 nm after 5 and before 60 minutes. The standard curve was plotted and the unknowns estimated.

2.5.3.3. Poly-glutamic acid assay.

A glutamine/glutamate determination kit based on the spectrophotometric measurement of L-glutamine and/or L-glutamate via enzymatic deamination of L-glutamine and dehydrogenation of L-glutamate with conversion of NAD^+ to NADH. was used to ascertain the amount of poly-l-glutamate in the bioconjugates prepared.

91

Materials:

(1) 1.0 ml of tris-EDTA-hydrazine buffer pH 9.0, prepared from a 1 in 19 ratio of hydrazine hydrate to tris-EDTA buffer, adjusted to pH 9.0)

(2) 0.10ml of 30mM β-Nicotinamide Adenine Dinucleotide (NAD) solution

(3)0.01 ml of 100 mM Adenosine 5'Diphosphate ADP solution.

Procedure.

Standard PLGlu solutions 0.0 to 0.5mg/ml were made up to 0.89 ml and added to solutions (1), (2) and (3), bringing the total reaction volume to 2.0 ml. Suitable dilutions of the unknowns were also prepared. The samples were mixed by inversion and their absorbances were read at 340 nm to obtain background reading. 0.02 ml of 1200 U/ml Glutamic Dehydrogenase (L-GLDH) was added to each sample, the solution again mixed by inversion and held at room temperature. The absorbances were read at 340 nm after 40 minutes until they remained constant. The background was subtracted from this for the net absorbance value. A graph of the poly-l-glutamate standards using mg/ml versus absorbance was drawn and the unknowns were determined from this graph.

2.5.4 Determination of lysozyme activity.

The enzymatic activity of lysozyme was measured by a modification of the assay developed by Shugar [15] and Perkins [16]. 0.02 ml of a 2 mg/ml lysozyme solution was added to 4.98 ml of a 40 mg/ml solution of *M. lysodeikticus* cells (or equivalent ratios), mixed for 10 seconds and then placed in a spectrophotometer. The decrease in turbidity at 450 nm was recorded at 30-second intervals for 3 minutes. The samples were mixed by inversion during the 30-second intervals. All results were expressed as the percent decrease in turbidity using the time zero turbidity to define the 100% level [17].

2.6   References.

[1]   C.D. Ellis, L.D. Margerum, R.W. Murray and T.J. Meyer, *Inorg. Chem.*, **1983**, 22, 1283.

[2]   E.M. Ryan, Ph.D Thesis, Dublin City University, Dublin, Ireland, **1991**.

[3]   G. Sprintschnik, H.W. Sprintschnik, P.P Kirsch and D.G Whitten, *J. Amer. Chem. Soc.*, **1977**, 99, 4947.

[4]   A.J. Bard, Luminescent Metal Chelate Labels and Means for Detection, U.S. Patent Application Number, PCT/US85/02153, **1986.**

[5]   J.N. Demas and G.A. Crosby, *J. Phys. Chem.*, **1971**, 75, 8, 991.

[6]   K. Makamura, *Bull. Chem. Soc. Japn.*, **1982**, 55, 2697.

[7]   J.N. Demas, Excited State Lifetime Measurements, Academic Press, London, **1983**.

[8]   P. Tijssen, Practice and Theory of Enzyme Immunoassays, Elsevier, New York, **1985**.

[9]   G.A. Means and R.E. Feeney, *Bioconj.Chem.*,**1990**, 1, 2.

[10]   D.J. Shannessy and R.H. Quarles, *J. Appl. Biochem.*, **1985**, 7, 347.

[11]   E.M. Ryan, R. O'Kennedy, M.M. Feeney, J.M. Kelly and J.G. Vos, *Bioconj. Chem.*, **1992**, 3, 285.

[12]   R.C. Nairn, Fluorescent Protein Tracing, 4th edition, Churchill Livingstone, New York, **1976**.

[13]   G.L. Peterson, *Anal Biochem.*, **1979**, 100, 201.

[14]   M.M. Bradford, *Anal. Biochem.*, **1976**, 72, 248.

[15]   D. Shugar, *Biochim. Biophys. Acta*, **1952**, 8, 302.

[16]   H.R. Perkins, *Royal Soc. Lond. Proc.*, **1967**, 167, 443.

[17]   B.L. Steadman, K.C. Thompson, C.R. Middaugh, K. Matsuno, S. Vrona, E.Q. Lawson and R.V. Lewis, *Biotech. Bioeng.*, **1992**, 40, 8.

Chapter 3.

Characterisation of Ru(II) polypyridyl complexes covalently bound to biomolecules.

3.1 Introduction.

In chapter 2, we described the procedures involved firstly in the preparation of various ruthenium polypyridyl complexes to be used as fluorescent labels, and secondly in their conjugation to selected biomolecules. Before one can apply these fluorescent complexes as probes of the dynamic behaviour of proteins, by using certain photophysical properties as the sensitive reporters, extensive characterisation of both the free labels and their protein-bound forms is necessary.

Firstly, the purity of the conjugates must be ascertained as one of the requirements of a good fluorescent probe is one which can easily be separated from the unbound label [1]. Otherwise, the photophysical properties of the free label may interfere with those of the bound form. One must also know how the spectroscopic properties of the ruthenium complexes are affected by their subsequent binding to biomolecules, hence the extensive characterisation of both forms. Finally, in order to understand the limits of the probes, one must verify the exact positioning of the labels on the protein and their affinity to the protein. For this reason, extensive studies regarding the effect of various conditions on the extent of various conjugation reactions were carried out.

This chapter will therefore deal with the chemical and biological characterisation of both the unbound ruthenium polypyridyl complexes and their corresponding bio-conjugate forms.

Compounds of the type $[Ru(L-L)_2(NH_2phen)]^{2+}$ and their isothiocyanate derivatives $[Ru(L-L)_2NCSphen]^{2+}$, where L = 2-2' bipyridyl (bpy), 1,10-phenanthroline (phen) and 4,7'-diphenyl-1,10'-phenanthroline (dpp), in addition to $[Ru(bpy)_2(COOH_2bpy)]^{2+}$ where $COOH_2bpy$ = 4,4'-dicarboxylic acid-2,2'-bipyridine and its succinimide ester derivative $[Ru(bpy)_2(esterbpy)]^{2+}$ were extensively characterised using chromatography, NMR, UV/vis, IR spectroscopy and fluorescence spectroscopy. The structures of some of the above mentioned complexes are depicted in Figure 3.1.
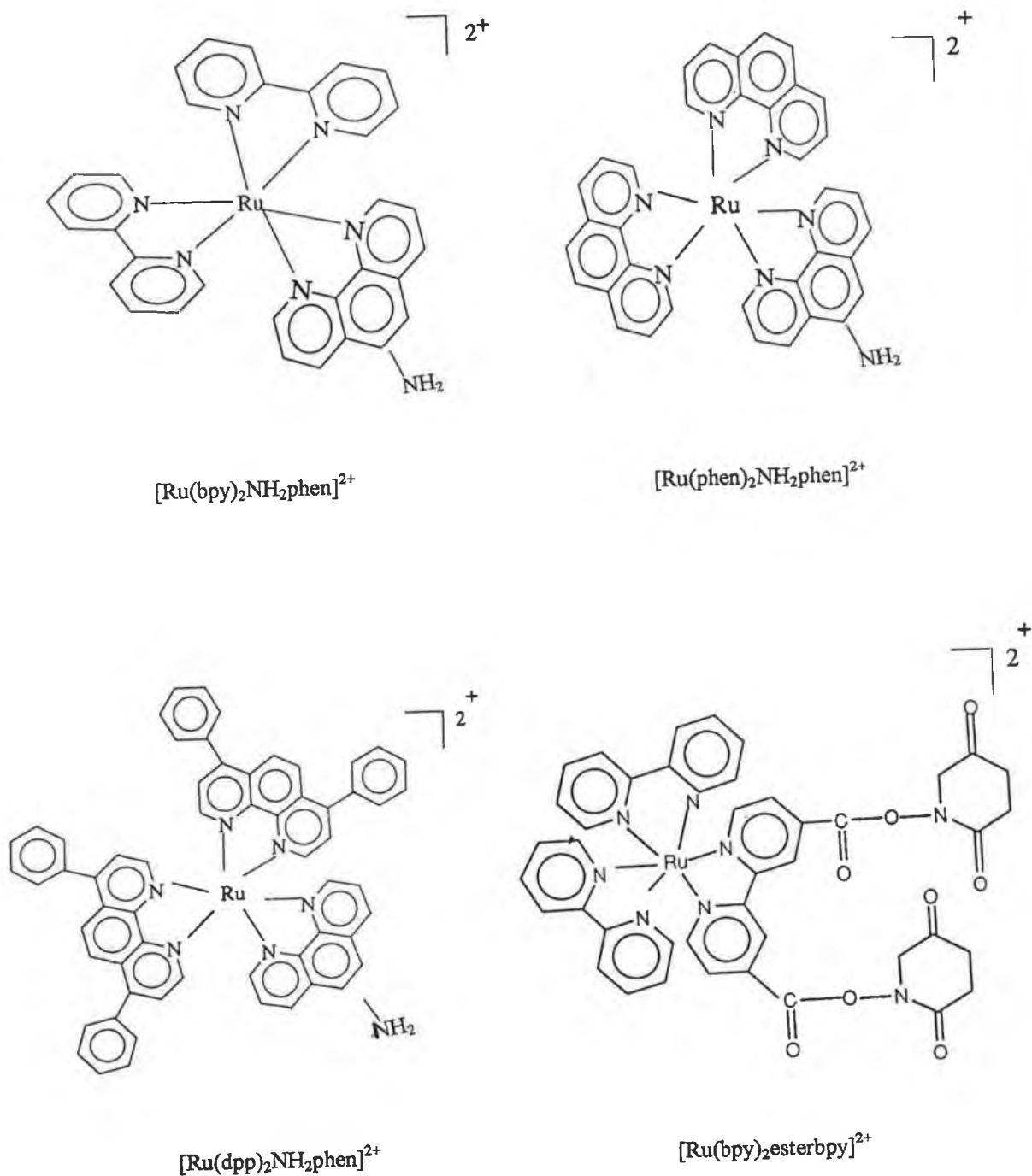
[Ru(bpy)$_2$NH$_2$phen]$^{2+}$

[Ru(phen)$_2$NH$_2$phen]$^{2+}$

[Ru(dpp)$_2$NH$_2$phen]$^{2+}$

[Ru(bpy)$_2$esterbpy]$^{2+}$

Figure 3.1 The structures of the Ru(II) polypyridyl complexes studied in this chapter.

Most of these same methods were used to characterise the protein-bound forms of these complexes where feasible, to investigate the effects of the binding to biomolecules on the spectroscopic properties of these fluorescent labels. In addition, the extent of the various conjugation reactions carried out was determined for all bioconjugates to examine the success of the various conjugation procedures. Finally the effect of the reaction conditions, the size and nature of the labels, the binding sites of the biomolecules chosen and the protein structure, on the conjugation ratio were investigated to more clearly understand the conjugation processes.

Below is a summary of all labels used and their various protein-bound forms, specifying the site of attachment of the labels on the biomolecule prepared. These compounds are listed in numerical order for further reference. Before the characterisation of the bioconjugates prepared is discussed, an introduction into the most widely used characterisation methods of proteins is appropriate.

Table 3.1. **Table of complexes and bioconjugates cited in this text**.

Ref. No. Complex	Ref. No.	Conjugate	Protein binding site
1. $[Ru(L-L)_2(NH_2phen)]^{2+}$	1a.	$Ru(L-L)_2(NH_2phen)^{2+}$: BSA	Carbohydrate moieties.
	1b.	$Ru(L-L)_2(NH_2phen)^{2+}$: BSA	Glutamic acid residues.
	1c.	$Ru(L-L)_2(NH_2phen)^{2+}$: IgG	Carbohydrate moieties.
	1d.	$Ru(L-L)_2(NH_2phen)^{2+}$: PLL	Terminal carboxylic acid.
	1e.	$Ru(L-L)_2(NH_2phen)^{2+}$: PLGlu	Glutamic acid residues.
2. $[Ru(L-L)_2(NCSphen)]^{2+}$	2a.	$Ru(L-L)_2(NCSphen)^{2+}$: PLL/BSA	Lysine residues.
	2b.	$Ru(L-L)_2(NCSphen)^{2+}$: PLGlu	Terminal amine.
3. $[Ru(bpy)_2(esterbpy)]^{2+}$	3a.	$[Ru(bpy)_2(esterbpy)]^{2+}$: PLL/BSA	Lysine residues.

3.1.1 Characterisation methods of proteins.

Various methods are used to characterise and/or follow changes in protein structure, which is indeed the eventual aim of this thesis, based on changes in their physical and chemical properties. Such variables include their hydrodynamic, spectral and chemical properties. Based on their hydrodynamic properties, one can study the folded state from their compactness, that is, their lower resistance to movement through the solvent, thus lower viscosity and greater rates of both translational and rotational movement and of sedimentation [2]. Due to a variety of environments of the chromophores of a folded protein and unique stereochemistry of the polypeptide chain, various spectral effects can be readily used to characterise, as well as to follow changes in the folded conformation in solution.

The absorbance of UV light is not very sensitive to conformation or environment, except for aromatic rings, such as phenylanaline, thyrosine and tryptophan residues where a shift in absorbance to a longer wavelength is observed in non-polar environments (i.e. the interior of proteins) and also when buried. This absorbance is not sensitive to changes in solvent, whereas that of aromatic groups on the surface may be perturbed significantly by the addition of glycerol, ethylene glycol and sucrose [2].

Fluorescence by aromatic groups is a much more sensitive method where the quantum yield may be either increased or reduced upon folding, a folded protein may therefore have higher or lower fluorescence intensity than the unfolded form. The close proximity of the aromatic groups in folded proteins usually results in very efficient energy transfer between them, therefore light absorbed by one chromophore may be transferred to another at higher wavelength, resulting in fluorescence [2].

Another spectral property which may be directly sensitive to polypeptide conformation is the optical rotatory dispersion of a polypeptide/protein, which can be studied by circular dichroism (CD). The polypeptide backbone absorbs, and is optically active in the far UV region, 240nm, with the magnitude of absorbance somewhat dependent upon conformation. These spectral characteristics are primarily

detected by polypeptide backbone conformation, especially secondary structure [3]. Figure 3.2 shows the CD spectra of poly-l-lysine (PLL) in α-helical, β and random-coil conformation [4]. This reflects primarily the conformation of the backbone. Folded proteins generally have significant absorbance in the near UV region owing primarily to the presence of aromatic side chains in assymetric environments.

Proton NMR is used to study protein structure in solution whereby different types of secondary structure are detected as the magnitude of specific interaction between hydrogen atoms depends upon the distance between them. Since specific interaction also occurs between atoms close in space but non covalently bonded, this provides semi-quantitative information about folded conformations [5].

The unique environment of reactive groups in folded proteins can have very substantial effects on their chemical properties. Notably, the environment can have an effect on the electronic state of the group, that is, its intrinsic reactivity or the steric effects on access to modifying reagents [2].
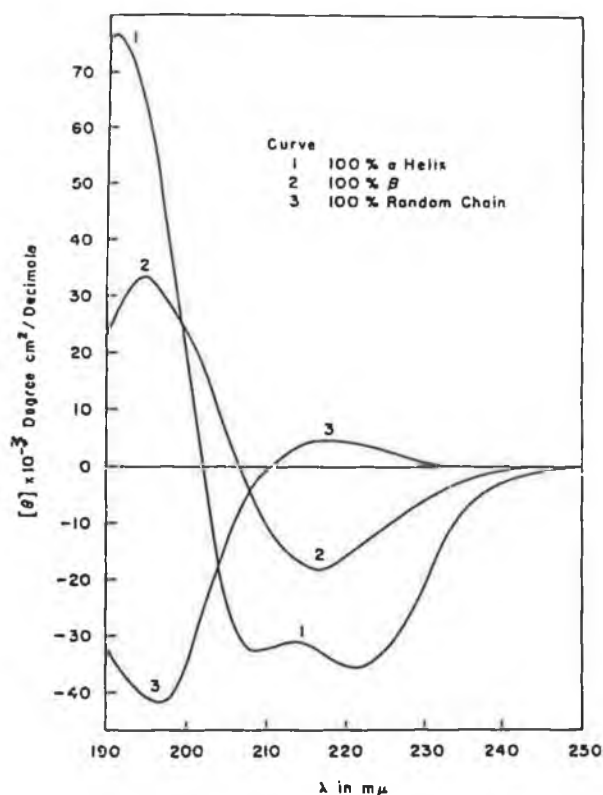

Figure 3.2 CD spectra of PLL in random-coil, β and α-helix conformation [4].

99

Such reagents include 2,4,6-trinitrobenzene sulfonate (TNBS) used to quantitate amino groups of the basic amino acid residues of proteins, such as lysine and arginine residues. This is accomplished via the spectrophotometric appearance of a new derivative which absorbs strongly at 367 nm [2].

Altered intrinsic reactivities of functional groups are often apparent from the perturbation of their pK_a values, which are affected by a wide variety of environmental and electrostatic effects. The titration behaviour of many proteins can be studied and followed by NMR [2]. pK_a values of different amino acid residues can vary widely, often over a range of 3-4 pH units (presumably owing to their different environments). Electrostatic interactions between such various groups can make their ionisation behaviour quite complex with unusual titration curves, since the pK_a values of a group will depend upon the ionisation of its neighbours [2].

The flexibility of protein structure can also be observed by various methods. Hydrogen exchange provides evidence for the mobility of the protein structure, as the internal groups of proteins react at a finite rate [2]. Aromatic side chains on the surface of a protein are quenched by diffusion controlled encounters with small molecules such as O_2 but also many internal residues are quenched only slightly less efficiently by neutral molecules, suggesting that they can diffuse through the interiors of proteins [2]. Such studies of fluorescence quenching of proteins are complicated by many factors, including varying quantum yields and possible energy transfer between different groups within the protein. Side chains on the surfaces of proteins have mobilities comparable to those in unfolded proteins, rotating at 10^{-11} to 10^{-8} sec. [2]. Such phenomena can be observed by fluorescence depolarisation, discussed in chapter 5.

X-ray diffraction is the only technique at present that can provide detailed structural information at an atomic scale. By collecting diffraction data over a range of temperatures or by using short pulse x-ray sources, one can learn something about dynamic aspects of the protein structure, averaged out by traditional methods [6]. Recently, protein secondary structure has been studied by fourier transform infrared/photoacoustic spectroscopy [7]. For secondary structure studies, the amide I

band (i.e. C=O structural vibration of the polypeptide backbone) is the most useful. Correlations between frequency and intensity of these bands with the various types of secondary structure of polypeptides such as α-helix and β-sheet, turns and random structures have been established, thus yielding quantitative estimation of protein secondary structure [7]. Photo-acoustic spectroscopy is suited because of its high sensitivity and it can be directly applied to solid samples. However, its usefulness for the study of protein secondary structure has not as yet been extensively explored.

A technique useful for experimental investigation of the energetics of folding/unfolding is direct scanning calorimetry (D.S.C.) which renders the direct determination and energetic description of protein folding possible. Protein folding/unfolding experiments are routinely conducted under conditions of reduced native state stability, which can be achieved by alteration of solution pH, the addition of chemical denaturants, or the chemical modification of proteins [8]. Because their unfolding is accompanied by positive heat capacity change, proteins can exhibit what is called cold denaturation (unfolding upon a decrease in temperature) [8].

Protein modelling by computer graphics is a modern method whereby protein structures can be fitted to electron density map by simultaneously displaying both with an interactive colour graphics program [6]. Much of the theoretical work on protein structure has concerned itself with attempting to accurately predict the final 3-D conformation of a protein from its amino acid sequence [6]. It is, however, only in recent years that significant progress has been made in obtaining detailed structural information on proteins using such a method.

In this chapter, no such modern techniques to characterise the dynamic aspects of proteins are used as the primary objective is to monitor how the luminescence behaviour of our fluorescent ruthenium complexes are affected by local structural variations of the bound biopolymer. However, such methods would have been useful in verifying that any changes in normal luminescence properties of the labels were indeed due to subsequent distortions induced in the covalently bound protein.

3.2. Results and discussion.

3.2.1. Chromatographic characterisation.

(1) High performance liquid chromatography (HPLC).

HPLC was used to characterise the unbound ruthenium polypyridyl complexes. The purity of the amino and isothiocyanate compounds was analysed using the HPLC method described in Section 2.2.3, while $[Ru(bpy)_2(COOH_2bpy)]^{2+}$ and its "active ester" were analysed using the same mobile phase at a lower pH of 2-3 using perchloric acid. The retention times of each compound are listed in Table 3.2.

Table 3.2 Retention times for the ruthenium polypyridyl compounds using HPLC.

Compound	Retention Time (min.)
$[Ru(bpy)_2(NH_2phen)](PF_6)_2$	3.34
$[Ru(bpy)_2(NCSphen)](PF_6)_2$	2.53
$[Ru(phen)_2(NH_2phen)](PF_6)_2$	2.58
$[Ru(phen)_2(NCSphen)]Cl_2$	2.10
$[Ru(dpp)_2(NH_2phen)]Cl_2$	1.65
$[Ru(dpp)_2(NCSphen)](PF_6)_2$	1.50
$[Ru(bpy)_2(COOH_2bpy)]^{2+}$	3.20
$[Ru(bpy)_2(esterbpy)]^{2+}$	3.00

Retention times of the compounds as listed above after separation in 80:20 $CH_3CN:H_2O$, with 0.10 M $LiClO_4$ as mobile phase. The flow rate was 2.5 ml/min.

The amino compounds were found to be 100% pure by HPLC after recrystallisation. The HPLC analysis of the isothiocyanate compounds [Ru(L-L)$_2$NCSphen](PF$_6$)$_2$ revealed impurities of approximately 2% , in some cases, which were due to the precursor amino compound as found in the literature [9]. However, these compounds were not recrystallised due to their instability in aqueous solution, and hence were used in their unrecrystallised forms for subsequent characterisation and conjugation procedures. The two isothiocyanate derivatives, [Ru(phen)$_2$NCSphen]$^{2+}$ and [Ru(dpp)$_2$NCSphen]$^{2+}$ were isolated as the dichloride salts while [Ru(bpy)$_2$NCSphen]$^{2+}$ was isolated as the PF$_6$ salt form.

(2) Size exclusion chromatography

Although some of the conjugates studied herein have previously been characterised, no attempts have been made to determine their purity, which upto now has been somewhat assumed [9]. As such assumptions need to be verified to determine the potential of our probes when bound to biomolecules, a method has been developed which allows the separation and identification of such conjugates using a size exclusion chromatographic technique.

The purity of the aqueous bio-conjugates prepared was determined using the size exclusion chromatographic technique described in section 2.2.4. There were two ultimate objectives behind using this technique. Firstly, it is obviously necessary to verify the success of dialysis as a means of purification i.e. to ensure that no free label is present in the conjugate solution. This is crucial if we wish to compare the photophysical properties of the protein-bound label to those of the unbound label. Secondly, it is necessary to be able to differentiate between the free protein and its modified form to ensure that the label is not merely bound to the protein electrostatically but indeed covalently bound. One may also be able to differentiate between various covalently modified proteins due to varying extents of modification.

Gel permeation chromatography, a particular type of size exclusion chromatography is a separation technique based on the application of a pressure to force macromolecules in solution form through a chromatographic column filled with porous beads [10]. The larger polymer molecules tend not to enter the pores of the beads and so pass through the column relatively quickly, whereas the smaller polymer molecules tend to diffuse through the pore structure of the beads and so take longer to pass through the column [10]. The eluted polymer is detected by its absorption in the UV region, say 215 nm where proteins absorb strongly. The relationship between retention time and relative molecular mass can be determined by calibrating the apparatus with polymer fractions, previously characterised by other methods, such as osmotic pressure, light scattering or viscosity [10]. However, for the purpose of our studies, qualitative analysis is adequate.

Based on this mechanism of separation, the larger macromolecules, in this case, the proteins, ranging in molecular mass from 65,000 to 100,000 should elute first with the free ruthenium complexes of molecular weights ranging from 900 to 1300 being eluted at a significantly slower rate. Indeed, on covalently binding the labels to the proteins, a further increase in size of the modified protein should be detected by a faster retention time. Depending on the sensitivity and resolution of the column used, it may also be possible to separate the same protein, modified to varying degrees due to different loadings of label bound to the biopolymer.

The retention time of each bioconjugate prepared is listed and is compared to the retention time of the appropriate free label and unconjugated protein in Table 3.3. From this table, we see that S.E.C. can indeed be used to substantiate the conjugation of the biomolecules in question, as it is possible to distinguish between unmodified and modified protein. In most cases, the difference in retention time between free and conjugated protein is less than one minute. As indicated previously, it may be theoretically possible to estimate the degree of conjugation of each protein, as through appropriate calibration, one could equate a certain decrease in retention time to a particular increase in molecular weight. From this, the number of labels bound could be calculated and the results obtained could be used to verify the real

conjugation ratios as calculated according to Nairn [1]. This would be useful as the method by Nairn does not take into account the presence of non-covalently bound label. Such quantitative analysis was not undertaken but is a possibility in further studies.

As outlined in Table 3.3, the retention times of the free labels studied are in the range 15 to 17 minutes, corresponding to molecular weights of the range 900 to 1250. In contrast, the proteins of molecular weights 60,000 to 100,000 are eluted more quickly, all eluting after approximately 8-10 min. The chromatogram typical of the protein BSA is depicted in Figure 3.3.

Table 3.3. Retention times of free Ru(II) complexes and proteins, and the conjugated proteins using size exclusion chromatography.

Complex/protein/conjugate		Retention Time (min)		
		L=bpy	L=phen	L=dpp
BSA	9.50			
PLL	9.20			
PLGlu	9.0			
$[Ru(L-L)_2NH_2phen]^{2+}$		16.2	16.0	16.0
$[Ru(L-L)_2NCSphen]^{2+}$		16.5	16.4	15.9
$[Ru(L-L)_2NH_2phen:PLGlu$		7.2	7.1	8.5
$[Ru(L-L)_2NH_2phen:PLL$		9.2	8.9	8.6
$[Ru(L-L)_2NH_2phen:BSA$ (1)		8.3	9.2	7.6
(2)		8.0	8.2	8.4
$[Ru(L-L)_2NCSphen:PLL$		8.1	9.0	8.6
$[Ru(L-L)_2NCSphen:PLGlu$		9.5	9.2	8.8
$[Ru(L-L)_2NCSphen:BSA$		8.9	8.0	7.6

Mobile phase used was 0.05M phosphate buffer pH 6.8.

Flow rate of 1.0 ml/min and the detector wavelength used was 215 nm.

As was found for all the biomolecules studied, the chromatogram of BSA reveals the presence of more than one peak. This may be due to presence of impurities or in the case of the protein BSA may be due to the proteins various separate components or subunits. However, in all such cases the predominant peak is the one which is listed and is used for reference. The primary objective in this section is the verification of the covalent modification of the proteins by the Ru(II) complexes and thereby to confirm the success of the conjugation procedures developed. As stressed earlier, this is possible by observing the shifts in the retention times of the proteins when the labels are covalently linked. On studying the chromatograms of several labelled proteins the retention time of the main peak of BSA is reduced on binding to labels as anticipated. One of the most significant shifts in retention time is achieved when $[Ru(dpp)_2NH_2phen]^{2+}$ labels are bound to BSA via glutamic acid residues, indicating that a large number of such labels bind to BSA in this manner and this chromatogram is displayed in Figure 3.4. Figure 3.4 demonstrates how the primary absorption peak of BSA of approximately 9.5 min is now apparent at a shorter retention time of 8.8 min. Again the smaller peaks at 12.0 min and 13.8 min may be impurities of the protein and do not appear to be due to free label because of their shorter retention time.

Another main objective of this study is the verification of the purity of such conjugates, thus ensuring that no free label is still present in the conjugate solution but that this indeed has been removed by dialysis as anticipated. It should therefore be possible to distinguish between free label, free protein and the covalently modified protein due to differences in their degree of retention in the separating column. For the purpose of this study and in an attempt to identify any unknown peaks the chromatogram of a conjugate is run and the peaks obtained are compared to those of the chromatogram of the same conjugate but with free ruthenium complex and/or free protein added to the sample. This should allow one to identify peaks due to free protein and/or free label in the chromatogram of the conjugate. As an example, Figure 3.5 depicts the chromatogram of $Ru(dpp)_2NCSphen:BSA$, while
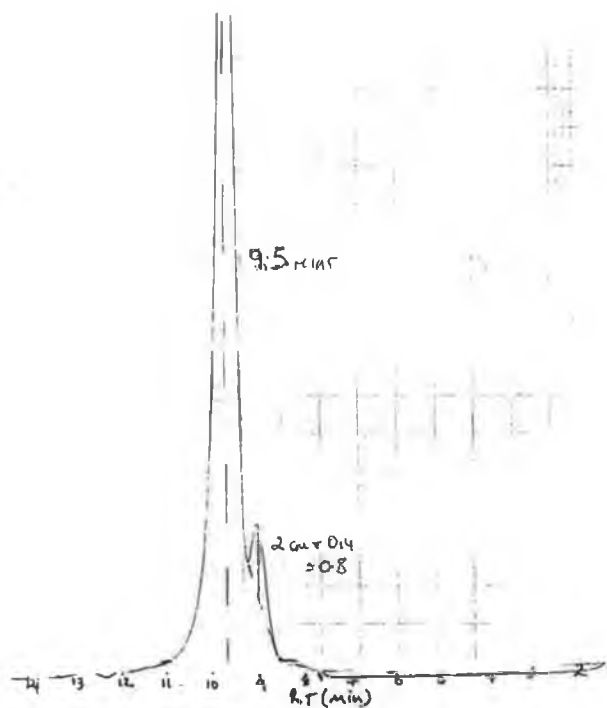
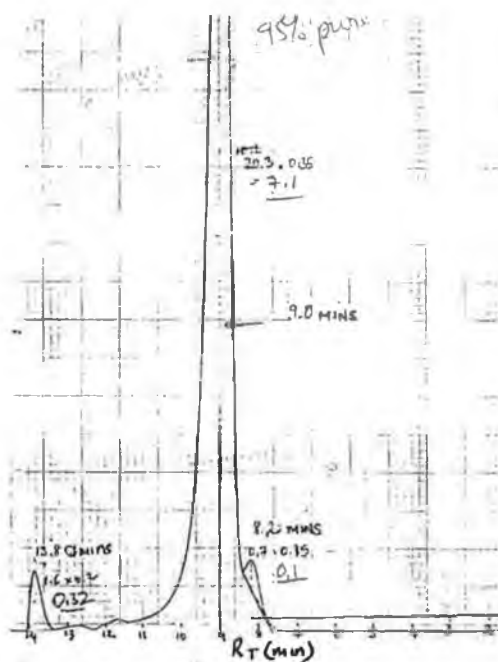*Figure 3.3 Typical chromatogram of BSA using size exclusion chromatography.*

Figure 3.4 Typical chromatogram of [Ru(dpp)$_2$NH$_2$phen:BSA (b) using size exclusion chromatography.

Figure 3.6 represents that of the same conjugate spiked with free label i.e [Ru(dpp)$_2$NCSphen]$^{2+}$. On comparing both chromatograms the primary absorption peak for the conjugate is unaffected at 8.9 min which would be anticipated as the conjugate should not be affected by the addition of ruthenium complex as this would not be covalently bound to the protein. There are also small peaks at 12.5 min and 14 min, the nature of which is uncertain. However, on adding the unbound label (See Figure 3.6) a significant peak appears in the chromatogram after approximately 18.5 min. Although this retention time does not correspond exactly to that of [Ru(dpp)$_2$NCSphen]$^{2+}$ (See Table 3.3), it is evident that this peak must be due to this label. Hence it would appear that the conjugate Ru(dpp)$_2$NCSphen:BSA does not contain impurites due to unbound label as no peak is evident in the range 16-20 min thereby confirming the usefulness of such studies in the identification of various peaks and the verification of the purity of a conjugate.

It must be noted that most chromatograms revealed small amounts of impurities due to free label, protein and other unidentified impurities, but for the purpose of our work the conjugates were deemed adequately pure for further studies. It would be difficult to determine the percentage purity of the conjugates from the chromatograms at the conditions used. This is because at 215nm both label and protein absorb strongly. In order to estimate the quantity of unbound label a wavelength unique to the absorption spectrum of the label would be necessary, eg 450 nm. This was not done however and hence rough estimates of the purity were made by comparing the peak sizes. In Table 3.3 the retention time of the predominant peak of each sample is listed for simplification.

It should also be possible to distinguish between biomolecules labelled to varying extents, due to contrasting increases in their molecular mass. However the difference in retention time would be minimal and hence this was not attempted.

It must be emphasised that these preliminary studies are merely an introduction into SEC and the results achieved are simplified. However initial results appear quite promising, allowing the separation of pure and labelled proteins and hence open the door to more advanced and complete analysis in future studies.

108
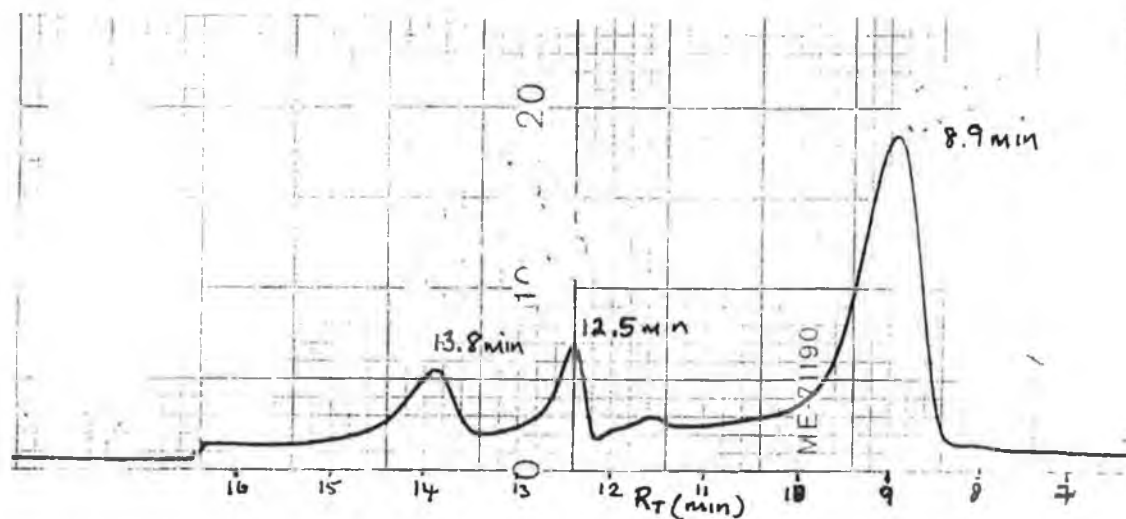
Figure 3.5 Typical chromatogram of Ru(dpp)₂NCSphen:BSA using size exclusion chromatography.
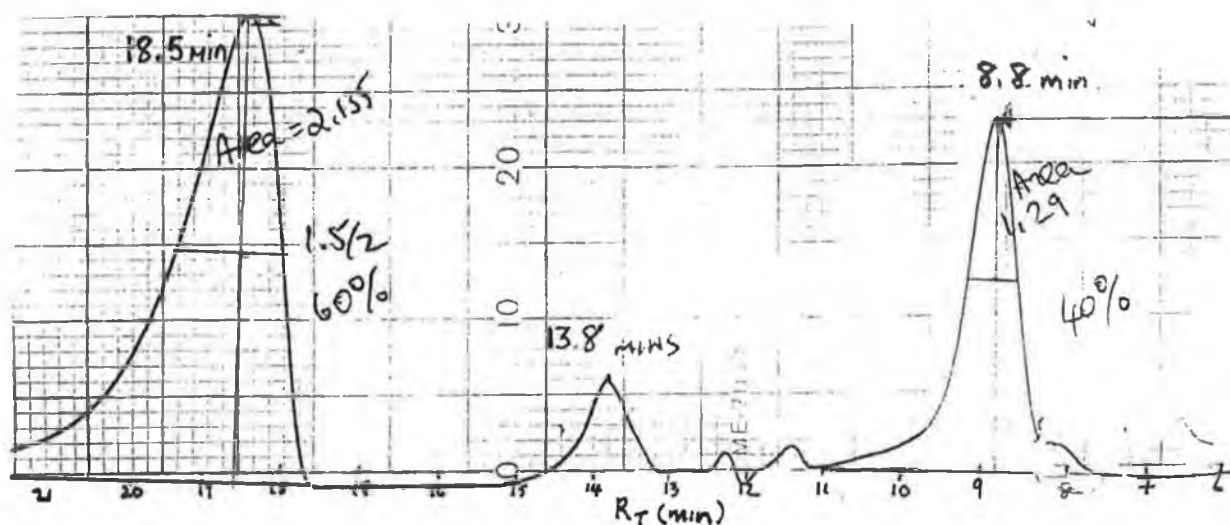
Figure 3.6 Typical chromatogram of Ru(dpp)₂NCS₂phen:BSA spiked with unbound label [Ru(dpp)₂NCS₂phen]²⁺ using size exclusion chromatography.

109

3.2.2. Infra-red spectroscopy.

Infra-red spectra were used in a purely qualitative manner to ensure the success of the derivatisation of the amino compounds to their respective isothiocyanate complexes, as the presence of the isothiocyanate group was confirmed by the presence of an infra-red band at about 2050cm^{-1}. The infra-red spectrum of the acidic complex [Ru(bpy)$_2$(COOH$_2$bpy)]$^{2+}$ was also obtained for characterisation purposes and is presented in Figure 3.7. The bands at 3400 cm^{-1} and 1650 cm^{-1} are typical of carboxylic acids. Meanwhile, Figure 3.8 depicts the infra-red spectrum typical of [Ru(dpp)$_2$(NH$_2$phen)]$^{2+}$ while that of its isothiocyanate derivative is presented in Figure 3.9.
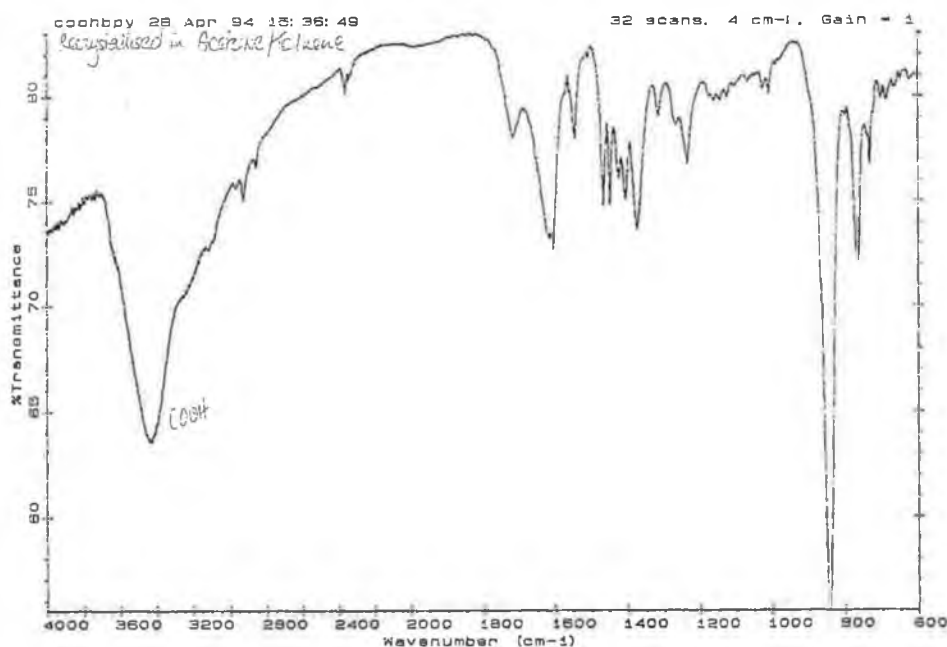
Figure 3.7. Infra-red spectrum of [Ru(bpy)$_2$(COOH$_2$bpy)]$^{2+}$

110
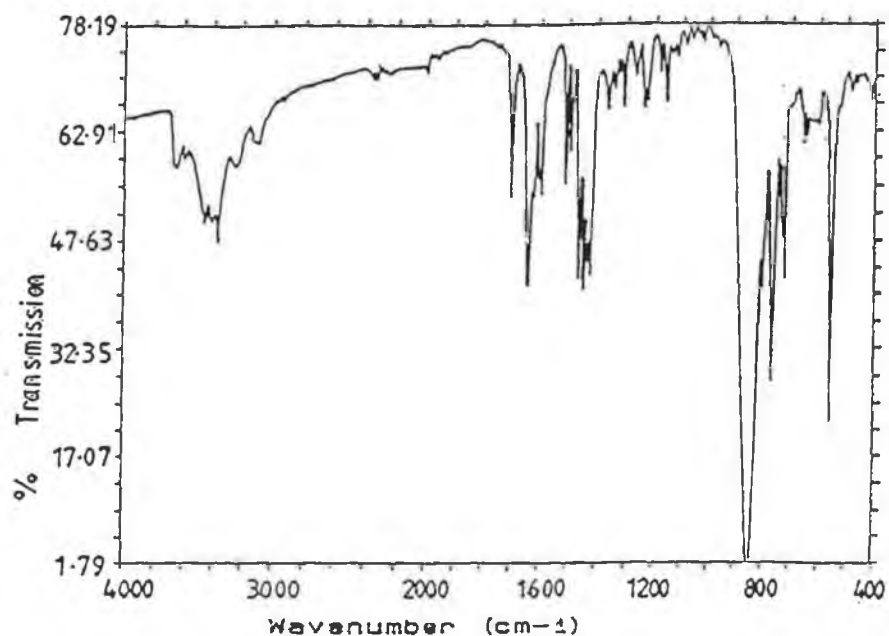
Figure 3.8. Infra-red spectrum of [Ru(dpp)$_2$(NH$_2$phen)(PF$_6$)$_2$].
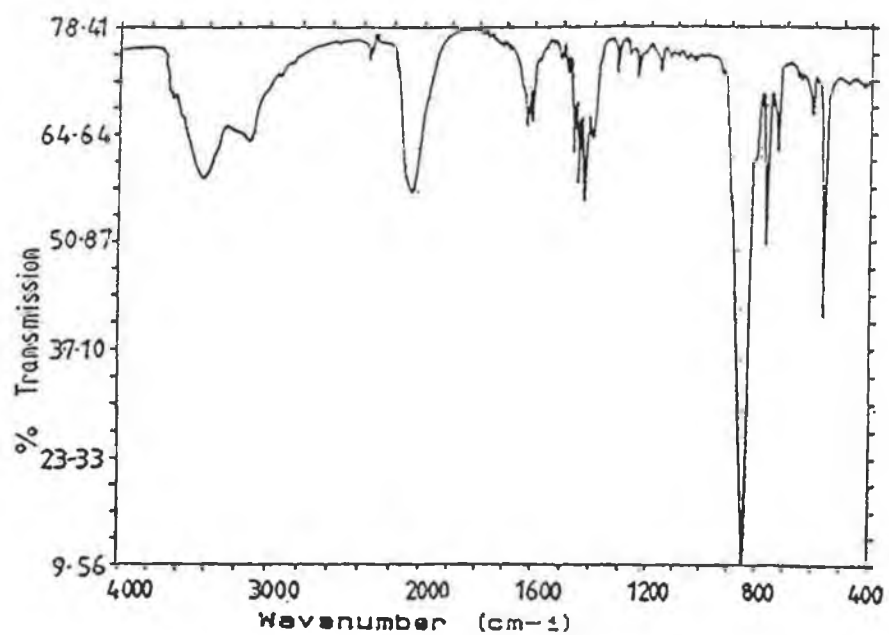
Figure 3.9. Infra-red spectrum of [Ru(dpp)$_2$(NCSphen)Cl$_2$].

3.2.3. Proton nuclear magnetic resonance spectroscopy.

The proton resonance signals obtained for the compounds have been assigned to the different protons by comparison with the literature for similar compounds [9]. NMR studies were essentially used to ascertain the purity of the ruthenium complexes prepared and to verify the formation of the isothiocyanate derivatives of the amino complexes studied.

The proton resonance signals of the compounds [Ru(bpy)$_2$(NH$_2$phen)](PF$_6$)$_2$] [Ru(phen)$_2$(NH$_2$phen)](PF$_6$)$_2$] and [Ru(dpp)$_2$(NH$_2$phen)](PF$_6$)$_2$] are reported in the literature [9]. As an example, the NMR spectrum of [Ru(bpy)$_2$(NH$_2$phen)](PF$_6$)$_2$] is depicted in Figure 3.10.
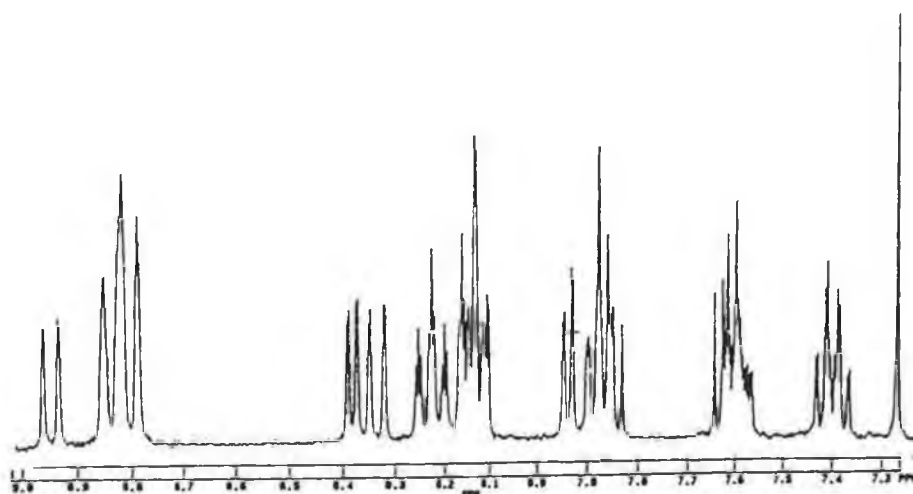
Figure 3.10. NMR spectrum of the complex [Ru(bpy)$_2$(NH$_2$phen)]$^{2+}$.

The NMR spectra of the isothiocyanate compounds were not assigned due to possible impurities of their amino precursors. Below, the NMR spectrum of the complex $[Ru(bpy)_2(COOH_2bpy)]^{2-}$ is depicted in Figure 3.11. Again, the proton resonance signals obtained for this compound have been assigned to the different protons by comparison with the literature [9]. The NMR spectrum of its hydroxysuccinimide ester was not however carried out as this complex was not isolated but remained in solution form.
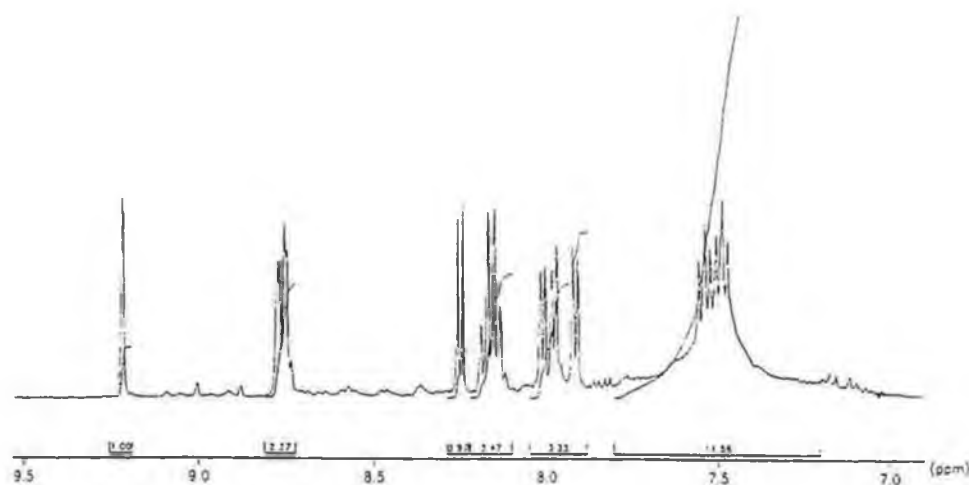
Figure 3.11. NMR spectrum of the complex $[Ru(bpy)_2(COOH_2bpy)]^{2-}$.

113

3.2.4. Determination of extent of conjugation reactions.

3.2.4.1. Introduction.

In this thesis, the conjugation of ruthenium polypyridyl complexes to various bio-molecules is carried out. The complexes have been bound at different sites on these biomolecules, using a variety of conjugation methods, the basis of which are discussed in Section 1.3.5.1. In Chapter 1, the difference between site-selective and side chain selective modifications of biomolecules is described. Much of the work carried out here involves side chain selective modification of the biomolecules in question, and as stressed earlier, under appropriate conditions, the reagents normally react only with the intended target side chain. An important point to be noted is the fact that complete modification of all targeted side chains in any conjugation reaction is not usually possible but the labelling efficiency does depend upon the protein, the modifying reagent and the reaction conditions [11], and these factors will be studied and discussed in this section.

In most cases, the extent of a conjugation reaction can be determined by either direct spectrophotometric measurements, amino acid analysis, or the use of radioactive reagents [11]. The extent of a reaction may often be increased by the use of more vigorous reaction conditions, for example, longer reaction times, larger excesses of reagent and the presence of denaturing agents such as urea. However, the use of more severe conditions usually leads to some decrease in side chain selectivity, greater risk of conformational change, and other disadvantages [11]. In this thesis, the methods chosen to measure the extent of the conjugation reactions involved direct spectrophotometric measurements. Three protein assays used to determine the concentration of protein in the bio-conjugate include the Folin-Lowry method [12], the Bradford method [13] and the glutamate assay kit, whose procedures are discussed in Section 2.3.4., while the conjugation ratios were calculated according to Nairn [1], as discussed in Section 2.3.3.

114

The Folin-Lowry method of protein determination is based on the Biuret reaction where proteins react with Cu^{2+} in an alkaline medium to produce Cu^+ and the detection of the phenolic moieties of tyrosine residues as well as the tryptophan residues by use of the Folin-Ciocalteu reagent, composed of phosphotungstic and phosphomolybdic acids [12]. The cupric ions form a coordination complex with the four nucleophilic amine groups from the peptide bonds, of the protein/PLL molecule. A Cu-protein/PLL complex yielded leads to the reduction of the phosphotungstic and phosphomolybdic acids to tungsten blue and molybdenum blue. Approximately 75% of this reduction process is due to the copper-protein complex, the remainder of which is due to tyrosine/tryptophan residues [12]. Therefore, the lysine residues are not involved in the protein binding process, which has significance, particularly in the accurate conjugation ratio determination of PLL.

The dye used in the Bradford assay is Coomasie Brilliant Blue G, and earlier reports suggest that the dye binds to the protein by electrostatic interactions of the sulphonic groups of the dye with protonated primary amino groups of the protein eg. lysine, N-terminal groups [14]. Other reports suggest an interaction with the arginine and lysine residues [15]. In any case, the dye appears to interact appreciably with lysine residues, which is to be noted, again particularly in the analysis of PLL, as this would lessen the effectiveness of this assay.

For the determination of the concentration of PLGlu, a glutamate/glutamine assay kit was employed which was based on the spectrophotometric measurement of poly-l-glutamate. The dehydrogenation of L-glutamate to α-ketoglutarate is accompanied by the conversion of NAD^+ to NADH [10], which can be subsequently measured spectrophotometrically and is proportional to the amount of glutamate that is oxidised.

Generally, modifications that have the least effect on side-chain character should have the least effect on protein structure and properties, which is an obvious priority in our study [11]. Modifications of lysine residues that retain their usual cationic charge have, for example, generally been found to have relatively little effect on the biological activities and other properties of many proteins. Because of this

115

and the fact that the ε-amino groups of lysine residues are usually among the most abundant and most accessible of the potentially reactive groups [16], the amino side group of the lysine residues are the side chains which are involved in much of the conjugation procedures of this thesis. Another side chain to be modified is the carboxylic acid side chain of glutamic acid residues, while site-selective modifications undertaken include the carbohydrate moieties of glycoproteins and the terminal amines and carboxylic acids of the polypeptide backbones of the biopolymers. The theory behind the various conjugation procedures used throughout this thesis is discussed in more depth in Section 1.3.5., while the procedures involved in carrying out such reactions are described in Section 2.3.2.

Initial studies were carried out in this area by Ryan, where the optimisation of conjugation conditions for some ruthenium-bound proteins was carried out [17]. The conjugation ratios of all bioconjugates prepared were determined in this thesis, rendering the comparison of the labelling efficiencies of various conjugation procedures possible. Furthermore the aim was to investigate the effects of the reaction conditions, (such as pH, temperature, reagents), as well as the structural forms of both the labels and the biomolecule on the reaction extents.

The effect of varying the nature and the size of the label, the structure of the protein and the exact binding site chosen on the protein on the extent of the conjugation reactions were investigated and are subsequently discussed.

3.2.4.2. Effect of original loading, label form and biomolecule.

Firstly, for most bioconjugates prepared, various loadings of ruthenium label were reacted with each biomolecule, and the resulting conjugation ratios of the bioconjugates determined. The biomolecules involved in such studies included the poly-amino acids, poly-l-lysine (PLL) and poly-l-glutamate (PLGlu), and the protein bovine serum albumin (BSA). In most cases initially, 10:1, 50:1 and 100:1 ratios of ruthenium label per protein molecule were originally reacted and the extent of the

116

reaction determined. $[Ru(bpy)_2NH_2phen]^{2+}$ was bound to PLGlu via the glutamic acid residues [1e], and to the protein BSA via the carbohydrate moieties [1a] while $[Ru(bpy)_2NCSphen]^{2+}$ was bound to both BSA and PLL via the lysine residues [2a]. The conjugation reaction conditions employed are discussed in Section 2.3.2. This study allowed us to compare the effectiveness of the different conjugation procedures and study the effect of the binding site and biomolecule form on the labelling efficiency as well as determining the reproducibility of initial work reported in the literature [9].

Table 3.4 lists the real conjugation ratios obtained for the $[Ru(bpy)_2(NCSphen)]^{2+}$-PLL conjugates [2a], while Table 3.5 lists the real conjugation ratios for the $[Ru(bpy)_2(NCSphen)]^{2+}$-BSA conjugates [2a]. Similarly, Table 3.6 represents such results for $[Ru(bpy)_2(NH_2phen)]^{2+}$-BSA [1a], each calculated using methods reported by Nairn [1] and Folin-Lowry [12].

The results presented in Table 3.4 show that, given that there are approximately 750 lysine residues on a PLL molecule, (molecular weight 109,000) the labelling efficiencies for each loading attempted are low. From an original loading of 10 moles of label per protein molecule, a final conjugation ratio of 5 was obtained, yielding a 50% labelling efficiency. This means that less than 1% of the total number of lysine residues in a PLL molecule have been covalently bound to the ruthenium labels, which is obviously a very low percentage. Of course, the labelling efficiencies have been calculated on the basis that all 750 lysine residues are available, which is never possible due to the conformation of the biomolecule, thereby increasing the actual labelling efficiency significantly. On attempting to bind 100 moles of label per PLL molecule, only 13 were found to actually bind, which is similar to the results achieved with a 50:1 loading. These low loadings only incorporate the modification of approximately 2% of the lysine residues present in a PLL molecule which appears minimal. These findings correlate well with initial reports from Ryan [9].

Hence, as can be seen from Table 3.4, the maximum conjugation ratios achieved for these PLL conjugates are between 10 and 15 moles of label per

biomolecule, achieved with initial loadings of 50-100:1. These low conjugation ratios would suggest that there is limited accessibility of the labels to the lysine moieties, most likely due to the structural conformation of the biopolymer, in this case PLL which will be studied in greater detail subsequently. Significantly, this study showed that attempting initial loadings beyond 100:1 ratios did not lead to higher conjugation ratios, as a saturation point appears to have been reached at loadings of 50-100:1. Furthermore, problems such as precipitation and other disadvantages are likely to increase, with too great an excess of reagents, thereby justifying our choice of 50:1 ratio as an optimum loading for further studies in this field. For this reason, a 50:1 loading was deemed suitable in the binding of the side chains of another poly-amino acid PLGlu. Even lower conjugation ratios are obtained for the PLGlu conjugates with a highest conjugation ratio of 5 achieved from an initial loading of 50:1. In addition to the hindering conformation of the biopolymer, another limiting factor in their modification would be the low reactivity of the carboxylic acids in the polypeptide in water [16]. For this reason, PLGlu was treated with a water soluble carbodiimide to activate these potential binding sites so that modification would be possible. However, the extent of the success of this activation reaction was not estimated and hence a low yield in this esterification process would result in fewer "available reactive binding sites" than originally anticipated. This is in contrast to the side chain modification of PLL where no prior activation of the lysine residues was necessary. This is due to the fact that the binding sites of these residues are more accessible due to the longer side chain length and the higher reactivity of their ε-amino groups thereby capable of reacting directly with the isothiocyanates to form stable thiourea bonds.

Another possible factor contributing to the low conjugation ratios of the poly-amino acids is the predominant conformation of the selected biomolecule, under the chosen reaction conditions. For example, PLL is known to adopt two different conformations, depending on the pH of the reaction. A helical form is adopted under basic conditions whereas a random coil structure is favoured under acidic and neutral conditions [10].

118

Table 3.4 Conjugation ratios obtained for various loadings of [Ru(bpy)$_2$ (NCSphen)]$^{2+}$:PLL conjugates.[2a]

Original ratio of Ru:PLL	Conjugation ratio (a)	Conjugation ratio (b)	Labelling efficiency[*] [(a)]	% lysines bound.[*] [(a)]
10:1	5	2	50%	< 1%
50:1	14	5	28%	2%
100:1	13	3	13%	2%

[*] *assuming there are 750 lysine residues per molecule of PLL (mol. wt. 109,000).*

(a) Protein concentration determined using the Folin-Lowry method [12].

(b) Protein concentration determined using the Bradford method [13].

Table 3.5 Conjugation ratios for various loadings of [Ru(bpy)$_2$(NCS phen)]$^{2+}$:BSA conjugates. [2a]

Original ratio of Ru:BSA	Conjugation ratio (a)	Conjugation ratio (b)	Labelling efficiency.	% lysines bound $
10:1	8	9	90%	15%
50:1	23	22	45%	45%
100:1	25	28	28%	50%

(a) Protein concentration calculated by Bradford method [13].

(b) Protein concentration calculated by Folin-Lowry method [12].

$ assuming 57 lysine residues per molecule of BSA [9].

Table 3.6 Conjugation ratios for [Ru(bpy)$_2$(NH$_2$phen)]$^{2+}$:BSA. conjugates. [1a]

Original Loading	Final Conjugation ratio (a)	Final Conjugation ratio (b)
10:1	3	5
50:1	4	4
100:1	4	5

(a) Protein concentration was determined by Bradford method [13].

(b) Protein concentration was determined by Folin-Lowry method [12].

In preliminary studies, pH 9 was deemed the optimum pH of conjugation [9, 17]. However at this pH, PLL is in a transition state, between the random-coil and α-helix conformations, and so may not be very reactive towards conjugation in this state, as well as being marginally stable. The same may be true of PLGlu, whose optimum pH for conjugation chosen as pH 4.8 (see section 1.4.4) is again in the pH range of the transition state. Hence, in later sections, similar conjugation reactions are carried out on regular biomolecules such as PLL, under different reaction conditions, such that the biomolecule is bound to the same labels when in different structural forms. This allows the investigation of how the secondary structure of a biomolecule may affect the extent of a particular conjugation reaction. Finally, another factor affecting the extent of a conjugation reaction may be the size and nature of the label, as steric hindrance of the ancillary ligands protruding from the backbone of the biomolecule may limit the number of labels which could bind to the biomolecule, in addition to the fact that some labels may be more reactive to certain modification sites than others, due to differences in hydrophobicity. From studying hyperchem structures of such PLL conjugates (see Chapter 5), however,

steric hindrance alone would not appear to be an adequate explanation for the low loadings achieved.

Moreover, to study the significance of the label structure and size, the same conjugation procedures were carried out, varying the ancillary ligands from bipyridine to phenanthroline to diphenylphenanthroline (i.e. increasing the bulkiness and hydrophobicity of the ancillary ligands) and the conjugation ratios compared and these experiments are described later in this chapter.

Table 3.5 presents the conjugation ratios achieved for $[Ru(bpy)_2NCSphen]^{2+}$ bound to the lysine residues of BSA [2a]. BSA was chosen for investigation as it is a natural protein with a more complex structure than synthetic polypeptides. This may give an insight into the effect of biomolecular form on the extent of conjugation reactions when bound to the same binding sites, as well as evaluating the potential of these labels in real biological processes.

At first glance, the loadings achieved may seem low, as for PLL. However, whereas the original 100:1 ratio yielded only a 13% labelling efficiency (13 moles of label per biomolecule) for PLL, the 100:1 ratio of BSA conjugate yielded almost 30% labelling efficiency. Also, significantly, there are only 57 lysine residues on the BSA molecule compared to 750 lysine residues per PLL molecule. Therefore, one would expect the conjugation ratios to be a lot higher for the PLL conjugates. This would seem to indicate that it is the structural form of PLL and/or the low reactivity of PLL towards the labels, that greatly restricts the number of fluorochromes which can bind to the lysine moieties of PLL. For both the PLL and BSA conjugates, the protein concentration was determined using both the Bradford method and the Folin-Lowry method. As for the PLL conjugates, the Bradford assay results in conjugation ratios that are lower than those obtained using the Folin-Lowry method, but one notes that the difference is greater for the PLL conjugates, due to the higher number of lysines. This correlates well with experiments of this kind in the literature, where the difference was explained in terms of where the reagents actually bind on the protein molecule [12, 14, 15]. The binding of the Bradford reagent to the lysine residues limits the validity of the results using this

method, particularly for PLL, as both the Bradford reagent and the Ru(II) complexes interact with the same groups on the protein/PLL molecule [15]. For this reason, the results discussed are those derived using the Folin-Lowry method of protein determination.

The labelling efficiencies achieved are quite high for BSA, with a maximum conjugation of 28 moles of label obtained, out of a possible 57 binding sites, hence 50% of all the lysine residues were modified. However, it is in fact known that less than half of these lysine residues are not available for reaction in albumins, although relatively hydrophilic, probably due to the complex structure of the folded protein [18], hence the labelling efficiency is actually much higher, approaching 100%. As the same labels and reaction conditions were used for PLL, it would appear that the variances in the secondary structures of PLL under the reaction conditions contribute significantly to such low conjugation ratios. Table 3.5 reveals a similar trend for these analogue BSA conjugates, whereby similar conjugation ratios were achieved starting from either 50:1 or 100:1 ratio of label to biomolecule. Again, the 50:1 loading was deemed optimum for further studies.

Table 3.6 presents similar data for $[Ru(bpy)_2NH_2phen]^{2+}$:BSA [1a] and again both the Bradford assay and the Folin-Lowry methods were used for analysis. In these cases, as the carbohydrate moieties have been modified, and these are not involved in the binding mechanisms of either the Bradford reagent or the Folin-Lowry reagents, both assays appear suitable for the determination of the protein concentration, and good correlation between both assays would be expected. Very similar results are indeed found, but for further work results from the Folin-Lowry method were employed.

The conjugation ratios are found to be somewhat lower than those obtained when labels were bound to the lysine residues of BSA [2a], with maximum conjugation ratios of 6 in this case compared to 23 previously (See Table 3.5). This however correlates well with initial studies in the literature [9], and would be expected, as the number of carbohydrate moieties in proteins such as albumins would be relatively small, fewer and less reactive than the lysine residues.

The protein BSA was treated, for this conjugation procedure as a glycoprotein. Other well known albumins such as ovalbumin are well recognised as glycoproteins, containing 1% by weight of carbohydrate where the oligosaccharide groups of most are covalently attached to the R groups of specific amino acid residues in the polypeptide chain [19]. Assuming the carbohydrates moieties are attached to BSA as to ovalbumin, they are found on the asparagine residues which are few in number but well spaced out on the BSA molecule. BSA, however, is not generally considered a glycoprotein, but for this purpose, was treated as such, and the above mentioned conjugation procedure was deemed to be successful for BSA. Although it is difficult for us to confirm the selective modification of the carbohydrate moieties in our case, using such a method, this procedure is specific for carbohydrate moieties and in the case of antibodies allows one to direct the label to a site removed from the antigen-binding region producing a more homogenously labelled antibody preparation [20].

For these conjugates, very similar results are achieved for initial loadings of both 50:1 and 100:1 and for further work the initial 50:1 loading was used, as beyond this ratio a saturation point is reached whereupon no corresponding increase in conjugation ratio is achieved and precipitation results. In brief, the low loadings achieved for the poly-amino acids as opposed to the natural proteins may be significant in learning more about the structures of such biopolymers in solution. However, the advantage of achieving such low loadings is that it renders studies on conformational changes more realistic since the presence of such few labels would have a minimal effect on the natural processes involved with biomolecules.

As mentioned earlier, to further our understanding and study the effect of both the reactivity and size of the labels on the extent of conjugation reactions, the same conjugation reactions were carried out on both PLL and BSA using $[Ru(L-L)_2(NCSphen)]^{2+}$ labels, where L = phen and dpp, thereby increasing the bulkiness and hydrophobicity of the labels. Figure 3.12 (a), (b) and (c) depict the computational models of $[Ru(L-L)_2(NCSphen)]^{2+}$ where L=bpy, phen and dpp respectively.
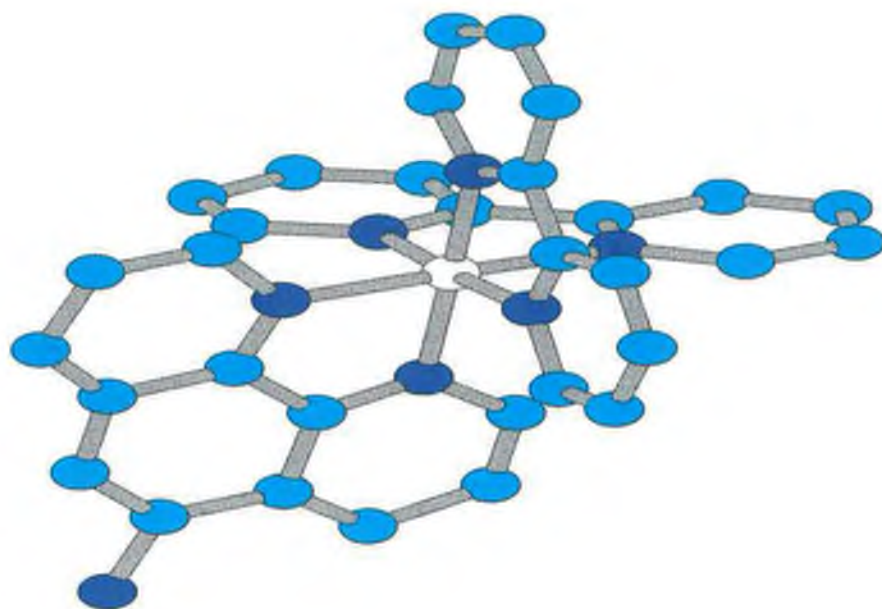
Figure 3.12 (a) Computational model of [Ru(bpy)₂ (NH₂phen)]²⁺, where pale blue = carbon, dark blue = nitrogen and white = ruthenium. The hydrogens have been removed for simplification purposes.
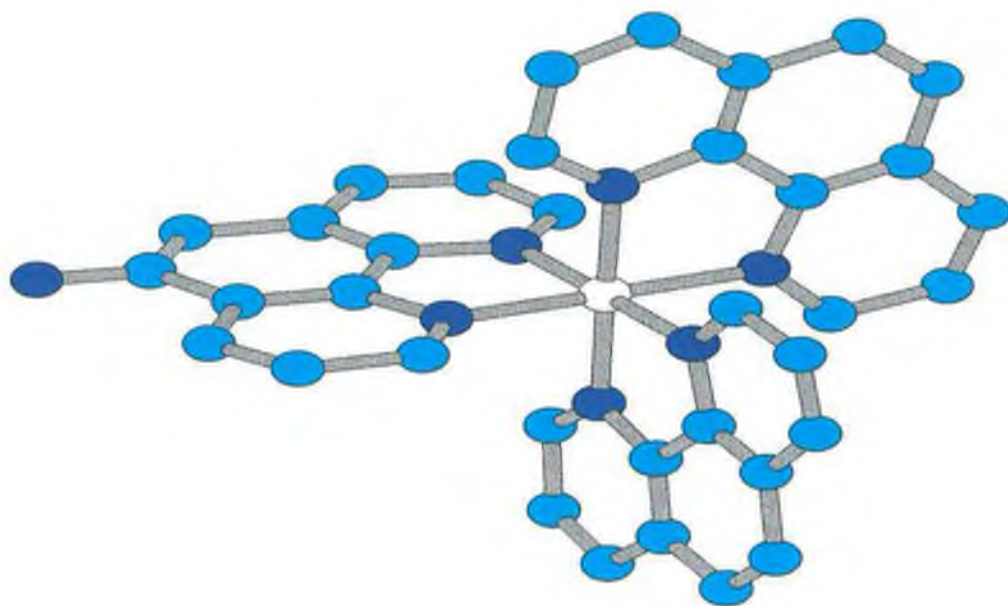
Figure 3.12 (b) Computational model of [Ru(phen)$_2$(NH$_2$phen)]$^{2+}$, where pale blue = carbon, dark blue = nitrogen and white = ruthenium. The hydrogens have been removed for simplification purposes.
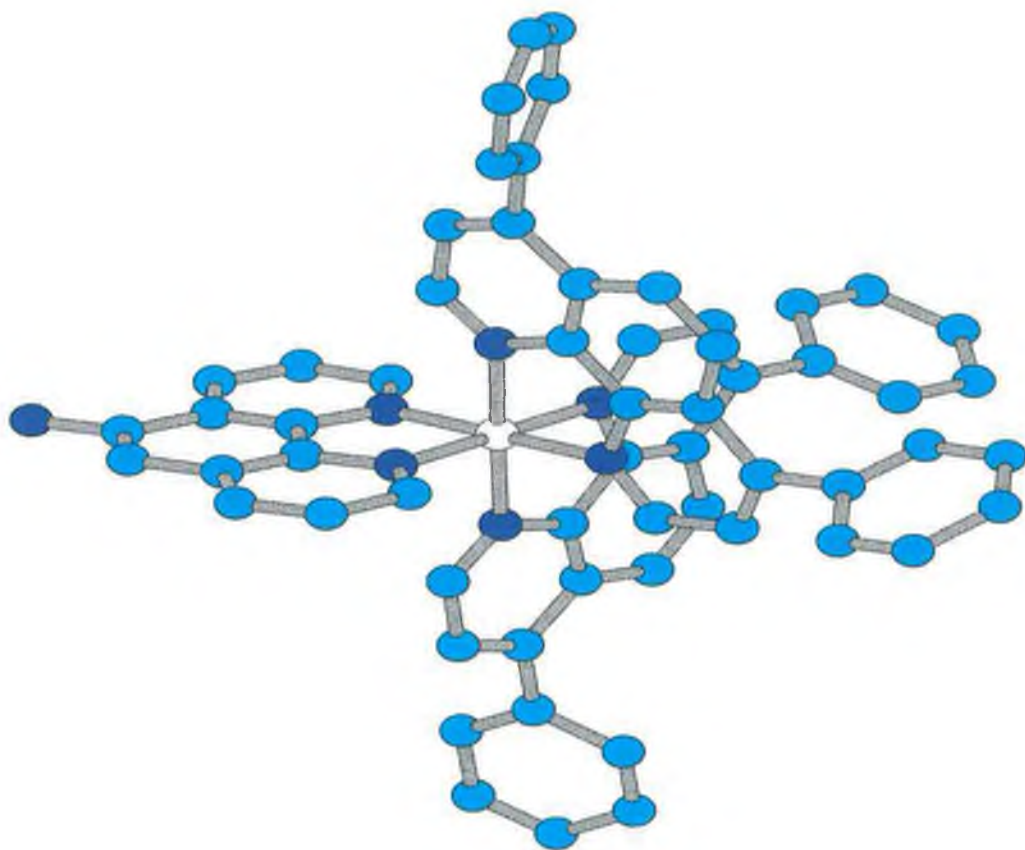
Figure 3.12 (c) Computational model of [Ru(dpp)₂(NH₂phen)]²⁺, where pale blue = carbon, dark blue = nitrogen, white = ruthenium. The hydrogens have been re-moved for simplification purposes.

This clearly illustrates the increase in bulkiness of the complex on varying the ancillary ligand from bpy to phen to dpp. Table 3.7 presents the conjugation ratios obtained for various loadings of [Ru(L-L)$_2$(NCSphen)]:PLL[2a] while Table 3.8 presents those of [Ru(L-L)$_2$(NCSphen)]:BSA [2a] (L= bpy, phen and dpp).

Table 3.7 Conjugation ratios calculated for various loadings of [Ru(L-L)$_2$(NCSphen)]$^{2+}$:PLL conjugates. [2a]

Original loading	Conjugation Ratio L=bpy $	Conjugation Ratio L=phen $	Conjugation Ratio L=dpp $
10:1	5	4	4
50:1	14	10	12

$ Protein concentration determined by Folin-Lowry method. [12]

Table 3.8. Conjugation Ratios obtained for various [Ru(L-L)$_2$(NCSphen)]$^{2+}$:BSA conjugates. [2a]

Original Loading	Conjugation Ratio L=bpy $	Conjugation Ratio L=phen $	Conjugation Ratio L=dpp $
10:1	9	6	9 (3)
50:1	25	20	28 (6)

$ Protein concentration determined by Folin-Lowry method. [12]

( ) Conjugation ratio determined in 0.01M carbonate buffer, pH 9.2

From Table 3.7 one can see that similar conjugation ratios are achieved on increasing the nature of the ancillary ligand of the labels from bpy to dpp ligands for the PLL conjugates. This would be expected as, at most, only 2% of all lysine residues present have been covalently modified and therefore the modified lysines would not be expected to be close enough to be further affected by steric hindrance. This also demonstrates, however, that the low loadings for PLL are not primarily due to the hydrophobicity or size of the label.

Table 3.8 reveals that the conjugation ratios determined where L= dpp are somewhat higher than those achieved with the smaller ligand bpy for equivalent BSA conjugates [2a]. This was not anticipated as almost maximum loading had already been achieved with the smaller less hydrophobic $[Ru(bpy)_2 (NCSphen)]^{2+}$ (i.e. almost all available lysine residues bound). Furthermore it would seem likely that the lysine residues are situated sufficiently close to each other in the compact folded structure of BSA, to be affected by a slight increase in bulkiness of the attached label. Therefore, lower conjugation ratios would be anticipated for $[Ru(dpp)_2(NCSphen)]^{2+}$. Meanwhile, the same effect would not be anticipated for the larger PLL molecule. However, another determining factor may be the lower affinity of these labels towards the hydrophilic lysines, due to the increased hydrophobicity of these labels, from L = bpy to dpp.

However, two possible explanations for our observations are (1) the presence of unbound label in the conjugate solution and (2) the intercalative/non-covalent binding of some labels to the biomolecule in addition to the covalently bound form, both leading to apparently higher conjugation ratios. Firstly, it is apparent that dialysis is less effective when separating hydrophobic molecules and this may affect the purification of proteins bound to such complexes as $[Ru(dpp)_2(NCSphen)]^{2+}$. Secondly, reports on ruthenium-DNA interactions concluded that intercalative binding affinity increases with increasing hydrophobicity of the ancillary ligands [21] possibly explaining higher than anticipated loading of the more hydrophobic label $[Ru(dpp)_2(NCSphen)]^{2+}$ to BSA. Furthermore, the same trends would not be expected when dealing with PLL due to its more open structure and lack of nega-

tively charged side groups on a PLL molecule. BSA, on the other hand, would be more susceptible to electrostatic interactions and intercalation due to its more compact folded structure and the presence of amino acids with negatively charged side groups facilitating electrostatic interactions with the positively charged Ru(II) complexes.

A chromatogram obtained for Ru(dpp)$_2$NCSphen:BSA (28:1) depicted in Figure 3.4 indicates impurities present apparently due to unbound label. However, extensive dialysis should have removed most of the unbound label. If these impurities were in fact due to electrostatically bound label, the ionic strength of the system should affect the degree of non-covalent interactions. Therefore, the same conjugation reaction was carried out using a buffer of lower ionic strength throughout the whole conjugation procedure ie. reaction and dialysis .0.01M carbonate buffer pH 9.2 was used as opposed to the usual strength of 0.10M. Interestingly, a significantly lower conjugation ratio of 6 was realised, indicating the elimination of much electrostatically or loosely bound ruthenium. Furthermore, the chromatogram of this conjugate indicates purification was achieved with the reduction of peaks due to free label rendering the real conjugation ratio for this reaction as 6 and not 28. These experiments would therefore suggest that non-covalent binding of [Ru(L-L)$_2$NCSphen]$^{2+}$ increases with increasing hydrophobicity of the ancillary ligand i.e. where L = dpp, whereas covalent binding decreases due to an increase in steric hindrance. The same experiment was carried out for when L=bpy and phen, but there was little change in the conjugation ratio on decreasing the ionic strength. This is due to the significant difference in hydrophobicity between the ancillary ligands studied. A set of experiments studying the effect of non-covalent linkage of the labels to the biomolecules on their emission lifetime are described later in this section and significantly, the results confirm the theory suggested here.

As above, similar experiments were carried out for [Ru(L-L)$_2$NH$_2$phen]$^{2+}$: BSA[1a] and [Ru(L-L)$_2$NH$_2$phen]$^{2+}$: PLGlu [1c] whereby the effect of the ancillary ligand of the label on the conjugation ratio was assessed. The results from these experiments are tabulated in Table 3.9 and Table 3.10 respectively.

129

Table 3.9 Conjugation ratios determined for [Ru(L-L)$_2$NH$_2$phen]$^{2+}$:PLGlu conjugates. [1e]

Original Loading	Conjugation Ratio L = bpy[$]	Conjugation Ratio L=phen[$]	Conjugation Ratio L=dpp[$]
10:1	4	5	6
50:1	5	6	10

$ Protein concentration was determined by Glutamic acid assay.

Table 3.10 Conjugation ratios determined for [Ru(L-L)$_2$NH$_2$phen]$^{2+}$:BSA conjugates. [1a]

Original Loading	Conjugation Ratio L=bpy $	Conjugation Ratio L=phen $	Conjugation Ratio L=dpp $
10:1	3	4	9
50:1	4	2	28 (15)

$ Protein concentration was determined by Folin-Lowry method. [12]
( ) Conjugation ratio determined in 0.01M carbonate buffer, pH 9.2.

Again, it is logical to compare any results obtained for the side chain modification of both synthetic biomolecules PLL and PLGlu. Table 3.9 shows that the maximum conjugation ratios for these PLGlu conjugates are similar but lower than those achieved for the analogous PLL conjugates, which would imply that the restricting factors found in the labelling of PLL are also true for PLGlu. In contrast

to PLL, the dpp based label led to a smaller increase in modification than the others. The discrepancy may however be due to the greater reactivity of the more non-polar $[Ru(dpp)_2NH_2phen]^{2+}$ to the non polar charged glutamic acid side chains, or indeed may merely be due to electrostatic binding of some label to the negatively charged molecule. The non-covalent interactions would not appear to be as significant however, as for BSA, probably due to the folded nature of BSA. Moreover, it is difficult to accurately compare conjugation ratios for PLGlu due to the necessity to activate the carboxylic acids prior to conjugation.

From Table 3.10 we can see that for the $[Ru(L-L)_2NH_2phen]^{2+}$:BSA conjugates [1a], the conjugation ratios determined for $[Ru(dpp)_2NH_2phen]^{2+}$ are notably higher than with the other two labels, with a maximum labelling efficiency of approximately 30% i.e. 15 out of 50 possible labels per molecule of BSA compared to 4-5 for $[Ru(bpy)_2NH_2phen]^{2+}$. This is quite a high conjugation ratio for such a specific conjugation process. Although the exact number of carbohydrate moieties on BSA are not known, the conjugation procedure used is known to be highly specific to such sites leading to homogenous labelling. Therefore, the contribution of electrostatic binding of the label to BSA to the overall conjugation ratio probably leads to the high values obtained for $[Ru(dpp)_2NH_2phen]^{2+}$ as significantly lower conjugation ratios are achieved in lower ionic strengths. However, this phenomenon will be discussed in greater detail in section 3.2.5.

3.2.4.3 Effect of nature of label.

In the previous section, we studied the effect of varying the size and hydrophobicity of similar labels on the extent of conjugation reactions. In this section, a ruthenium label of a different nature was chosen and bound to the same binding sites of PLL and BSA as the isothiocyanate derivatives i.e. the side groups of the lysine residues. This was to confirm that the nature of the label was not the principal cause of such low loadings of PLL.

Section 2.1.3. describes the synthesis of $[Ru(bpy)_2(COOH_2bpy)]^{2+}$ while section 2.3.2.3. outlines the conjugation procedure in binding the esterified derivative to the lysine residues of both PLL[3a] and BSA[3a]. Table 3.11 presents the conjugation ratios achieved for various loadings of the $[Ru(bpy)_2(esterbpy)]$:PLL/BSA conjugates while comparing the results to the other side chain modification reagents used.

As can be seen from Table 3.11, for both PLL and BSA, the isothiocyanate derivatives leads to greater labelling efficiency than with the ester. This would not have been expected, however, as preliminary studies by Eleanor Ryan PhD. revealed conjugation ratios similar to the isothiocyanates [9]. A possible explanation, however, may be related to the activation of the carboxylic acids to the ester form which again was not 100% efficient and so whose purity may affect the extent of the conjugation reaction.

Table 3.11. Conjugation ratios for 50:1 $[Ru(bpy)_2esterbpy]^{2+}$:PLL[3a] and $[Ru(bpy)_2esterbpy]^{2+}$:BSA[3a] conjugates.

Complex	Conjugation ratio-PLL *	Conjugation ratio-BSA*
$[Ru(bpy)_2esterbpy]^{2+}$	6	10
$[Ru(bpy)_2NCSphen]^{2}$	13	23

* Protein concentration was determined using the Folin-Lowry method [12].

3.2.4.4. Effect of protein binding site.

As well as binding to the side groups of amino acid residues of poly-amino acids, ruthenium complexes were also covalently bound to the terminal groups of these biopolymers. In order to carry this out, the conjugation procedures were modified to

permit binding to the terminal amine and carboxylic acid of the polypeptide chain backbone. Hence, $[Ru(L-L)_2NH_2phen]^{2+}$ was bound to the terminal carboxylic acid of the PLL chain [1d] and $[Ru(L-L)_2NH_2phen]^{2+}$ bound to the terminal amine of the PLGlu chains [2b], both via amide bonds.

In addition to binding to the lysine residues of BSA, a second side-chain modification reaction was carried out, whereupon ruthenium complexes were bound to the acidic glutamic acid residues present in the biomolecule. Labels were not bound to the terminal groups of BSA however, as due to the presence of both carboxylic acids and amines in the side groups of various amino acids, specific modification of the terminal binding sites could not be ensured. The conjugation ratios of such bioconjugates were calculated and are presented below in Table 3.12 and Table 3.13.

As well as assessing the success of the individual conjugation reactions, the estimation of such conjugation ratios are useful in the verification of the selectivity of the various conjugation procedures.

Table 3.12 Conjugation ratios of 50:1 $[Ru(L-L)_2NH_2phen]^{2+}$:PLL [1d] and $[Ru(L-L)_2NCSphen]^{2+}$:PLGlu. [2b]

Conjugate	Conjugation ratio L = bpy	Conjugation ratio L = phen	Conjugation ratio L = dpp
Ru(L-L)$_2$NH$_2$phen:PLL*	1	2	3
Ru(L-L)$_2$NCSphen:PLGlu§	2	1	4

Protein concentration was determined using the Folin-Lowry method [12].

§ *Protein concentration was determined using the glutamate assay.*

133

Very low conjugation ratios would be anticipated on binding labels to the terminal carboxylic acids and amino groups of biomolecules as there is only one terminal carboxylic acid and amine per polypeptide chain, as opposed to 57 lysine residues in the protein BSA, 750 lysine residues in PLL and 640 glutamic acid residues in PLGlu, which are theoretically the number of binding sites available for previous conjugation reactions studied.

From Table 3.12 we see that for PLL and PLGlu, an average conjugation ratio of 1 was achieved with the nature of the label having little effect on the extent of the reaction. This would be expected due to the uniqueness of such binding sites per polypeptide chain. Slightly higher loadings achieved with $[Ru(dpp)_2NH_2phen]^{2+}$ may be due to the apparent lower efficiency of dialysis of hydrophobic molecules. Nevertheless, these universal low loadings suggest that the conjugation method developed to exclusively modify the terminal groups of the polymer chains is indeed selective. It must be noted that there are means to detect the terminal groups of proteins and such methods could be used in future studies to confirm such site-selective binding processes.

The conjugation ratios of $[Ru(L-L)_2NH_2phen]^{2+}$: BSA bound via the glutamic acid residues [1b] are outlined in Table 3.13. A loading of 1 was obtained for both $[Ru(bpy)_2NH_2phen]^{2+}$:BSA and $[Ru(phen)_2NH_2phen]^{2+}$:BSA compared to 23 labels per biomolecule when bound via the lysine residues, which is surprising considering there are 67 glutamic acid residues per BSA molecule compared to 57 lysine residues per biomolecule. However, with $[Ru(dpp)_2NH_2phen]^{2+}$, upto 20 glutamic acid residues appear to be modified, in this case showing these labels to be much more efficient in this particular labelling procedure, in particular the latter. However, this high labelling efficiency appears again to be due to extensive non-covalent binding of the label. On reducing the ionic strength of the buffer system throughout the complete conjugation procedure, a high loading of 18 was still achieved indicating that a decrease in ionic strength merely improved the efficiency of dialysis but did not remove the tightly bound label. As discussed in page 129 dialysis also appears to be less efficient when separating hydrophobic molecules rationalising the

unusually high apparent conjugation ratios here. However, it may also be possible in this case, that the more hydrophobic label is more reactive to these binding sites.

As already mentioned, the lysine residues are normally more accessible and reactive than the glutamic acid residues, due to the higher reactivity of the ε-amino group of its side chain and longer chain length, and so this would explain why, on average, the lysine residues are the most efficiently modified binding sites. However, unlike the lysine residues of BSA, the exact number of glutamic acid residues which are actually " available" for modification per BSA molecule is not known, thereby rendering the comparison of the conjugation ratios of both amino acids difficult.

Table 3.13. Conjugation ratios for [Ru(L-L)$_2$NH$_2$phen]$^{2+}$:BSA [1b] bound via the glutamic acid residues.

Complex	L = bpy	L = phen	L = dpp
[Ru(L-L)$_2$NH$_2$phen]$^{2+}$:BSA	1	2	20 (18)

$ Protein concentration was determined using the Folin-Lowry method [12].
( ) Conjugation ratio determined in 0.01M carbonate buffer, pH 9.2.

3.2.4.5 Effect of reaction conditions.

The optimum reaction conditions used when carrying out various conjugation procedures are presented in Section 2.3.2., Chapter 2 [11, 15]. It was decided to investigate the effect of pH and temperature of reaction on the extent of conjugation reactions in an attempt to more clearly understand the reasons for low labelling efficiencies, particularly concerning the synthetic biomolecules, PLL and PLGlu. The topic concerning the effect of chemical denaturants is addressed briefly.

135

The optimum pH for the conjugation of PLL and BSA via their lysine residues was initially investigated in the literature [9]. It was found that pHs 7-9 gave similar conjugation ratios while conjugation was found not to occur at lower pHs. This increase in conjugation ratios as a function of pH was explained in the literature to be most likely due to the greater deprotonation of the amino group of the lysines at higher pH values, thereby providing additional sites for reaction with the isothiocyanate group of the label [17]. The pH alone would not be an adequate explanation for the low binding to PLL as the lysines in BSA would be similar, although the presence of various amino acids in the chain would modify their pK_a somewhat.

Significantly however, the pK_a of the amino groups of lysines is very close to the pH at which the reactions were carried out for PLL and hence, PLL is known to be in a transitional state between a random-coil conformation and it's helical form.

In order to investigate whether the structural conformation of the poly-amino acids predominant under the reaction conditions would have a major effect on the extent of the reactions, conjugation reactions were carried out for both PLL and PLGLu, under conditions at which the poly-amino acids would be expected to be totally helical, to learn if more or less efficient labelling would be achieved under such conditions. Table 3.14 presents the conjugation ratios achieved for PLL, BSA and PLGlu conjugates at higher temperatures (where PLL is known to adopt a β-sheet conformation), various pHs (pH 11 for PLL and BSA) (optimum pH 9.2) and pH 3 for PLGlu (optimum pH 4.8) where their helical forms are expected to prevail.

(1) Effect of pH.

From Table 3.14 we can attempt to deduce the effect of the reaction pH on the extent of the conjugation process. A change in pH has many different effects on the reactants in a conjugation process. Firstly, the pH may affect the reactivity and

stability of the labels as, for certain reactions, it may be the protonated/unprotonated form of the label that reacts with the binding site of the biomolecule.

The pK_a of the binding sites of the biomolecule is also very important, notably in the reactions we are considering [16]. For example, in the side-chain modification of PLL and BSA, it is the deprotonated form of the amino groups, of pK_a 10, which react with the isothiocyanates to form a thiourea bond [16]. This explains why no conjugation was found to occur at acidic pHs whereas the optimum pH of conjugation was determined to be approximately pH 9, where the vast majority of amino groups would be deprotonated. The pH also obviously affects the most stable conformation of the biomolecule, in particular the more dynamic synthetic biopolymers. In addition to the pH sensitivity of the secondary structures of many poly-amino acids in solution, most proteins are found to become unstable and therefore may become unfolded to some extent above pH 11, while generally found in their most stable state around their isoelectric point.

Table 3.14 Conjugation ratios for [Ru(bpy)$_2$ (NCSphen)]$^{2+}$:PLL, [Ru(bpy)$_2$(NCSphen)]$^{2+}$:BSA and [Ru(bpy)$_2$(NH$_2$phen)]$^{2+}$:BSA(a) under extreme reaction conditions.

Conjugate	(a)	(b)	(c)	(d)
[Ru(bpy)$_2$NCSphen]$^{2+}$:PLL	14	2	2	4
[Ru(bpy)$_2$NCSphen]$^{2+}$:BSA	23	7	6	8
[Ru(bpy)$_2$NH$_2$phen]$^{2+}$:BSA	6	2	2	4

(a) Conjugation ratios determined with initial loading of 50:1, under optimum reaction conditions specified in Section 2.3.2.4. and 2.3.2.5.

(b) Conjugation was carried out at pH 11 for PLL & BSA. (c) Conjugation was carried out at 50°C. (d) 8 M urea was added to the conjugation reaction mixture.

From Table 3.14 we see that on carrying out the same conjugation at a higher pH of 11 for PLL, a significant decrease in the extent of reaction is apparent, with modification of only 2 sites achieved, as opposed to an optimum of 14. As the α-helix is the favoured conformation at pH 11 [10], this would suggest that more lysine residues are actually available for binding when PLL is in the random-coil conformation than when in the rigid α-helical form. However, as for proteins, under such extreme basic conditions, the polypeptide may become destabilised and hence less reactive to modification. A similar experiment was attempted on PLGlu at pH 3. However, as an amino label was used, it was necessary to elevate the pH in order to dissolve the label, rendering such a study difficult. Table 3.14 reveals that BSA is less well modified at pH 11, and this would be expected as BSA, an acidic protein would be somewhat denatured at such high pHs.

Hence, as preliminary experiments indicated, no conjugation took place under acidic conditions and we find less conjugation at pH 11 than at pH 9. This correlates well with initial reports that pH 9 is the optimum pH of such conjugation reactions.

This illustrates the importance of verifying the optimum pH of conjugation reactions and shows us that the pH and pH sensitive conformations of the biomolecules are not adequate explanations for such low labelling of PLL and PLGlu. Furthermore, this highlights the complexity behind conjugation reactions and the number of parameters affecting their success.

(2) Effect of temperature.

As stressed previously, PLL is known to adopt a β-sheet conformation when heated to 50^0 C for 15 minutes [4]. From Table 3.14, we see that, as for the pH modified conjugate, the conjugation reaction carried out at 50^0C leads to significant loss in conjugation. This correlates well with our earlier theory that non-random conformations such as α-helix, β-sheet yield less efficient labelling. We would not expect to be able to differentiate between secondary structures of a similar nature

such as the α-helix and β-sheet using ruthenium complexes as probes and therefore would expect similar results for both structural forms. Such information is not however known of PLGlu and so it would be difficult to interpret results here. On carrying out the same experiment on BSA conjugates, lower conjugation ratios were calculated, but less affected than with PLL. Another possibility is the lower stability of the labels at elevated temperatures although absorption spectra of heated labels did not show any changes. The most stable forms of proteins are temperature dependent, with most proteins becoming denatured beyond a critical temperature. BSA, like most serum albumins, would not be expected to be fully unfolded at a relatively mild temperature of 50 ^{0}C, and so it is not clear why lower conjugation ratios are achieved under such conditions. In short, this experiment yields little information on the thermostability of proteins/poly-amino acids but rather verifies the complexity behind such biological procedures. Nevertheless, the lower conjugation ratios would not appear to be due to the thermostabilty of the covalent bonds involved between label and biomolecule, i.e. thiourea and amide bonds, as further studies in the next chapter indicate the reversibity of the effect of heat, dismissing the idea of decomposition. Consequently, a method, such as DSC, to recognise unfolding of the protein, or CD spectra to differentiate between secondary structures, would be necessary to make more definite conclusions possible from such a fundamental study.

(3) Effect of chemical denaturants.

As pointed out earlier, the addition of some chemical denaturants to the reaction mixture may increase the extent of a conjugation reaction [11]. To investigate this possibilty in our conjugates, 8 M urea was added to PLL, PLGlu and BSA conjugates. However, from Tables 3.14, the opposite effect was noted for all biomolecules, resulting in lessening the extent of such reactions particularly on binding to lysine residues of PLL and BSA.

Denaturants such as urea and guanidine may denature proteins by increasing the solubility of non-polar molecules, such as amino acid side chains, thereby diminishing the magnitude of the hydrophobic effect by upto one third [2]. This effect should be adequate to produce unfolding of proteins. Specific interactions between denaturant and protein is implied while urea molecules even permeate the interior, perturbing the close-packed interior by occupying small cavities [2].

Hence denaturation of BSA may occur, leading possibly to the lower reactivity of the binding sites in question. For $[Ru(bpy)_2NCSphen]^{2+}$:BSA [2a] a significant drop in the number of labelled sites is implied, while only a slight decrease in modification is indicated for $[Ru(bpy)_2NH_2phen]^{2+}$:BSA [1a]. This may be due to the fact that the lysines and oligosaccharides, on different positions along the BSA molecule may be affected by varying degrees by any unfolding or local conformational changes induced by urea. However, on determining the lifetimes of conjugates prepared with urea, very little change was observed, which indicates little change in the local environment of the labels along the polymer chain, questioning any significant structural changes in the denaturation of BSA under such conditions. An important point to note is that denaturation does not necessarily induce detectable physical changes in proteins, but may rather involve influences on folded conformations of the polypeptide chain upon which its biological properties may be critically dependent [2].

Another point to note however, is that on studying the effect of urea on the decay behaviour of the unbound labels used, the decay lifetimes of the labels decreased, indicating that chemical denaturants affect the spectroscopic properties of the labels, which may subsequently affect their affinity to binding to the biomolecules. Therefore, the lower conjugation ratios may be merely due to the effect of urea on the reactivity of the labels. Again, simultaneous means to study conformational variances of such biopolymers in more depth would be a major advantage in such work.

Another likely explanation is that the thiourea bond formed between the lysines and label is rendered less stable by chemical denaturants than the stabilised

amine bonds between label and carbohydrate moieties. This interpretation is strengthened by the fact that similar effects are seen for PLL as for the former BSA conjugates, i.e. dramatic drop in conjugation ratio, of which thiourea bonds are also involved in the conjugation. However, it is difficult to study the reversibility of the effects of urea as its removal is a prerequisite.

In brief, it must be concluded that the initial reaction conditions are indeed the optimum conditions for the reactions concerned. Also, any change in such conditions has a critical effect on the success of the conjugation procedures, verifying the unpredictable and complicated dynamic behaviour of biomolecules.

3.2.5. UV/vis and emission spectroscopy.

The absorption and emission data on the unbound ruthenium complexes, in addition to their protein-bound forms are presented in Table 3.15, while Figures 3.13 and 3.14 depict the absorption and emission spectra typical of unbound [Ru(II) complexes and their various bio-conjugate forms.

For all the compounds studied, the maximum wavelength of the lowest energy absorption occurs at 450-470 nm. Upon conversion to their isothiocyanate derivatives, the maximum of absorption (and emission) is shifted very slightly, in most cases to higher energies. Upon conjugation, the visible region in the absorption spectrum of the bioconjugates is not affected by absorbance by the biomolecules since this occurs in the ultraviolet region. Hence, any changes in the absorption in this area of the spectrum should reflect changes in the spectroscopic properties of the ruthenium complexes upon conjugation to biomolecules. All compounds studied emit at room temperature with emission maxima ranging from 600-625 nm.

On conjugation of the labels to the biomolecules, slight variations in the maxima of absorption and emission are induced, indicating subsequent changes in spectroscopic properties of the labels upon binding. Generally, binding to the protein BSA leads to more pronounced shifts in absorption/emission maxima than with syn-

thetic biomolecules used, although even in most cases the shifts are only in the range 2-5 nm, which are still minimal and indeed within instrumental error range.

Table 3.15. Electronic data for ruthenium complexes and bio-conjugate forms.

Compound	Conjugate		Absorption	Emission (nm)
$[Ru(bpy)_2(NH_2phen)]^{2+}$			456 (4.15)	612
$[Ru(bpy)_2(NH_2phen)]$ -	BSA		460	615
	poly-l-glutamate		458	610
	poly-l-lysine		458	614
$[Ru(bpy)_2(NCSphen)]^{2+}$			454 (4.18)	610
	BSA		460	615
	poly-l-lysine		458	615
	poly-l-glutamate		456	614
$[Ru(phen)_2NH_2phen]^{2+}$			452 (4.24)	602
	BSA		456	603
	poly-l-glutamate		455	602
	poly-l-lysine		456	604
$[Ru(phen)_2(NCSphen)]^{2+}$			454 (4.16)	608
	BSA		460	605
	poly-l-lysine		460	605
	poly-l-glutamate		456	608
$[Ru(dpp)_2NH_2phen]^{2+}$			462 (4.32)	620
	BSA	(a)	475	625
		(b)	465	618
	poly-l-glutamate		478	625
	poly-l-lysine		465	620
$Ru(dpp)_2(NCSphen)]^{2+}$			460 (4.25)	618
	BSA		470	624
	poly-l-lysine		465	625
	poly-l-glutamate		468	624
$[Ru(bpy)_2(COOHbpy)]^{2+}$			460 (4.20)	642
$[Ru(bpy)_2 (esterbpy)]^{2+}$			460 (4.18)	655
	BSA		465	655
	poly-l-lysine		465	655

(a) All spectra and extinction coefficients (log ε) were measured in 0.10M carbonate buffer, pH 9.2, at room temperature.

(b) Ruthenium complexes were firstly dissolved in a minimal volume of acetone.

142

The conjugates of $[Ru(dpp)_2NH_2phen]^{2+}$ and in particular $[Ru(dpp)_2NCSphen]^{2+}$, exhibit more significant changes, with the absorption and emission maxima of the label, changing by upto 6-8 nm upon conjugation, thereby indicating that the emitting properties of such labels are significantly affected by the bound biomolecule. This is possibly due to the tighter binding of the complexes and stronger electrostatic interactions involved with the folded protein.
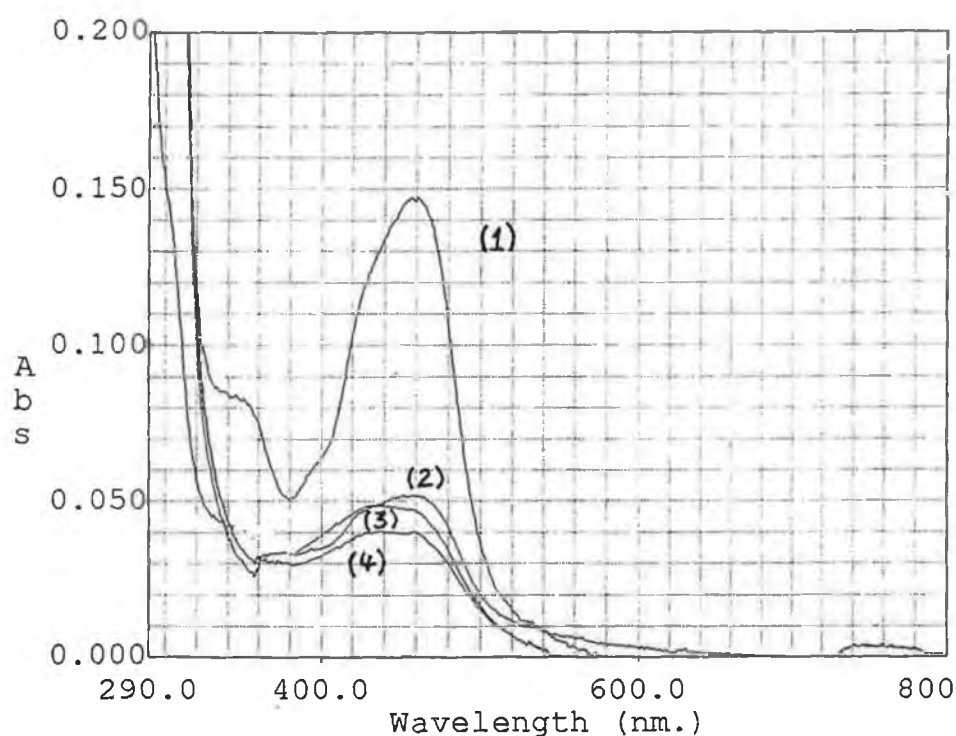
Figure 3.13. Typical absorption spectra of (1) $[Ru(dpp)_2NCSphen]^{2+}$ and when covalently bound to (2) BSA, (3) PLL & (4) PLGlu.
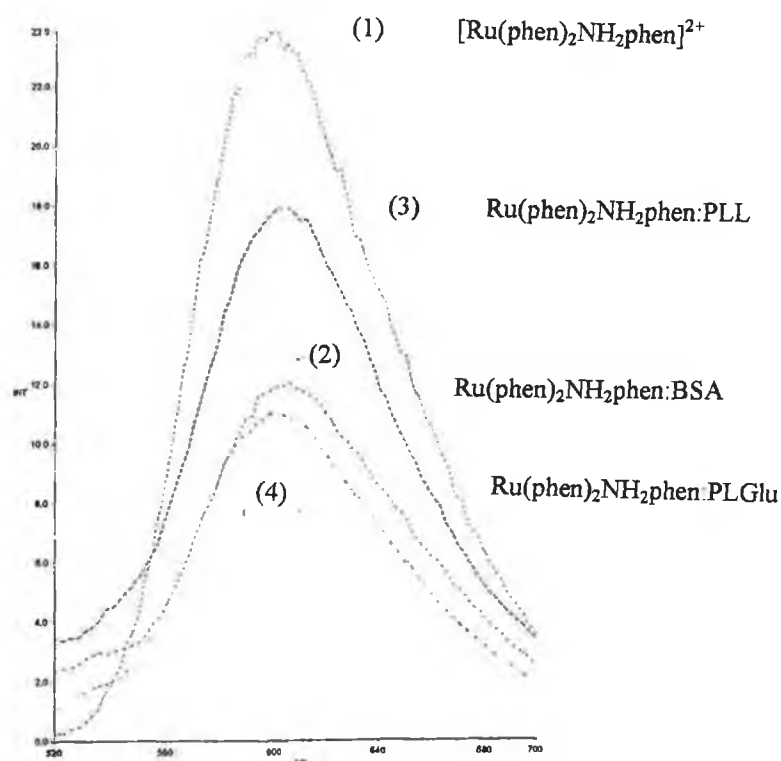
Figure 3.14 Typical emission spectra of (1) [Ru(phen)₂NH₂phen]²⁺ and when
covalently bound to (2) BSA, (3) PLL & (4) PLGlu.

3.2.6 Emission lifetime measurements.

The emission lifetimes of the ruthenium polypyridyl complexes, both when unbound and when covalently bound to selected biomolecules were measured using the system described in Section 2.2.8., Chapter 2. The measurements were carried out in aerated and degassed solutions, in 0.10M carbonate buffer, pH 9.2, unless otherwise stated. As noted in the literature [9, 17], most of the protein-bound complexes display essentially double exponential decay behaviour, with one emitting component significantly longer than the other. Hence, from the preliminary experiments carried

out in Section 2.2.9, equation 2.3 was deemed a suitable model for the analysis of such complexes [22]. However, it is necessary to recognise the physical limitations of this approximation, as this neglects the fact that the measured fluorescence decay profile is an average signal from all molecules excited by the light. Thus, if a fluorescent molecule is subject to a heterogeneous environment, one has to calculate the decay profile of fluorescence as an average over the distribution of relaxation rates [22]. In this study, a double exponential equation was found to suffice in most cases as described in equation 2.6.

In contrast, the excited state decay of the unbound ruthenium complexes can be fitted by single exponential kinetics. Hence equation 2.5, the monoexponential decay law may be used in data analysis of such compounds [22] (See Section 2.2.9). An emission decay profile typical of a ruthenium complex analysed using such a monoexponential decay model and equation 2.5 is depicted in Figure 3.15 while the decay profiles of a protein-bound label, analysed using the single and double exponential decay models mentioned above, are displayed in Figure 3.16 and Figure 3.17 respectively. These clarify the reasoning behind differentiating between whether a single or multi-exponential decay model gives the best fit for a given sample, which was already discussed in Section 2.4.9.1. Figure 3.16 shows that on analysing the conjugate with the single exponential model, significant deviations are observed in contrast to the minimal error achieved for the unbound label in Figure 3.15 (See equation 2.7), confirming that this sample possesses more than one emitting component. On using the double exponential decay model for the same sample, the elucidation of two emission lifetimes lead to a very small error in the calculations as observed in Figure 3.17(b). The lifetimes of the free Ru(II) complexes obtained by using equation 2.5 are presented in Table 3.16 (a) when the samples are aerated, deoxygenated and oxygenated. Table 3.16 (b) discloses the lifetimes of the various emitting components of the protein-bound labels when aerated and deoxygenated which were calculated using the multi-exponential decay law (equation 2.6).

145

20 mV/Div

.2 us/Div

4.23

2.05

0   0.8E+00

time (microseconds)
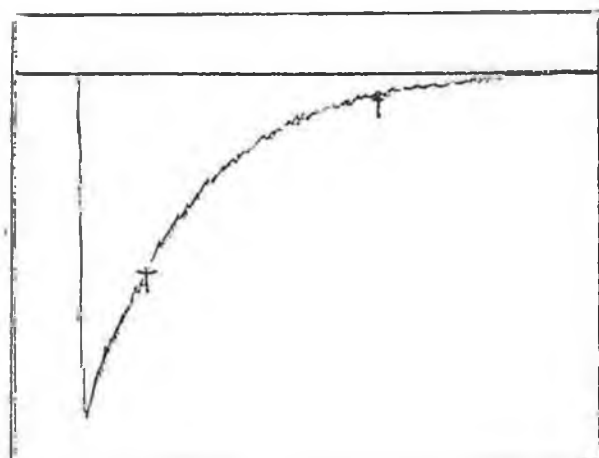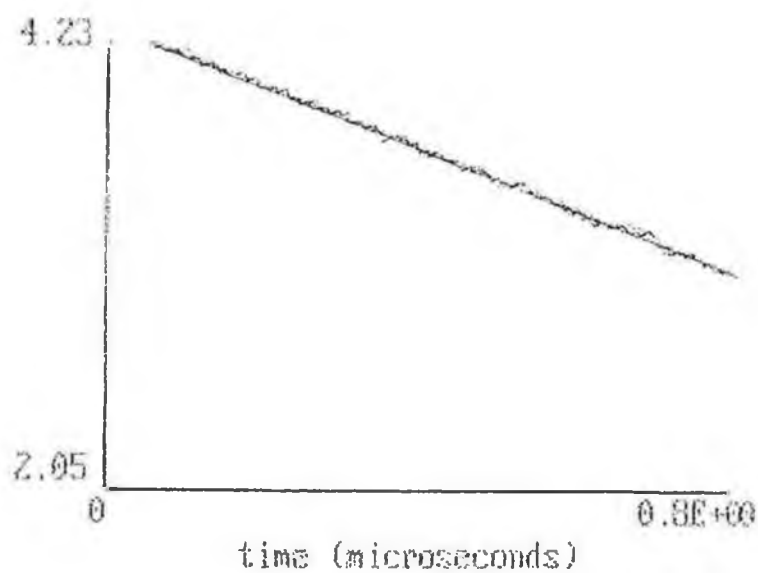
Figure 3.15 (a) Emission decay profile of [Ru(dpp)₂NCSphen]²⁺.
   (b) Weighted residual plot for a single exponential fit.

4 mU/Div

.14 us/Div

2.75

0.86

0

0.8E+00

time (microseconds)
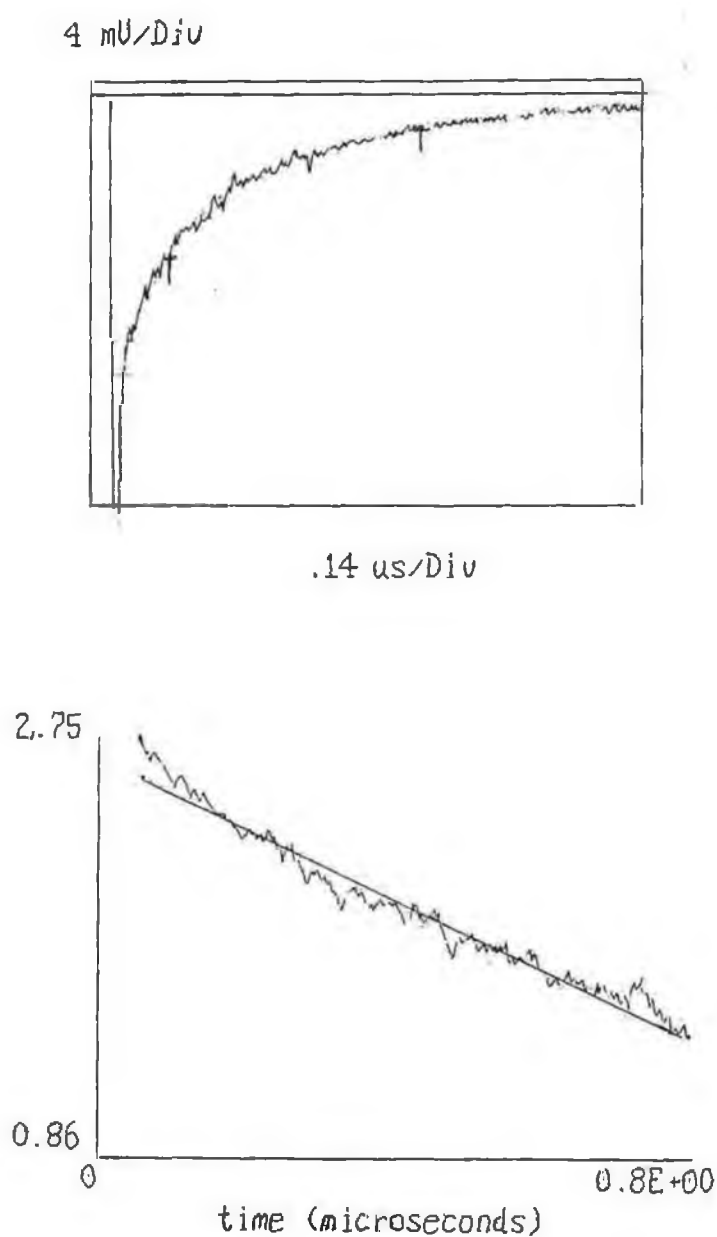
Figure 3.16 (a) Emission decay profile of Ru(dpp)₂NCSphen:BSA.

(b) Weighted residual plot for a single exponential fit.
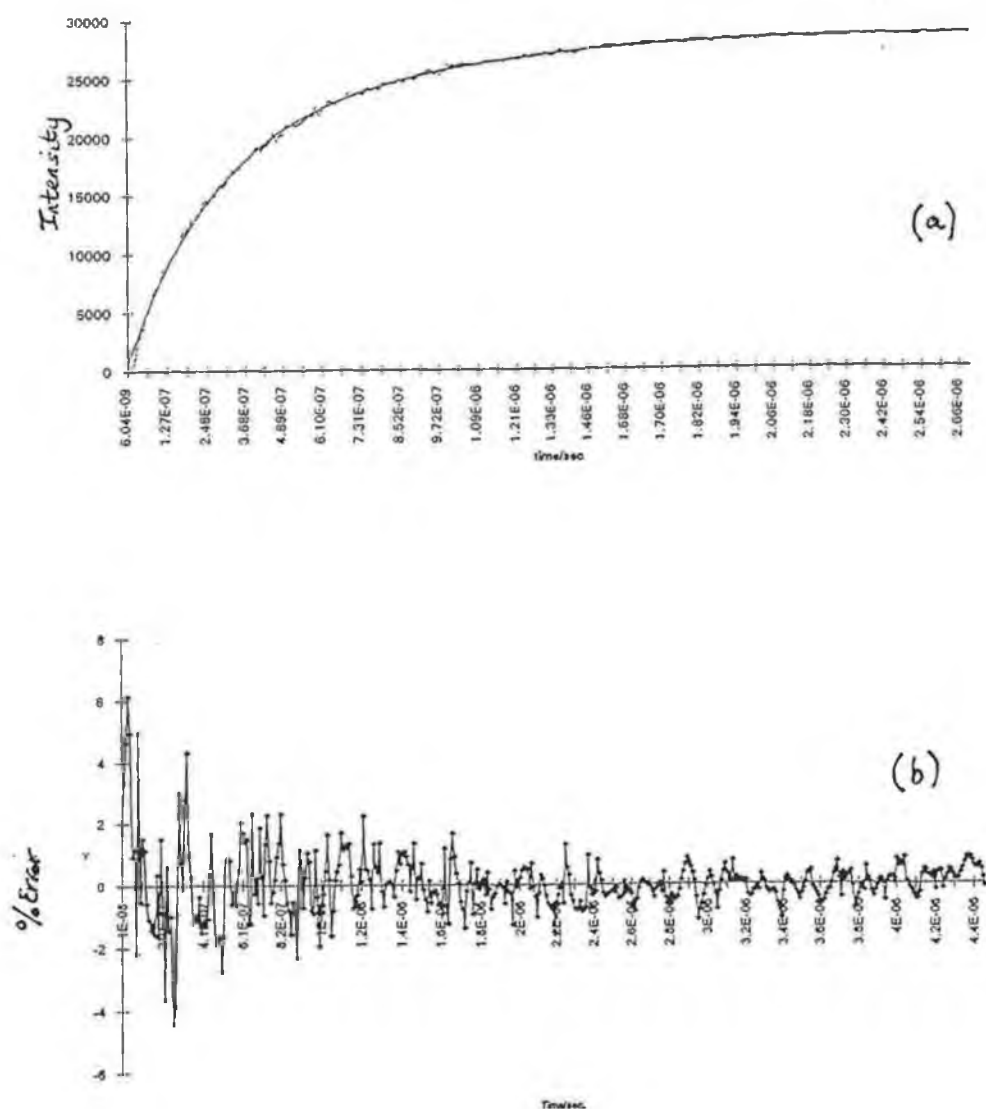
Figure 3.17 (a) Emission decay profile of Ru(dpp)$_2$NCSphen:BSA.
(b) Weighted residual plot for a double exponential fit.

As stated previously, all the free labels used display single exponential decay, thereby possessing a single emission lifetime. From Table 3.16 (a) it can be seen that the emission lifetimes of the complexes are efficiently quenched by oxygen, in particular the amino complexes and their isothiocyanate derivatives with the lifetimes being reduced by half on oxygenation.

Table 3.16 (a) Emission decay lifetimes for the unbound ruthenium complexes, measured in 0.10M carbonate buffer, pH 9.2.

Complex	Lifetimes (ns)		
	[a] Oxygenated	Aerated	[a] Argon
$[Ru(bpy)_2NH_2phen]^{2+}$	185	350	600
$[Ru(phen)_2NH_2phen]^{2+}$	230	530	800
$[Ru(dpp)_2NH_2phen]^{2+}$	430	700	1300
$[Ru(bpy)_2NCSphen]^{2+}$	200	450	650
$[Ru(phen)_2NCSphen]^{2+}$	230	550	1100
$[Ru(dpp)_2NCSphen]^{2+}$	270	650	1300
$[Ru(bpy)_2(COOHbpy)]^{2+}$	220	350	480
$[Ru(bpy)_2(esterbpy)]^{2+}$	210	330	460

Samples were dissolved in acetone and made up in 0.10 M carbonate buffer, pH 9.2.

[a] 0.2ml sample was added to 0.10M carbonate buffer, pH 9.2, and the solutions were treated with argon/oxygenated for 30 mins.

This is to be expected, as oxygen is one of the few species which efficiently quenches the excited state lifetime of $[Ru(bpy)_3]^{2+}$ and its derivatives. Furthermore, the lifetimes obtained correlate well with those in the literature [9]. The decay lifetime of the acidic complex $[Ru(bpy)_2(COOH_2bpy)]^{2+}$ and its ester form appear to be less influenced by the quenching effects of oxygen which also correlates with findings for similar compounds in the literature [23].

3.2.6.2. Protein-bound ruthenium complexes.

As stressed earlier, upon binding to the biomolecules in question i.e. PLL, BSA and PLGlu, the ruthenium complexes display essentially double exponential decay kinetics. The first point to note from the aerated solutions in Table 3.16 (b), when compared to those of the free labels in Table 3.16 (a), is that in most cases the protein-bound labels possess one lifetime significantly longer than that of the free label and another lifetime of similar duration or shorter than that of the free label. For every label used, the BSA-bound form exhibits notably greater enhancements of lifetimes than found using the synthetic biomolecules, PLL and PLGlu. In particular, for the labels, $[Ru(dpp)_2NH_2phen]^{2+}$ and $[Ru(dpp)_2NCSphen]^{2+}$ when bound to BSA, striking lifetime enhancements are evident, whereby the longer lifetime obtained is upto four times longer than that of the same free label, while the shorter lifetime is approximately of the same durationas that of the free label. This observation is in correlation with the more pronounced changes in the absorption and emission spectra of the same protein-bound complexes. This may again be due to the tighter binding of these complexes resulting from the stronger electrostatic interactions between the more hydrophobic labels and the proteins. However, although not to the same extent, all protein-bound labels studied do exhibit enhanced lifetimes to some degree when compared to their unbound counterparts.

150

Table 3.16 (b) Emission decay lifetimes for protein-bound ruthenium complexes, measured in 0.10M carbonate buffer, pH 9.2.

Conjugate	Conjugation ratio	Lifetime (ns)	
		Aerated	Argon [a]
[Ru(bpy)$_2$NH$_2$phen] / BSA (a) [1a]	4	760 (65), 270(35)	1000 (40), 390(60)
[Ru(phen)$_2$NH$_2$phen] / BSA (a)	5	930(60), 350 (40)	1100 (50), 380 (50)
[Ru(dpp)$_2$NH$_2$phen] / BSA (a)	15	2000 (60), 500 (40)	2800 (70), 650 (30)
[Ru(bpy)$_2$NH$_2$phen] / BSA (b) [1b]	1	850 (70), 370 (30)	1100 (60), 360 (40)
[Ru(phen)$_2$NH$_2$phen] / BSA (b)	2	1000 (60) 360 (40)	1300 (50), 520 (50)
[Ru(dpp)$_2$NH$_2$phen] / BSA (b)	20	1800 (65), 270 (35)	2400 (70), 450 (30)
[Ru(bpy)$_2$NCSphen] / BSA. [2a]	21	930,(65), 250 (35)	950 (52), 350 (48)
[Ru(phen)$_2$NCSphen] / BSA	25	1100 (65), 310 (35)	1200 (60), 390 (40)
[Ru(dpp)$_2$NCSphen] / BSA	28	3500 (65), 830 (35)	3700 (65), 820 (35)
[Ru(bpy)$_2$(esterbpy)] / BSA [3a]	6	990 (25), 320 (75)	1200 (45), 500 (55)
[Ru(bpy)$_2$NCSphen] / PLL [2a]	12	680 (65), 390 (35)	730 (70), 450 (30)
[Ru(phen)$_2$NCSphen] / PLL	15	1250 (60), 370 (40)	1100 (60), 400 (40)
[Ru(dpp)$_2$NCSphen] / PLL	12	1650 (90), 410 (10)	1700 (80), 200 (20)
[Ru(bpy)$_2$(esterbpy)] / PLL [3a]	6	405 (80), 180 (20)	640 (50), 290 (50)
[Ru(bpy)$_2$NH$_2$phen] / PLL [1d]	1	500 (85), 180 (15)	800 (85), 290 (15)
[Ru(phen)$_2$NH$_2$phen] / PLL	2	750 (90), 270 (10)	1100 (75), 350 (25)
[Ru(dpp)$_2$NH$_2$phen] / PLL	4	1050 (90), 490 (10)	1500 (80), 550 (20)
[Ru(bpy)$_2$NH$_2$phen] / PLGLu [1e]	5	520 (80), 210 (20)	780 (80), 180 (20)
[Ru(phen)$_2$NH$_2$phen] / PLGlu	6	670 (50), 400 (50)	1100 (50), 350 (50)
[Ru(dpp)$_2$NH$_2$phen] / PLGlu	10	980 (60), 280 (40)	1400 (60), 400 (40)
[Ru(bpy)$_2$NCSphen] / PLGlu [2b]	1	520 (75), 240 (25)	840 (90), 240 (10)
[Ru(dpp)$_2$NCSphen] / PLGlu	4	1240 (85), 590 (15)	2100 (85), 580 (15)

[a] *0.2 ml sample was added to 0.10M carbonate buffer, pH 9.2, and deoxygenated under argon for 30 mins.*

Figures in ( ) represent the proportion of each emitting species determined from the pre-exponential decay functions, as described in equation 2.3.

151

Before more detailed studies could be carried out on the decay behaviour of the protein-bound labels, it was necessary to verify that the double exponential behaviour of the conjugates was indeed due to the covalently bound label and not merely electrostatically bound forms. For this purpose, a set of experiments were carried out whereby free Ru(II) complexes were mixed with free protein under conditions not apt for covalent bond formation, and the immediate effect of the non-covalently bound protein on the emission lifetime of the label was investigated. Similar concentrations of both label and biomolecule were used as for the conjugation reactions in an attempt to keep conditions constant. Table 3.17 below displays the results of such studies.

Table 3.17 Effect of mixing ruthenium complexes with proteins on the emission lifetime of the label in aerated 0.10M carbonate buffer pH 9.2.

$[Ru(L-L)_2NH_2phen]^{2+}$ [ns]	Lifetime (ns) label + PLL.	Lifetime (ns) label + PLGlu	Lifetime (ns) label + BSA
L = bpy, [350]	350	380	320
L = phen, [530]	450	490	430
L = dpp [800]	780	1000 (70) 400 (30)	1500 (70) 260 (30)

( ) Figures in brackets represent the pre-exponential factors of the emitting components as determined from the decay function $\Phi(t) = [(A_1(1-exp(-k_1t))+(A_2(1-exp(-k_2t))] $ *[22].*

The information outlined in Table 3.17 is quite significant in two respects. Firstly, it reveals how the emission lifetime and single exponential decay behaviour of the labels are unaffected by the presence of the synthetic biomolecule PLL. This verifies that the double exponential nature of decay of their conjugates is primarily due to covalently bound label and not induced by electrostatically bound complex. However, on mixing $[Ru(dpp)_2NH_2phen]^{2+}$ with PLGlu, double exponential kinetics become apparent, with one lifetime slightly elevated when compared to that of the unbound label. As regards the natural protein BSA, the decay lifetimes of the complexes $[Ru(bpy)_2NH_2phen]^{2+}$ and $[Ru(phen)_2NH_2phen]^{2+}$ are also unperturbed by the presence of this protein. The interesting discovery in this study is the striking effect that unmodified BSA has on the decay behaviour of the free label $[Ru(dpp)_2NH_2phen]^{2+}$. Double exponential decay kinetics of the non-covalently bound ruthenium complex results from the presence of BSA, where the longer lifetime is almost twice that of the free complex and whose shorter lifetime is significantly less than that of $[Ru(dpp)_2NH_2phen]^{2+}$. This observation would appear to substantiate our assumption that $[Ru(dpp)_2NH_2phen]^{2+}$, due to bulkier ancillary ligands and increased hydrophobicity, partakes in significant electrostatic interactions with the protein. Table 3.18 summarises the lifetimes obtained for $[Ru(dpp)_2NH_2phen]^{2+}$:BSA linked in both non-covalent and covalent manners.

The greater enhancement of the longer lifetime of the complex when covalently bound to BSA indicates that this enhanced lifetime is indeed due to a combination of covalently and electrostatically bound label along the biopolymer. As the double exponential decay appears to originate from a composite of several decays from labels at various positions along the protein, the shorter lifetime may be a quenched bound form of the label, possibly linked electrostatically as this lifetime is little affected by covalent linkage. The similar but less obvious effect noted for the decay of $[Ru(dpp)_2NH_2phen]^{2+}$:PLGlu may be due to the electrostatic interactions between Ru(II) complexes and the negatively charged PLGlu.

153

Table 3.18 Effect of ionic strength on conjugation ratio and emission lifetimes of [Ru(dpp)$_2$NH$_2$phen]$^{2+}$: BSA[1a,1b] and [Ru(dpp)$_2$NCSphen]$^{2+}$: BSA [2a].

Conjugate	Conj.Ratio1,	lifetimes1 (0.1M)	Conj Ratio2,	lifetimes2 (0.01M)
[Ru(dpp)$_2$NH$_2$phen]$^{2+}$: BSA (a)	28:1	2400 (60), 650 (40)	15:1	2000 (70), 500 (30)
[Ru(dpp)$_2$NH$_2$phen]$^{2+}$: BSA (b)	20:1	2200 (65), 320 (35)	18:1	1800 (65), 270 (35)
[Ru(dpp)$_2$NCSphen]$^{2+}$:BSA	15:1	3500 (65), 830 (35)	6:1	2900 (70), 600 (30)

( ) Figures in brackets represent pre-exponential factors of the emitting components from the decay function $\Phi(t) = [(A_1(1-exp(-k_1t)) + (A_2(1-exp(-k_2t))] $ *[22].*

[*]Conjugation ratios determined according to Nairn [1].

As mentioned earlier, the scale/strength of electrostatic interactions seems to be affected by the ionic strength of the system. However, on mixing ruthenium complexes and biomolecules under the same conditions but at a lower ionic strength using 0.01M carbonate buffer, similar lifetime enhancements result, indicating that a decrease in ionic strength only removes the more loosely bound label.

Salt is often used to increase the ionic strength of a system. Interestingly, NaCl was added to the mixture of [Ru(phen)$_2$NH$_2$phen]$^{2+}$ and BSA. Although the lifetime of the label was unaffected by the non-covalently bound protein under standard conditions, double exponential decay resulted in the presence of NaCl, indicating that the electrostatic interactions indeed increase with ionic strength.

The double exponential nature of the decay of such bio-conjugates as observed in Table 3.16 has been attributed to the presence of labels on the same binding sites but along different locations of the biomolecule, thereby possibly under different local environmental effects, to which Ru(II) complexes are very sensitive. This being the case, PLL conjugates may be expected to display single

exponential decay behaviour, as PLL is made up of only lysine residues, indicating homogenous environments for the labels, regardless of their position along the PLL molecule. Double exponential analysis was required for the best fit for most PLL conjugates, however one significant feature is that these conjugates are not as clearly " double exponential " as the BSA conjugates, in the sense that single exponential analysis gave a reasonable fit. This is more evident from the analysis of decay curves obtained from the single exponential decay analysis of such samples than from the fractions of each emitting component estimated from the relevant pre-exponential factors using double exponential analysis. This would be explained by the fact that BSA is composed of several types of amino acids along a chain and hence, labels bound to one particular type of binding site may still have variances in their surroundings, depending on their exact location along the polymer chain. It is important to remember the nature of the analysis of multi-exponential decays as it is merely a mathematical approach to solving an equation. Hence, the apparent single exponential nature of the lifetimes of such conjugates may actually be due to the less significant difference between both lifetimes in the more homogenous environment of PLL, to which the functions used are less sensitive (See 2.4.9.1) However, the uneven distribution of the labels along the PLL polypeptide chain may lead to heterogeneity of these labels, thereby rationalising the double exponential nature of the decay. In brief, it is likely that the emission decay of the conjugates is much more complicated and complex than treated and therefore the elucidation of two lifetimes is merely an averaging process.

The exact nature of the various emitting components of the protein-bound labels is uncertain. The enhanced lifetimes of the protein-bound labels, as suggested in the literature [17], may be due to a combination of factors. One important component is (1) a decrease in vibrational activity of the label when held in the more rigid environment of the biomolecule. This would appear to be a fundamental contributing factor, despite the uncertainty of the extent of increase of rigidity of such complexes as opposed to when in the free form. Based on results, BSA would appear to hold the labels more rigidly than the synthetic polypeptides, which is very

155

likely, due to the compact folded nature of such albumins, in contrast to the more open nature of the polypeptide chains of PLL and PLGlu as well as the capacity for stronger electrostatic interactions. However, this factor alone would not adequately explain variances in degrees of enhancements between different labels bound to various sites on the same biomolecule. Moreover, the rate of enhancement may depend on the predominant conformation of the biomolecule under the reaction conditions. This rationalisation would explain results obtained in the chapter 5, whereby the degree of enhancement of the lifetime of the bound label appears to be noticeably influenced by the local conformational variances inherent in the biomolecule involved, evident on studying secondary structural variances in synthetic poly-amino acids and denaturation of BSA.

Another factor influencing the enhancement of lifetimes, on binding to large biomolecules, may be (2) the protection of the label from quenching, by O_2 in particular, in the sheltered environment of the biomolecule. BSA, a natural globular protein has a more complex folded structure than the regular poly-amino acids and therefore contains more sheltered pockets, incorporating in essence a hydrophobic core and hydrophilic surface. Hence, a combination of theory (1) and (2) would explain the greater enhancement of the BSA-bound labels when compared to those bound to other biomolecules. Assuming (2) is particularly true for BSA, by removing oxygen from the BSA-bound labels their longer lifetimes should be less influenced than those in the more open environments of the PLL/PLGlu-bound labels, which is indeed observed in most cases (See Table 3.16). However, the degree of enhancement of the lifetimes and the quenching efficiency of oxygen on the label varies with the site of attachment of the label on the biomolecule, probably due to different affinities of the binding sites towards various labels involved. Moreover, the specific conformation of the biomolecule at the binding site and hence the local environment surrounding the label would appear to be an important determining factor in the degree of enhancement and sensitivity of the lifetimes. As an example, one can compare and contrast the lifetimes of a side-chain modified and a site-specific modified biomolecule when aerated and

156

degassed. For example, the longer lifetime of a label bound to the side chains of PLL i.e. $[Ru(L-L)_2NCSphen]^{2+}$ is more enhanced but less efficiently quenched than that of a label bound to the end of the polymer chain i.e $[Ru(L-L)_2NH_2phen]^{2+}$. Furthermore, the longer lifetimes of the conjugates, notably those of BSA are much less effectively quenched by oxygen than those of the unbound labels. This supports the former evidence that the spectroscopic properties of the labels are greatly affected by the close approach of the biomolecules.

An important phenomenon noted for these conjugates however, is the fact that the degree of conjugation actually affects the longer lifetime of the label. This is most evident on analysing the lifetimes of conjugates of similar nature but with different numbers of labels covalently bound. One example is $[Ru(phen)_2NCSphen]^{2+}$:PLL whereby lifetimes of 1200 ns and 370 ns are noted with 15 labels bound while lower lifetimes of 810 ns and 300 ns are obtained with 6 labels bound. This denotes the notable effect of the loading of label on lifetimes of certain conjugates, particularly the longer lifetime, and indicates that this phenomenon may actually be a primary contributing factor for the lower lifetimes of $[Ru(L-L)_2NH_2phen]^{2+}$:PLL (1-3 labels) compared to $[Ru(L-L)_2NCSphen]^{2+}$:PLL (12-15 labels). However, the sensitivity of the lifetime and quenching efficiency of the label to the conformation of the biomolecule and/or the local environment of the label will be explained and discussed in greater detail in chapter 5.

Another consideration with such lifetime studies is (3) an increase in the energy gap between the emitting state and the metal centred deactivating states of the label upon binding to the biopolymer, the extent of which may vary between labels. This proposal may explain why, on binding various types of label to the same binding sites on say BSA, the lifetimes of certain labels are more significantly affected than others. As well as (1) and (2), the further increase in lifetime observed for such conjugates may be consistent with differences in the spectroscopic characteristics of the excited state complex. A change in the term $A_i exp(-\Delta E_i/RT)$ which describes the population of the anti-bonding d-d state may lead to the inhibition of the deactivating pathway due to the MLCT$\rightarrow$dd transition. To

157

investigate this proposal, temperature dependent lifetime analysis would be necessary, which was not actually carried out, as low temperature work on aqueous samples is very difficult.

A more likely explanation however, for the striking lifetimes of [Ru(L-L)$_2$NH$_2$phen]$^{2+}$ and [Ru(L-L)$_2$NCSphen]$^{2+}$ bound to BSA is the contribution of non-covalent binding of the more hydrophobic labels to the longer lifetime. As already mentioned, the presence of the bulkier and more hydrophobic ancillary ligand dpp leads to greater stacking capacity and stronger electrostatic interactions of the labels with biomolecules. Hence, the most enhanced lifetime may be a composite of several decays, emanating from covalently and electrostatically/intercalatively bound labels at different locations along the protein molecule. This suggests that an electrostatically bound label may possess similar photophysical properties to the covalently bound label.

Spectroscopic characterisation of the protein-bound labels has already indicated significant electrostatic interactions between the more hydrophobic labels and the protein BSA. Indeed, the possibility of intercalative binding cannot be dismissed. As mentioned earlier, on decreasing the ionic strength of the buffers in the conjugation reactions, it is possible to reduce electrostatically bound labels to BSA. To study the effect of non-covalently bound Ru(II) on the lifetimes of the BSA-bound labels, the lifetimes of the conjugates in both 0.01M and 0.10M carbonate buffer are listed in Table 3.18 on page 154.

Significantly as anticipated, the [Ru(dpp)$_2$] based conjugates are the only ones whose lifetimes vary significantly with ionic strength and these same labels bound to PLL or PLGlu do not show such sensitivity to ionic strength changes. On removing much of the electrostatically bound ruthenium by decreasing the ionic strength of the buffer throughout, notable decreases in lifetimes are found for the corresponding conjugates, indicating their contribution to the longer lifetime, in particular. However, this effect could be predominantly due to the greater efficiency of dialysis in removing the loosely bound label in lower ionic strengths and hence the lower lifetimes resulting from lower conjugation ratios.

The next debatable question, the nature of the shorter lifetime of the protein-bound labels has already been addressed briefly. Again, the main possibilities include the presence of unbound label or a non-covalently bound form susceptible to quenching, probably of an electrostatic nature. The presence of a quenched bound species would be the most likely explanation, based on the assumption that dialysis would have removed most of the unbound ruthenium. However, on using size exclusion chromatography to determine the purity of the bio-conjugates prepared, although most conjugates were determined to be at least 90% pure, there was in most cases still small amounts (< 5%) of unbound labels which had not been removed even by extensive dialysis. However, even for these samples, only approximately 70% of the decay emanates from the longer lived species, and so it is unlikely that these minute impurities are the sole reason for double exponential decay kinetics displayed by such conjugates. Dialysis would appear to be least effective in the removal of the more hydrophobic molecules, notably the labels $[Ru(dpp)_2NH_2phen]^{2+}$ and $[Ru(dpp)_2NCSphen]^{2+}$. For this reason, buffers of lower ionic strengths were used throughout the whole conjugation procedures to further purify such conjugate solutions. Interestingly, the shorter lifetimes of most of the conjugates studied appear to be much less effectively quenched by oxygen than those of unbound label, further indicating a quenched bound form. Nevertheless, the possibility that the short lifetimes of the conjugates are partly due to unbound label cannot be dismissed. For the majority of conjugates prepared, the longer lived emitting component constitutes between 60% and 80% of the total decay. However, the behaviour of the shorter lifetimes varies with the protein and so its nature appears to be quite complex. It is more likely that the shorter lifetime is primarily due to unbound label interacting in some form with the protein, most probably in an electrostatic manner. Although the PLL and PLGlu conjugates do not appear to interact electrostatically in a significant way, there are probably still some weak interactions taking place, particularly with the negatively charged PLGlu polypeptide.

Effect of protein binding site.

(1) BSA

The lifetimes obtained for the BSA-bound labels, bound to three different sites-(1) the lysine residues; (2) the glutamic acid residues; and (3) the carbohydrate moieties are quite similar, although in all three cases, the longer lifetimes of the complexes bound via the lysine residues are slightly longer than via the other two binding sites. This may be due to the various environments of the different binding sites. Glutamic acid and asparagine residues, to which it is assumed that the carbohydrate moieties are attached, are non-polar charged amino acids, lysine being basic while the other two are acidic [10]. The difference in charge of the binding sites on binding of the postively charged Ru complex may result in some sites being more hydrophobic than others and hence more sheltered in the protein interior. Albumins, being globular proteins, undergo compact folding with very little internal space for water molecules, whereby much of the hydrophobic R groups on the amino acid side chains are situated in the interior, and the vast majority of the hydrophilic R groups are located on the exterior. However, all the amino acids chosen here as binding sites are relatively hydrophilic and the difference in lifetimes may be due rather to the higher number of labels bound to the lysine residues. This is consistent with reports that the lifetimes of such complexes seem to depend on the affinity of the medium (in this case, the side groups of amino acids) for the hydrophobic ligands of the labels. The amino groups of the lysine residues of BSA are indeed the most reactive towards modification [1, 17]. Preliminary studies showed that for equivalent conjugate types, the lifetimes of the more extensively labelled biomolecule are accordingly higher, thereby rationalising the higher lifetimes of the more extensively labelled lysine residues. Another contributing factor may the greater influence of electrostatically bound label due to the longer chain length of lysine residues.

All three types of BSA conjugates are equally influenced by the removal of oxygen, with slight increases in both lifetimes apparent. As anticipated, the lifetimes

are less influenced than that of the free label, probably due to sheltering and their increased rigidity when bound to proteins. Interestingly however on oxygenating the samples, much more efficient quenching of labels bound to the lysine residues is evident. The higher quenching rates would be explained in terms of the longer side groups of lysine residues, which would render the labels more accessible to the quenching effects of oxygen, in particular.

(2) PLL

On comparing the lifetimes of the complexes bound to the lysine residues [2a] to those bound to the terminal groups of the polypeptide chain [1d], one can see from Table 3.16(b) that in most cases both lifetimes are higher when bound to the lysine residues Again, this may be merely due to the more extensive binding of the labels to such sites. Also, the complexes bound to the end of the chains display almost single exponential decay kinetics, with the higher lifetime incorporating 90% of the decay, in some cases. This may be due to the smaller number of terminal groups and hence the more unique environment of the label. These complexes also appear to be more effectively quenched by oxygen, perhaps because they are not as susceptible to the sheltering effect of the side groups of the lysine residues. The shorter lifetime shows little change on degassing, which would suggest this is not unbound label, which is itself very effectively quenched by oxygen. Again, however, due to the complexity of the decay of such conjugates and the problems associated with their analysis, a definite explanation is impossible.

(3) PLGlu

On comparing the lifetimes of the complexes when bound to the glutamic acid residues to those bound to the end of the chains, the lifetimes are similar for both sites, a

161

sites, a contributing factor possibly being the low labelling efficiency of both sites. However, the complexes bound to the end of the chains are more efficiently quenched by oxygen, as for PLL, as well as the longer lifetime contributing to upto 90%. This again would be anticipated due to the regular primary structure of PLGlu and the positioning at the end of the chain which is more open than the side groups of the glutamic acid residues. Overall however, the longer lifetimes are more sensitive to oxygen quenching than those bound to BSA as anticipated due to the absence of sheltered pockets in the synthetic biomolecules.

3.3   Conclusion.

The ultimate objective of work carried out in this chapter was the extensive characterisation of Ru(II) polypyridyl complexes when covalently bound to proteins prior to investigation into their potential as fluorescent probes capable of monitoring conformational variances of the bound biopolymers. This is essential as extensive knowledge of the spectroscopic and luminescent properties of both the free labels and those covalently bound to the proteins as well as their purity is a prerequisite to understanding their probing characteristics.

Firstly, both the unbound ruthenium polypyridyl complexes and their protein-bound forms are characterised using chromatographic and spectroscopic techniques. A chromatographic procedure based on size exclusion is developed to determine the purity of the resultant bio-conjugates and hence this proves useful in determining the success of the various conjugation reactions attempted. Such studies indicate that although some conjugates still contain small amounts of unbound label, not quantified but approximately < 5%, this would not appear to have a significant effect on the probing capabilities of the samples.

The electronic measurements of the labels and their protein-bound forms confirm earlier work done, namely that absorption and emission characteristics of the

labels are not significantly affected by such binding. However, as reported in the literature [17] significant changes in the decay behaviour of the labels are noted on conjugation in the form of double exponential decay kinetics and enhanced lifetimes. However, it is important to note that the multi-exponential analysis of the decay lifetimes of the conjugates is merely a mathematically based solution and the elucidation of two lifetimes for most bioconjugates may be a result of the averaging of several lifetimes. These same studies indicate that the enhanced lifetimes of the conjugates are indeed mainly due to both the decrease in vibrational activity of the label when held in the more rigid environment of a biomolecule, and the protection of the label from quenching effects in the sheltered environments of the biomolecules. This would explain why the conjugates of BSA, a rigid and compact globular protein, with many sheltered pockets, yield the most enhanced lifetimes, least affected by quenching effects of oxygen, in particular. Our studies further suggest that the variances in the decay behaviour of various protein-bound labels are indeed due to the nature of the specific modification sites chosen on the biomolecules, that is the local environment of the biomolecule, as well as the absolute conformation of the bio-polymer in question. This strongly indicates that the decay kinetics of the label will be susceptible to conformational variances of the bound biopolymers and therefore give rise to their probing potential.

The most dramatic increases in lifetimes are noted for $[Ru(dpp)_2NH_2phen]^{2+}$ and $[Ru(dpp)_2NCSphen]^{2+}$ bound to BSA and this appears to be partly due to extensive electrostatic interaction between these hydrophobic molecules and the protein. The shorter lifetime appears to be due to a quenched bound form of label, probably bound in a non-covalent manner. The possibility of intercalation taking place also cannot be dismissed.

Labels are bound to various sites on three biomolecules, BSA, PLL and PLGlu. Very efficient binding is achieved on the natural protein BSA, whereby the lysine residues are found to be the most accessible and reactive, as anticipated. Low labelling efficiencies are achieved on both synthetic polypeptides, PLL and PLGlu, the reasons for which are not definite but which appear to be due to the marginal

stability of their conformational forms, and hence the lower accessibilty of the binding sites.

A method is developed to selectively modify terminal groups on the biomolecules as well as their side groups permitting the comparison of the potential of site-selective and side-chain modification reagents as probes of protein structure, subsequently dealt with in the following chapter.

The effect of reaction conditions, such as pH, temperature, and reagents on the extent of various conjugation reactions is studied. This study confirms the fact that optimum pH and temperature had been originally chosen for all conjugation reactions studied and that any deviations from these optimum conditions dramatically reduce the number of binding sites labelled, possibly due to induced unfolding/conformational variances of the biomolecule. However, no definite information regarding the stability of the biomolecules involved could be deduced without the simultaneous use of other characterisation methods commonly used for proteins.

In brief, the groundwork behind understanding the spectroscopic and luminescent properties of the bio-conjugates has been accomplished, allowing us to move on to study and compare the potential of these various labels as probes, capable of monitoring conformational variances these biomolecules undergo in solution, which is addressed in the next chapter.

3.4   References.

[1]   R.C. Nairn, Fluorescent Protein Tracing, Churchill Livingstone, 4th edition New York, **1976.**

[2]   T.E. Creighton, Proteins, Structures and Molecular Properties, 2nd edition, W.H. Freeman & Co., New York, **1984**.

[3]   P.C. Kahn, *Methods Enzymol.,* **1979**, 61, 339.

[4]   N. Greenfield and G.D. Fasman, *Biochem.,* **1969**, 8, 10, 4108.

[5]   O. Jardetzky and N.G. Wade-Jardetzky, *Ann. Rev. Biochem.,* **1971**, 40, 605.

[6]   K.M. Ulmer, *Science,* **1983,** 219, 666.

[7]   S. Luo, C-Y.F. Huang, J.F. Mᶜ Clelland and D.J. Graves, *Anal. Biochem.,* **1994**, 216, 67.

[8]   D.T. Haynie and E. Freire, *Anal. Biochem.,* **1994**, 216, 33.

[9]   E.M. Ryan, PhD. Thesis, Dublin City University, **1991**.

[10]   A.L. Lehninger, Biochemistry, Worth Publishers Inc., New York, **1979**.

[11]   G.E. Means and R.E.Feeney, *Bioconj. Chem.,* **1990**, 1, 2.

[12]   G.L. Peterson, *Anal Biochem.,* **1979**, 100, 201.

[13]   M.M. Bradford, *Anal. Biochem.,* **1976**, 72, 248.

[14]   S. F. de St. Groth, R.G. Webster and A. Datyner, *Biochim. Biophys. Acta,* **1963**, 71, 377.

[15]   S.J. Compton and C.G. Jones, *Anal. Biochem.,* **1985**, 151, 369.

[16]   M. Brinkley, *Bioconj. Chem.,* **1992**, 3, 1, 2.

[17]   E.M. Ryan, R. O'Kennedy, M.M Feeney, J.M. Kelly and J.G. Vos, *Bioconj. Chem.,* **1992**, 3, 285.

[18]   A. Canfi, M.P. Bailey and B.F. Rocks, *Analyst,* **1989**, 114, 1407.

[19]   R.S. Nezlin and Y.K. Sykulev, *Molecul. Immun.,* **1982**, 19, 347.

[20]   D.J. Shannessy and R.H. Quarles, *J. Immun. Methods,* **1987**, 99, 153.

[21]   A.M. Pyle, J.P. Rehmann and R. Meshoyrer, *J. Am. Chem. Soc.,* **1989**, 111, 3051.

[22]   J.N. Demas, Excited State Lifetime Measurements, Academic Press, London, **1983**.

[23]   J.W. Park, J. Ahn and C. Lee, *J. Photochem., Photobiol. A: Chem.,* **1995**, 86, 89.

Chapter 4.

The pH sensitivity of the absorption and emission spectra of protein-bound Ru(II) polypyridyl complexes.

4.1   Introduction.

In earlier chapters, we have described various procedures involved in labelling poly-
amino acids and proteins with ruthenium based fluorescent complexes and also have
characterised all protein-bound complexes prepared. In the remaining chapters, our
aim is to investigate the potential of such fluorescent labels to monitor conforma-
tional changes which the bound biomolecules undergo in solution, thereby acting as
probes of their dynamic behaviour. In this chapter the sensitivity of the absorption
and emission spectra to conformational changes of the bound biomolecules, induced
by pH changes and chemical denaturants are monitored, while chapter 5 will deal
with the potential of the decay lifetimes of the labels as probes.

However, in order to understand how the label may function as such a probe,
a discussion on the properties of a good fluorescent probe is undertaken and the
particular advantages displayed by ruthenium complexes will be summarised. Finally,
a summary of the physical properties of the biomolecules in solution is necessary in
order to visualise the phenomena we wish to monitor before an in depth study of
their probing capabilities are discussed.

4.1.1. Properties of a good fluorescent probe [1].

As the aim of this thesis is to use ruthenium polypyridyl complexes as fluorescent
probes, one must consider the requirements for such probes, thereby ensuring the
applicability of such complexes in our area of interest;

> (1) The fluorochrome should possess chemical groups which will form stable
> covalent bonds with protein molecules or be easily converted to such a
> reactive form without destroying the fluorescent structure. It should not
> possess any other groups which might react with the primary reactive group
> or give any unwanted by-products.

167

(2) It should be easy to separate unbound from the bound fluorescent probe.

(3) The probe should possess a high quantum yield of fluorescence, which should not decrease upon conjugation.

(4) It should be possible to conduct the conjugation reaction under mild conditions so that the conformation of the biomolecule is not disturbed.

(5) The probe should be photostable/stable under normal storage conditions not differing materially in its properties from the unconjugated protein.

(6) The probe should exhibit a large Stokes shift so that the scattered analysing light does not interfere with the signal.

(7) The conjugation procedure should be as simple and as rapid as possible.

The incorporation of spectroscopic and fluorescent labels has been extensively investigated and developed in recent years, in particular to characterise certain structural features of proteins. This is due to extensive attempts to substitute radioactive labels with nonradioactive counterparts, the prime examples including enzymatic, fluorescent and spectroscopic labels [2]. Although radioactive labels are quite versatile and can be detected at very low concentrations, they are expensive, hazardous, and their use requires sophisticated equipment and trained personnel [3].

The choice between fluorescent probes or radioactive isotopes is governed by the type of information sought. Where the material to be detected is present in minute amounts, radioactive labelling would normally be chosen, due to the decreased sensitivity obtained with fluorescence, partly due to the samples own fluorescence (autofluorescence) [3]. The intense background has however been overcome by the use of time-resolved fluorescence and labels with a long emission decay, including some Ru(II) polypyridyl complexes [4]. Some other problems associated with fluorometric analysis include the scattering of light and quenching of the fluorescence by oxygen, heavy atoms and concentration quenching due to the location of probes in close proximity to each other [3, 5].

Nevertheless, for most purposes, the greater convenience and the greater safety of the fluorescence technique is preferred. A commonly used label for proteins, such as insulin, is the dye fluorescein isothiocyanate (FITC) extensively used in various fluorescence immunoassay methods and in fluorescence microscopy. However FITC is susceptible to fading in the presence and absence of oxygen, found to be due to organic peroxides, hydroperoxides and oxyradicals [4]. Intensely fluorescent conjugates have also been prepared from 1-dimethylaminonaphthalene-5-sulphonic acid (DANS) and rhodamines which show a less intense fluorescence than FITC conjugate but are more stable to photobleaching (fading) [6]. Lanthalide chelates due to their much extended decay lifetimes and the large Stokes shift they exhibit are also used in time-resolved fluorimetry [7].

Fluorescence is used, as well as for labelling biomolecules, in immunology, mainly in fluorescence microscopy for studying various types of cells, tissues, bacteria, etc. [8]. Usually the sample to be analysed is detected with an antibody which is labelled with a fluorescent species. Quantitative fluorescent immunoassay techniques include fluorescence polarisation methods, fluorescence quenching methods, fluorescence enhancement techniques and fluorescence excitation transfer methods.

Ruthenium polypyridyl complexes fulfil the requirements of a good fluorescent probe, in addition to absorbing strongly in the visible region and yielding long lived emission, rendering them suitable as fluorescent probes of biomolecules. Varied methods of binding such complexes to enzymes, antibodies and other proteins have found important applications in their labelling and in fluorometric immunoassays. However, these will be discussed in greater detail in chapter 5.

4.1.3 Physical properties of poly-amino acids.

Polypeptides are long chains of amino acids bound together while poly-amino acids are basically simple models of proteins with a regular primary structure ie. amino acid composition. Proteins are much more complex with up to 20 different amino

acids bound together. For this reason, much work has been carried out on studying and understanding polypeptide structures in order to further our understanding of the complex nature of protein structure and properties.

The most natural state of a polymer is considered to be a random coil conformation. However, other conformations will be adopted if sufficient interactions are possible, within or between molecules [9]. Many synthetic poly-amino acids adopt a few such regular conformations that are also found in natural proteins resulting from the regularity of the primary structure. In brief, the secondary structure of polypeptides are basically structures due to hydrogen bonding on forming a three dimensional structure, examples being α-helices and β-sheets which are illustrated in Figure 4.1.

The α-helix is the most predominant of polypeptide regular secondary structures with the atoms of the backbone packed closely together, making very favourable Van der Waals contacts. Both α-helices and β-sheets are involved in main chain amino and carboxyl groups participating in hydrogen bonds to each other, with α-helices having 3.6 residues per turn and hydrogen bonds between carboxyl groups and the amino groups three amino acids ahead of it, thus leaving only the first amino group and the last carboxyl group not involved in hydrogen bonds [9]. This leads to a net dipole that gives a partial positive charge at the amino end and a partial negative charge at the carboxyl end. This is known to be the most stable secondary structure for proteins [10]. The polypeptide properties stabilise the molecule into this more rigid form by (a) hydrogen bonds, (b) ionic bonds and (c) hydrophobic interactions [9].

The side chains project out of the helix conformation and do not interfere with the stereochemical properties of the α-helix. Although considered the most natural conformation for polypeptides, it is, however only marginally stable in solution and amino acids differ in their propensity to adopt this conformation [11]. For example, alanine, glutamine and methionine are good α-helix formers while serine, proline, glycine and threonine are very poor.

In general, uncharged groups on the side chains permit the formation of stable α-helical units while charged groups of like sign, such as the COO$^-$ ions of carbonyl glutamyl residues and the NH$_3^+$ groups of the lysyl/arginine residues cause the destabilisation as a result of charge repulsion. Although apparently rigid structures, α-helices are usually dynamic systems in solution, being rapidly formed and unfolded 10^5 to 10^7 times/sec. α-helix to random coil transitions can occur in polypeptides upon changing temperature or solvent, or by altering the pH of the medium, where the equilibrium can be shifted from a totally random to totally helical form [10].
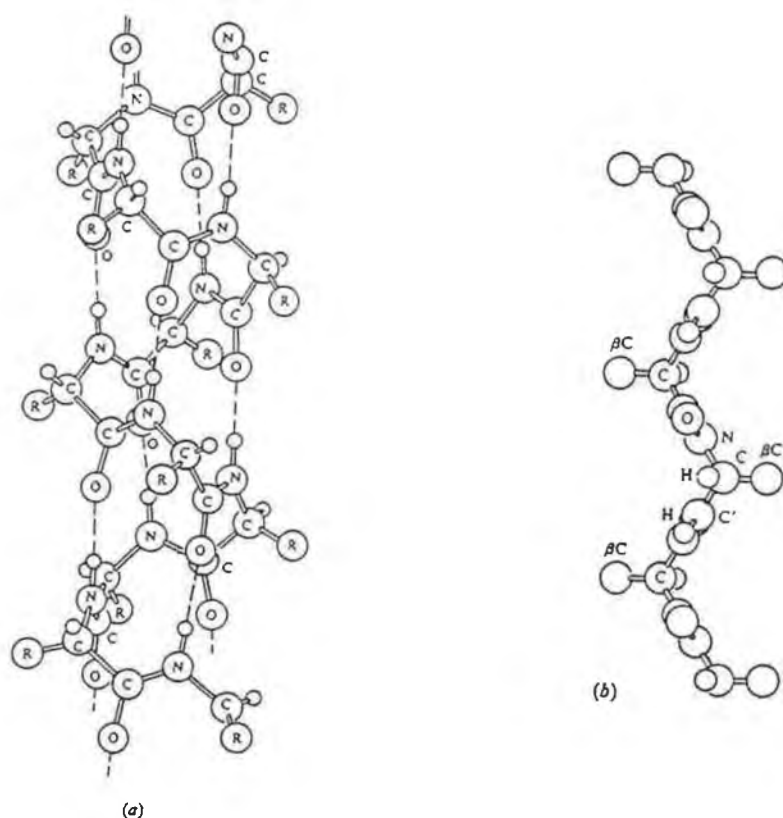

Figure 4.1. Structural forms of (a) α-helix and (b) parallel β-sheet [11].

This is a very abrupt and fast process (10^{-5} to 10^{-7} sec) and is a co-operative system. The initiation of the α-helix in a random coil is the slowest and energetically the most unfavoured step, whereas the subsequent growth of the α-helix nucleus is rapid and relatively favoured. Owing to the difficulty of nucleation, individual polypeptide molecules tend to be either entirely helical or disordered [11].

By gradually varying the nature of the medium, say by adding strongly interacting solvent (eg. trifluoroacetic acid) or pH changes in aqueous solution, or a change in temperature, a sudden change in physical properties results in a conformational change in the polymer molecule from the rigid helical structure to the non-rigid random coil structure [10].

Most synthetic polypeptides can be induced into α-helices by dissolving in dichloroacetic acid whereas β-sheets are favoured in solutions of formic acid [10]. Where side chains can ionise, the pH is important as electrostatic repulsions drive the ionised form into the random coil state where the distance may be maximised [10]. For example, poly-l-lysine is found to be in the random coil conformation below pH 10. In explanation of this phenomenon, the pK_a of the side group of lysine in poly-l-lysine is pH 10 so that, above this pH, all the amino groups are deprotonated, (See equation 4.1) thus allowing α-helical formation (due to the absence of charge repulsion of the NH_3^+ groups) [11].

$$NH_3^+ \Leftrightarrow \quad NH_2 \quad + \quad H^+ \qquad\qquad (4.1)$$

The effect of pH on the secondary structure of PLL, monitored by changes in the polypeptides optical rotation is illustrated in Figure 4.2. PLL conjugates also have varied applications from their use as polar tracers for cell lineage tracing in embryonic cells [12], to displaying antiviral and anticancer activity [13], to acting as powerful agents for aggregation of blood platelets [14].

Poly-l-glutamate (PLGlu) also possesses an ionisable group on its side chain, in this case a carboxylic acid on the glutamic acid residues.

$$COOH \quad \Leftrightarrow \quad COO^- \quad + \quad H^+ \quad (4.2)$$

The pK_a of the carboxyl group is pH 4.8 so above this pH, the COOH group is converted to COO^- and the random-coil conformation would then be favoured. This correlates well with the fact that PLGlu is found in the helical form at pH 4 whereas at pH 7 the random coil form is favoured [15].
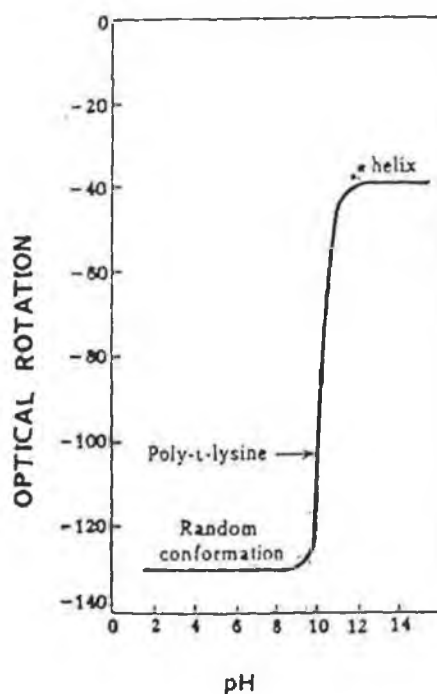

Figure 4.2 Effect of pH on the secondary structure of PLL.

173

The aim of the work in this thesis is to investigate the ability of ruthenium polypyridyl labels to monitor such structural changes in biomolecules, via their luminescent properties, under conditions at which conformational changes of the bound biopolymer in solution are induced. In this chapter, the effects of pH and chemical denaturants on the energy and intensity of the absorption and emission spectra are investigated.

Similar studies were carried out on a natural protein, bovine serum albumin, of which much less is known of its pH dependent dynamic behaviour. As expected, the interpretation of the results is a lot more difficult due to the complexity of its structure. As well as various forms of secondary structures present, proteins have tertiary or three dimensional structural forms, as well as undergoing a folding process, constituting their quaternary structure.

4.1.3. Physical properties of proteins.

Protein structure is usually discussed in terms of four levels. The primary structure is the amino acid sequence while the secondary structure is any regular local structure of a linear segment of polypeptide chain. More specific to natural proteins are the tertiary structure i.e. the overall topology of the folded polypeptide chain and the quaternary structure which is the aggregation of the polypeptides by specific interactions [9].

The molecular state in real polymers differs from the hypothetical unperturbed state, in that such polymers have finite dimensions as well as attractive and repulsive forces, both within the molecules and with the solvent [11]. Most proteins have helical regions of varying length interspersed with regions of random coil. Most proteins of biological significance differ dramatically from synthetic polypeptides of random or simple repetitive conformation and from structural proteins. These globular proteins have a smaller diameter in solution, being nearly spherical in shape. These physical properties do not change in a continuous manner

as the environment is altered, for example, by changing temperature, pH, pressure, as do random polypeptides. Instead, they exhibit little or no change, until a point is reached where there is a dramatic change in physical properties, and invariably a loss in biological function. This leads to protein denaturation, which leads to a structure much more like a random polypeptide than like the original protein.

The secondary structure in proteins is generally somewhat distorted. Generally, there are various classes of secondary structures found in proteins. Amino acids with branched or bulky side chains, such as valine, ileucine and threonine, or aromatic rings, such as phenylanaline, threonine and tryptophan occur most frequently in β-sheets [11]. The remainder most often occur in α-helices, except for those with short polar (serine, aspartine, aspartate) or special side chains (glycine, porcine) most often found in reverse turns.

As with polypeptides, the forces involved in the maintenance of secondary and tertiary structure include interpeptide and side chain hydrogen bonds, ionic bonds and hydrophobic bonds [15]. It is believed that there is a relationship between primary and higher order structures of proteins. As a result, the restoration of proteins to their native states following the initial loss of native structure, indicating a non-random process is observed.

As the distribution of the α-helix is one of the most important features of the process of protein denaturation [10], poly-amino acids are simple models of proteins and are ideal substrates for model processing of protein denaturation. The aim of folding polypeptide chains is to arrive at a more stable structure in aqueous solution, collapsing into a conformation where hydrophobic interactions dominate [11].

The stable conformation will remain until perturbed by a change in conditions. As the folded conformation of certain proteins is only marginally stable under the best of conditions, it may be disrupted merely by change in environment, a rise in temperature, variation of pH, increase in pressure or addition of denaturant. Thus, there are many conformations between the native state of a protein molecule and that in which the protein chain is completely denatured.

As the environment is altered towards conditions favourable for unfolding, there is initially little change with increases in flexibility, but within a rather limited range of conditions it then becomes fully unfolded [11]. For example, nuclease experiences acid-induced unfolding over a pH range of 0.30 pH units. As for random coil to helix transitions in model polypeptides, this is a co-operative transition where each of a number of groups can be ionised only if all do so simultaneously. Unfolding is a two state phenomenon with only fully folded and unfolded states present.

Denaturation does not require the rupture of covalent bonds i.e. cleavage of the primary structure and hence it is sometimes possible to reverse denaturation by the removal of the agent. It rather involves the disruption of some folded conformation of the polypeptide chain upon which it's biological properties are often critically dependent [9]. A particular treatment of a protein may, for example, drastically alter biological activity though extensive physical measurements reveal slight or no change in structure. Examples of denaturation by heat is frequently irreversible but by urea is usually reversible [15].

When a protein has substantial net charge, electrostatic repulsion between ionised groups might cause unfolding since such repulsion would be minimised in the unfolded state. The unfolded state may approach random-coil state for disordered polypeptides for urea, nonrandom conformation is apparent for acid and heat denatured states while denaturation by ultraviolet irradiation, organic solvents, guanidinium chloride, LiBr and detergents may lead to very different denatured states [15].

4.2 Results and Discussion.

From the above discussion, the complexity of the dynamic behaviour of proteins in solution is evident. Nevertheless, the significant effect of parameters such as pH, solvent and temperature on the physical properties of biomolecules has been emphasised. This chapter deals with inducing conformational changes in the proteins labelled with ruthenium complexes by varying the pH in particular but also temperature and reagents, and monitoring corresponding variations in the spectroscopic properties, namely the energy and intensity of the absorption and emission spectra of the bound label. In this respect, it will be possible to deduce the potential of these fluorescent complexes as probes of biological structures. The unbound ruthenium complexes are used as controls to ensure that any variations in the spectroscopic properties of the bound label are indeed due to conformational variances of the bound protein and not merely due to the behaviour of the free complexes.

4.2.1. pH sensitivity of absorption spectra.

As mentioned earlier, the absorbance of UV light is not very sensitive to conformation or environment, and so is limited in its potential to follow changes in the folded conformation of a protein in solution [11]. Nevertheless, the polypeptide backbone absorbs in the UV region 240nm, with the absorbance intensity of the protein dependent to some extent upon the conformation on the biomolecule. Folded proteins are also known to exhibit significant absorbency in the UV region 250-300nm [9]. Figure 4.3 illustrates the absorption spectrum of BSA at various pHs, verifying the pH sensitivity of absorbency of proteins at 240 nm, presumably due to conformational changes/unfolding of the protein under such extreme conditions. Although variations are apparent these are not sensitive enough to yield information on conformational changes and it is exactly for this reason that the

177

highly fluorescent ruthenium complexes absorbing strongly in the visible region were bound to the biomolecules.
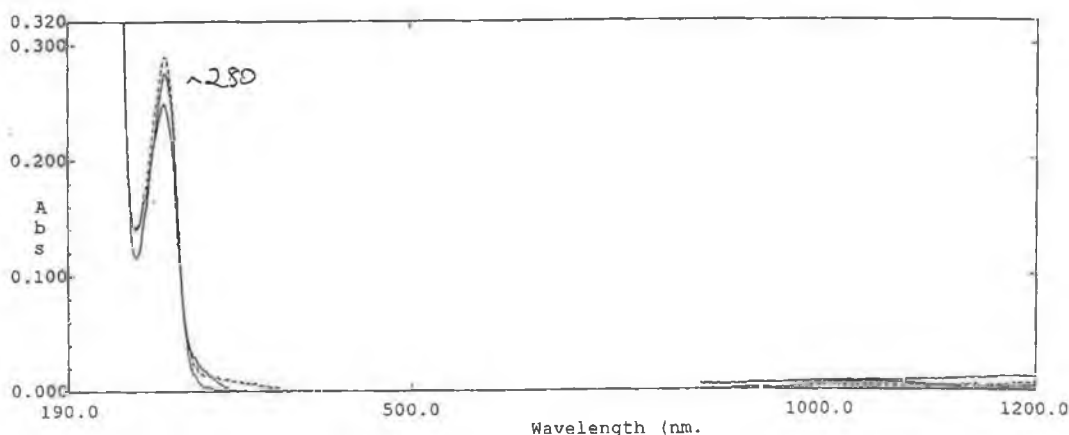

Figure 4.3. pH sensitivity of the absorption spectrum of BSA.

Prior to studying the pH sensitivity of the absorption spectra of the protein-bound labels, a study of the variability of absorbencies of the unbound labels in the range 290-700 nm was studied from pH 2 to pH 12 both to investigate any evidence of protonation/deprotonation effects and to check the stability of such complexes under such conditions. This has the additional purpose of ensuring that any changes in the absorption spectra of the protein-bound labels are not merely due to the decomposition of the free label. Figure 4.4 illustrates the effect of pH on the absorption spectrum of $[Ru(bpy)_2NH_2phen]^{2+}$ while Figure 4.5 depicts the pH sensitivity of the absorption spectrum of the isothiocyanate derivative $[Ru(bpy)_2NCSphen]^{2+}$.

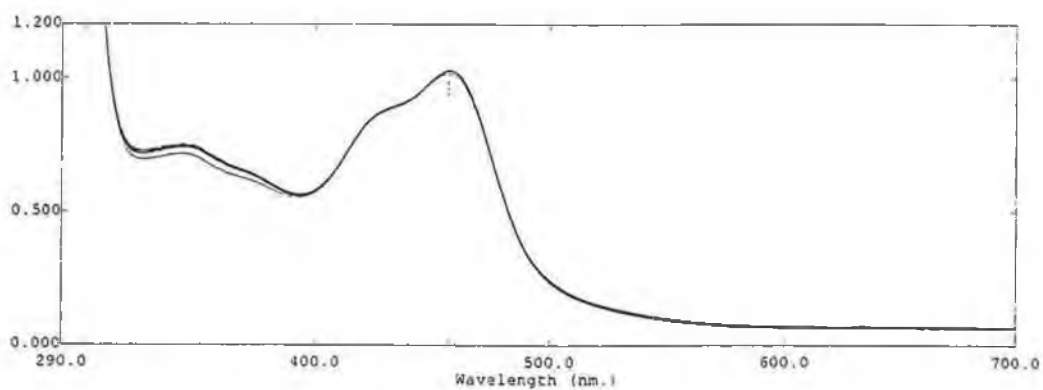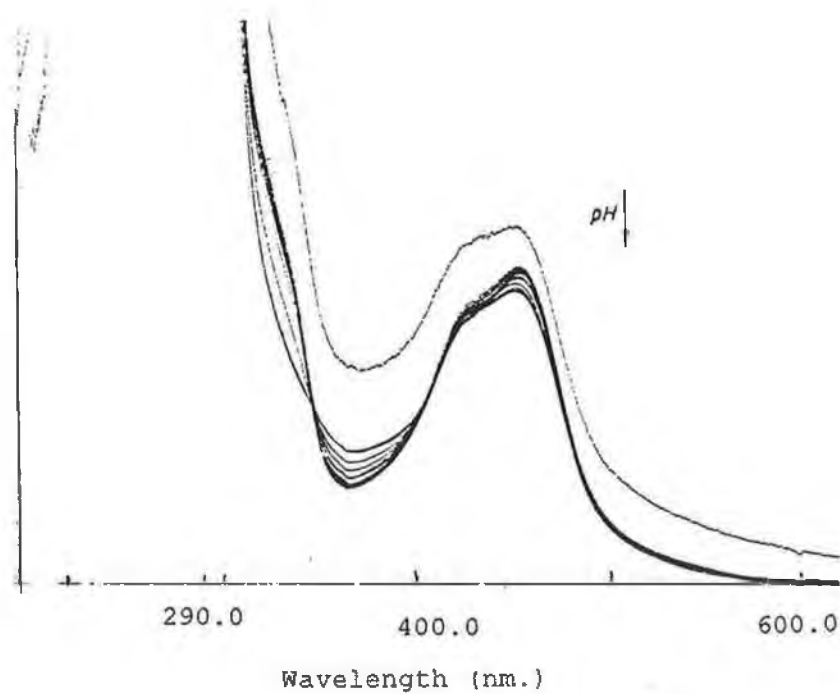*Figure 4.4 Effect of pH on the absorption spectrum of [Ru(bpy)₂NH₂phen]²⁺.*

Figure 4.5 pH sensitivity of the absorption spectrum of [Ru(bpy)₂NCSphen]²⁺.

179

From Figure 4.4 above, it is evident that the absorbencies of the complexes $[Ru(L-L)_2NH_2phen]^{2r}$ in the visible region are almost totally insensitive to pH in the range pH 2-12 in that the wavelengths and intensities of maximum absorbance are not shifted. This indicates the stability of such complexes even at pH extremes but also provides no evidence of protonation of the amino group present on one ligand as may be expected. The UV/vis spectra of the isothiocyanate derivatives on the other hand reveal a change in form in terms of the intensity of absorbance peaks and the energy of the peaks on increasing the pH as depicted in Figure 4.5. Above pH 9, the energy of the absorption spectrum in the MLCT and MC region changes and the form appears to return to that of the amino precursor, indicating that decomposition of the complex to its amino precursor may take place under such conditions. This correlates with reports in the literature [17], that the complexes are not very stable in aqueous solution reverting back to the precursor amino complex under such conditions.

In contrast both the energy and intensity of the absorption spectra of both $[Ru(bpy)_2COOH_2bpy]^{2+}$ and its ester form i.e. $[Ru(bpy)_2(esterbpy)]^{2+}$ are very sensitive to pH, due to protonation/deprotonation effects. On increasing the pH of $[Ru(bpy)_2COOH_2bpy]^{2+}$ above pH 2, the form of absorbance spectrum changes with the main absorbance peak of the label increasing in intensity while its wavelength shifts from 460 nm to 480 nm. This phenomenon has already been reported for similar acidic complexes in the literature [16]. Such characteristics are explained in terms of the presence of the carboxylic acids on the label. The pK_a of these groups is approximately 2, and above this pH the two carboxylic acids present are in the dissociated state, displaying different spectroscopic behaviour to the non-dissociated state. The ester form displays similar unusual pH dependent spectroscopic behaviour shown in Figure 4.5. However the increase in intensity and shift in absorbance maximum occurs above pH 3, indicating a shift in the pK_a of the carboxylic acid, perhaps due to the modification of the neighbouring group. A possible explanation for the protonation influences observed in the absorption spectrum of the "ester" would be the hydrolysis of the ester in acid and/or base leading to its decomposition

180

to its acidic precursor. However the reversibility noted for the changes in the absorption spectra imply otherwise, indicating the stability of the ester under such conditions. Rather, the esterification of only one of the reactive carboxylic acids appears to be the cause of such absorbencies. The pH sensitivity of the UV spectrum of the "ester" is depicted in Figure 4.6.
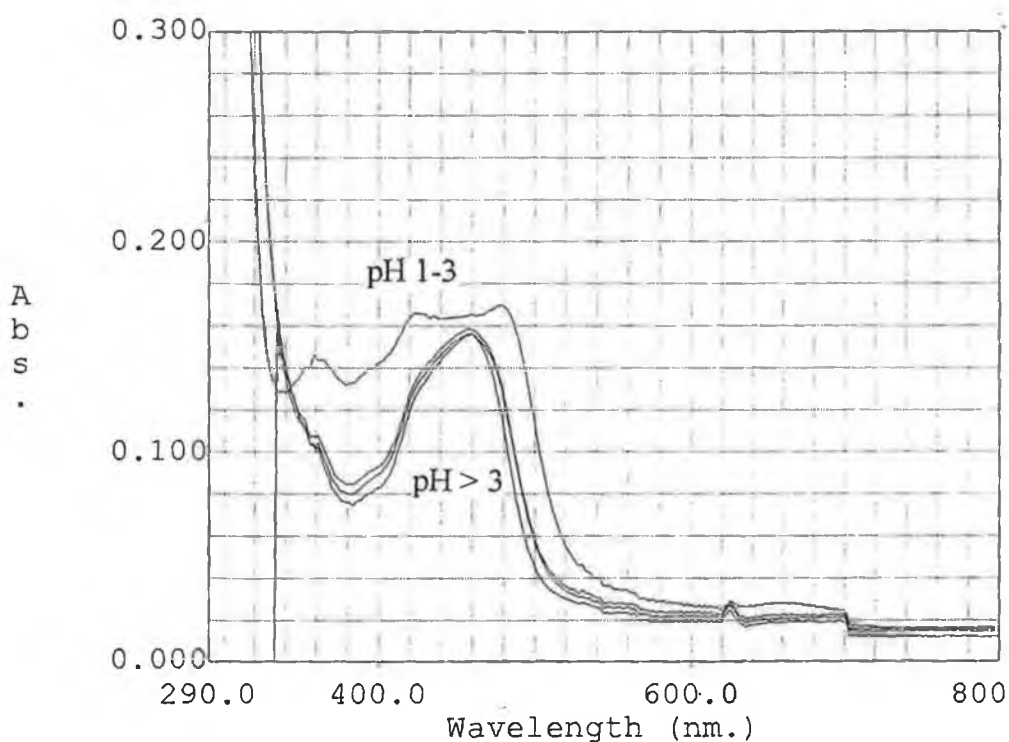
Figure 4.6 Effect of pH on the absorption spectrum of [Ru(bpy)$_2$esterbpy]$^{2+}$

As previously stressed, upon conjugation the visible region in the absorption spectrum of ruthenium complexes is not notably affected by the absorbencies due to the bound biomolecules, as these occur in the UV region. Absorption spectra were obtained for the various protein-bound labels from pHs 2-12. These were run for the following purposes; (1) to observe how the binding of the protein to the relevant functional group (NH$_2$, NCS, ester) of the label influences the ligand on the labels

181

absorbencies due to their protonation effects; (2) to ensure that decomposition of the bioconjugate does not occur at pH extremes and (3) to observe the sensitivity of the labels absorption in the visible region to acid-induced conformational variances of the bound biomolecule. Figure 4.7 depicts the absorption spectrum of $Ru(dpp)_2NH_2phen:BSA$ upto 1200 nm where absorbencies due to the protein may be evident while Figure 4.8 illustrates the pH sensitivity of the absorption spectrum of $Ru(phen)_2NCSphen:PLL$, restricted to the visible region where the label absorbs strongly (290-700 nm). As for the unbound label, the absorbencies of the protein-bound label $Ru(dpp)_2NH_2phen:BSA$ reveal very little sensitivity to pH with the absorption peaks merely appearing broader and of different intensity at lower pHs. Otherwise, the effect of the protein binding on the UV-visible spectrum of the label is negligible indicating as expected that the absorbencies of the label are not sensitive to any conformational variances of the protein. The spectrum of $Ru(phen)_2NCSphen:PLL$ in Figure 4.8 shows that the variations for the unbound label observed for the isothiocyanate at 350 nm possibly due to its decomposition are no longer apparent. This would be anticipated as the binding of the NCS group to the protein would lead to its stabilisation. Slight variations in the absorption spectra of the protein-bound labels are observed particularly at 300-400 nm but appears to be merely due to the turbidity of the protein solution at certain pHs.

It is apparent from these spectra that the covalent bonds formed between label and biomolecules are stable and resistant to pH extremes. This is a prerequisite to their use as probes of biological structures, particularly when the acid-induced conformational variations of the biomolecules are to be followed. Finally, as suspected, although some variations in absorption intensities in the ultraviolet region are noted due to conformational effects of the proteins, variations in the visible absorbencies of the protein-bound label are almost negligible, deterring their use as a probe in the detection of their acid-induced conformational variances.
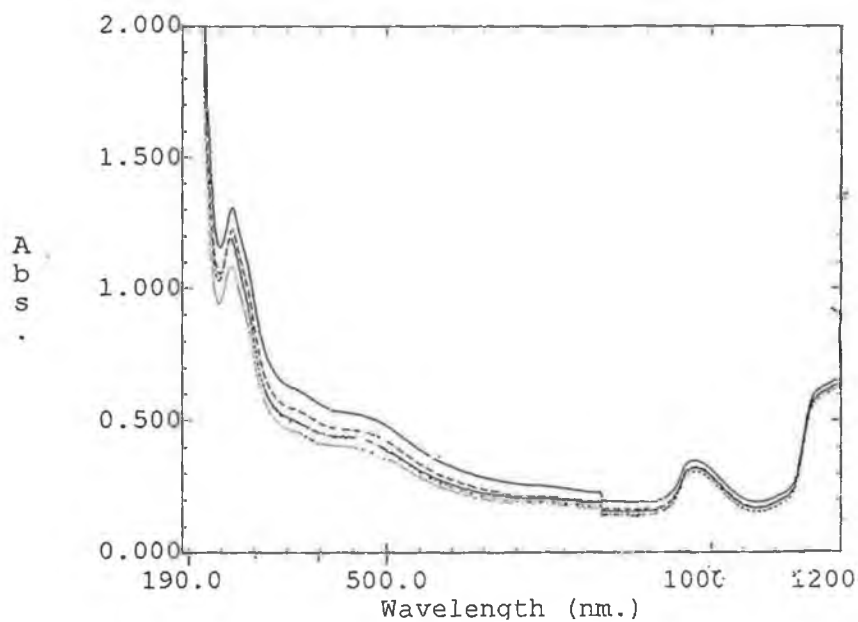
Figure 4.7 pH sensitivity of absorption spectrum of Ru(dpp)₂NH₂phen:BSA.

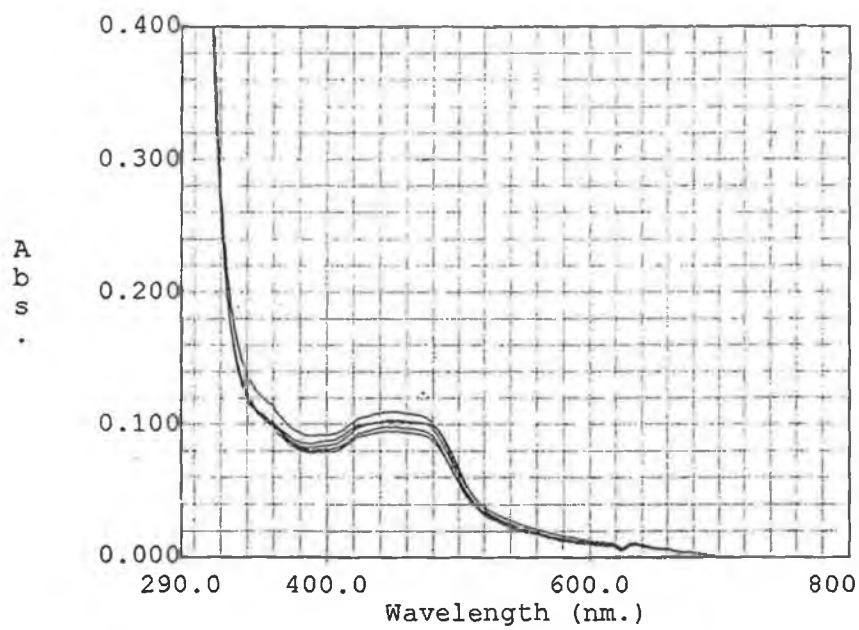*Figure 4.8 pH sensitivity of absorption spectrum of Ru(phen)₂NCSphen:PLL.*

4.2.2. pH sensitivity of the emission spectra.

Proteins are the only biopolymers that are known to fluoresce, due to the presence of the natural fluorophores tyrosine and tryptophan [18]. Such residues have a low quantum yield and are very sensitive to the polarity of the surrounding solvent with the emission maximum for tryptophan ranging from 330 nm in a hydrophobic environment to 355 nm in water [18]. Recently it has been deemed possible to reveal protein dynamics by fluorescence methods involving anisotropy measurements and fluorescence quenching [18]. However, as we are interested in the fluorescence of the labels bound to proteins the molecules are excited at 450-470 nm and the emission observed at 600-620 nm is that of the label with no interference from the unmodified protein.

For reference however, the influence of pH on the emission characteristics of the unmodified proteins was firstly examined. Figure 4.9 depicts the effect of pH on the emission spectrum typical of BSA whose emission maximum occurs at 320-360 nm. One notes that the intensity of the emission is very low. As expected, the emission intensity and wavelength varies from acidic to basic pHs with conformational changes possibly due to unfolding apparently inducing the variations at pH extremes, particularly striking under alkaline conditions. On the other hand the emission spectrum of the synthetic biomolecule poly-L-lysine is less affected by pH extremes, presumably due to the fact that PLL does not actually "unfold", being a synthetic biomolecule which has no quaternary structure but rather experiences changes in its secondary structure. Indeed, a study of the pH sensitivity of the emission intensity of the fluorescence of proteins reveals more clearly the sensitivity of their fluorescence to acid-induced conformational changes. The quantum yields of the fluorescence of the proteins used in this study are calculated by comparing the emission intensity of their fluorescence to that of tryptophan after normalising their absorption intensity close to their λ_{max}. The pH sensitivity of the intrinsic fluorescence of the various biomolecules concerned is tabulated in Table 4.1.

184

It is assumed that the sensitivity of the fluorescence intensity of the protein bovine serum albumin to pH changes reflect its sensitivity to acid induced conformational changes due to the sensitivity of the emitting species to its local environment. The emission intensity of BSA is particularly reduced above pH 8, indicating structural changes and possibly unfolding at such pHs. This is more significant than the drop at acidic pHs, probably due to the fact that BSA is an acidic protein and hence would be expected to become fully unfolded at basic pHs. Figure 4.10 contrasts the effects of pH on the emission intensity of the natural fluorescence of proteins and poly-amino acids.
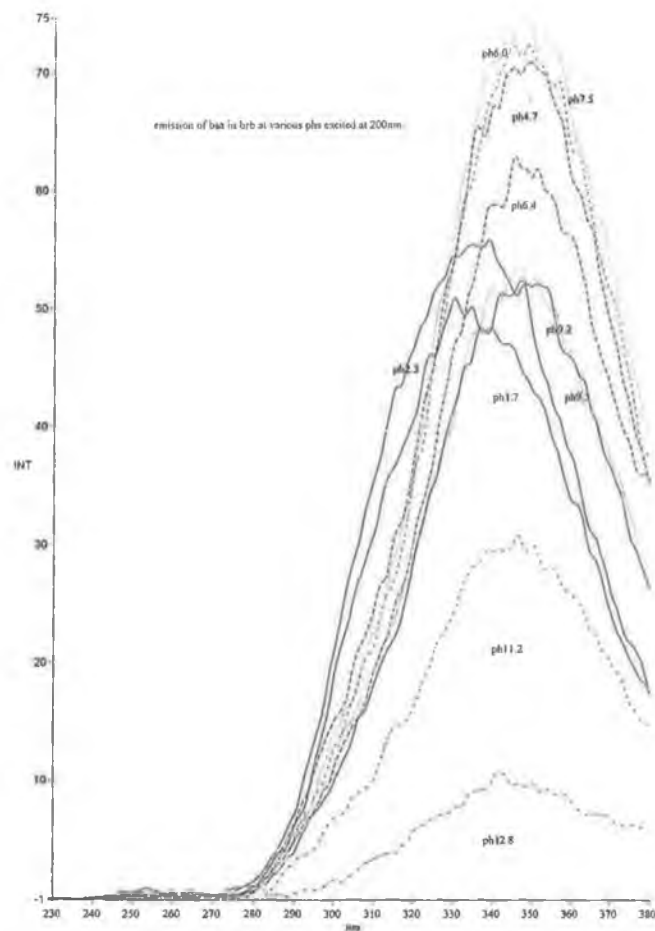
Figure 4.9 pH sensitivity of the intrinsic fluorescence of BSA.

Table 4.1 pH sensitivity of the emission intensity of the fluorescence of (a) bovine serum albumin, (b) poly-l-lysine and (c) poly-l-glutamate.

Protein	Quantum yield of emission (λ_{emiss} = 330-350 nm)					
	pH 2	pH 4	pH 6	pH 8	pH 10	pH 12
Bovine serum albumin	0.22	0.25	0.74	0.48	0.045	0.015
Poly-L-lysine	0.032	0.20	0.20	0.20	0.35	0.75
Poly-L-glutamate	0.10	0.12	0.10	0.12	0.15	0.10

The quantum yield values given are the emission intensities of the fluorescence of the proteins compared to that of free tryptophan of the same absorbance using the equation $\phi_{em} = (A_s \, / \, A_{ref})$ where A_s and A_{ref} are the integrated areas / heights of the emission band of sample and reference complex respectively.

Figure 4.10 pH sensitivity of the quantum yields of emission of the proteins (1) BSA (2) PLL and (3) PLGlu.

186

In general, the fluorescence is less intense for the poly-amino acids. Indeed PLL/PLGlu would not be expected to fluorescence as they do not possess tyrosine or tryptophan residues the prime fluorescent residues. However, as a wavelength not unique to the absorption of such residues was us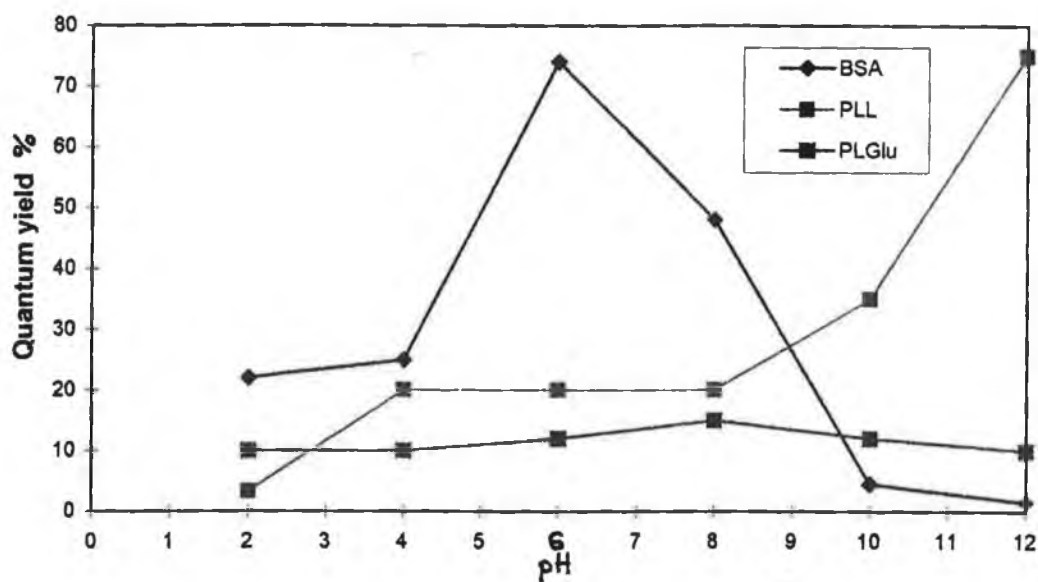ed to excite the proteins, other low emissions were picked up. The use of tryptophan as a reference for all proteins despite the fact that PLL/PLGlu do not contain these may explain the pH sensitivity of the low emission of the synthetic biomolecules. Nonetheless less dramatic pH induced variations would be expected as it is not a question of unfolding but of local secondary structural changes occurring. These studies merely confirm what was anticipated, including the low intensity of the fluorescence of the proteins, the difficulty of quantitative analysis and the significant effect of solvent but also the sensitivity of the intrinsic fluorescence of proteins to conformational variances.

However, as the fluorescence of the labels is the issue here, the next step involved determining the potential of the emission spectra of the labels when bound to proteins to monitor their acid-induced conformational variances. Hence the emission spectra of the unbound labels are initially studied. The intensities of all the emission spectra of the free labels used are quite sensitive to pH while the energies of the emission maxima are not shifted significantly. Figure 4.11 illustrates how the intensity of the emission of $[Ru(dpp)_2NH_2phen]^{2+}$ is at a minimum at very acidic pHs. Although the general trend shows the intensity to increase with increasing pH, the maximum emission intensity is observed from pH 7-10. Furthermore, λ_{max} shifts to a slightly lower wavelength at very basic pHs, although the shift is probably within instrumental error (2-4 nm). The decrease in emission intensity at acidic pHs which was found to be reversible on addition of base is consistent with the effects of protonation of the emitting ligand on the emission spectrum for Ru(II) complexes. As variations in the absorption spectrum due to protonation effects are not apparent, the possible protonation effects noted in the emission spectrum indicate that the excited state of the complex is probably more basic than that of the ground state. It would be indeed possible to calculate the excited state pK_a^* of the complex by using the following equation ;

$$pK_a^* = pH_i + \log (\tau_a/\tau_b) \qquad\qquad (4.1)$$

where pH_i is the inflection point of the emission intensity vs pH curve. This is called the "apparent pK_a^* " as these values need to be corrected if the protonated (τ_a) and deprotonated (τ_b) complexes have different emission lifetimes.

Figure 4.12 represents the pH susceptibility of the emission of $[Ru(L-L)_2NCSphen]^{2+}$ whereupon a decline in emission intensity is noted at high pHs i.e. above pH 10. Again, in correlation with the observations of the absorption spectra, this may be due to reversion of the complex back to its amino precursor. However the same is probably not true for $[Ru(bpy)_2esterbpy]^{2+}$. Above pH 3, a change in the form of the emission spectrum is evident whereby an increase in emission intensity and striking shift in emission maximum from 680 nm to 656 nm is observed, again indicating the dissociation of COOH. As the pK_a of the excited state complex is higher than that of the ground state it would appear that the excited state complex is less acidic. Again, the variations in the emission spectrum observed are reversible with further addition of acid/base, dismissing the possibility of decomposition of the complex and further confirming that both carboxylic acids were not successfully reacted with the hydroxysuccinimide (see section 2.2.3).
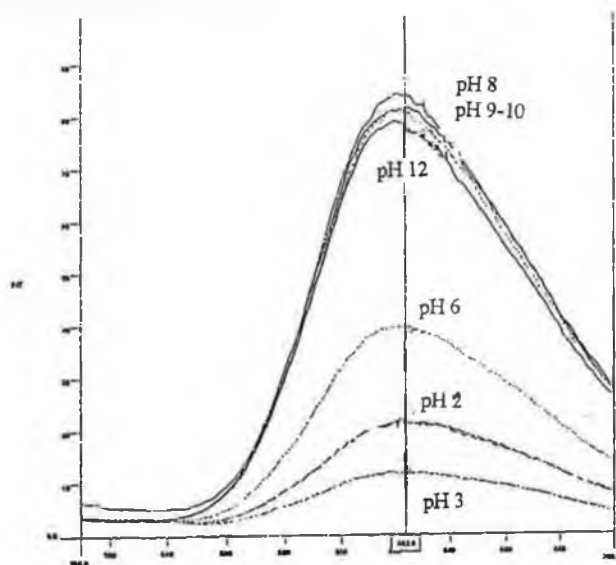
Figure 4.11 pH sensitivity of emission spectrum of $[Ru(dpp)_2NH_2phen]^{2+}$.
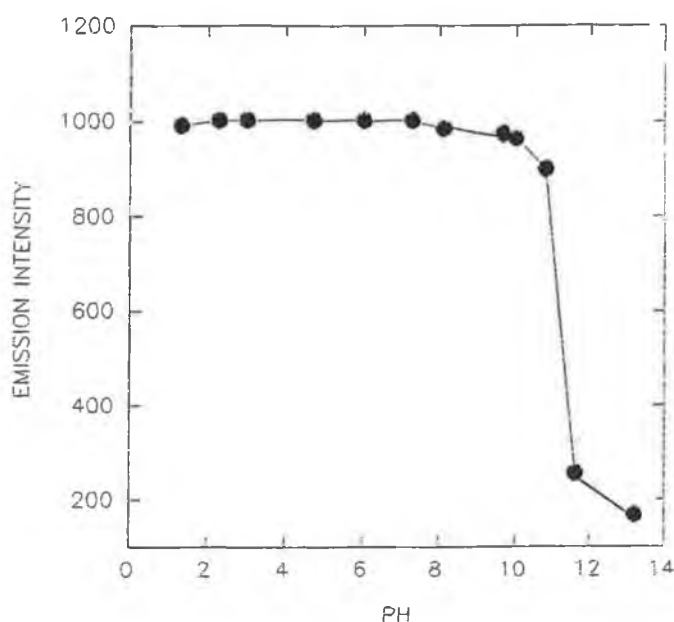
Figure 4.12 pH sensitivity of the emission intensity of [Ru(dpp)$_2$NCSphen]$^{2+}$.

Another important issue concerning the emission of these ruthenium complexes is the effect of conjugation to proteins on their quantum yield, as a minimal effect is desired to render these complexes suitable as fluorescent probes. The quantum yield of a compound is defined as the fraction of molecules that emit a photon after excitation by the source [19] and is determined by comparing the emission intensity of a sample to that of a reference compound whose quantum yield is known, in this case [Ru(bpy)$_3$]$^{2+}$ at a wavelength where both samples absorb equivalently. The estimation of the quantum yield of emission of the protein-bound labels and comparison to those of the free labels is rendered difficult due to the fact that the free label possesses only one emitting species while the protein-bound forms display multi-exponential decay kinetics. Therefore, changes in the contributing ratios of the two emitting components of the protein-bound labels would influence

the quantum yield determination and render comparison difficult. However, a brief study was carried out to approximate the effect of conjugation on the apparent quantum yield of emission of these labels (ϕ_{em}).

Firstly, the ϕ_{em} of the Ru(II) complexes, unbound and when bound to proteins were determined according to the method of optically dilute measurements described by Demas and Crosby [19] and as outlined in section 2.4.1. $[Ru(bpy)_3]^{2+}$ whose quantum yield is known to be 0.028 is suitable as the reference compound as it has no overlap between absorption and emission, is soluble in the same solvents (hence there is no need for refractive index correction) [19], and has similar absorption and emission spectra to the complexes being studied.

Table 4.2 Effect of protein-binding on the apparent quantum yields of emission of Ru(II) complexes in 0.10 M carbonate buffer, pH 9.2.

Complex/Conjugate	Quantum yield	
$[Ru(bpy)_2NH_2phen]^{2+}$	0.025	
$[Ru(bpy)_2NH_2phen]$:BSA	0.025	
$[Ru(phen)_2NH_2phen]^{2+}$	0.020	
$[Ru(phen)_2NH_2phen]$:BSA	0.018	
$[Ru(phen)_2NH_2phen]$:PLGlu		0.024
$[Ru(phen)_2NCSphen]^{2+}$	0.040	
$[Ru(phen)_2NCSphen]$:BSA		0.060

Normalisation of absorbance intensity was carried out prior to emission measurement.

$\phi_{em}=0.028(A_S/A_{ref})(n_S/n_{ref})^2$ *where A_S and A_{ref} are the integrated areas of the emission band of the sample and reference respectively and n_S and n_{ref} are the solvent refractive indices of the sample and reference solutions respectively [19].*

The first point to note is that the quantum yields of emission of the unbound labels at low concentrations are all quite similar i.e. 0.007 to 0.015 which is quite low. It is difficult to compare absolute quantum yield values of ruthenium complexes when bound to proteins as the exact concentrations of ruthenium is difficult to quantify and variations in concentrations are unavoidable. A table of quantum yields for free and various protein-bound labels is outlined in Table 4.2.

These results verify the minimal effect that the covalent linkage to proteins has on the quantum yields of emission of the Ru(II) polypyridyl complexes which is indeed a prerequisite to their successful application as luminescent probes. However, the extent and nature of the effect of the conformational variances of a protein bound to such complexes on their emission spectra will determine the probing capacity of their emission.

Figure 4.13 depicts the pH sensitivity of the emission of the label $[Ru(bpy)_2NH_2phen]^{2+}$ when bound to PLGlu. The noticeable decline in emission intensity between pH 4 and pH 5 is all the more significant when one considers the transition from an α-helical conformation to a random-coil which poly-L-glutamate is known to undergo at approximately such a pH range [22]. Furthermore, the fluorescence of the unbound label $[Ru(bpy)_2NH_2phen]^{2+}$ does not display such behaviour at pH 4-5 (See Figure 4.11), which suggests that such behaviour is indeed due to the changes in secondary structure of the biomolecule.

Figure 4.14 depicts the influence of pH on the fluorescence of the conjugate $Ru(bpy)_2NCSphen:PLL$. Interestingly, the wavelength of maximum emission (λ_{max}) shifts slightly from 608 nm below pH 9 to 605 nm at pHs 9-12 while the intensity decreases significantly above pH 10, at approximately the pH at which the random-coil to α-helix transition occurs. However, on comparing with the behaviour of the corresponding unbound label (See Figure 4.12) the variations are of the same nature as those of the unbound label in the sense that the intensity decreases dramatically above pH 9-10. However, on binding the NCS group to the proteins the unstability of such a complex (or indeed its protonation) should no longer be a phenomenon, suggesting that the decrease in emission intensity typical of the

191

unbound label should no longer be evident. Therefore, it may be possible that such variations are indeed due to the conformational changes of the bound polypeptide.
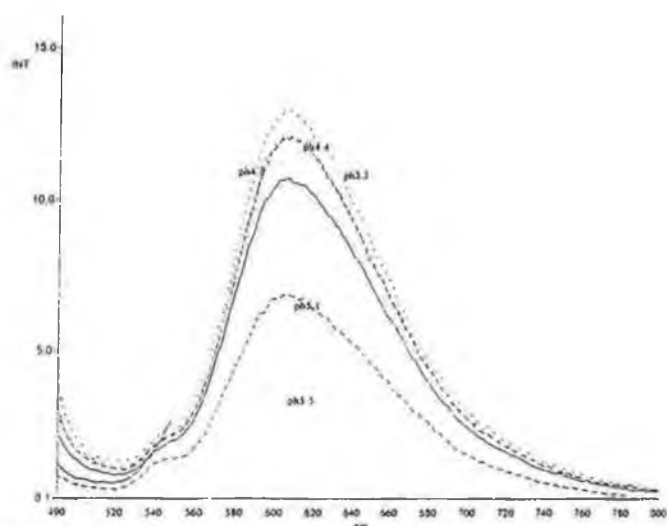

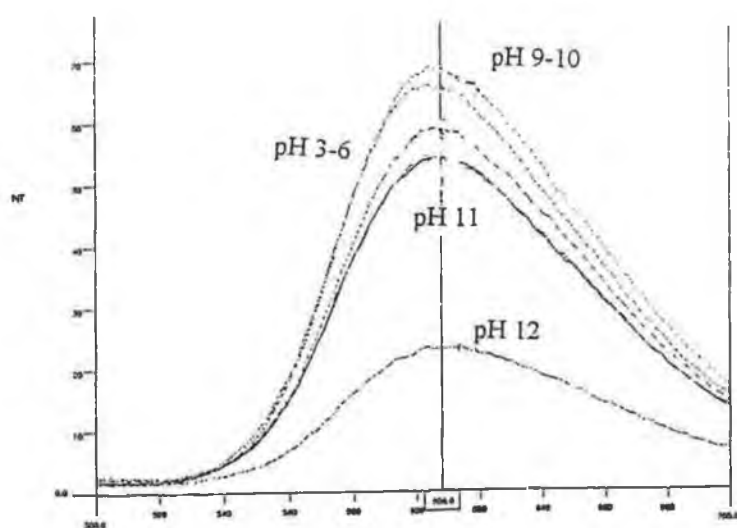*Figure 4.13 pH sensitivity of the emission spectrum of Ru(bpy)$_2$NH$_2$phen:PLGlu.*

Figure 4.14 pH sensitivity of the emission spectrum of Ru(bpy)$_2$NCSphen:PLL.

192

Thus far, we have found that the emission spectra of the complexes [Ru(L-L)$_2$NH$_2$phen]$^{2+}$ and [Ru(L-L)$_2$NCSphen]$^{2+}$ when bound to biomolecules are somewhat sensitive to the acid-induced secondary structure changes of the poly-amino acids poly-L-lysine and poly-L-glutamate. However, as a result of the pH sensitivity of the emission spectra of the free labels some of the effects of the bound biomolecule may be masked thereby restricting its potential in certain pH ranges. An extreme case is the complex [Ru(bpy)$_2$esterbpy]$^{2+}$ whose absorption and emission spectra do not change significantly on the binding of the biomolecules. The spectra typical of carboxylic acid complexes for the protein-bound label is probably due to the fact that the unbound reactive group has not been esterified, hence interfering with any effects the protein may have on the other esterified group. For this reason, the remainder of this section concentrates on the study of the amino and isothiocyanate complexes.

The propensity of the emission spectra of [Ru(L-L)$_2$NH$_2$phen]$^{2+}$ and [Ru(L-L)$_2$NCSphen]$^{2+}$ to monitor acid-induced denaturation of a natural protein was also studied. As an example, the emission spectrum of Ru(dpp)$_2$NCSphen:BSA from pHs 2 to 12 is depicted in Figure 4.15. In this case a dramatic decline in emission intensity is observed above pH 9 and below pH 3, indeed more dramatic than the decline seen for the corresponding unbound label. Although this indicates that such an effect may be due to the acid-induced unfolding of the protein as most proteins are most stable between pHs 4 and 9 (similar to pH range of maximum intrinsic fluorescence of BSA), the exact effects are vague and difficult to confirm, again due to the pH susceptibility of the labels fluorescence.

However, the use of the amino complex to bind the protein gives a clearer picture as the fluorescence of the complexes [Ru(L-L)$_2$NH$_2$phen]$^{2+}$ does not decrease appreciably in intensity at pHs above pH 9, at which the protein is believed to become unfolded. Figure 4.16 reveals a notable reduction in emission intensity of [Ru(L-L)$_2$NH$_2$phen]: BSA above pH 9, which indicates that this does not merely mirror the spectroscopic effects of the unbound label but rather is associated with the conformational variability of the bound protein.

193
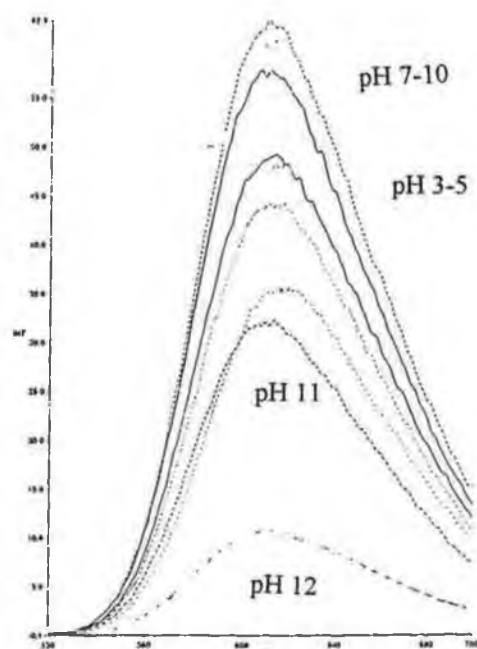
Figure 4.15 pH sensitivity of the emission spectrum of Ru(dpp)₂NCSphen:BSA.
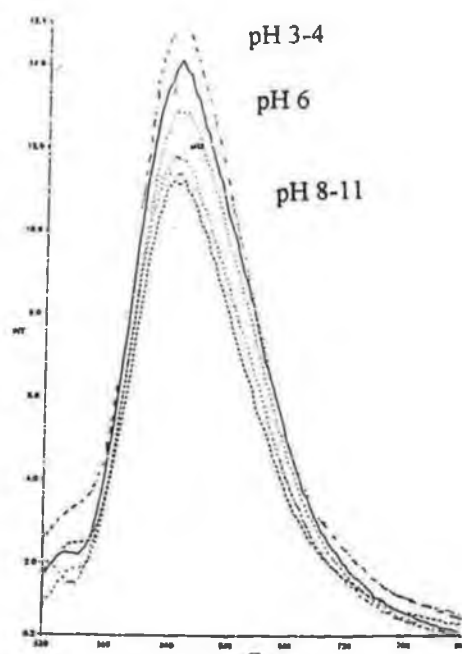
Figure 4.16 pH sensitivity of the emission spectrum of Ru(bpy)₂NH₂phen:BSA.

194

Table 4.3 pH sensitivity of quantum yields of emission of [Ru(L-L)$_2$NCSphen]:BSA and [Ru(L-L)$_2$NH$_2$phen]:BSA.

Conjugate	Quantum yield (φ)					
	pH 2	pH 4	pH 6	pH 8	pH 10	pH 12
Ru(bpy)$_2$NH$_2$phen:BSA	0.006	0.005	0.018	0.022	0.02	0.008
Ru(phen)$_2$NH$_2$phen:BSA	0.006	0.004	0.006	0.017	0.002	0.003
Ru(dpp)$_2$NH$_2$phen:BSA	0.0025	0.0045	0.003	0.003	0.002	0.0008
Ru(bpy)$_2$NH$_2$phen:BSA	0.006	0.005	0.018	0.022	0.02	0.01
Ru(bpy)$_2$NCSphen:BSA	0.004	0.005	0.01	0.016	0.01	0.004
Ru(phen)$_2$NCSphen:BSA	0.06	0.065	0.068	0.07	0.055	0.015
Ru(dpp)$_2$NCSphen:BSA	0.028	0.035	0.070	0.040	0.008	0.003
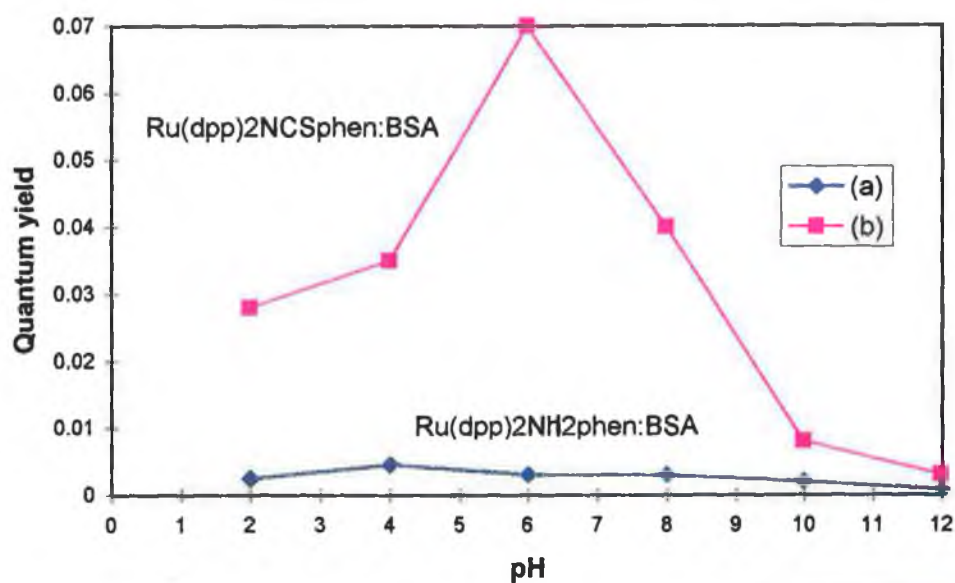
Figure 4.17 pH sensitivity of intensity of the fluorescence of (a)Ru(dpp)$_2$NH$_2$phen:BSA and (b) (Ru(dpp)$_2$NCSphen:BSA.

Nevertheless, to clarify this effect of the bound protein on the emission intensity of the labels, Table 4.3 lists the quantum yields of emission of Ru(II) complexes when bound to bovine serum albumin at various pHs, thereby outlining their sensitivity to pH changes. Again, these values are listed merely to give an indication of the absolute effect of the protein on the emission spectra of the labels.

This table of results basically highlights the fact that the apparent quantum yields of emission of the ruthenium complexes when bound to a natural protein such as bovine serum albumin are very sensitive to pH changes. The quantum yields of emission are significantly reduced at pH extremes in particular at very alkaline pHs i.e from pHs 9-12 as was already concluded for the emission spectra of the protein-bound labels. Significantly, this table together with Figure 4.17 reveal how the emission intensity of the Ru(II) complexes bound to proteins behaves in a similar fashion to the intrinsic fluorescence of such proteins (see Figure 4.10) at pH extremes.

As stated earlier, the reason for changes in emission intensity is likely to be due to unfolding or denaturation of the protein at both extremes of pH but particularly at basic pHs. It is not clear why exactly the emission intensity of the label decreases so dramatically when the bound protein unfolds but merely establishes a possible link between emission intensity variations of the fluorescent labels and the acid-induced conformational variances of both synthetic biomolecules and natural proteins. However, the pH susceptibility of the emission spectra of the unbound labels and possible protonation effects somewhat restricts their suitability to monitor structural variances of bound proteins.

Earlier studies have already revealed that the emission lifetime of the Ru(II) complexes is the luminescent property most affected by the subsequent binding to proteins. This, in addition to the fact that there is usually correlation between emission lifetime and emission intensity variations lead us to the study of the sensitivity of the decay lifetimes of the labels to the conformational variances of the bound protein.

4.3 Conclusion.

The photophysical properties of ruthenium polypyridyl complexes when covalently bound to the natural protein bovine serum albumin and the synthetic poly-amino acids, poly-l-lysine and poly-l-glutamate are explored further in this chapter. The ultimate objective in this chapter is to assess the sensitivity of the spectroscopic properties, namely the energy and the intensity of the absorption and emission spectra of such fluorescent complexes to the acid-induced conformational variances occurring in the bound protein and hence to determine their potential to act as probes of such variations.

The absorption spectra of the unbound labels $[Ru(L-L)_2NH_2phen]^{2+}$ are not susceptible to pH effects (pH 2-12), suggesting that protonation of the amino group does not take place but also indicating the stability of such complexes even at extreme pHs. The change in form of the absorption spectra of $[Ru(L-L)_2NCSphen]^{2+}$ indicate that these complexes may revert back to their precursor amino complexes at extremes of pHs while the succinimide ester of $[Ru(bpy)_2COOH_2bpy]^{2+}$ possesses an absorption spectrum typical of its precursor, indicating that the two carboxylic acids were not successfully esterified. However, even though the pH sensitivity of the protein-bound labels reveal changes in absorption intensity and slight shifts in wavelengths of maximum absorbance (λ_{max}) particularly at high pHs, not solely due to the unbound complex, these variations are not sensitive enough to successfully probe the bound proteins.

However, a study of the effect of bound biomolecules on the pH sensitivity of the emission spectra of the labels reveals changes in emission intensity which do not appear to be merely due to the behaviour of the unbound complexes but rather as a consequence of the acid-induced conformational variances of the bound proteins. For both poly-amino acids, PLL and PLGlu, significant decreases in the labels' emission intensity appear to correlate with the pHs at which the transition from α-helix to random coil of the biomolecule is favoured. However, it must be noted that the emission spectra of the labels, particularly those of $[Ru(L-L)_2NCSphen]^{2+}$ are

197

themselves somewhat susceptible to pH, thereby limiting their potential as probes of acid-induced conformational variations. In the case of the ester form of $[Ru(bpy)_2COOH_2bpy]^{2+}$ the emission properties due to the protonation/deprotonation effects of the carboxylic acid, indicating that only one of the COOH groups is esterified, are still evident on binding of the label to proteins and this restricts the use of these complexes as efficient probes.

Furthermore the amino and isothiocyanate complexes when bound to BSA, a protein most stable between pH 4 and 9, display diminished emission intensities at very acidic and highly alkaline pHs, probably due to the unfolding of the protein at such pH extremes. The greater pH sensitivity of the quantum yields of emission of the labels is used to illustrate more clearly the effect of the protein on the emission intensities of the label. However, due to the presence of two or more emitting components in the decay of the protein-bound label compared to the single exponential kinetics of the free label, the quantum yields of emission may not be a true representation.

The intrinsic fluorescence of the proteins is studied briefly in order to show the effect of conformational changes on the emission intensity, here described in terms of the quantum yield of emission, using tryptophan as a reference. BSA is the most fluorescent of the biomolecules studied and the most sensitive to pH extremes, presumably due to the unfolding process occurring under such conditions while less significant changes in the fluorescence of the synthetic poly-amino acids are apparent.

In brief, the emission spectra of the labels are indeed somewhat influenced by the conformational changes of the bound proteins, whereby changes in the secondary structure from α-helical to random coil conformation for poly-amino acids and unfolding of the proteins appear to lead to significant reductions in their emission intensity. However, the pH susceptibility of the emission spectra of the labels and protonation/deprotonation effects themselves restricts their usefulness in this area and renders the study of the labels more difficult, leading to the subsequent study of the more sensitive emission lifetime of the labels in the following section.

4.4   References.

[1]   R.C. Nairn, Fluorescent Protein Tracing, Churchill Livingstone, 4th edition New York, **1976.**

[2]   M.J. O'Sullivan, J.W. Bridges, V. Marks, *Annu. Clin. Biochem.*, **1979**, 6, 221.

[3]   A.J. Bard, Luminescent Metal Chelate Labels and Means for Detection, U.S. Patent Application Number, PCT/US85/02153, **1986.**

[4]   W. Bannwarth and D. Schmidt, *Tetr. Lett.*, **1989**, 30, 1513.

[5]   R.S. Davidson, Transition Metal Complexes and Method for Time-Resolved Luminescence Binding Assay, International Application No., 8704523, **1987.**

[6]   S.G. Weber S.G., U.S. Patent Application Number, 4,293,310, **1981.**

[7]   R.S. Davidson, M.M. Hilchenbach, *Photochem. Photobiol.*, **1990**, 52, 2, 431.

[8]   W. Bannwarth, *Anal. Biochem.*, **1989**, 181, 216.

[9]   A.L. Lehninger, Biochemistry, Worth publishers Inc., New York, **1979.**

[10] G. Giacometti, *J. Phys. Chem*, **1980**, 67.

[11] T.E. Creighton, Proteins:Structures and Molecular Properties, 2nd edition, W.H. Freeman & Co., New York, **1993.**

[12] G. Degols, J.P. Leonetti, C. Gaynor, M. Lemaitre and B. Lebleu, *Nucleic Acids Res.*, **1989**, 17, 9341.

[13] E. Hurwitz, I. Stancovski, M. Wilchek, D. Shouval, H. Takahashi, J.R. Wands and M. Sela, Bioconj. Chem., **1990**, 1, 285.

[14] L.& M. Mester, B. Kraska and J. Crisba, *J. Carbohy. Nucleosides Nucleotides*, **1979**, 6, 2, 149.

[15] H.R. Mayler, E.H. Cordes, Basic Biological Chemistry, Harper & Row Publishers, New York, **1968.**

[16] J.W. Park, J.A. Chongmok Lee, *J.Photochem. Photobiol., A,* **1995**, 86, 89.

[17] E.M. Ryan, PhD. Thesis, Dublin City University, **1991.**

[18] D. Gerard, B. Lux, A. Follenius and M.C. Kilhoffer, *Spectrosc. Biol. Mol. (Proc. Eur. Conf. 1st).,* **1985**, 393.

[19] J.N. Demas and G.A. Crosby, *J. Phys. Chem.*, **1971**, 75, 8, 991.

Chapter 5.

The use of decay lifetimes of protein-bound Ru(II) polypyridyl complexes as probes of conformational variances.

5.1   Introduction.

In the preceding chapter it was concluded that the energy and intensity of both the absorption and emission spectra of ruthenium polypyridyl complexes studied are not suitable variables to monitor conformational variances of the bound proteins. This chapter concentrates on the use of the emission lifetimes of the labels as the reporters which were shown in chapter 3 to be the most influenced by protein-binding. The sensitivity of the decay lifetimes of the fluorescent labels to changes in secondary structures of poly-amino acids and unfolding of proteins induced by acid and chemical denaturants was investigated to determine the usefulness of such probes in real biological processes. In the final section, the labels were bound to the enzyme lysozyme allowing one to determine the effect, if any that the binding of labels has on the funciton of the enzyme. The effects of denaturation on the decay behaviour of the labels were also investigated by monitoring the effects of pH and chemical denaturants on the activity of the enzyme towards its substrate. The ultimate objective here was to identify the potential of such fluorescent complexes in real biological matrices.

Below is a summary of further applications of fluorescent complexes in natural biological processes stressing the wide range of possible applications. Various applications of synthetic macromolecules such as poly-l-lysine are also discussed which is of relevance to the work carried out in this thesis.

5.1.1. Use of Ru(II) polypyridyls as probes for biomolecules.

Various ruthenium polypyridyl complexes have been prepared and coupled to proteins, albumins, antibodies and oligonucleotides. The use of the esterified derivative of $[Ru(bpy)_2(COOH_2bpy)]^{2+}$ where $COOH_2bpy$ = 2,2'- bipyridine-4,4' dicarboxylic acid in the conjugation of the proteins bovine serum albumin and anti-

rabbit immunoglobulin has been reported, with the immunological activity of the antibody after conjugation shown to be retained by immunofluorescence [1]. This complex has also found applications in a time-resolved fluorescence immunoassay [1]. (See Figure 5.1.) When bound to bovine serum albumin, detection was carried out using electrochemiluminescent techniques. Ruthenium concentrations of 1×10^{-11} M were detected using this method.

A ruthenium polypyridyl sulphonyl chloride has also been conjugated to human IgG [2] while $[Ru(bpy)_2((CONCS)_2bpy)]^{2+}$ where CONCS = diacylisothiocyanate, has been conjugated to antibodies [2]. Another such complex coupled to sheep and rabbit anti-mouse IgG is $[Ru(bpy)_2(4,4'\text{-dichloro-}methylbpy)]^{2+}$ as depicted in Figure 5.2, which reacts with a free amino group that attacks the chloromethyl group and displaces the chloride [1]. Retention of immunological reactivity is demonstrated by fluorimetric analysis.

Weber describes the use of some ruthenium complexes in photoelectrochemical immunoassays and also reports the use of the 3-0-morphinyl ester of $[Ru(bpy)_2(4,4'COOHbpy)]^{2+}$ as a label in determining morphine [3]. The basis behind this is that the label transfers an electron to a quencher when photoexcited and the resulting oxidised molecule is subsequently reduced with an electron from an electrode of the flow cell held at the suitable potential. This electron is measured as photocurrent and hence the amount of free labelled analyte is determined by the photocurrent signal [3].

The use of various ruthenium complexes attached to immunologically active material for use in time-resolved immunoassays has also been reported [4]. For such work, the lifetime of the luminescence is suitably longer than 20 ns such that it exhibits a lifetime substantially longer than that of the background luminescence of the assay environment. Hydroxysuccinimide esters, chloroformate, isothiocyanate and sulphonyl chlorides derivatives of ruthenium polypyridyl complexes were subsequently conjugated to anti-thyroid stimulating hormone and human IgG and are also applicable in time-resolved immunoassay techniques [4].
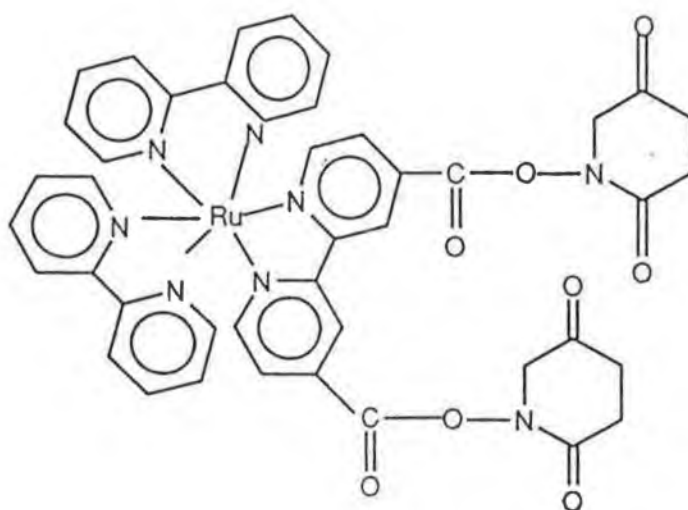
Figure 5.1. Structure of the di-N-hydroxysuccinimide ester of the complex

[Ru(bpy)$_2$(4,4'COOHbpy)]$^{2+}$
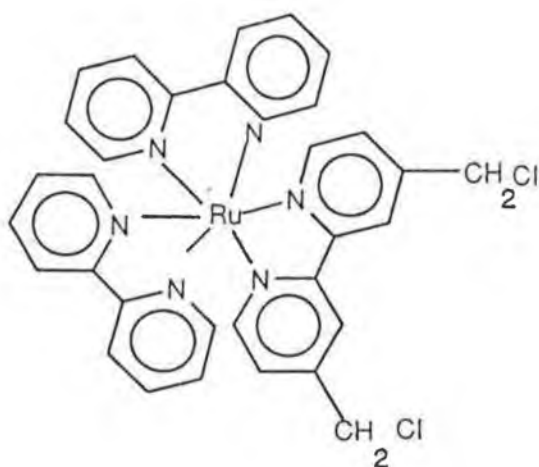
Figure 5.2. Structure of the complex [Ru(bpy)$_2$(4,4'-dichloromethylbpy)]$^{2+}$.

The use of ruthenium bathophenanthroline complexes to label oligonucleotides has previously been mentioned [4, 5]. The products formed are measured by time-resolved fluorescence with a detection limit below 10^{-14} M. Decay lifetimes of the order of μ sec are obtained. These complexes are thermodynamically very stable, chemically inert and show strong and long lasting fluorescence after excitation by light pulses of short duration, which renders them suitable for time-resolved measurement methods in their detection [5].

The covalent attachment of multiple fluorophores to DNA containing phosphorothionate diesters leading to the highly sensitive detection of single-stranded DNA is reported [6]. The incorporation of multiple fluorophores or other nonradioactive labels into nucleic acids allows significant enhancement of detection limit by increasing the amount of signal present for a given quantity of nucleic acid while not altering the characteristics of the DNA [6].

Recently, the covalent linkage of ruthenium polypyridyl complexes to polypeptides and immunoglobulins has been reported to lead to significant changes in decay lifetime and behaviour of the label [7], prompting our investigation of the potential of related complexes as fluorescent probes in the study of biomolecules and their conformations.

5.1.2 Fluorescence in immunoassays.

Fluorescence immunoassays have been widely used for the detection of drugs, antigens and other biological molecules based on a number of spectral properties, including the use of fluorogenic substrates in the ELISA assays, long lived emission, chemiluminescence, the use of fluorescence resonance energy transfer (FRET) to detect antigen-antibody association, fluorescence polarisation to measure changes in the rotational correlation times, and fluorescence quenching or enhancement.

Fluorescence lifetimes and quantum yields of many different fluorescent groups and their sensitivities to quenching by various substances can for example be

used to evaluate environments close to the residues to which those groups have been attached. Fluorescence energy transfer measurements are also widely used to estimate distances between certain internal or intrinsic chromophores and various selectively introduced extrinsic fluorescent labels [8].

Fluorescence methods are also widely used to study the rotational dynamics of proteins and other macromolecules, the physical basis behind these measurements being the polarisation or anisotropy of the emitted light when the sample is excited with a vertically polarised light. The extent of polarisation of the emitted light depends upon the extent of random Brownian motion of the molecules that occurs during their excited state lifetimes [9]. As a labelled antigen binds to the antibody, its rotation slows down and the degree of polarisation increases. The polarised light from metal-ligand complexes possess many advantages to render them suitable in biophysical and clinical chemistry including a wide range of lifetimes, absorption and emission maxima obtainable by a suitable choice of metal and ligand. Information on the rotational motion is possible over a time range extending to about three times the fluorescence lifetime [10], which indicates that long lived ruthenium complexes can measure processes such as protein folding. Recent work by Demas et al. involving the direct measurements of rotational correlation times of luminescent Ru(II) molecular probes has led to their use as dynamic probes of motions of macromolecular systems [10].

Initial studies by Terpetschnig and co-workers incorporated the study of the potential of certain ruthenium complexes as anisotropy probes [11]. Symmetrical species such as $[Ru(bpy)_3]^{2+}$ had not previously been used as anisotropy probes due to their apparent low polarisation of luminescence. However, the less symmetrical Ru-complex $[Ru(bpy)_2(dcbpy)]^{2+}$ was studied, where dcbpy = 2,2'-bipyridine-4,4'-dicarboxylic acid, as it displays high anisotropies in the absence of rotational motions [11]. The intensity and anisotropy decays of $[Ru(bpy)_2(dcbpy)]^{2+}$, when covalently bound to human serum albumin, concanavalin A, human immunoglobulin G (IgG) and ferritin were measured, demonstrating their ability to measure rotational motions

205

on the 10 ns to 1.5 µs timescale [11]. Such studies confirm that the anisotropy decays of the Ru-labelled proteins are sensitive to the size and/or shape of the proteins. Furthermore, in solutions of increasing viscosity the Ru-complex displays a slower anisotropy decay as protein diffusion is slowed.

Based on these preliminary studies, Terpetschnig reports fluorescence polarisation [12] and FRET immunoassays [13], based on such ruthenium complexes. The steady-state polarisation of the antigen human serum albumin (HSA), labelled with $[Ru(bpy)_2(dcbpy)]^{2+}$ where dcbpy = 4,4'-dicarboxyl-2,2'-bipyridine, is sensitive to the binding of its antibody anti-HSA, resulting in a 200% increase in polarisation [12]. On labelling HSA with $[Ru(bpy)_2(NCSphen)]^{2+}$, its association with the antibody labelled with a non-fluorescent absorber, Reactive Blue is detectable by a decreased quantum yield of Ru-HSA, a decrease in its fluorescence lifetime and an increase in its fluorescence anisotropy [13].

Because the photophysical properties of $[Ru(bpy)_3]^{2+}$ are sensitive to local environmental factors, it is also suitable as a luminescent probe of antibody binding pockets, according to Shreder and co-workers, involving the use of time-resolved luminescence in the photophysical investigation of polyclonal antibodies elicited via immunization with a $[Ru(bpy)_3]^{2+}$-methyl viologen hapten [14]. Antigen-specific polyclonal antibodies are produced when the immune system is challenged by infection or immunization. A complete characterisation of the functional distribution of such antibodies in a polyclonal immune response is vital in understanding how the immune system functions, having applications in several fields, from medicine to catalytic antibodies. Contrary to common belief that polyclonal immune responses are highly heterogenous, $[Ru(bpy)_3]^{2+}$ when bound by the entire hapten-specific polyclonal IgG sample, exhibits surprisingly homogenous photophysical behaviour, indicating that the entire polyclonal response may be essentially monoclonal, with all the hapten-specific antibodies being genetically related. Alternatively, the different antibodies could be genetically unrelated but simply recognise the hapten in a similar fashion [14]. (See Figure 5.3)
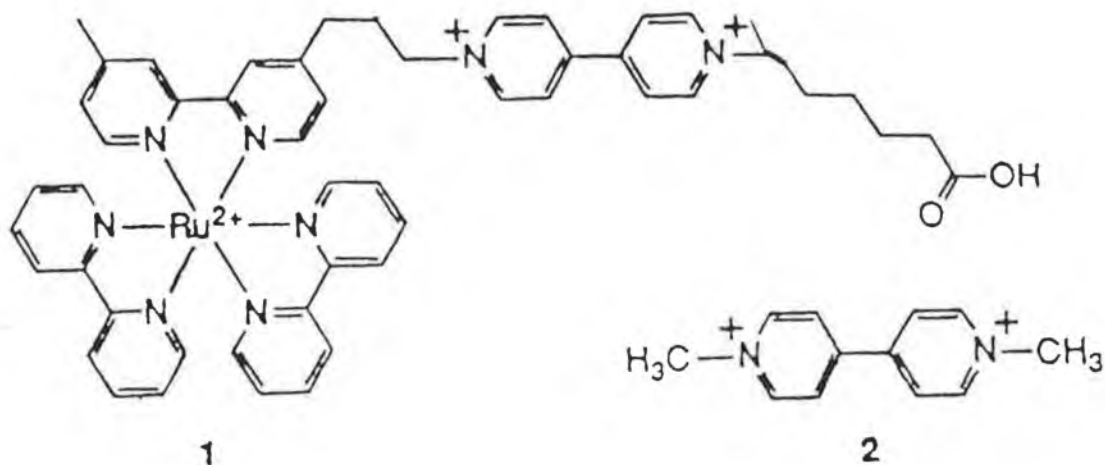
Figure5.3 (1) [Ru(bpy)₃]²⁺ -methyl viologen hapten and (2) methyl violegen [14].

5.1.3 Applications of poly-amino acids.

In addition to the use of certain poly-amino acids in the study of real biological processes due to their analogy to basic proteins, many poly-amino acids have found important applications in their own right. In order to establish the importance of such synthetic biomolecules in the areas of clinical and biomedical chemistry, a brief summary of various significant biological applications of such molecules is given below.

Synthetic macromolecules have great potential in a number of areas of clinical application including their use as carriers of drugs (for example, for cancer

chemotherapy, antigenic determinants (for vaccines), hormones, and gamma emitting radionuclides (for use as radiopharmaceuticals) [15].

One such application important in biodistribution studies and radiopharmaceutical development involves the labelling of branched polypeptides with a poly-L-lysine backbone with radioiodines and radiometals [15]. Groups of branched polypeptides , having the general formula poly[Lys-(X_i-DL-Ala$_m$)] (XAK) are water soluble, biodegradable, and possess a large number of α-amino groups rendering them suitable for simple and efficient conjugation to drugs or other agents, while polycationic polypeptides (regardless of their branch structure) are cleared rapidly from their circulation [15].

Yoshimura and co-workers have reported the characterisation of thyroidal membrane-bound Mg-adenosinetriphosphatase, activated by trypsin or poly-L-lysine. This activation is reportedly due to an increase in the maximal velocity of the hydrolysing reaction without a change in the affinity of the enzyme for its substrate. Indications were that the alteration of ATPase activities is dependent on the basicity of the poly-amino acid, as acidic poly-amino acids had no effect [16].

Fiume and co-workers have reported the conjugation of the antiviral agent adenine arabinoside monophosphate (ara-AMP) with a low molecular mass lactosaminated poly-L-lysine. This led to an increase in the chemotherapeutic index of the antiviral drugs used in the treatment of chronic hepatitis B and more selective delivery to hepatocytes via Ashwell's receptor which recognises galactosyl terminating glycopeptides [17]. The conjugate was also found to be devoid of acute toxicity even at high dose in contrast to free poly-L-lysines.

The toxic effects of poly-L-lysine itself are associated with its polycationic character and are probably caused by the binding of the electronegative charges present on the cell. Coupling of lactose molecules by reductive amination preserves the cationic character of lysine ε-amino groups , but the bound lactose and coupled ara-AMP (negatively charged) probably hinder the binding of the conjugate to the electronegative groups of cell membranes. The conjugate is very soluble in water, allowing the administration of a pharmalogically active dose in a small volume [17].

208

Another medical application of poly-L-lysine is its use in the study of the non-enzymic reaction between glucose and the free amino groups of proteins, which has significance due to its possible implication in the development of long-term diabetic complications [18]. Due to the large number of free ε-amino groups (known as reactive sites in the glycation processes) in PLL, it was chosen as the model compound in order to increase the yield of the glycation processes. This glycation process is the first of a complex series of reactions that determine the formation of fluorescent insoluble products, the advanced glycation end products of melanoidins. The accumulation of such products on long-lived proteins is one of the most important damage factors determining diabetic complications. Lapolla and co-workers have studied the products arising from the interaction of glucose and poly-l-lysine using pyrolysis/gas chromatography/mass spectrometry [18].

Studies have shown that PLL and other polycations influence endothelial functions and activate certain enzymes involved in the caseinolytic activity of the erythrocyte multicatalytic proteinase. Investigations of the physiological role of these enzymes are rendered difficult by complicated multi-stage purification processes. Here, the purification of CLP by a simple one-step method using poly-L-lysine was developed by Nagamatsu [19]. In this study, low concentrations of PLL were found to stimulate the release of elactase (CLP) and cathepsin G from leukocytes in vitro, and was particularly useful as a reagent for the fractionation of CLP in a simple chromatographic procedure.

Finally, an interesting application involving amino acids is their use as photoactivatable DNA-cleavage agents. Saito and Takayama report novel water-soluble l-lysine derivatives possessing a naphthalimide chromophore that can induce efficient, highly specific selective cleavage of double stranded DNA upon photoirradiation at 320-380 nm [20].

5.2 Results and discussion.

5.2.1. pH sensitivity of decay lifetimes.

It has been noted that the decay lifetime of the labels studied here is the luminescent property most influenced by their subsequent binding to biomolecules. The decay kinetics and lifetime are substantially changed upon conjugation. For this reason it was assumed that the decay lifetimes of the labels would be the most susceptible to conformational variances taking place in the bound biomolecule and in this sense they would act as the sensitive reporters. This section involves the pH sensitivity of the decay lifetimes of each label when bound to various biomolecules.

In section 4.1.3 the pH sensitivity of the conformational forms of two poly-amino acids in particular was described. As their dynamic behaviour is well documented under such conditions [21], in addition to their use as model compounds to study more complex biological processes [15-20], such biomolecules were again chosen as model compounds to study the capability of Ru(II) complexes to follow regular structural changes of these bound biomolecules. In the first section, the acid induced conformational variances of regular synthetic poly-amino acids, namely their random coil to α-helix transitions were studied using the decay lifetimes of the labels as a probe. A similar study was then undertaken with a natural protein, bovine serum albumin, to assess the potential of such probes in natural biological processes while the last section involves the monitoring of the loss of activity of the enzyme lysozyme again using the decay lifetimes as the reporter.

In order to ensure that any fluctuations in the decay of the protein-bound label are indeed due to corresponding structural changes in the bound biomolecule and not merely due to pH susceptibility of that particular free label, a study of the pH dependence of the decay lifetimes of all the unbound ruthenium complexes was initially carried out. Table 5.1 and 5.2 list the lifetimes of the complexes [Ru(L-L)$_2$(NH$_2$phen)]$^{2+}$ and [Ru(L-L)$_2$(NCSphen)]$^{2+}$ where L=bpy, phen and dpp, at various pHs, when degassed and aerated. As stressed in chapter 3, all these

ruthenium complexes exhibit single exponential decay behaviour. Figure 5.4 compares the pH sensitivity of the decay lifetimes of the aerated $[Ru(bpy)_2NH_2phen]^{2+}$, $[Ru(bpy)_2NCSphen]^{2+}$ and $[Ru(bpy)_2esterbpy)]^{2+}$. Approximately $1.10^{-4}M$ label was initially dissolved in DMF and diluted with Britton Robinson buffer. The pH was increased/decreased by the addition of 2 m NaOH/ 2 M Hcl, samples were taken at a range of pHs, allowed to stand at room temperature and then analysed. Degassing of the solution involved gently bubbling argon through the dilute label solution over a 30 minute period in cuvettes to remove the oxygen after which the cuvettes were sealed and the lifetimes of the samples analysed.

The decay lifetimes of aerated $[Ru(bpy)_2NH_2phen]^{2+}$, $[Ru(phen)_2NH_2phen]^{2+}$ and $[Ru(dpp)_2NH_2phen]^{2+}$ show slight variations with pH with average lifetimes of 350-400 ns, 500 ns and 700-750 ns exhibited respectively. $[Ru(dpp)_2NH_2phen]^{2+}$ appears to be the most efficiently quenched by oxygen with the lifetimes increasing more than twofold, on treating with argon to remove the oxygen. When samples were deoxygenated in particular, a notable increase in each of the labels lifetimes was obtained above pH 6 and in correlation with the changes in the emission intensity of the labels at such pHs a likely explanation is that the protonation of the complexes leads to an increase in emission lifetime, allowing one to calculate the excited state pK_a^* of the complexes according to equation 4.1.

On comparing the results for the amino complexes, each isothiocyanate derivative possesses a longer lifetime than its respective amino precursor, ranging from 450ns (bpy) to 600ns (phen) to 850ns (dpp). Although these complexes display lifetimes not very sensitive to pH a decrease in the lifetimes is noted for each at pHs 10-12 which correlates with the pH range at which decreases in emission intensity and changes in the absorption spectrum were noted. This further indicates the decomposition of these complexes back to their amino precursors although the lifetimes at pH 10-12 are higher than the lifetimes of their respective amino complexes. Lower lifetimes could also however be due to protonation of the complex.

Table 5.1 pH dependence of decay lifetimes of degassed and aerated samples of [Ru(L-L)$_2$NH$_2$phen]$^{2+}$.

pH	L=bpy lifetime (ns)	L=phen lifetime (ns)	L=dpp lifetime (ns)
	(a),(b)	**(a), (b)**	**(a), (b)**
2.0	500, 380	800, 500	1600, 740
4.0	530, 360	820, 500	1800, 720
6.0	620, 360	880, 520	1800, 750
9.0	630, 370	900, 520	1700, 800
11.0	620, 340	890, 500	1800, 800
12.0	650, 350	870, 470	1500, 750
13.0	680, 360	980, 510	1480, 730

(a) Samples were deoxygenated with argon for 30 mins; (b) Aerated samples. Error of lifetimes calculated is approximated to be +- 5%.

Table 5.2 pH dependence of decay lifetimes of degassed and aerated samples of [Ru(L-L)$_2$NCSphen]$^{2+}$.

pH	L=bpy lifetime 1 (ns)	L=phen lifetime 1 (ns)	L=dpp lifetime 1 (ns)
	(a), (b)	**(a), (b)**	**(a), (b)**
2.0	720, 490	990, 500,	1700, 800
4.0	700, 450	1060, 600	1850, 840
7.0	750, 460	1100, 640	1700, 850
9.0	760, 450	1170, 620	1600, 860
10.0	740, 460	1120, 630	1560, 890
12.0	700, 420	1000, 580	1600, 830

(a) Samples were deoxygenated wtih argon for 30 mins.; (b) Aerated samples. Error of lifetimes calculated is approximated to be +- 5%.

$[Ru(bpy)_2esterbpy]^{2+}$ and its precursor show variability in their emission lifetimes, as in their absorption and emission spectra. As for the emission intensity, an increase in lifetimes was notable from pH 4-6 upwards. Again this jump is probably due to the deprotonation of the carboxylic acid and hence as the deprotonated complex has a longer lifetime than the protonated one, the real excited state pK_a could be calculated taking the change in lifetimes upon protonation into account using equation 4.1. Indeed the excited state lifetime of the "ester" is at a minimum at less than 300 ns while a jump to 400 ns is noted at such a pH range. Another point to note is the minimal effect degassing of the samples has on the lifetimes, with the lifetimes only increasing by a third on degassing. This change in lifetime could also be explained by the hydrolysis of the ester in acid/base but the reversibility and reproducibility of the variations contradict this. The protonation effect of the lifetimes of this label is illustrated in Figure 5.4 where it is compared to the pH susceptibility of the lifetimes of $[Ru(bpy)_2NH_2phen]^{2+}$ and $[Ru(bpy)_2NCSphen]^{2+}$.
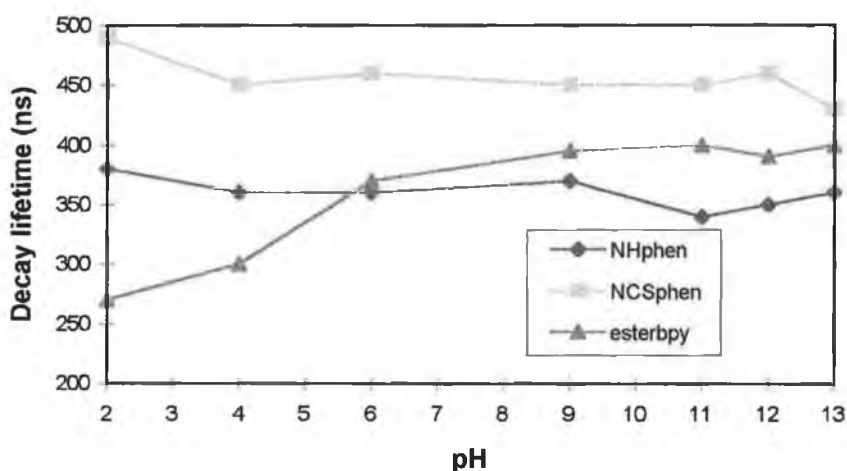
Figure 5.4 pH dependence of luminescence lifetimes of aerated (a)
$[Ru(bpy)_2NH_2phen]^{2+}$ (NHphen), (b) $[Ru(bpy)_2NCSphen]^{2+}$(NCSphen) and (c)
$[Ru(bpy)_2esterbpy]^{2+}$ (esterbpy).

These preliminary studies of the controls would lead us to believe that while the amino and isothiocyanate complexes appear suitable to probe pH dependant conformational variances due to their immunity to pH influences, the irregular pH induced decay behaviour of the carboxylic acid derivative may complicate matters when used as probes of such variations.

5.2.1.1 Effect of protein type.

For the lifetime analysis of the protein-bound labels, each conjugate solution was diluted further with Britton Robinson buffer (the dilution depended on the concentration of label in the conjugate). The pH was increased/decreased by the addition of 2 M NaOH/ 2 M HCl and samples were taken at a range of pHs. These samples were allowed to stand at room temperature for the "aerated " readings while "degassing" involved the bubbling of argon through each sample in cuvettes for 30 mins with care so as not to denature the protein. The cuvettes were then sealed and immediately analysed by laser excitation. Oxygenation of the samples involved bubbling oxygen through the solutions in cuvettes for 15 mins, sealing the cuvettes and immediately analysing by laser excitation.

(1) pH sensitivity of PLL-bound complexes.

Ruthenium complexes were bound to the side chains of the lysine residues of PLL using both isothiocyanate complexes and dicarboxylic acid derivatives. However, ruthenium amino complexes were also bound to the terminal carboxylic acid groups of the polypeptide backbone of PLL. This allowed the comparison of the probing capabilities of the labels when bound to different locations on the biopolymer. Table 5.3 lists the decay lifetimes of $[Ru(bpy)_2NCSphen]^{2+}$:PLL conjugates at various pHs, when degassed and aerated, while Figures 5.5 and 5.6 graphically illustrate such behaviour. The results obtained for the aerated and degassed

$[Ru(phen)_2NCSphen]^{2+}$:PLL and $[Ru(dpp)_2NCSphen]^{2+}$:PLL conjugates are listed in Table 5.4. Although absolute lifetime values are higher in Table 5.4, we see that the trend is the same as we vary the ancillary ligand on the label, suggesting that the nature of the additional polypyridyl ligand has no bearing on probing potential.

As previously noted, the two lifetimes obtained consist of one lifetime significantly longer than the free form while the shorter lifetime is slightly shorter than the free form. The longer lived species may be a composite of several decays from complexes bound to the same type of binding site but at different locations along the PLL molecule. However, taking all the parameters involved in the interaction of ruthenium polypyridyl complexes with biomolecules into account, it would be expected that the excited state decay behaviour of the conjugates may be quite complicated and impossible to define precisely and that, in this case double exponential analysis is the most suitable approach.

Figure 5.5 outlines how at room temperature the two lifetimes of the PLL-bound labels are relatively constant upto a pH of approximately 9 or 10, whereupon a significant drop in both is observed. Significantly as already explained, poly-l-lysine is known to be in a random-coil conformation at pH 7, but at pH 12, is known to be totally helical, with this random coil to α-helix transition occurring at approximately pH 10 [21]. A likely explanation for the longer lifetime of the bound label below pH 10 is the protection from quenching by O_2 in particular, in the sheltered environment of the polypeptide when in the random coil conformation. It is proposed that above pH 10, when PLL is in the non-random helical form, the side chains to which the ruthenium labels are bound, are protruding from the α-helix, rendering them more accessible to various quenching agents, particularly oxygen, leading to the observed reduction of emission lifetimes. On removing oxygen from the same samples with argon, multi-exponential decay is again found. However, in some cases triple as opposed to double exponential analysis gave a better fit, the reason for which is not clear. Interestingly, below pH 10 the labels decay behaviour is very similar to that of the aerated samples. To be noted is the fact that above pH 10, all three lifetimes show little change across the entire pH range.

215

Since on degassing the samples, the quenching affects of oxygen should be minimised, the bound labels' emission lifetime should be quite uniform over the whole pH range. This is indeed found and can be clearly seen from Figure 5.6. On the other hand, on oxygenating the samples, although all the lifetime components would be expected to be affected somewhat, an equivalent or indeed a more significant drop in lifetimes is anticipated at pH 9-10, as the label is more susceptible to oxygen quenching under the specified alkaline conditions. On adding oxygen, a significant drop is noted only for the longer lifetime, indicating that the shorter lifetime is a form of label quenched by some other means. Figure 5.7 depicts a molecular model of PLL labelled with one ruthenium complex when PLL is in the random coil conformation. This illustrates more clearly the projection of the complex from the α-helix when covalently bound to a side chain of the polypeptide.

An important experiment carried out was the confirmation of the reversibility of such variations, to ensure that any observations made were due to reversible structural conformational changes of the bound protein and to dismiss such possibilities as decomposition of the conjugate. Furthermore, these similar experiments carried out on the free labels permit us to conclude that the unusual pH dependent behaviour is indeed due to the pH dependent dynamic behaviour of PLL in solution.

An important question already addressed in chapter 3 is the nature of the lower lifetime of the protein-bound label. A lifetime similar to that of the unbound label may indicate such an explanation but the fact that this lifetime exhibits pH dependent decay behaviour different to that of the unbound label plus the fact that dialysis and/or size exclusion chromatography should have removed most of the unbound label would dismiss the possibility that the lower lifetime is merely due to the unbound label.

Table 5.3 pH dependence of decay lifetimes of 50:1 Ru(bpy)₂NCSphen:PLL in deoxygenated, aerated and oxygenated solutions.

pH	Degassed lifetimes 1, 2,3 (ns) [a]	Aerated lifetimes 1, 2 (ns) [b]	Oxygenated lifetimes 1, 2 (ns)
2.0	90 (10), 350 (45), 700 (45)	250 (35), 900 (65)	200 (50), 660 (50)
4.0	80 (15), 390 (45), 690 (40)	260 (35), 940 (65)	170 (50), 680 (50)
8.0	40 (15), 260 (30), 820 (55)	240 (30), 860 (70)	170 (50), 610 (50)
10.0	40 (15), 350 (40), 860 (45)	220 (30), 790 (70)	180 (35), 540 (65)
11.0	50 (15), 340 (40), 790 (45)	190 (40), 530 (60)	150 (40), 250 (60)
12.0	45 (15), 370 (55), 900 (30)	120 (30), 410 (70)	160 (50), 280 (50)
13.0	50 (10), 340 (45), 790 (45)	70 (30), 400 (70)	140 (50), 240 (50)

* Values in parentheses are the emitting components pre-exponential factors in percent.

Table 5.4 pH dependence of decay lifetimes of aerated Ru(phen)₂NCSphen:PLL and Ru(dpp)₂NCSphen:PLL.

pH	L = phen Lifetimes 1, 2 (ns)	L = dpp Lifetimes 1,2 (ns)
2.0	320 (35), 840 (65)	450 (25), 1200 (75)
5.0	340 (35), 810 (65)	420 (30), 1230 (70)
8.0	320 (35), 860 (65)	400 (30), 1150 (70)
10.0	250 (30), 690 (70)	280 (25), 1000 (75)
11.0	220 (25), 560 (75)	250 (25), 800 (75)
12.5	200 (25), 530 (75)	220 (25), 700 (75)

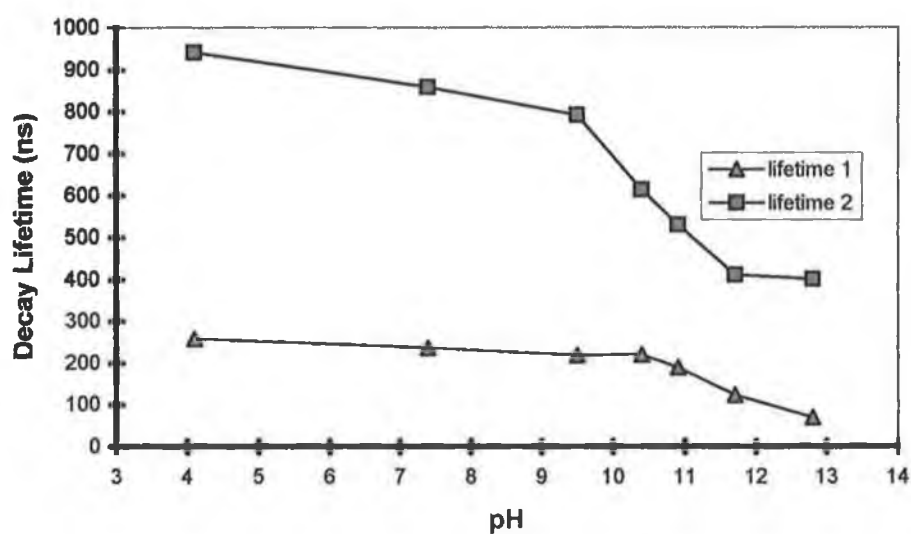** Values in parentheses are the emitting components pre-exponential factors in percent.*

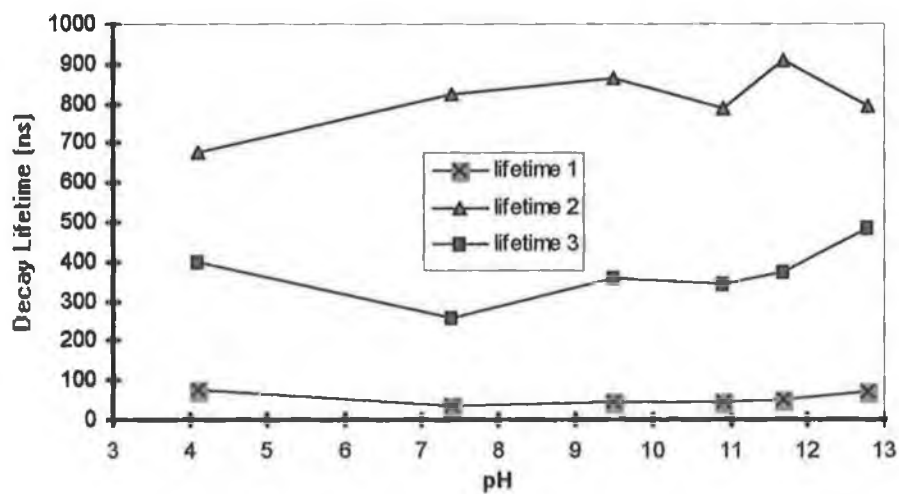Figure 4.12. pH dependence of luminescence lifetimes of aerated
Ru(bpy)₂NCSphen:PLL.

Figure 4.13 pH dependence of luminescence lifetimes of degassed
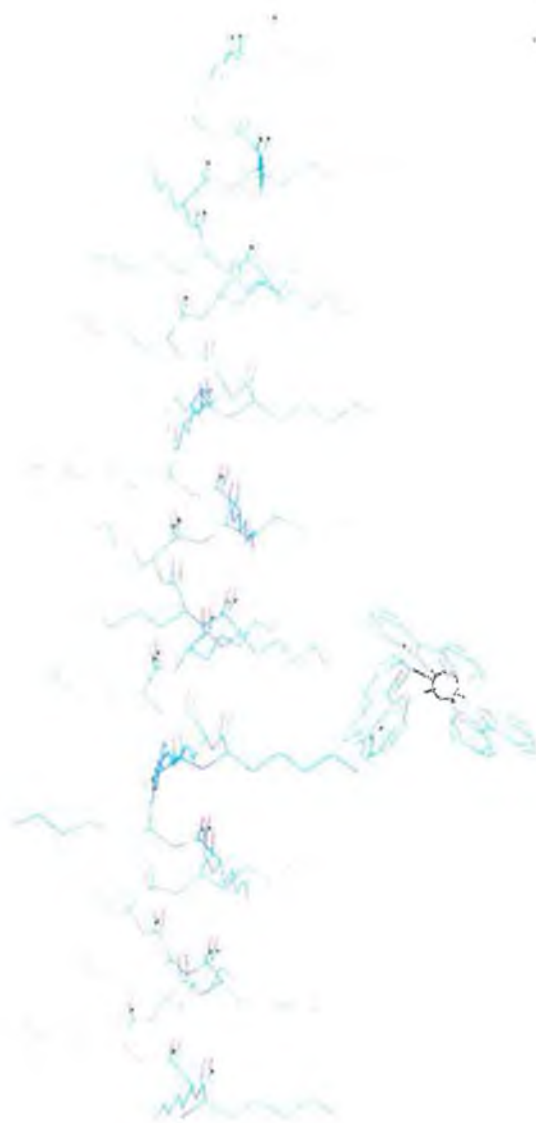Ru(bpy)₂NCSphen:PLL.

Figure 5.7 Computational model of Ru-labelled PLL with PLL in the α-helical form.

At certain pHs of our studies the lower lifetime is actually significantly lower than that of the unbound label which would indicate that quenching of the label via either energy or electron transfer by the protein is taking place. However, there is no direct evidence to support this theory and it must be remembered that the analysis of the multi-exponential decaying samples is based on mathematics and hence the values are not absolute. A similar pH study was carried out for the PLL conjugate using the succinimide ester as the label. Before any analysis of results is possible, however, it must be remembered that this label displays spectroscopic properties highly sensitive to pH variations, with significant variances in absorption, emission maxima and emission lifetimes on increasing the pH (See Chapter 4). Table 5.5 presents the lifetimes of the conjugate in question over a wide pH range. Again, double exponential decay is apparent for the protein-bound label, however, the longer lifetime is on average only slightly higher than that of the unbound label form, while the lower lifetime of the bound label is considerably lower than the same. From Table 5.5, it is evident that there is a change in decay behaviour of the bound label between pH 7 and 9. Firstly, while the protein-bound label displays essentially single exponential decay behaviour at acidic pHs (the lower lifetime contributes to only 8%), double exponential decay is more noted under neutral/alkaline conditions. Furthermore, as well as an increase in the contribution of the lower lifetime both lifetimes are shown to increase in duration above pH 7, a phenomenon which was found to be reversible. On degassing the samples very little change in lifetimes is noted as for the unbound labels, indicating that the protein-bound labels has photophysical properties very similar to those of the free label. This again may be due to the presence of an unreacted carboxylic acid group of the label not bound to the biomolecule.

These results appear to be in direct contrast to the other side-chain modification reagents of PLL whereupon a drop in lifetimes was obtained in alkaline conditions. Furthermore the changes are noted at the lower pH of 7 and hence would not appear to be due to the structural variances inherent of PLL. Rather, as for the other spectroscopic properties, changes at pH 7 would appear to

correspond to the excited state pK_a of a carboxylic acid of the label. As the label is bound to the PLL molecule via one of the modified carboxylic acids present the decay behaviour may actually be governed by the unusual decay behaviour of the other unbound and unreacted carboxylic acid. This indicates that in order for Ru(II) polypyridyls to be used as efficient labels, only one functional group should be present and the unbound label should not be sensitive to the conditions which one wishes to study.

Table 5.5 pH dependence of lifetime components of Ru(bpy)₂esterbpy:PLL when degassed and aerated.

pH	Degassed lifetimes 1,2 (ns)	Aerated lifetimes 1,2 (ns)
2.6	190 (65) 370 (35),	60 (10), 280 (90)
6.4	290 (55), 640 (45)	60 (10), 350 (90)
9.0	400 (65), 770 (35)	180 (30), 430 (70)
10.0	400 (70), 700 (30)	120 (15), 390 (85)
11.0	380 (70), 750 (30)	220 (35), 440 (65)
12.0	350 (70), 720 (30)	240 (45), 480 (55)

As emphasised earlier, in addition to binding labels to PLL via the side chains of the lysine residues, suitable labels and reaction conditions were chosen to lead to the binding of ruthenium complexes to the terminal carboxylic acid groups of the polypeptide chains via stable amide bonds. As before, the pH dependence of the decay lifetimes of such labels when bound to such binding sites was investigated, to determine the effect of the binding site of the label on the biomolecule on the probing potential of these ruthenium labels. Table 5.6 presents the data describing the pH dependence of the lifetimes of the complexes $[Ru(L\text{-}L)_2NH_2phen]^{2+}$ bound to PLL, when degassed and aerated. It is evident that these labels behave in a different manner, compared to those bound to the PLL side chains. Firstly, under

aerated conditions, the amino complexes actually display essentially single exponential decay behaviour with lifetimes simliar to those of the unbound labels.

The pH sensitivity of the decay behaviour of the conjugates above is somewhat similar to that of the unbound form, in that the lifetime is not very sensitive to pH changes. However, on carrying out the appropriate protein assays, the actual binding of such labels to PLL was verified.

Table 5.6 pH dependence of decay lifetimes of aerated $Ru(L-L)_2NH_2phen$:PLL.

pH	Lifetimes 1, 2 (ns)		
	L = bpy	L = phen	L = dpp
2.0	480 (90), 80 (10)	580 (80), 200 (20)	900 (90), 220 (10)
4.0	620 (90), 80 (10)	520 (85), 190 (15)	840 (80), 100 (20)
6.0	590 (85), 100 (15)	550 (80), 220 (20)	940 (85), 100 (15)
8.0	540 (90), 100 (10)	560 (80), 200 (20)	800 (75), 100 (20)
11.0	510 (90), 80 (10)	500 (80), 120 (20)	800 (75), 100 (25)
12.0	540 (80), 100 (20)	560 (60), 220 (40)	830 (85), 80 (15)

This would indicate that the labels, when bound to the terminal groups of polypeptide chains, are not subject to significant changes in local environment, despite the secondary structural variances taking place in the bound PLL molecule. This phenomonen may be explained in terms of the exact position of the binding sites of PLL in question, and how they are affected by corresponding conformational changes in the biopolymer. While the side chains of the amino acid residues in a polypeptide are known to be projecting out from the polypeptide backbone, the only carboxylic acid groups present in PLL are the terminal groups of each amino acid which bind to the terminal amino groups of another amino acid in the polypeptide chain to form peptide bonds, and so theoretically the only carboxylic acid available for binding to the labels in PLL is the terminal group of

each polypeptide chain in a PLL molecule. As stressed previously, on binding the ruthenium labels to the protruding amino acid side chains, the labels susceptibility to quenching by oxygen, dramatically increases, as PLL undergoes a structural transition from a random-coil to rigid helical form. In contrast to this, the terminal groups would not be expected to experience much change in environment located at the end of polypeptide chains, and based on this assumption, a structural variance of the biomolecule should not lead to significant changes in the quenching rate of oxygen on the label. Furthermore as addressed in chapter 3, the predominance of the longer lifetime may be due to the more homogenous nature of the bound label due to the uniqueness of the binding site. On removing oxygen from such samples both lifetime components are not significantly affected, increasing only slightly. These results clearly indicate the limited potential of these labels when bound to the end of polypeptide chains and confirm the importance of the location of the label on the biomolecule in their use as sensitive probes of conformational variances inherent in the biopolymer.

(2) PLGlu-bound complexes.

To confirm our theory on the probing of PLL, poly-l-glutamate (PLGlu) was chosen and a similar line of investigation was carried out. Again suitable labels were chosen which could bind to the side chains of glutamic acid residues, and the pH dependence of the decay lifetimes of the protein-bound labels is examined. Table 5.7, with Figures 5.8 and 5.9 reveal the pH susceptibility of the lifetime components of such protein-bound labels when aerated and degassed respectively. As before, double exponential decay kinetics is observed for the PLGlu conjugates. As anticipated, the decay lifetimes of the aerated samples in correlation with those bound to PLL, are shown to be greatly affected by the pH of the medium as revealed in Figure 5.8. This is in response to resulting conformational changes of PLGlu from an α-helix at pH 4 to random-coil conformation at pH 7 [22], which is illustrated in Figure 5.9 by the pH dependence of its optical rotation. In this case,

the enhanced lifetimes from pH 4 upwards are induced when the biomolecule is in the random coil form. Figure 5.8 compares the lifetime of the unbound label to the two lifetime components of the PLGlu-bound label highlighting the effect of the polypeptide on the lifetime of the label. On studying the effect of removing oxygen from the samples there is no such jump in the longer lifetime component at any pH, however the shorter lifetime does show an increase after pH 5-6 indicating that the shorter lifetime experiences quenching effects other than oxygen. Nevertheless, from the sensitivity of the longer lifetimes to oxygen quenching it is apparent that the sensitivity of the excited state of these labels to their local environment in addition to the differential quenching by oxygen when the label is in various environments is the basis behind the propensity of these labels to monitor structural variances in poly-amino acids. As for PLL, the experiment was repeated for the larger labels $[Ru(phen)_2NH_2phen]^{2+}$ and $[Ru(dpp)_2NH_2phen]^{2+}$ to ensure that the probing nature of the label is not significantly affected. The results for such studies are presented below in Table 5.8. This reveals that the same observations are found for such labels with more enhanced lifetimes at each pH.

Table 5.7 pH dependence of decay lifetimes of Ru(bpy)$_2$NH$_2$phen:PLGlu conjugates in aerated and degassed solutions.

pH	Aerated lifetimes 1,2 (ns)	Degassed lifetimes 1, 2 (ns)
3.0	190 (25), 430 (75)	280 (30), 920 (70)
4.0	170 (20), 550 (80)	250 (25), 880 (75)
4.4	160 (25), 690 (75)	-----------------
5.0	230 (35), 870 (65)	230 (30), 830 (70)
6.0	245 (35), 780 (65)	480 (30), 900 (70)
8.0	220 (45), 800 (55)	440 (25), 880 (75)
10.0	200 (50), 700 (50)	-----------------

Values in parantheses are the emitting components pre-exponential factors given in percent.
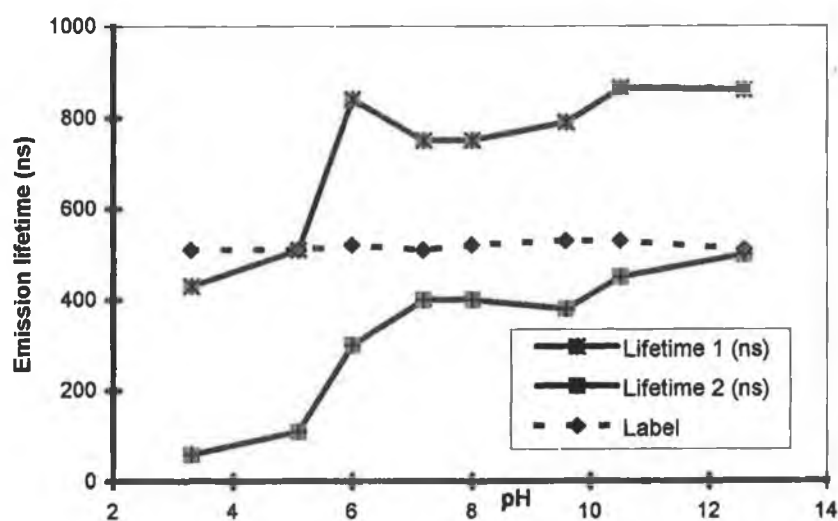
Figure 5.8 pH dependence of both lifetime components of aerated Ru(bpy)$_2$NH$_2$phen:PLGlu.
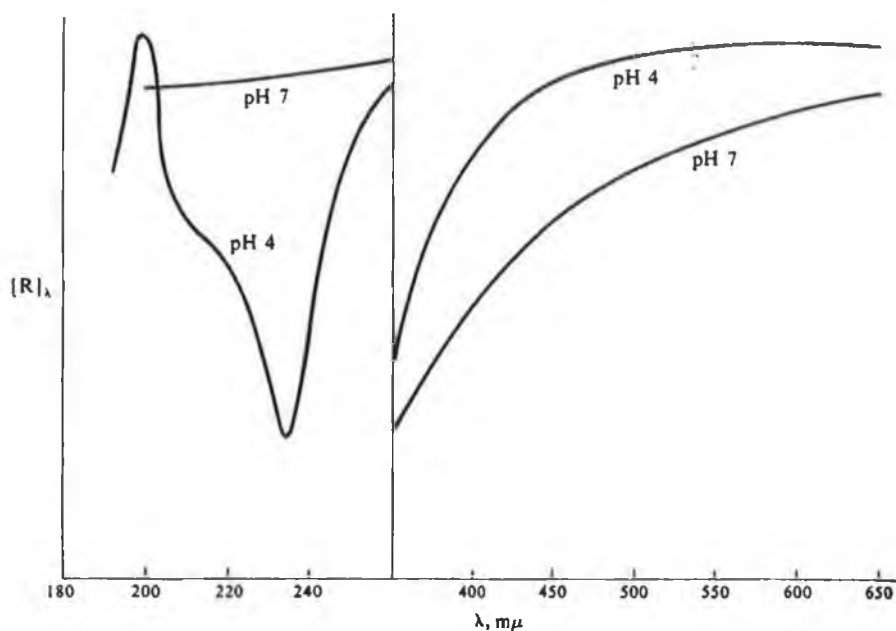

Figure 5.9 Variation of optical rotation as a function of wavelength for poly-L-glutamate at pH 4 (helical) and pH 7 (random coil) [22].

Table 5.8 pH dependence of decay lifetimes of aerated

$Ru(L-L)_2NH_2phen:PLGlu$ conjugates where L=phen and dpp.

pH	Aerated lifetime (ns)	
	L = phen	L = dpp
3.0	60 (30), 430 (70)	200 (40), 840 (60)
4.5	120 (30), 500 (70)	210 (35), 820 (65)
5.0	110 (35), 510 (65)	230 (45), 800 (55)
6.0	300 (50), 940 (50)	240 (45), 820 (55)
7.0	450 (50), 850 (50)	600 (50), 1180 (50)
9.5	420 (45), 800 (55)	700 (50), 1220 (50)
11.0	460 (70), 870 (30)	600 (50), 1100 (50)

* Values in parantheses are the emitting components pre-exponential factors given in percent.

One interesting point to be noted from Tables 5.7 and 5.8 is that above pH 5-6 where an enhancement of both lifetimes is observed, there is a corresponding increase in the contribution ratio of the shorter lifetime towards the total decay. A jump from 30% to 70 % is noted, the reason for which has not been ascertained.

Following the order of investigation carried out for the PLL conjugates, isothiocyanate derivatives were bound to the terminal amino groups, situated at the end of each polypeptide chain found in a PLGlu molecule. While Table 5.9 displays the lifetimes of the above conjugates, Figure 5.10 displays the pH dependence typical of the lifetime components of $Ru(dpp)_2NCSphen:PLGlu$ when aerated.

From Figure 5.10 it is evident that the longer lifetimes are enhanced to a significant degree when compared to the lifetime of the corresponding unbound label verifying the influence of binding on the lifetime of the label. However, when comparing Figure 5.10 to Figure 5.8 one notes that the effect of pH on both lifetime components is negligible compared to the side-chain modified PlGlu molecule.

Table 5.9 pH dependence of decay lifetimes of aerated

Ru(L-L)₂NCSphen:PLGlu where L= bpy and dpp.

pH	lifetimes (ns) L = bpy	lifetimes (ns) L = dpp
2.0	160 (25), 700 (75)	380 (50), 1400 (50)
4.0	100 (30), 600 (70)	220 (55), 1220 (45)
6.0	180 (40), 540 (60)	390 (35), 1200 (65)
8.0	200 (40), 550 (60)	590 (20), 1240 (80)
10.0	280 (45), 590 (55)	600 (20), 1270 (80)
12.0	270 (35), 600 (65)	400 (20), 1150 (90)

* Values in parantheses are the components pre-exponential factors in percent.
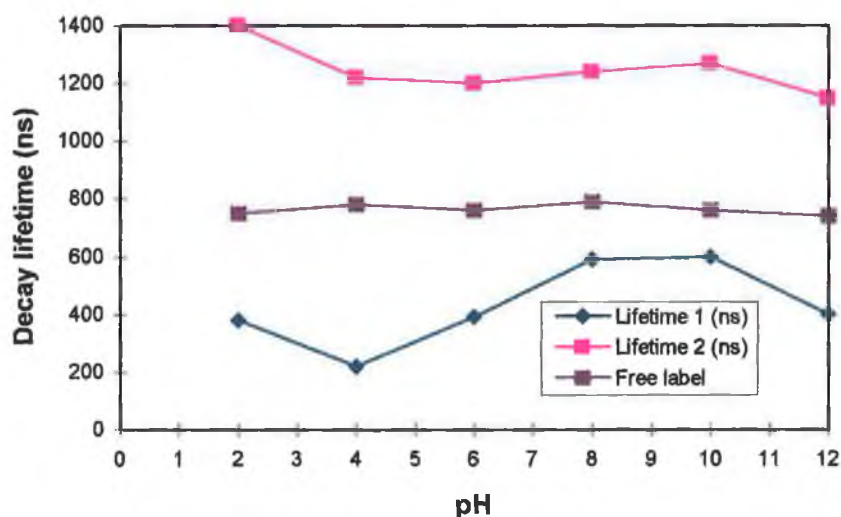

Figure 5.10 pH dependence of the decay lifetimes of aerated
Ru(dpp)₂NCSphen:PLGlu.

As for PLL, this difference in behaviour is most likely due to the difference in sensitivity to oxygen quenching when the labels are situated on different binding sites along the biopolymer. On removal of oxygen, the longer lifetimes are significantly enhanced while the shorter lifetime components are only slightly increased further supporting the theory that the short lifetime component is due to some quenched bound form of label and not unbound label.

(3) BSA-bound complexes.

As labels bound to the side chains of poly-amino acids have proved successful in confirming changes in secondary structure already known, the next step was the labelling to a natural protein. The overall objective here was to investigate the possibility of monitoring more complex conformational variances unique to proteins, such as folding/unfolding processes.

The natural protein chosen for these studies was the globular protein, bovine serum albumin, whereupon both side chain and site-specifiic modification were effected using the same ruthenium labels. Table 5.10 presents the pH dependence of both lifetime components for the aerated forms of both $Ru(L-L)_2NCSphen:BSA$ and $Ru(bpy)_2esterbpy:BSA$. Meanwhile Figure 5.11 depicts both their pH dependent decay behaviour under aerated conditions. In both cases here, the labels are bound to BSA via the lysine residues and so similar behavioural trends should be noted for both the labels, as the local environment of both would be under the same influences at pH extremes.

In contrast to the regular poly-amino acids, whereby the exact effect of specific pH changes on their conformation is well documented, the exact effect of pH on the structures of real proteins, such as BSA is much more complex and more difficult to follow or monitor. However BSA is an acidic protein, and being a serum albumin is most stable at acidic to neutral pH [22]. As a protein is most stable

around its isoelectric point [21], denaturation/unfolding probably occurs at more alkaline pHs. As anticipated, more complicated behaviour and less easily interpreted results are found for the BSA conjugates compared to that of PLL and PLGlu. As opposed to a step or jump in lifetimes being observed at a particular pH, the BSA conjugates do not exhibit such simple behaviour. However, as stated earlier, denaturation may only involve the disruption of some folded conformation upon which its biological properties may be critically dependent [21]. This being the case, on denaturing with acid/base, no change in structure close to the label may be observable although their biological activity may be dramatically affected.

Table 5.10 pH dependence of decay lifetimes of Ru(bpy)$_2$NCSphen:BSA and Ru(bpy)$_2$esterbpy:BSA at room temperature, in aerated solutions.

pH	Ru(bpy)$_2$NCSphen:BSA lifetimes 1, 2 (ns)	Ru(bpy)$_2$esterbpy:BSA lifetimes 1, 2 (ns)
2.9	200 (30), 810 (70)	120 (35), 480 (65)
4.0	230 (30), 800 (70)	240 (40), 750 (60)
7.0	150 (30), 710 (70)	180 (30), 680 (70)
9.0	210 (25), 800 (75)	220 (35), 700 (65)
10.0	130 (25), 790 (75)	180 (25), 620 (75)
11.0	130 (35), 580 (65)	90 (30), 390 (70)
12.0	100 (40), 480 (60)	100 (25), 400 (75)
13.0	130 (30), 390 (70)	

* Values in parentheses are the pre-exponential factors given in percent.

permit us to recognise unfolded states simply from variations in the decay lifetimes of the protein-bound labels.

Significantly, when aerated, both labels bound to the side chain lysine residues exhibit similar decay patterns across a wide pH range which was anticipated. On removing oxygen however from these samples, although lifetimes are enhanced to a certain degree, there is little change in the overall trend with the lowest lifetimes still achieved at basic pHs. This is in contrast to the effects seen for the polypeptides PLL/PLGlu which indicates that the contributing factors are more complex for natural proteins. Figure 5.12 illustrates the more striking changes in lifetimes induced by variations in pH for the label $[Ru(dpp)_2NCSphen]^{2+}$ indicating that this label is more sensitive to environmental changes and therefore would have greater potential as a probe for biological structures. However, such effects may be also more pronounced for such labels due to significant electrostatic interactions that these hydrophobic complexes appear to undergo with proteins. Furthermore interchalation may also be a contributing factor as would be suggested when a change in ionic strength leads to lower conjugation ratios (See Table 3.18) as the ionic strength of a system affects the propensity of a complex to interchalate into a biological structure.

As already discussed, it is possible to target ruthenium complexes to the glutamic acid residues present in BSA. Although the labels are bound to different sites along the biopolymer similar effects are observed on varying the pH except that the lifetimes are enhanced, but this was previously dealt with in Chapter 3. This would be anticipated as our probes would not be expected to be sensitive enough to differentiate between various amino acid residues along the biopolymer.

The next step involved the study of the pH sensitivity of Ru(II) complexes bound to carbohydrate moieties present on the biomolecule i.e. the conjugates Ru(L-L)$_2$NH$_2$phen:BSA(a), constituting site selective modification. Table 5.12, together with Figure 5.13 represent the pH sensitivity of the emission lifetimes of such samples.

231

Table 5.11 pH dependence of decay lifetimes of degassed and aerated Ru(dpp)$_2$NCSphen:BSA conjugates.

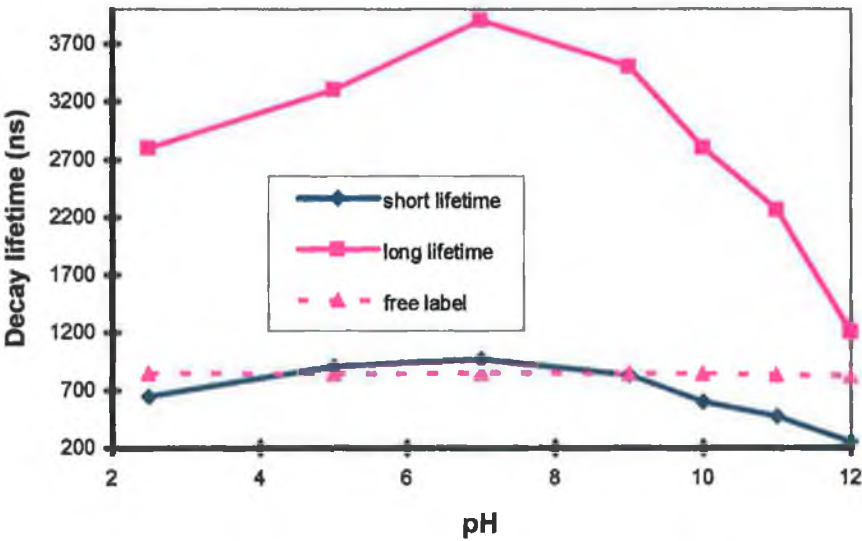| pH	Lifetimes (ns)	
	Degassed	Aerated
2.5	710 (40), 2900 (60)	650 (45), 2800 (55)
5.0	830 (40), 3200 (60)	910 (40), 3300 (60)
7.0	750 (30), 3700 (70)	970 (30), 3900 (70)
9.0	820 (30), 3700 (70)	830 (30), 3500 (70)
10.0	850 (30), 3100 (70)	600 (30), 2800 (70)
11.0	870 (30), 3140 (70)	470 (35), 2260 (65)
12.0	520 (30), 2330 (70)	250 (25), 1200 (75)

Figure 4.19. pH dependence of both lifetime components of aerated Ru(dpp)$_2$NCSphen:BSA.

Table 5.12 pH dependence of decay lifetimes of Ru(L-L)$_2$NH$_2$phen:BSA at room temperature in aerated solutions where L=bpy and dpp.

pH	L=bpy lifetimes 1, 2 (ns)	L=dpp lifetimes 1, 2 (ns)
2.0	70 (25), 680 (75)	220 (45), 1080 (55)
4.0	370 (25), 1130 (75)	410 (45), 1900 (55)
6.0	295 (30), 930 (70)	380 (40), 1700 (60)
8.0	270 (35), 760 (65)	520 (40), 2250 (60)
9.0	300 (20), 620 (80)	420 (50), 1600 (50)
10.0	80 (20), 560 (80)	-------------------------
11.0	90 (20), 480 (80)	300 (45), 1200 (55)
12..0	120 (20), 470 (80)	210 (40), 880 (60)

Again, for the more hydrophobic labels of the form [Ru(dpp)$_2$NH$_2$phen]$^{2+}$, more pronounced variations in lifetimes of their protein-bound form induced by pH variations. Again a contributing factor may be the substantial electrostatic effects and/or intercalation which these complexs experience with proteins. When compared to labels bound to the lysine residues as revealed in Figure 5.12, the lifetimes are more notably affected in very acidic conditions when bound to the carbohydrate moieties, showing significant reduction. This difference may be due to the difference between the local environments of both binding sites when denatured in acidic conditions. Certain local conformational changes may occur at low pHs which affect the carbohydrates more than the lysine residues. However, this theory is difficult to verify and more advanced studies would be necessary to confirm such proposals.
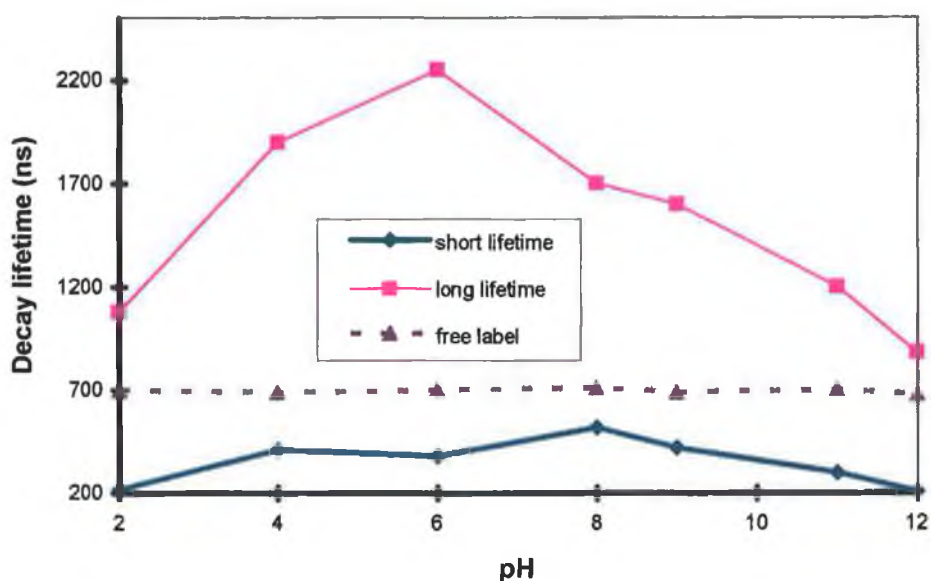
Figure 5.13 pH dependence of both lifetime components of aerated
Ru(dpp)$_2$NH$_2$phen:BSA (a)

One can conclude from the above study that our probes are more effective in the monitoring of predictable and regular conformational variances of simple biomolecules. As there are many more complicating factors involved in the structural deviations of natural proteins such as BSA with much less known of their exact nature one would not expect our fluorescent probes to give us detailed information on their pH dependent dynamic behaviour. All that is apparent from our studies is that extremes of pH, particularly alkaline conditions lead to structural variances which lead to a reduction of the labels lifetimes, the reason for which is unclear. This would be expected as serum proteins would be quite acidic and sensitive to pH, with unfolding expected to occur at such pH extremes. Later in this section, studies on denaturation of such proteins by chemical denaturants will be carried out in an attempt to determine the usefulness of our probes in examining such unfolded states.

5.2.1.2 Effect of reaction conditions.

(1) Temperature effects.

So far in our work, the conjugation reactions studied have involved mild conditions such that the native structure of the biomolecule should not be disturbed, thereby permitting us to study the natural conformational variances inherent in the biomolecules in question. The ultimate objective in this section is the manipulation of some of these conditions in an attempt to induce variations in the natural structural forms of the biomolecule. Thereafter, the effect of such variations on the decay behaviour of the bound labels are monitored. The variables chosen include temperature and reagent effects and after labelling the proteins under such extreme reaction conditions the same pH dependent lifetime studies are carried out on the modified bio-conjugates taking note of any significant changes.

Certain conjugation reactions were carried out at an elevated temperature of 50 ^{0}C, namely the side-chain modification of PLL and BSA. For this study the conjugation procedure was carried out as normal (i.e. at 4 ^{o}C), samples were taken at various pHs and each sample was then heated to 50 ^{0}C, in order to maintain the required temperature while analysing the samples by laser excitation. The lifetimes for heated Ru(L-L)$_2$NCSphen:PLL are presented in Table 5.13.

The first point to note is the fact that shorter lifetimes were obtained at higher temperatures for both PLL and BSA, which was anticipated due to the increase of efficiency of deactivation pathways of Ru(II) complexes at such elevated temperatures [23]. However, the most significant observation of this study is the fact that at 50^{0}C, the lifetimes are no longer sensitive to pH variations for Ru(L-L)$_2$NCSphen:PLL. This correlates well with the fact that PLL at 50^{0}C does not undergo a pH dependent structural transition, but rather adopts a non-random type β-sheet conformation somewhat similar to the α-helical form earlier discussed [24]. These probes would not be expected to be sensitive enough to differentiate between two such similar non-random conformations as α-helices and β-sheets. Hence, the

label when bound to PLL in the β-sheet conformation would be expected to behave in a very similar fashion to when in the helical form due to the equivalent local environments of the labels when bound to both. Another significant observation is the reversibility of this experiment which indicates that these heat induced structural variations are indeed reversible and that PLL reverts back to its random coil conformation on cooling down the conjugate solution. Such an effect would further support our theory and would make the decomposition of the bioconjugate an unlikely explanation for any effects noted at such elevated temperatures.

Table 5.13 pH dependence of emission lifetimes of aerated $Ru(L-L)_2NCSphen:PLL$ at 50^0C where L=bpy and phen.

pH	L= bpy lifetime 1, 2 (ns)	L=phen lifetime 1, 2 (ns)
3.0	60 (20), 360 (80)	200 (20), 500 (80)
6.0	45 (15), 420 (85)	190 (20), 530 (80)
9.0	65 (30), 390 (70)	220 (15), 530 (85)
11.0	60 (35), 370 (65)	220 (15), 510 (85)
12.0	65 (30) 400 (70)	120 (15), 480 (85)

For the heated samples of $Ru(L-L)_2NCSphen:BSA$ the lifetimes of the samples at every pH are shorter than the corresponding sample at room temperature as for the PLL conjugates, again explained by the spectroscopic properties of the label [23], and not due to any conformational effects of the bound protein. However, no significant change in the pH sensitivity of their luminescence lifetimes is evident in

that the lifetimes still show dramatic reduction at pH extremes, particularly at pHs 9-12. It was anticipated that if the chemical were to unfold the protein the acid-induced denaturation effects would no longer be evident. This is not the case however, which would indicate either that the temperature of 50° C is not high enough to cause denaturation in BSA or that the heat induced structural variations are minimal and of a different nature to the acid-induced conformational changes. This renders such studies on proteins inconclusive and in order to complete such studies much higher temperatures should be used in an attempt to fully denature the protein BSA.

(2) Effect of chemical denaturants.

As discussed in chapter 3, the various proteins were treated with denaturing agents including urea and guanidine by allowing them, both in solution form, to react together at 4 °C and the normal procedure of conjugating the labels to the resulting protein solution was carried out (See section 2.3). In section 3.2.4.5, the effect of chemical denaturants on the success of the conjugation reactions has been discussed, whereas this section incorporates the study of the effect of the denaturing agents on the acid-induced conformational variances of the bound biomolecules.

Firstly a study of the pH sensitivity of the lifetimes of conjugates prepared with 1 M solutions of chemical denaturants added (guanidine/urea) was carried out. On comparing the acid-induced decay behaviour of Ru(L-L)$_2$NCSphen:BSA when treated with urea to the normal conjugate as described in Table 5.11 the trend observed is very similar in that significant drops in both lifetime components are still evident at alkaline pHs. The similar pH sensitivity in the presence of urea indicates either of two main possibilities, one being the ineffective denaturation of the protein using urea possibly due to the requirement of a higher concentration of urea. This would mean that the lifetime reductions judged to be due to denaturation at pH extremes would still be evident. The second explanation may be that the denaturation induced by urea may not lead to significant structural disruptions and hence the acid-

induced denaturation would still be evident in such conjugates, having a stronger effect on the label. However, on removing oxygen from all urea treated samples, the resulting increases in both lifetime components are more significant than those not treated with urea. This indicates that the urea treated samples are more susceptible and accessible to the quenching effects of oxygen most likely due to some form of structural disruption having taken place. In the case of Ru(L-L)$_2$NCSphen:PLL very little change is observed in their acid induced decay behaviour on treating with urea, except that again the samples appear more accessible to the quenching effects of oxygen.

To establish the concentration of denaturant required to affect the lifetimes of the labels and thus possibly alter the proteins conformational properties, the effect of increasing concentrations of guanidine on the emission lifetimes of the protein-bound labels was determined and is described below. Table 5.14 outlines the influence of various concentrations of guanidine on the emission lifetimes of both conjugates Ru(dpp)$_2$NH$_2$phen:BSA and Ru(dpp)$_2$NCSphen:PLL.

Table 5.14 Effect of increasing concentrations of guanidine (Guan) on the lifetimes of Ru(dpp)$_2$NH$_2$phen:BSA and Ru(dpp)$_2$NCSphen:PLL, pH   9.2

Conc Guan (mol/l)	Ru(dpp)$_2$NH$_2$phen:BSA Aerated lifetimes 1, 2 (ns)	Ru(dpp)$_2$NCSphen:PLL Aerated lifetimes 1, 2 (ns)
0.0	1650 (55), 380 (45)	800 (65), 300 (35)
2.0	1370 (60), 270 (40),	820 (80), 210 (20
4.0	1340 (65), 290 (35),	850 (65), 330 (35)
6.0	1270 (80), 340 (20)	820 (75), 290 (25)
10.0	1240 (75), 390 (25)	780 (75), 260 (25)

It was anticipated that one may possibly be able to estimate the approximate concentration of denaturant necessary to unfold the protein by observing the gradual reduction of the lifetimes of the labels to a minimum level with increasing concentrations of denaturant. Essentially, we can deduce from Table 5.14 that the longer lifetime of the BSA-bound label is significantly reduced after adding 2.0 M guanidine whereas the shorter lifetime varies less appreciably The longer lifetime continues to decrease further but much more gradually upto 10 M guanidine and as the errors in the lifetimes are approximately 5% these changes in lifetime at 2 M guanidine are insignificant. The most significant lifetime reductions with 2 M added would suggest that the chemical has unfolded/denatured the protein at such a concentration assuming the minimisation of the emission lifetimes is an indication of complete denaturation.

Table 5.14 also reveals the contrasting effect the denaturant has on the PLL-bound label at various pHs. In contrast to the reduction of the decay lifetimes for the BSA conjugate, a slight increase in the longer lifetime is noted with the addition of denaturant, however the variations are within the range of experimental error. However, it must be noted that the emission lifetimes of the same PLL-bound label at a higher pH of pH 12 experience significant enhancements. This may be due to the recognised effect of denaturants such as guanidine and lithium chloride on the conformation of PLL [25]. Although PLL is a synthetic biomolecule which does not undergo the same unfolding process as natural proteins, reports reveal that both chemical denaturants and other salts do indeed affect the secondary conformational changes inherent in PLL [25], which are closely related to its biological activity [15]. This proposedly occurs by making PLL unstable in water via the destruction or minimisation of the hydrogen-bonded structure of water surrounding the non-ionised peptide [25]. Hence the guanidine may de-stabilise the α-helix favoured at pH 12, thereby restoring PLL to a random coil conformation where the more enhanced lifetimes of the bound labels have been evident. On the other hand, PLL at pH 9 is probably still in the random coil conformation which would not be affected by the denaturant.

239

Hence, one can see that the denaturation induced by chemical denaturants may possibly be monitored by the reduction in decay lifetimes of the protein-bound labels but only if an optimal concentration of denaturant is added which depends on the chemical used and the nature of the protein. This would explain the minimal effect of 1 M guanidine on the pH sensitivity of the PLL and BSA bound complexes. In contrast, on increasing the concentration of guanidine to where a decline in decay lifetime of the label is noted, the influence on the pH sensitivity of the labels is probably due to the unfolding of the protein in the presence of guanidine. From these studies it is evident that the higher concentration of guanidine greatly decreases the pH sensitivity of the decay lifetimes of the labels when bound to both PLL and BSA. In the case of $Ru(bpy)_2NCSphen$:PLL with urea the emission lifetimes from pH 2 to pH 12 are quite similar, being of similar duration to those of the conjugate at acidic to neutral pHs when PLL is in the random coil conformation. This would indeed be anticipated if as suggested the guanidine does destabilise the α-helix returning it to the random coil form. This being the case, PLL would be in the random coil form at all pHs in the presence of guanidine explaining the similarity of the decay lifetimes of the PLL-bound labels at all pHs.

On the other hand the emission lifetimes of the BSA-bound labels are reduced, rendering them of similar duration to those normally achieved at highly alkaline pHs in the absence of urea. This is probably due to the unfolding effect of the denaturant guanidine on the protein. The difference in the effect of 1 M and 5 M guanidine on the pH sensitivity of the decay lifetimes of the protein-bound labels would appear to be due to the fact that 1 M guanidine is not concentrated enough to affect the conformational forms of the proteins while 5 M is sufficiently concentrated to exert its reducing affect on the protein. Hence the labels are somewhat sensitive to the denaturation which the proteins undergo in the presence of chemical denaturants such as urea and guanidinium chloride although they appear to be less sensitive than for acid-induced conformational variances of the same proteins.

5.2.2 Lysozyme activity studies.

5.2.2.1 Introduction.

Although the capability of the emission lifetimes of the ruthenium complexes to detect conformational changes of the protein BSA has been indicated in the previous section, some of the major restrictions include the inability to establish the effect of the label on the function and natural structure of the protein and the lack of information on and understanding of the conformational properties of BSA. Under extreme reaction conditions such as pH extremes it was merely assumed that unfolding of the protein had taken place and therefore that any changes in emission lifetime/intensity of the bound label were likely to be due to structural variances of the biomolecule emanating from the unfolding process.

In this section, the same labels are covalently bound to the enzyme, lysozyme. Lysozyme is present in tears, nasal mucus, tissues and milk and acts by catalysing the hydrolysis of a polysaccharide that is a major constituent of the cell wall of certain bacteria [26]. The polymer is formed from β (1-4)-linked alternating units of *N*-acetyl glucosamine (NAG) and *N*-acetylmuramic acid (NAM) as depicted in Figure 5.14 and the hydrolysis of these 1,4-β linkages by lysozyme destroys the cell walls of many airborne gram positive bacteria [26]. Lysozyme contains small regions of pleated sheet, little α-helix and large regions of random coil. The molecule has a deep central cleft that harbours a catalytic site with six subsites that bind various substrates and inhibitors [26]. The cleft contains nonpolar side chains of amino acids for binding the nonpolar regions of the substrate, and hydrogen-bonding sites for the acylamino and hydroxyl groups. Small distortions occur in the enzyme structure at the active-site binding cleft when the inhibitor is bound ie. the enzyme undergoes a small conformational change [27]. The binding sites of lysozyme are approximately complementary in structure to the structures of the substrates as the nonpolar parts of the substrate match up with nonpolar side chains of the amino

241

acids [27]. The reactive part of the substrate is firmly held by this binding next to acidic, basic or nucleophilic groups on the enzyme.

The enzymatic activity of lysozyme, which is dependant on its structure can be measured by determining the loss of substrate in this case the bacteria *M. lysodeikticus* per unit of time and was determined using modified methods of Shugar [28] and Perkins [29], subsequently described in section 2.5.4. The primary objectives of this study were twofold; (1) to determine the effect if any of the covalently bound label on the natural stability and activity of the enzyme (and hence on its original conformation); (2) to investigate the correlation between the deactivation of the enzyme and changes in decay lifetimes of the protein-bound label, thereby determining the potential of these complexes in biological applications.
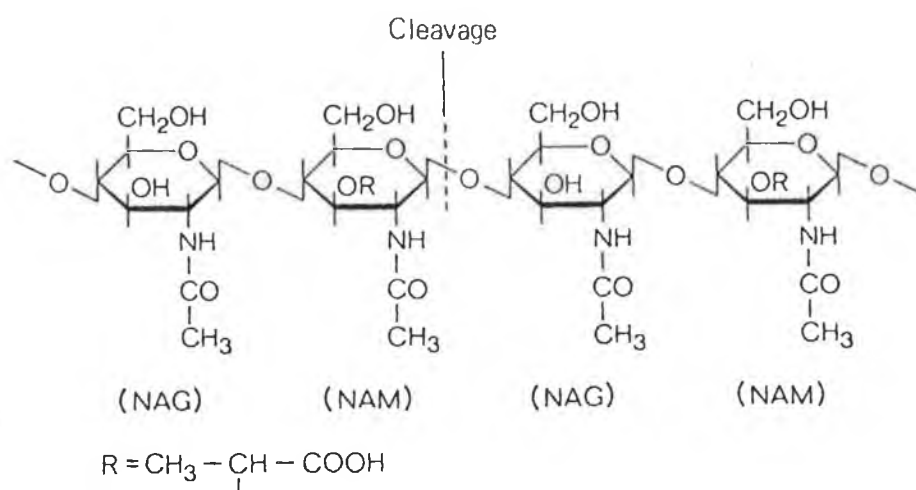

Figure 5.14 The polysaccharide substrate of lysozyme found in bacterial cell walls.

Firstly, the effect of pH and protein denaturants on the activity of pure lysozyme was determined to ascertain the conditions under which the enzyme becomes totally deactivated. The Ru(II) complexes were bound to the enzyme via the carbohydrate moieties ($Ru(L-L)_2NH_2phen:LYS$) and the lysine residues ($Ru(L-L)_2NCSphen:LYS$) as was done for BSA and PLL (See sections 2.3.1 & 2.3.5). The effect of the label on the activity of the enzyme was determined under similar conditions in order to ensure that the labels do not have adverse affects of the natural conformation variances of the protein. The sensitivity of the decay lifetimes of the lysozyme (LYS)-bound labels to pH changes and to chemical denaturants was then studied in attempts to find correlations between deactivation of the enzyme and a decrease in decay lifetime of the label. Table 5.16 lists the loadings achieved and the decay lifetimes of the various lysozyme conjugates prepared.

Table 5.16 Conjugation ratios and lifetimes of 10:1 $Ru(L-L)_2NH_2phen:LYS$ and $Ru(L-L)_2NCSphen:LYS$, 0.05M carbonate buffer, pH 8.2.

Conjugate	Conjugation ratio	Decay lifetimes 1, 2 (ns)
$Ru(bpy)_2NH_2phen:LYS$	1	650 (70), 250 (30)
$Ru(phen)_2NH_2phen:LYS$	1	700 (70), 280 (30)
$Ru(dpp)_2NH_2phen:LYS$	3	800 (75), 350 (25)
$Ru(bpy)_2NCSphen:LYS$	3	750 (80), 260 (20)
$Ru(phen)_2NCSphen:LYS$	3	780 (70), 300 (30)
$Ru(dpp)_2NH_2 phen:LYS$	1	850 (75), 380 (25)

Conjugation ratio was calculated according to Nairn [30].

The protein concentration was determined using the Folin-Lowry assay [31].

As seen from the information above, very low loadings are achieved for all labels bound to lysozyme. The less efficient binding compared to BSA may be due to the smaller number of lysine residues per lysozyme molecule ie. 6 and/or the more compact structure of the enzyme. As with all protein-bound labels studied, double exponential decay kinetics is evident. However, as was found for the same labels bound to BSA, on mixing the label $[Ru(dpp)_2NH_2phen]^{2+}$ with lysozyme and analysing immediately (hence, no covalent linkage has occurred), double exponential decay kinetics results, indicating substantial electrostatic interactions between such labels and the enzyme. Indeed a possibility may be the intercalation of the label into the folded structure of the enzyme, a phenomenon already witnessed, particularly between Ru(II) complexes and DNA [32] and which already has been proposed to occur between Ru(II) labels and the protein BSA. For this reason, the other smaller labels were used mainly in the remainder of this section. One unusual aspect is the low lifetimes obtained for $Ru(dpp)_2NH_2phen:LYS$, both when this label is bound to lysozyme via the carbohydrate moieties and glutamic acid residues. This suggests that the label has some adverse affect on the enzyme, but this topic will be addressed subsequently.

(1) pH effect:

A correlated study between the pH sensitivity of the enzyme activity of pure and labelled lysozyme and the decay lifetimes of the lysozyme-bound labels was carried out. The deactivating effect of pH on the various lysozyme conjugates is outlined in Table 5.17 where they are compared to the behaviour of the non-labelled lysozyme. This study allows one to determine the effect of such modification on the activity of the enzyme and the effects of modification on the conformational stability of the protein at extremes of pHs.

When the activity of enzymes is measured at several pH values, the optimal activity is typically between pH 5 and pH 9 [27]. This was indeed the case for

lysozyme whereby it was most active at breaking down the cell wall of the bacteria *M. lysodeikticus* between pHs 5 and 8 while almost totally inactivated at more extreme pHs (See Table 5.17(a)). There are two likely explanations for such behaviour. (1) Enzyme denaturation may occur at pHs lower and higher than the optimal pH range. (2) Alteration in the charged state of the enzyme and/or substrate with pH may lower the reaction rate [27]. The enzyme may undergo changes in conformation when the pH is varied. A charged group distinct to the region may be necessary to maintain the active tertiary or quaternary structure. As the charge is changed with pH, the protein may unravel, become more compact causing a decline in activity. Depending on the severity the activity may or may not be restored when the enzyme is restored to the optimal pH. In this case the activity of lysozyme is partially restored when the pH is brought back to the optimal pH 6-7.

Table 5.17 pH sensitivity of the activity of (a) lysozyme (b) Ru(bpy)$_2$NH$_2$phen:LYS,(c)Ru(bpy)$_2$NCSphen:LYS, (d)Ru(phen)$_2$NH$_2$phen:LYS, (e)Ru(dpp)$_2$NH$_2$phen:LYS(a) and (f) Ru(dpp)$_2$NH$_2$phen:LYS(b).

| pH | Enzyme activity | | | | | |
	(a)	(b)	(c)	(d)	(e)	(f)
2.6	0.001	0.001	0.001	0.005	0.001	0.000
4.6	0.001	0.002	0.002	0.010	0.001	0.000
6.2	0.009	0.002	0.004	0.008	0.001	0.002
8.2	0.005	0.004	0.002	0.000	0.000	0.001
9.2	0.001	0.000	0.004	0.000	0.000	0.000
10.2	0.001	0.000	0.002	0.000	0.000	0.000

On studying the activity of the various lysozyme conjugates, the first point to note is the general reduction of maximum activity which may be merely due to the physical affect/steric hindrance of the label on the reaction with the substrate. However the optimal pH range where maximum activity of the enzyme is noted to be still approximately between pH 4 and pH 8, indicating the minimal effect of most of the covalently bound labels on the stability and pH susceptibility of the enzyme. The fact that most of the labelled forms of lysozyme behave similarly to the unmodified lysozyme indicate that the binding sites of the labels on the enzyme are not located on the active site, critical to the binding of the enzyme to the substrate. Lysozyme modified by labels bound to the carbohydrate moieties and lysine residues is still quite active indicating that these sites are not critical to the activity of the enzyme.
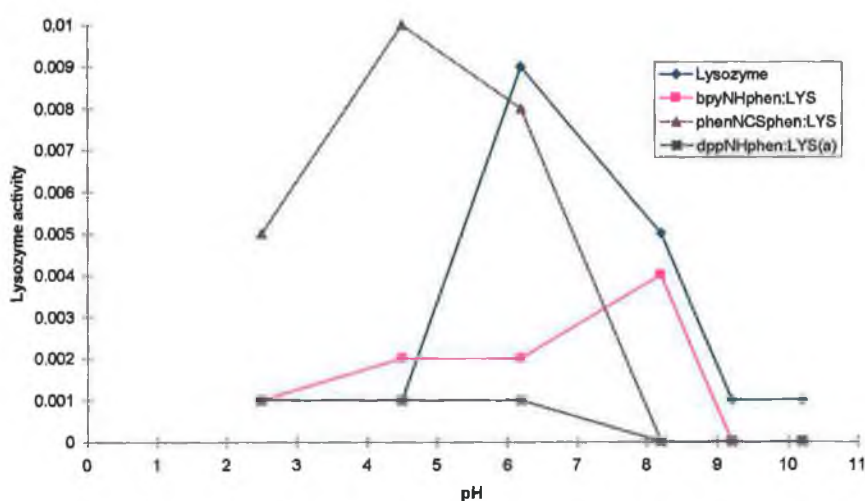

Figure 5.15 The pH sensitivity of the activity of lysozyme and various lysozyme conjugates, (a) Ru(bpy)$_2$NH$_2$phen:LYS (b) Ru(phen)$_2$NH$_2$phen:LYS and (c) Ru(dpp)$_2$NH$_2$phen:LYS(a).

One exception however appears to be the label $[Ru(dpp)_2NH_2phen]^{2+}$ when bound to lysozyme via the glutamic acid residues $(Ru(dpp)_2NH_2phen:LYS(b))$ and via the carbohydrate moieties $(Ru(dpp)_2NH_2phen:LYS(a))$ whereby the enzyme appears to be almost totally inactivated with only low activity observed at pHs 6-8. This suggests that the hydrophobic complex adversely affects the stability and conformational properties of the enzyme. Another possibility is that the binding of such a large molecule to lysozyme may cause steric hindrance, thereby preventing the substrate from binding as efficiently. Another possible explanation is the importance of glutamic acid residues in the binding of the enzyme to substrate which is confirmed by reports whereby the modification of all the carboxylic acids of the glutamic acid residues by treating with aminomethanesulphonic acid and carbodiimide results in a total loss of activity of lysozyme [33]. The effect of the bound Ru(II) complexes on the pH sensitivity of lysozyme activity is outlined in Figure 5.15.

Although the lysine residues and carbohydrate moieties do not appear to be critical to the activity of lysozyme, Figure 5.15 reveals a slight difference in the activity patterns of lysozyme. The labelling of lysozyme via lysine residues (Table 5.17(c)) appears to activate the enzyme at high pHs whereas the modification of the carbohydrate moieties has an activating effect on the enzyme at low pHs. This is probably due to the change in charge that these labels impose on the sites.

On determining the significance of pH on the activity of lysozyme, the pH sensitivity of the lifetimes of Ru(II) labelled lysozyme was determined. To illustrate this phenomenon, the pH sensitivity of the emission lifetimes of $Ru(bpy)_2NCSphen:LYS$ is tabulated in Table 5.18 and graphically represented in Figure 5.16. The decrease in lifetimes particularly at high pHs is evident for both conjugates of lysozyme as was found for the labels bound to the protein BSA earlier in this chapter. Again this indicates denaturation or some unfolding or change in conformation of the enzyme at extremes of pH. The emission intensity of these protein-bound labels is also very sensitive to pH variations with the most intense emission at acidic to neutral pHs (i.e. pH 3-6), in correlation with the pH range

where lysozyme in free and labelled form is at its most active and where the labels display the longest lifetimes.

Table 5.18 pH sensitivity of decay lifetimes of (a) Ru(bpy)₂NCSphen:LYS and (b) Ru(phen)₂NCSphen:LYS, 0.01 M carbonate buffer pH 8.2.

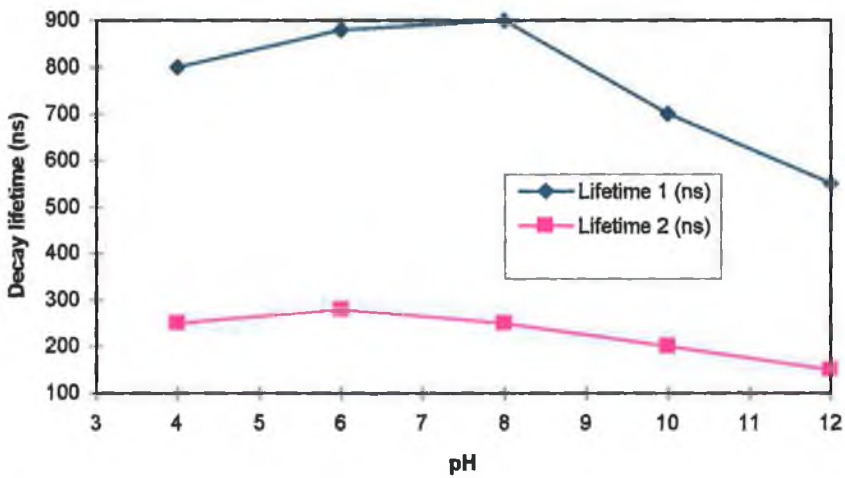| pH	(a) Decay lifetimes 1, 2 (ns)	(b) Decay lifetimes 1, 2 (ns)
4.0	800 (70), 250 (30)	900 (75), 300 (25)
6.0	880 (70), 280 (30)	1000 (70), 280 (30
8.0	900 (70), 250 (30)	950 (75), 250 (25)
10.0	700 (65), 200 (35)	850 (70), 240 (30)
12.0	600 (70), 150 (30)	650 (70), 200 (30)

Figure 5.16 pH sensitivity of the emission lifetimes of Ru(bpy)₂NCSphen:LYS.

Hence, these results confirm that there is indeed a close association between the loss of activity of the enzyme lysozyme due to either denaturation at pH extremes or conformational changes due to changes in charges and the decline in decay lifetimes of the enzyme-bound labels. This correlates well with the promising results found in the monitoring of the acid-induced denaturation of the protein BSA using the decay lifetimes of the bound labels.

(2) Effect of chemical protein denaturants:

This section involves the determination of the deactivating effect of chemical denaturants on the enzyme lysozyme in an attempt to correlate such deactivation with changes in the decay lifetimes of the labels bound to the same enzyme, as was confirmed previously in the case of acid-induced denaturation. One of the primary objectives is the elucidation of the approximate concentration of guanidine necessary to deactivate/denature the enzyme when unmodified and when labelled with Ru(II) polypyridyls. This should allow one to estimate the effect of such protein modification on the stability of the protein under such adverse conditions. An illustration of the effects of denaturants on both the activity of the labelled lysozyme and the emission lifetimes of the label bound to lysozyme is given in the following section. Table 5.19 and Figure 5.17 reveal the effect of guanidine on the activity of the labelled enzyme while Table 5.20 and Figure 5.18 illustrate the susceptibility of the emission lifetimes of the labels to such a chemical denaturant. Table 5.19 reveals that although the addition of the denaturant guanidine leads to loss of activity of lysozyme, there is a minimum concentration of the chemical required to fully deactivate the protein, below which little loss of activity of the enzyme is noted. This is probably due to the co-operative nature of the denaturation of the protein as discussed in section 4.1.4. Figure 5.17 discloses that approximately 2 M guanidine is necessary to deactivate the natural lysozyme. While the enzyme is still 95% active after adding 1.2 M guanidine an increase of another 1.2 M leads to

249

almost total loss of activity. In the case of the labelled enzyme, slightly higher concentrations (3.6 M) of denaturant are necessary to induce total loss of activity of lysozyme and the denaturation curve reveals a less abrupt loss of activity. This suggests that the labelling of the enzyme with these Ru(II) complexes actually has a stabilising effect on the enzyme against the reducing properties of the denaturant, possible due to steric hindrance.

Table 5.19 Effect of guanidinium chloride (Guan) on the enzyme activity of lysozyme (LYS) and lysozyme conjugates pH 8.2.

| Lysozyme/conjugate | Enzyme activity (vs [Guan]) | | | | | |
	0.00 M	0.90 M	1.20 M	2.40 M	3.60 M	4.80 M
lysozyme	0.013	0.013	0.011	0.001	0.001	0.004
Ru(bpy)$_2$NH$_2$phen:LYS(a)	0.008	0.007	0.007	0.005	0.001	0.001
Ru(bpy)$_2$NCSphen:LYS	0.005	0.005	0.006	0.004	0.000	0.000

Error of activity is approximately =- 0.001

Table 5.20 Effect of guanidinium chloride on the emission lifetimes of lysozyme conjugates pH 8.2.

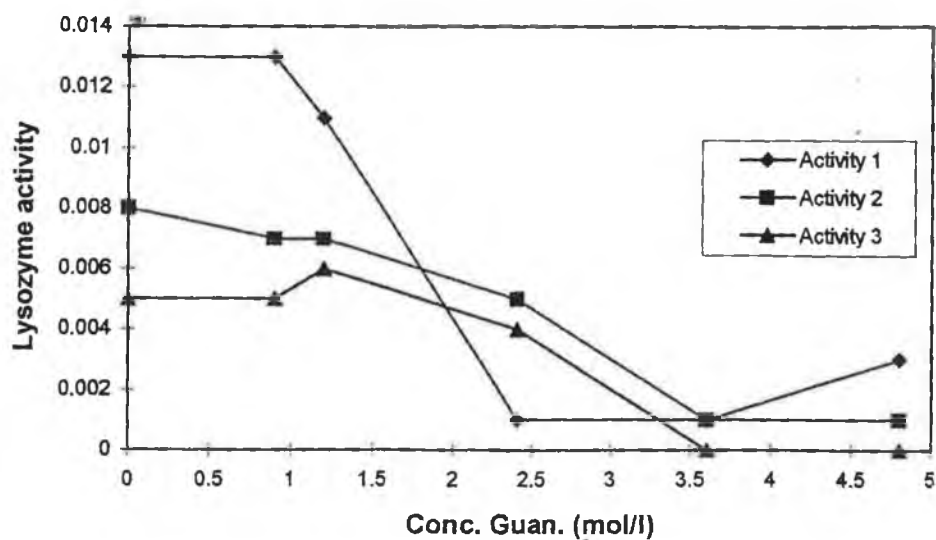| Conc. Guan. (mol/l)	Ru(bpy)$_2$NH$_2$phen:LYS	Ru(bpy)$_2$NCSphen:LYS
0.00 M	900 (70), 250 (30)	950 (75), 250 (25)
1.20 M	880 (75), 260 (25)	960 (75), 260 (25)
2.40 M	800 (70), 230 (30)	900 (75), 240 (25)
3.60 M	740 (65), 200 (35)	780 (70), 200 (30)
4.80 M	650 (65), 190 (35)	700 (65), 180 (35)

Figure 5.17 Effect of guanidine (Guan) on the enzyme activity of (1) lysozyme, (2) Ru(bpy)₂NH₂phen:LYS (NH₂phen:LYS) and (3) Ru(bpy)₂NCSphen:LYS pH 8.2 (NCSphen;LYS)
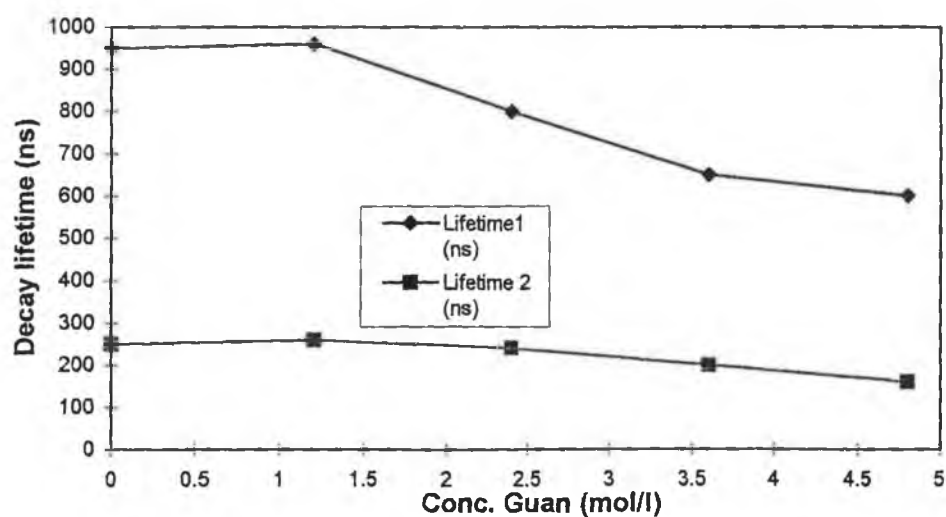

Figure 5.18 Effect of guanidine on the emission lifetimes of Ru(bpy)₂NCSphen:LYS pH 8.2.

Regarding the effect of chemically induced denaturation on the labels bound to lysozyme, the sensitivity of the emission lifetimes of the same labelled enzymes outlined in Table 5.20 and presented in Figure 5.18 reveals that the longer lifetime in particular is affected by guanidine. The emission lifetime of one label of duration 950 ns when bound to the 100% active enzyme diminishes to a minimum duration of 700 ns after the addition of approximately 4 M guanidinium chloride, a concentration sufficient to totally deactivate the enzyme as verified in Figure 5.17. A levelling off of the lifetime above concentrations of 3.6 M indicate that total deactivation/denaturation of the enzyme has indeed been achieved. As for the deactivation by pH, this study appears to confirm the association between the loss of activity or denaturation of the enzyme and the reduction of decay lifetimes of the labels bound to the deactivated enzyme.

In conclusion, the results of these studies allow us to emphasise the following interesting points. Firstly, they indicate that the labels do have some effect on the stability and activity of the enzyme which varies depending on the nature and position of the binding sites in relation to the active site of the enzyme. In particular the labels bound to the glutamic acid residues have adverse affects on the enzyme, causing almost a total loss of activity, proposed to be due to the critical positioning of such residues in the active site of lysozyme. However, the conformational variations of the enzyme induced by both pH and chemical denaturants do not appear to be affected by the covalently bound labels which is very important in the probing of such "inherent" variances. Furthermore, there are indeed correlations between loss of activity and possible denaturation of lysozyme, and the reduction of the decay lifetimes of the covalently bound labels which had earlier been proposed for the protein BSA. This thereby strongly strengthens our case regarding the potential of these labels in monitoring denaturation of proteins in real biological processes as well as the more fundamental secondary structure changes in synthetic poly-amino acids.

5.3 Conclusion.

Studies in chapter 4 verified that while the emission spectra of the protein-bound Ru(II) complexes are influenced by the conformational variances of the bound biomolecule the variations in intensity are not sensitive or specific enough to be used as efficient probes. This chapter investigates the potential of the emission lifetimes of the labels as probes to the proteins conformational variations, whereby various conformational changes are induced in the proteins and the sensitivity of the emission lifetimes of the bound labels to such variations are investigated.

As the influence of pH on both the secondary structure of polypeptides and the 3-D structure of proteins is widely known, these are the conformational changes primarily studied. As anticipated the sensitivity of the decay lifetimes to pH is striking and appears to be dependent on the form of bound biomolecule. This phenomenon is explained to be due to the fact that the lifetimes of the ruthenium complexes are affected by their local environment and hence local structural variations of the bound biomolecule are discerned by subsequent modification in the decay kinetics of the bound labels. The propensity of the labels to differentiate between random and non-random secondary structures including random coil and α-helices in synthetic poly-amino acids is verified as such structural variances lead to significant changes in emission lifetimes. This capability appears to be primarily due to the greater sheltering effect of the biomolecule of random structure on the ruthenium complex from certain quenching effects in particular oxygen. In this respect their probing qualities are based on the difference in the efficiency of oxygen quenching on the lifetime of the labels excited state due to changes in their immediate surroundings. The next step incorporated the study of the efficacy of such probes to monitor more complex structural variations in real proteins such as folding/unfolding processes. The decay lifetimes of the labels also appear to be susceptible to the unfolding process of natural proteins, induced both by pH extremes and by chemical denaturation. Certain folding/unfolding processes of the protein studied, in particular acid-induced denaturation apparently lead to reduction

253

of the lifetimes of the bound labels, probably due to the more open and accessible structure of the protein when unfolded rather than local environmental effects noted for the synthetic biomolecules. However, due to the unavailability of more thorough biological procedures the unfolding of the protein by extremes of pH and by chemical denaturants was not confirmed but can only be assumed.

For this reason, the second main objective was to broaden our scope on the study of real biological processes by investigating the labelling of the active enzyme, lysozyme with the same Ru(II) complexes. Firstly, the effect of labelling on the activity of the enzyme is determined to ensure that such modification does not de-stabilise, deactivate or induce structural deviations in the protein which would adversely affect our studies. In order to verify that unfolding or denaturation of the enzyme does indeed take place, the loss of activity of lysozyme towards a specific substrate is used as the indicator of denaturation. The enzyme remains active on binding the various labels, however the nature of the binding site of the label on the enzyme does affect its activity, probably due to the various positions of the site in relation to the active site of the enzyme. On binding to the glutamic acid residue, a total loss of activity results, thereby indicating that certain glutamic acids are essential in the binding of the enzyme to substrate, which correlates with reports in the literature [33]. Furthermore, the label $[Ru(dpp)_2NH_2phen]^{2+}$ deactivates the enzyme to a significant degree, possibly due to its large size and/or its hydrophobic nature causing conformational variations.

The denaturation of the labelled lysozyme by pH and chemical denaturants is followed and the decay lifetimes of the labels are simultaneously monitored to investigate the influence of protein deactivation on the lifetimes of the labels. According to our studies, both natural lysozyme and its various labelled forms are most active at pHs 4-8 and significantly, the most enhanced lifetimes of the protein-bound labels are indeed evident at such a pH range. Furthermore, the denaturing effect of guanidine is revealed by the combined loss of activity of the enzyme and decline in emission lifetimes of the label. This study allows one to approximate the concentration of denaturant required to deactivate the enzyme. Such results are

254

promising as they indicate the possibility of using such labels in real biological matrices without adverse effects on the protein nature.

In conclusion, the fluorescent Ru(II) complexes chosen appear to be successful as probes of certain conformational variances of the bound biomolecules whereby the decay lifetime of the excited state of the fluorescent label acts as the sensitive reporter, both of secondary structure changes of polypeptides and unfolding processes of natural proteins. This appears to be primarily due to the sensitivity of the labels excited state to the local environment in addition to its susceptibility to quenching effects, particularly that of oxygen. Finally, in most cases the labels appear to have little effect on the natural conformational properties of the proteins concerned which is a critical factor in their use of probes of real biological systems. However this obviously depends upon the position of the label on the biomolecule concerned and should be examined prior to any probing studies.

5.4   References.

[1]   A.J. Bard, Luminescent Metal Chelate Labels and Means for Detection, U.S. Patent Application Number, PCT/US85/02153, **1986.**

[2]   R.S. Davidson, Transition Metal Complexes and Method for Time-Resolved Luminescence Binding Assay, International Application No. 8704523., **1987**.

[3]   Weber S.G., U.S. Patent Application Number, 4,293,310, **1981.**

[4]   W. Bannwarth and D. Schmidt, *Tetr. Lett.,* **1989**, 30, 1513.

[5]   W. Bannwarth, *Anal. Biochem.,* **1989**, 181, 216.

[6]   N.E. Conway and L.W. McLaughlin, *Bioconj. Chem.,* **1991**, 2, 452.

[7]   E.M. Ryan, R. O'Kennedy, M.M. Feeney, J.M. Kelly and J.G. Vos, *Bioconj. Chem.,* **1992**, 3, 285.

[8]   D. Gerard, B. Lux, A. Follenius and M.C. Kilhoffer, *Spectrosc. Biol. Mol., (Proc. Eur. Conf. 1st),* **1985**, 393.

[9]   A.O. Ozinskas, H. Malak, J. Joshi, H. Szmacinski, J. Britz, R.B. Thompson, P.A. Koen and J.R. Lakowics, *Anal. Biochem.*, **1993**, 213, 264.

[10]   B.A. DeGraff and J.N. Demas, *J. Phys. Chem.*, **1994**, 98, 12478.

[11]   E. Terpetschnig, H. Szmacinski, H. Malak and J.R. Lakowics, *Biophys. J.*, **1995**, 68, 342.

[12]   E. Terpetschnig, H. Szmacinski and J.R. Lakowics, *Anal. Biochem.*, **1995**, 227, 140.

[13]   H.J. Youn, E. Terpetschnig, H. Szmacinski and J.R. Lakowics, *Anal. Biochem.*, **1995**, 232, 24.

[14]   K. Shreder, A. Harriman and B.L. Iverson, *J. Am. Chem. Soc.*, **1995**, 117, 2673.

[15]   M.V. Pimm, S.J. Gribben, G. Mezo and F. Hudecz, *J. Lab. Comp. Radio pharm.*, **1994**, 36, 2, 157.

[16]   Y. Yoshimura, K. Kondo, M. Nishida, J. Kawada and R. Tanaka, *Chem. Pharm. Bull.*, **1992**, 40, 2, 423.

[17]   L. Fiume, G. D. Stefano, C. Busi and A. Mattioli, *Biochem. Pharm.*, **1994**, 47, 4, 643.

[18]   A. Lapolla, C. Gerhardinger, L. Baldo, D. Fedele, D. Favretto, R. Seraglia and P. Traldi, *Org. Mass Spec.*, **1992**, 27, 183.

[19]   Y. Nagamatsu, J. Yasamoto, A. Kanamoto, Y. Tsuda and Y. Okada, *Chem. Pharm. Bull.*, **1992**, 40, 6, 1634.

[20]   I. Saito and M. Takayama, *J. Am. Chem. Soc.*, **1995**, 117, 5590.

[21]   A. Lehninger, Biochemistry, Worth Publishers Inc., New York, **1979**.

[22]   H.R. Mahler, E.H. Cordes, Basic Biological Chemistry, Harper & Row Publishers, New York, **1968**.

[23]   A. Juris, V. Balzani, F. Barigelletti, S. Campagna, P. Belser and A. Von Zelewsky, *Coord. Chem . Rev.*, **1988**, 84, 85.

[24]   R. Townsend, T.F. Kumosinski, S.N. Timasheff, G.D. Fasman and B. Davidson, *Biochem. Biophys. Res. Commun.*, **1966**, 23, 163.

[25]   S. Watanabe and T. Saito, *Int. J. Peptide Protein Res.*, **1985**, 26, 439.

[26] R.K. Murray, Harpers Biochemistry, 23rd edition, Prentice Hall Int. London, **1993**.

[27] A. Fersht, Enzyme Structure and Mechanism, 2nd edition, W.H. Freeman & Co., New York, **1985**.

[28] D. Shugar, *Biochim. Biophys. Acta.*, **1952**, 8, 302.

[29] H.R. Perkins, *Royal Soc. Lond. Proc.*, **1967**, 167, 443.

[30] R.C. Nairn, Fluorescent Protein Tracing, 4th edition, Churchill Livingstone, New York, **1976**.

[31] G.L. Peterson, *Anal. Biochem.*, **1979**, 100, 201.

[32] S. Satyanarayana, J.C. Dabrowiak and J.C. Chaires, *Biochem.*, **1993**, 32, 2573.

[33] Y. Eshdat, A. Dunn and N. Sharon, *Proc. Nat. Acad. Sci. USA*, **1974**, 71, 1658.

Chapter 6.

Final remarks.

6.1 Summary and final remarks.

This thesis involves the investigation of the photophysical properties of a range of Ru(II) polypyridyl complexes when covalently bound to various synthetic and natural biomolecules. Chapter 1 gives a general introduction into several aspects involving ruthenium chemistry. Firstly, an introduction into the various spectroscopic properties of Ru(II) complexes is given, with particular emphasis placed on the advantages these complexes possess to render them suitable as luminescent probes. A literature survey on current applications of such complexes in biological matrices is carried out, including the interactions of Ru(II) polypyridyls with DNA, their use in cancer treatment and various uses when bound to enzymes and antibodies from stabilising agents to models of novel drugs. This aims to illustrate the wide range of applications possible and their potential in the probing of biological materials. Finally the various techniques involving the covalent modification of proteins are discussed in order to understand the methods used and reactions involved in covalently binding the labels to the proteins in this thesis.

Chapter 2 deals with the synthesis of the ruthenium complexes and the specific procedures used in the conjugation of these labels to the proteins. In this chapter, the experimental details of the different physical measurements used for the elucidation of the properties of the ruthenium complexes both in the free form and when bound to proteins are given. Finally, studies were carried out on the decay of ruthenium complexes to investigate the accuracy and reliability of the functions/models used to analysis the nature of the decay and determine the emission lifetimes of the various emitting components of the luminescent probes. From this study the suitability of the single exponential decay law to elucidate the lifetime of the unbound labels and a multi-exponential decay law for the lifetimes of the various emitting species of the protein-bound labels is confirmed.

The ultimate objectives behind this thesis include the covalent linkage of Ru(II) polypyridyl complexes to proteins via specific binding sites and the investigation into the potential of these complexes as fluorescent probes capable of

monitoring conformational variances which the bound biomolecules undergo in solution, in particular the secondary structure changes in polypeptides and the unfolding processes in real proteins.

In chapter 3, the methods developed to selectively bind Ru(II) complexes to the (1) lysine residues (2) carbohydrate moieties (3) glutamic acid residues and (4) terminal amino/carboxylic acid groups of the biomolecules studied were carried out and the spectroscopic and the luminescent properties of such protein-bound labels were investigated as extensive characterisation of the complexes and the assessment of their probing properties were prerequisites to any further applications as luminescent probes. There were therefore three main aims behind the work carried out in chapter 3. Firstly, it was intended to successfully bind labels to the specific sites mentioned on each biomolecule in a covalent manner. Secondly, the verification of the purity of both the free complexes and their protein-bound forms was essential to deem any results obtained reliable. Finally, extensive analysis of the spectroscopic and luminescent characteristics of the fluorescent labels in their free form and when bound to proteins was fundamental in understanding the sensitivities of their various spectroscopic properties to changes in their surroundings, namely in the form of conformational variances of the bound biomolecules.

The most important conclusions from the studies carried out in chapter 3 are summarised herein. Firstly, methods were developed to bind the labels selectively to both the side groups of the amino acid residues and to the terminal groups of the polypeptide chain of both synthetic and natural proteins. A chromatographic method was developed based on size exclusion to distinguish the unbound from the protein-bound label. It had previously been assumed that most conjugates would be pure as dialysis should have removed all unbound label. However, small amounts of impurities due to free label ($< 5\%$) were identified but as quantitative analysis was not carried out, the exact purity of the conjugates was not ascertained. Nonetheless, for the purpose of the remainder of the work, the conjugates were deemed to be adequately pure to be studied as probes as the presence of unbound label in minute quantities did not appear to adversely affect the probing capabilities of the labels.

260

The emission lifetime of the label revealed the greatest potential as a sensitive reporter of the bound biomolecules as in most cases the duration and kinetics of the lifetime were significantly affected when bound to a protein. The change from single to multi-exponential decay kinetics and the enhancement of lifetimes of the labels when bound to proteins were proposed to be most likely due to a combination of factors, including the decrease in vibrational activity of the label when held in the more rigid environment of the biomolecule and the protection of the label from various quenching effects, particularly that of oxygen. Further studies concluded that the specific binding site chosen on the protein as well as the absolute conformation of the protein in question have an important bearing on the changes incurred on the decay lifetimes of the protein-bound labels. Evidence from size exclusion chromatography and conjugation ratio calculations suggested that the larger more hydrophobic complexes such as $[Ru(dpp)_2NH_2phen]^{2+}$ experience strong electrostatic interactions with proteins in addition to the anticipated covalent linkage whereas this was not the case for the synthetic biomolecules studied. Therefore, although these hydrophobic labels appear to be the most sensitive to conformational variances of the bound proteins, the probing potential may be adversely affected or indeed exaggerated by the interference from electrostatically bound label.

The labelling efficiency of various Ru(II) complexes to selected proteins was studied, concluding that the success of conjugation varies notably between synthetic and natural biomolecules and between various labels, with evidence of very efficient labelling of bovine serum albumin, particularly on the lysine residues. In contrast low loadings were achieved on the same sites on poly-L-lysine. The reason for this discrepancy is not evident but may be related to the reactivity of the biopolymer. In summary, the main achievements of these studies include the discernment of all relevant properties of the ruthenium complexes to be used as labels and the successful site and side chain modification of both natural and synthetic biomolecules which led the way to the investigation of their probing capabilities and limits in chapter 4 and 5.

In chapters 4 and 5, more detailed studies are carried out involving the determination of the potential of these labels to monitor conformational variances of the bound biomolecule in solution using various spectroscopic and luminescent properties of the label as the probes. The overall aim in these two chapters therefore was to study the effect of conformational variances of the conjugated biomolecules on various spectroscopic properties of the complexes, including their absorption and emission spectra and their emission lifetimes. The effect of pH and denaturants on such spectroscopic and luminescent properties of the protein-bound labels were investigated as these two parameters in particular are known to induce significant conformational changes in polypeptides/proteins. Chapter 4 concentrated on the investigation of the sensitivity of the absorption and emission spectra of the labels to the conformational variances of the proteins while Chapter 5 incorporated the study of the emission lifetimes of the labels.

The reason for choosing the pH as a variable was because the predominant form of secondary structure of the synthetic poly-amino acids poly-L-lysine and poly-L-glutamate, the subject of our studies, are known to be highly dependent on pH. The secondary structure of the basic PLL changes from random-coil conformation to an α-helical form above pH 10 approximately, due to the deprotonation of the amino groups of the lysine residues permitting such a regular structure to form. In contrast, the random coil conformation is the predominant form of PLGlu at neutral and basic pHs (i.e. above pH 5) due to the repulsion of the deprotonated carboxylic acid groups of the glutamic acid residues preventing the formation of α-helical structure. An important point to note is the similarities in conformational variances of synthetic polypeptides and proteins, hence their use as models in the study of protein unfolding and furthermore their structure is critical to their biological activity as is found for proteins. Finally, although definite information on the exact structural forms of the proteins BSA and the enzyme lysozyme are not given at various pHs, it is known that some denaturation/unfolding of such proteins takes place at very low and high pHs.

By studying the pH sensitivity of the absorption and emission spectra of the protein-bound labels, the limit of these properties to monitor conformational variances of the proteins was realised. In particular the absorption spectra of the labels were not influenced to any significant extent by any structural changes of the bound biomolecule. The pH sensitivity of the emission spectra of the labels were however found to be influenced by the bound protein, presumably due to its acid-induced conformational variances. However the exact effect of the protein on the emission spectra was difficult to evaluate due to the complex pH sensitivity of the emission spectra of the free labels.

In Chapter 5, the potential of the emission lifetimes of the labels of the form $[Ru(L-L)_2NH_2phen]^{2+}$ and $[Ru(L-L)_2NCSphen]^{2+}$ as probes was realised with promising results while the label $[Ru(bpy)_2esterbpy]^{2+}$ was no longer studied due to the complex pH sensitivity of its absorption and emission properties displayed in Chapter 4. Significantly, it was concluded that as the acid-induced random coil- α-helix/ α-helix-random coil transition of the polypeptides PLL and PLGlu in solution took place, the emission lifetimes of both emitting components of the bound labels decreased/increased dramatically, strongly supporting the theory that the lifetimes of such labels act as sensitive reporters to such conformational variances. However, an important discovery is the fact that such monitoring was only successful on binding the labels to the side groups of the polypeptides. This is proposed to be due to the more noticeable change in environment of such groups on occurrence of conformational changes when compared to the labels bound to the groups at the end of the polypeptide chains.

Similar studies on BSA revealed significant enhancement of lifetimes approximately between pHs 3-8 while notable lifetime decreases were evident at pH extremes, particularly above pH 9, where the protein is at its least stable. However, although such decreases in lifetimes of the labels were likely to be due to unfolding of the protein at both extremes of pH particularly noticeable under alkaline conditions, there was no proof that unfolding did take place. In contrast to the polypeptides, such observations did not vary significantly with the site of attachment

263

of the label on the protein, probably due to the global effect of the unfolding on the protein and all labels.

In brief, the promising results obtained in this section verify the success of the fluorescent complexes in monitoring certain conformational variances of proteins but also indicate that more definite proof is required. Due to the uncertainties associated with the nature of unfolding of the protein BSA, the final section in chapter 5 dealt with similar denaturation studies carried out on the enzyme lysozyme whereby loss of enzyme activity was used as an indication of protein denaturation. Furthermore, a study of the effect of labelling on the natural conformational properties of the enzyme was possible by comparing the activity of the unbound and modified lysozyme at various conditions. Combined studies of the emission lifetime of the bound labels and the enzyme activity at pH extremes and in the presence of chemical denaturants were carried out in order to establish an association between protein denaturation and decay lifetime reduction of the labels and hence verifying the promising results indicated with BSA.

Indeed, as anticipated there was found to be a relationship between the reduction of the decay lifetimes of the labels when bound to lysozyme and loss of activity of the enzyme (i.e. denaturation). Both acid-induced denaturation and unfolding in the presence of guanidine were verified by the total loss of activity of the enzyme towards its substrate which indeed correlated with significant reductions in the decay lifetimes of both emitting species of the enzyme-bound label. As would be expected the nature of the label and binding site on the enzyme did influence the effect of modification on the enzyme activity and perhaps even its conformational properties. However, most labels bound to the lysine residues and carbohydrate moieties had a minimal effect on the stability and conformational properties of the enzyme while the loss of activity of the labelled enzyme may have been due to modification of binding sites near the active site which would influence the binding of the substrate. The importance of the position of the binding site on the enzyme was demonstrated by the loss of activity of lysozyme when a label was bound to the glutamic acid residues as these sites are known to be crucial in the binding between

264

enzyme and substrate in the active site. Studies of the pH sensitivity of the activity of lysozyme concluded that the enzyme was most active at pHs 5-8 as found for most proteins and this was not influenced significantly by the bound labels in most cases. This is of critical importance as the aim was to study the natural structural changes of the enzyme in solution rather than merely monitor the effects of the bound label on its dynamic behaviour.

By analysing the emission lifetimes after increasing quantities of denaturant a levelling off of lifetime appeared to indicate the approximate concentration of denaturant required to denature the enzyme. This phenomenon was already suggested for BSA and was indeed confirmed for lysozyme where a good correlation between the complete deactivation of the enzyme and the minimisation of the decay lifetimes of the labels was evident. Contrasting effects were earlier noted for the PLL-bound labels whereby the addition of denaturants when PLL was in the α-helical form actually led to enhancements of lifetimes, proposed to be due to their destabilising effects on the hydrogen bonded α-helix and subsequent return to the random-coil conformation, where the labels display enhanced decay lifetimes.

In conclusion, the emission lifetimes of most Ru(II) polypyridyl complexes of the form $[Ru(L-L)_2NH_2phen]^{2+}$ and $[Ru(L-L)_2NCSphen]^{2+}$ when bound to biopolymers were found to be particularly sensitive to the secondary structure changes of synthetic polypeptides but also denaturation of natural proteins and loss of activity of enzymes induced both by pH variations and chemical denaturants. As, in the majority of cases the labelling of the proteins did not appear to adversely affect the conformational properties of the protein, the results of these studies are promising in the use of such labels in the probing of real biological matrices but emphasise the importance of studying the nature of the label and the position of the binding site on the protein beforehand.

6.2 Future work.

Our photophysical studies of various protein-bound ruthenium(II) polypyridyl complexes in solution have unveiled the potential certain such complexes display in relation to their ability to monitor conformational changes which the bound proteins undergo via variations in the emission lifetimes of the bound fluorescent labels. However, the limit to their applications in their own right must be appreciated. In this thesis, some assumptions are made as regards the conformational variances which these proteins are undergoing. For example, it is assumed that the protein bovine serum albumin becomes unfolded at pHs above 9. Future work of this nature could be substantiated by the combined use of protein characterisation techniques. Such methods include differential scanning calorimetry (D.S.C.) which analyses the energetics of unfolding or circular dichroism studies (C.D.) for polypeptides as the optical rotation of polypeptides is dependent on its secondary structure, allowing the differentiation of α-helix, β-sheet and random-coil conformations. This would allow more definite conclusions to be made regarding the sensitivity of the labels to the unfolding/conformational changes of the bound proteins. Nevertheless, initial studies involving the labelling of the enzyme lysozyme proved successful, yielding promising results. However, the investigation of the unfolding processes of enzymes and proteins, (eg. to substantiate the relationship between the unfolding of lysozyme and its loss of activity) combined with such protein characterisation methods would be invaluable to the study of such probes.

Another important area which was not approached but may prove invaluable is polarisation studies of the protein-bound labels which allow the study of the rotational dynamics of proteins and other macromolecules based on the polarisation or anisotropy of the emitted light when the sample is excited with a vertically polarised light. The extent of polarisation of the emitted light depends upon the extent of random Brownian motion of the molecules that occurs during their excited state lifetimes. One of the unclear issues in this thesis is the nature of the shorter lifetime of the decay of the various protein-bound labels and the use of polarisation

studies may allow the determination of the nature of such a lifetime, often similar to that of the unbound label. This technique may also allow one to differentiate between electrostatically and covalently bound labels which is of critical importance in determining the true potential of such fluorescent complexes as probes of biological matrices.